THE GEOLOGY OF SAINT HELENA ISLAND, SOUTH ATLANTIC

Ian Baker 1968

Thesis submitted for the Degree of Doctor of Philosophy in the University of London

ABSTRACT

The island of St. Helena is formed by two deeply eroded basaltic shield volcanoes, active from approximately 15 to 7 million years ago. The smaller north-eastern volcano is partly buried beneath the flanks of the younger, more complex south-western shield. Linear dyke swarms are preserved in the central areas of both volcanoes.

Over 400m of altered breccias of probable submarine origin form the core of the north-eastern volcano, the bulk of which consists of approximately 800m of subaerial lavas and interbedded pyroclastics.

The south-western volcano has been divided into three major stratigraphic units. The 500m thick Lower Shield is composed of five alternating sequences of lava flows and pyroclastics in approximately equal amounts. The Main Shield is built dominantly of more than 800m of lava flows. A marked unconformity separates extrusives of the Upper Shield from the main mass of the volcano. The constituents of the Upper Shield (270m preserved) are basalts and younger trachyandesites which originated from an area on the flanks of the south-western shield. Later trachytic and trachyandesitic flows are locally present on the eastern flank. A number of trachytic and phonolitic intrusions into the central area and flanks of the south-western shield are the latest major volcanic products.

Sixteen individual arcuate intrusions of three distinct structural types are described, all but one occurring in the south-western volcano. Their maximum dimension in plan varies from 25m to approximately 1000m.

Volumetrically, the exposed rock types are: basalts + trachybasalts = 95% (approx. 75% and 20% respectively); trachyandesites = 4%; trachytes and phonolites = 1%. Ankaramites are abundant in the Lower Shield of the south-western volcano. Trachytic and trachyandesitic rocks are exceptionally rare in the north-eastern volcano, but occur at a number of levels throughout the south-western shield.

The volcanic products belong to the alkali olivine basalt - trachyte - phonolite assemblage. Chemically and petrographically the rocks exhibit regular variations from ankaramites to phonolites; these variations are interpreted as the result of differentiation of a parental, weakly nepheline normative (approx. 4%) basaltic magma. Late stage differentiates are markedly undersaturated, containing up to 16% normative, and nearly 15% modal nepheline. The late, highly alkaline, intrusive rocks exhibit regular compositional variations outwards from the centre, and are believed to be products of a differentiated magma chamber at a high level in the volcanic pile.

A number of small amphibole-bearing monzonitic and syenitic xenoliths are interpreted as inclusions picked up by the late intrusions when they passed through a thin, nearly consolidated, differentiated sheet.

The petrochemistry of the St. Helena rocks is compared with that of other islands in the Atlantic, and a possible mechanism for producing an outward increase in degree of undersaturation away from the mid-Atlantic Ridge is proposed.

ACKNOWLEDGEMENTS

I would like to thank all of the people on St. Helena who made field work possible. In particular I am indebted to the Peters family of Blue Hill School, the Peters family of Sandy Bay Beach, Mr. and Mrs. K. Thomas of Levelwood School, Mr. and Mrs. Maurice Thomas of Longwood, Mr. and Mrs. Edward Williams of Horse Ridge, and Mrs. Moyce and Mrs Richards of the Consulate Hotel, Jamestown, for their hospitality and many kindnesses.

The warm friendship of Mr. and Mrs. Alan Johns and Mr. and Mrs. Ralph Hilling was a continual feature of my stay on St. Helena, and I am deeply grateful to them.

I wish to thank the Government Secretary of St. Helena for arranging one of my boat trips round the island.

The provision of a number of copies of the topographical map by the Geographical Department of the War Office is gratefully acknowledged.

I am indebted to S.E. Haggerty for identifying the opaque minerals and for valuable discussion in this field, and to R. Berlin for assistance during the X-ray and optical spectrographic determinations of trace elements.

I am very grateful to Dr. D.A.B. Pearson (now of the Institüt für Palaeontologie, Tübingen) for introducing me to the processes of photographic printing.

I am indebted to Dr. G.D. Borley for critically reading this manuscript and for her many helpful suggestions. I also wish to thank the following for critically reading specific sections: J.G. Jones (II and IX), W.I. Ridley (III), Dr. N. Price (IV), Dr. M.J. Abbott (V and VIII). Discussion with these and may others is gratefully acknowledged.

I would like to thank Mrs. Julia Kelland for typing the manuscript.

The receipt of a Natural Environment Research Council Studentship is gratefully acknowledged.

The continual encouragement of my wife during this course of study and especially during the last few months of writing this thesis cannot be sufficiently acknowledged.

TABLE OF CONTENTS

SECTION I

INTRODUCTION

1. Geography.

The volcanic island of St. Helena lies in the South Atlantic at latitude 16°S, longitude 5°40'W, over 800km east of the crest of the Mid-Atlantic Ridge. The mainland of Africa is over 1800km to the east, and the Brazilian coast lies some 3000km to the west. The nearest other volcanic islands are Ascension, 1200km to the north-west, and Tristan da Cunha, 2150km to the south (Fig. 1). St. Helena rises to a height of nearly 830m (Mount Actaeon) above sea level; the ocean floor is a further 4400m down, resulting in a total height of over 5km for the volcanic pile.

The island, although in the tropics, is cooled by the south-east trade winds and the western extension of the Benguela current, and the climate is very pleasant. Because of the highly irregular topography, temperature and precipitation vary considerably over the island. The central high ground probably receives more than 100cm of rain each year, while the coastal regions often receive less than 25cm. These rainfall variations have produced a more or less barren coastal belt, and thickly vegetated ground above about 450m.

The island, 120km^2 in area, has a coastline of precipitous cliffs (200-500m high), with streams that reach the sea via narrow, deep valleys, arranged more or less radially. Overall the topography is rugged, resulting in good exposures (except on very high ground) which are frequently inaccessible. A topographical map with contours at

FIGURE 1: THE SOUTH ATLANTIC

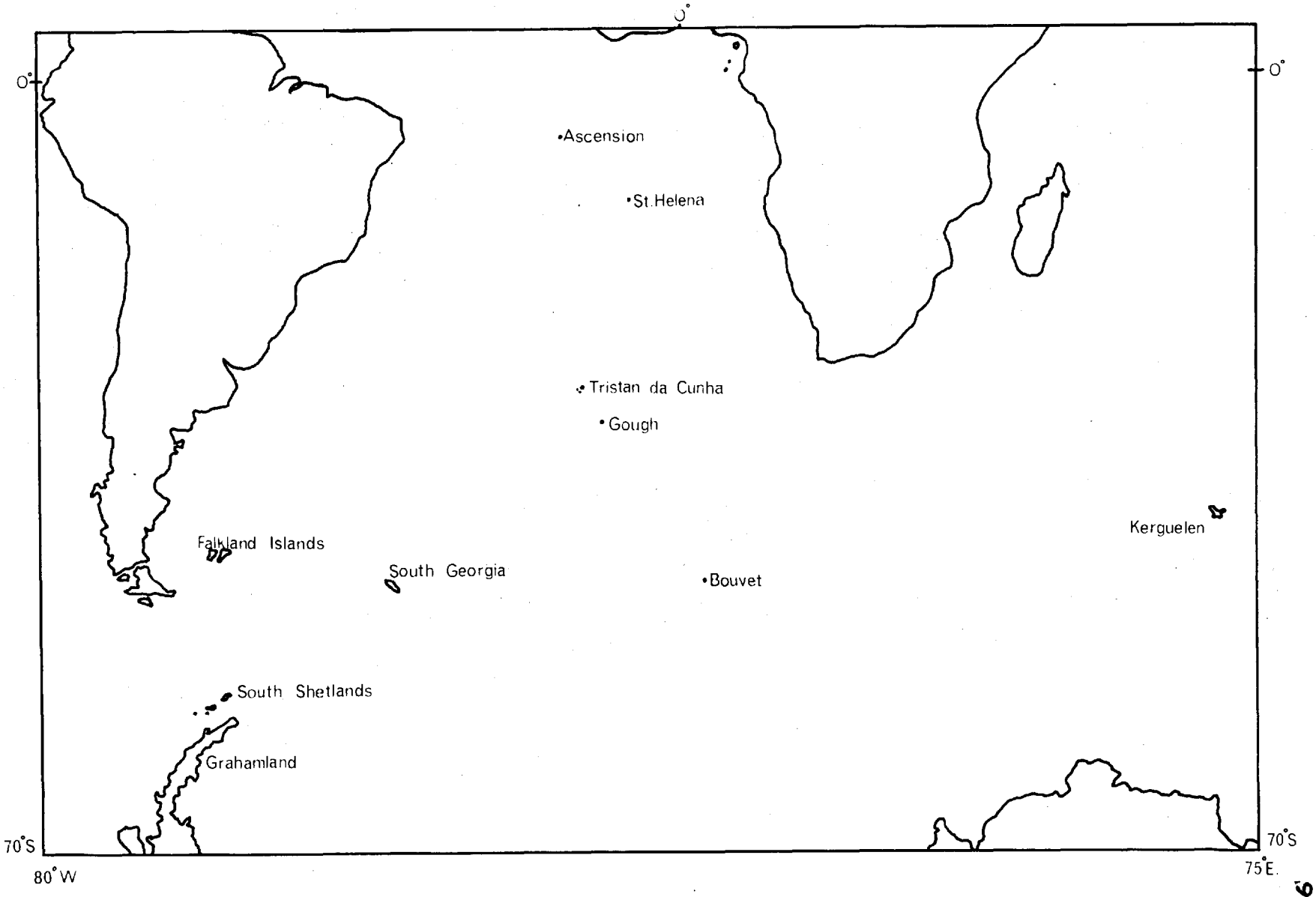

100m intervals is shown in Enclosure 1, together with place names used extensively in the text. Place names will be indicated on most of the maps and diagrams, but Enclosure 1 has been prepared especially to avoid overcrowding of lettering and obscuring detail in geological maps.

The most striking topographic feature is undoubtedly the erosional ampitheatre of Sandy Bay, with its rim of high ground separating it from the rest of the island. This area which is the most complex geologically, is also the most dangerous, especially in the south and south-west, where few tracks exist and fishermen's paths are rare and little used. It is of considerable significance that the last stronghold of wild goats is in the area of Lot's Wife, the Asses Ears and Devil's Hole.

Bathymetric data for the area around St. Helena (Fig. 2) has been compiled from Admiralty Plotting Chart 5331 (1:1,000,000), with additional data from one run by H.M.S. Protector (April, 1966) supplied by F.J. Davey of the University of Birmingham. The position of the 50 fathom line, and of off-shore shoals, has been compiled from Melliss (1875) and Admiralty Chart No 1771, and is shown in Fig. 3.

The 50 fathom line is on average about 2km from the present coast line. Only 5km further out the water is 1500 fathoms (2750m) deep, the slope of the mountain then decreases slightly, especially to the west. The diameter of the island at the 2300 fathom (4200m) line is about 85km east - west and 75km north - south, the irregularity in the east - west contour being in the western radius (Fig. 2).

One continuous sounding run to the west has recorded a bathymetric high only 125m below sea level which is featured as a prominent submarine peak by Heezen and Tharp (1961). The soundings suggest that this pile is smaller than

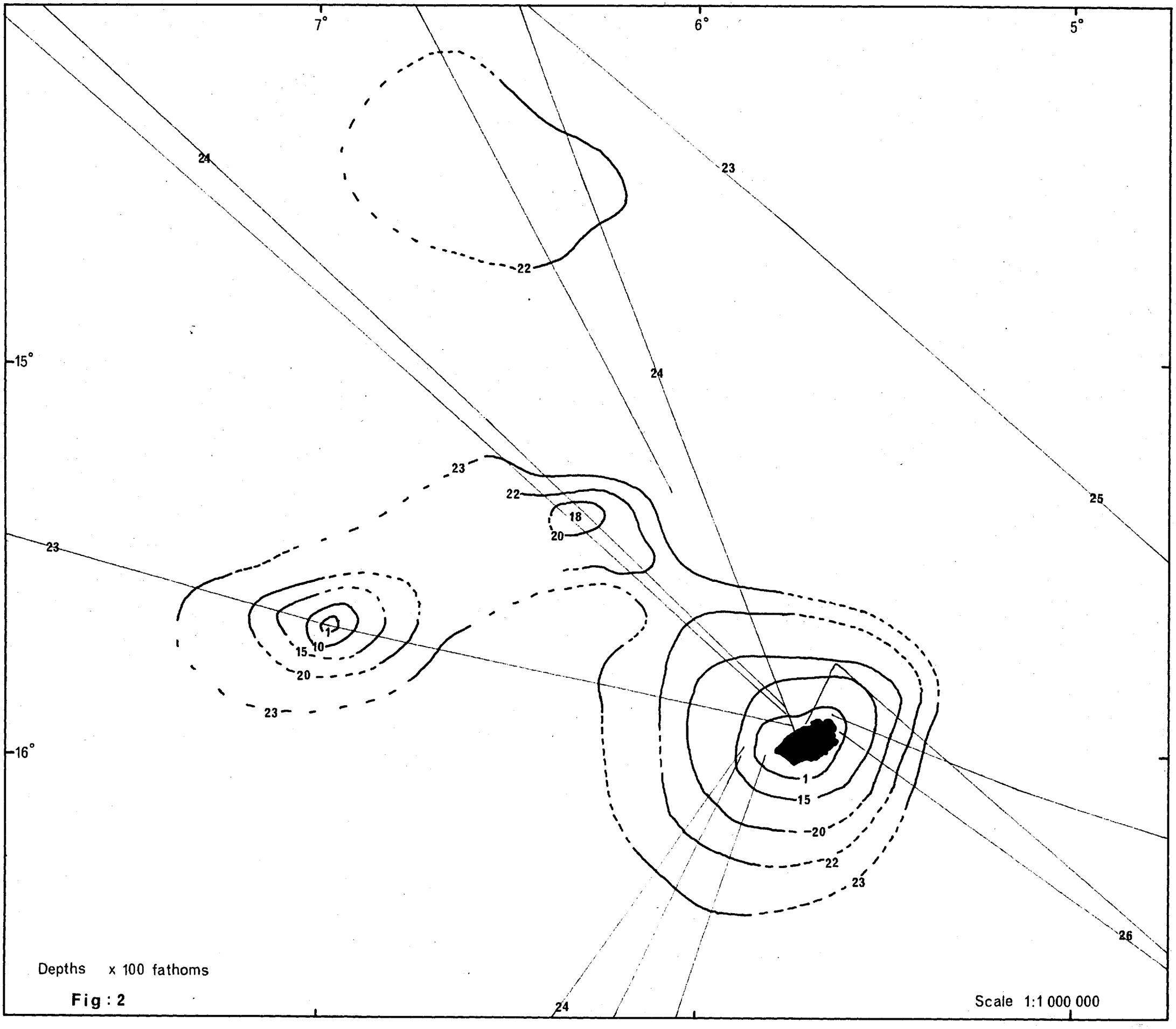
7°
6°
5°
15°
16°
24
23
22
24
23
22
18
20
23
1
15
10
20
23
1
15
20
22
23
25
26
24
Depths x 100 fathoms
Scale 1:1 000 000

Fig : 2

FIGURE 2:

Bathymetry of the area around St. Helena plotted in hundreds of fathoms. Faint lines represent sounding lines taken from Admiralty plotting chart (see text).

Note: general slope of ocean floor west to east; smaller conical seamount 120km WNW of St. Helena, and slight bathymetric high ENE of that. The broad ill-defined area 160-200km NNW of St. Helena is of uncertain shape.

St. Helena, and may well represent a completely submarine volcano which failed to reach the ocean surface. A further slight rise (to 1800 fathoms) appears to be present 80km north-west of the island. The Protector recorded an uncorrected depth of 3022 fathoms (5450m) only 200km south-east of the island.

2. Geology.

> "The geological structure of this remarkable land has often been curtly described in the few words 'it is volcanic', and the explanation as often considered sufficient, inasmuch as the truth of such an assertion cannot be doubted, even by the most casual observer. This rocky pile, however, so briefly dismissed as troublesome to inquire into, presents not a few points, in searching out truth, well worthy of the student's attention. The manner of its formation, together with the time occupied therein, and the period that has elapsed in bringing it to the present shape and dimensions, are each subjects affording unusual interest in reading that page of nature's book which throws light upon the ancient geography of the South Atlantic region". (Melliss, 1875).

Charles Darwin visited St. Helena during the homeward voyage of the Beagle in 1836. He spent four days on the Island, and established a succession of basal submarine lavas, basaltic series (lavas and pyroclastics), feldspathic series (lavas) and late phonolitic intrusives. He believed that the hollow of Sandy Bay represented the original explosion crater of a single volcano, the anomalous dips of the north-east being the result of uplift and tilting (Darwin, 1872).

A remarkably accurate account of the geology is given by J.R. Oliver (1869), a Captain in the Artillery. He recognized that a number of irregularities in the topography were erosional features and were not the results of 'upheaval', a popular mechanism invoked at the time. He believed that the north-eastern dyke swarms represented the oldest part of the

structure, and suggested that The Barn and King and Queen Rocks possibly represented an earlier volcano than the main mass of the island. Oliver also recognized the later "feldspathic lavas" of the east coast, and established their presence on much of the high ground inland. The earlier basalts and those later lavas could have originated from different localities, although he believed the later lavas to be from Sandy Bay. He described one major alkaline dyke, and believed Sandy Bay to be the initial "confused" crater.

Melliss (1875) accepted the theory of a single volcano, with its crater in Sandy Bay, producing thick basaltic layers and late feldspathic lavas of Horse Point and Stone Tops. He connected many of the Sandy Bay alkaline dykes into one sinuous major dyke, and accounted for anomalous dips by assuming widespread tilting. These early accounts of the geology make very enjoyable reading, and that of Oliver requires special credit. Darwin's chapter in "Naturalist's Voyage Round the World" gives a delightful contemporary view of the island.

The standard geological work on St. Helena is that of Daly (who spent a month on the island in 1922), published 40 years ago (Daly, 1927). Daly established the existence of two volcanoes, both fed by fissures - an older, smaller one in the north-east, and the major one centred in Sandy Bay. He described highly altered basal rocks of uncertain origin in both centres, believing them equivalent. Daly opposed the idea of later feldspathic lavas, the classic exposure of which, between Turk's Cap and Prosperous Bay, he interpreted as being formed of later flows from the north-eastern volcano. He showed the ampitheatre of Sandy Bay to be the result of erosion, not explosion, and suggested the existence of three major alkaline dykes in this same region. Daly believed the alkaline intrusives and flow domes to be the very latest volcanic products.

In general terms much of Daly's field interpretation is correct, but in many specific cases his interpretations are wrong, undoubtedly because of the briefness of his visit. However, Darwin's, and especially Oliver's, accounts are also correct in broad terms, in spite of Darwin's misinterpretation of the gross volcanic structure. From the point of view of the field geology and its interpretation the works of these three authors should be viewed equally, in the light of the briefness and date of their visits.

Two periods of field work were spent on the island, between July and October 1964, and November 1965 and April 1966. The first season was spent in reconnaissance mapping and collecting a large suite of specimens, and the second in detailed mapping and collecting further material for laboratory study. The War Office topographical map (Ref. no. 1853) of 1904 (with modifications, 1941) is on the whole quite accurate. This map was photocopied and enlarged to a scale of approximately 1 : 7,400 and the whole island was mapped geologically on this scale.

A short summary of the volcanic history of the island interpreted during these two visits is given below, to act as a guide during the following detailed discussions of the structure of the volcanoes.

The island was formed by the coalescence of two broad basaltic shield volcanoes: a smaller, older, very highly eroded mass in the north-east, and the major eroded south-western shield centred in Sandy Bay (Fig. 3). The lavas and interbedded pyroclastics forming the bulk of both shields were erupted dominantly through fissures, preserved as impressive dyke swarms in the deeply eroded centres of the volcanoes. A third, late, eruptive centre, believed to be in the area of the Peaks, poured out thick sequences of basaltic

FIGURE 3:

Broad geological subdivisions of the island. North-eastern volcano lies inside the ticked line, with erosional 'window' in James Valley. South-western volcano - blank; lavas of the upper shield - L; eastern flank flows (later than upper shield) - stippled; late highly alkaline intrusive rocks - black.

Dashed line is 50 fathom line, dots S mark positions of shoals. Note irregularities in the outline in the south-west, and south-east (see text). The overall NE-SW elongation of the island is closely paralleled by the 50 fathom line - compare with the direction of dykes.

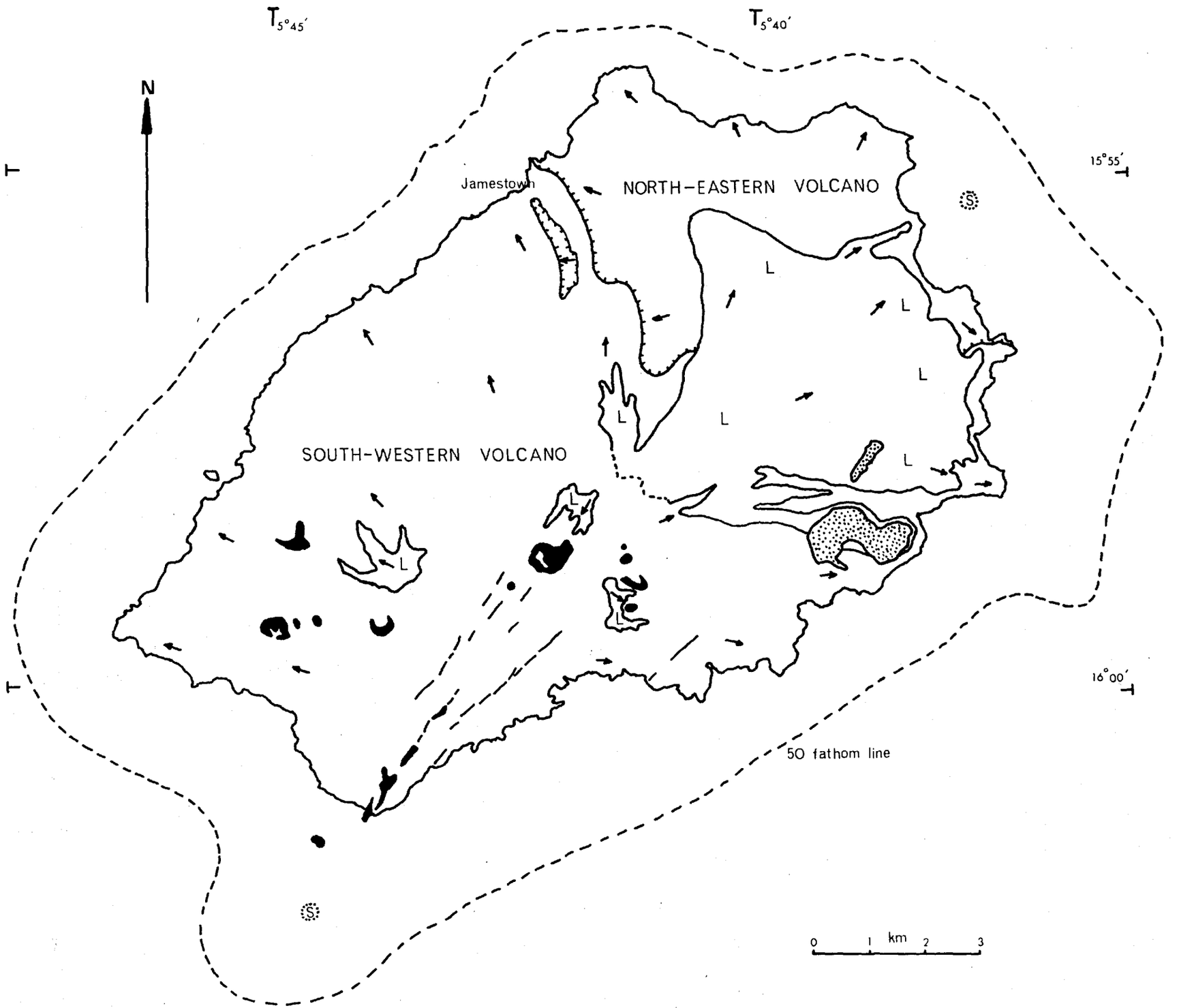
T5°45′
T5°40′
N
T
15°55′
Jamestown
NORTH-EASTERN VOLCANO
SOUTH-WESTERN VOLCANO
L
S
16°00′
50 fathom line
0 1 km 2 3

FIGURE 3

and later intermediate lavas to flood highly eroded parts of both shields, especially in the east of the island between Turk's Cap Ridge and Sharks Valley (Fig. 3). In the east of the island, in the Stone Tops area, a complicated sequence has been established for younger local (intrusive and extrusive) activity.

The south-western shield was intruded by a large number of highly alkaline dykes and individual parasitic bodies much later than the constructive phases of the shield as a whole. The late individual parasitic intrusives (and a number of earlier isolated intrusions) are frequently controlled by small scale arcuate fractures. These structures are discussed separately in Section IV.

Large areas of the island have been extensively altered, producing brightly coloured, clay-rich materials, often very difficult to identify and correlate. Much of the high ground, inside the coastal rim, is affected, and while much of the alteration can be explained by weathering, hydrothermal activity must have been locally very severe.

SECTION II

THE NORTH-EASTERN VOLCANO

1. Introduction.

Rocks of the deeply eroded north-eastern shield extend south-easterly to King and Queen Rocks, south-westerly into the upper reaches of Rupert's Valley, and westerly to James Valley (Fig. 4). In the west and south-east they are buried beneath flows of the main shield group of the south-western volcano, and from the head of Rupert's Valley easterly to Prosperous Bay they are overlain by lavas of the upper shield series. The oldest rocks, breccias of probable submarine origin, are overlain by pyroclastics of probable subaerial origin and the thick shield-forming mass of basaltic flows and pyroclastics.

2. Basal Breccias.

The oldest rocks of the north-eastern volcano are breccias, the form and structure of which is largely obscured by intense dyke swarms. The area of these old rocks presents a monotonously uniform appearance - highly eroded, yellow-brown, irregular, narrow ridges and valleys. Most of the area is inaccessible, and much is covered in detrital material making systematic work impossible (Plate 7).

a. Field relations.

The breccias consist of unsorted fragments of very variable size grade never exceeding 0.5m in diameter (Plate 1A). Locally they may form vague planar units about 0.5m thick, which suggest dips of 15-25^{o} north-easterly beneath

FIGURE 4:

Geology of the deeply eroded north-eastern volcano; note the erosional 'window' exposed for nearly 2km in the lower parts of James Valley.

Note also the overall high dip values of the shield-forming extrusives compared to the south-western volcano; and the restriction of abundant parasitic pyroclastics to high levels in the shield.

A-A and B-B are lines of dyke counts approximately perpendicular to the main Knotty Ridge dyke swarm - for explanation see text.

5°43' 5°41' 5°39'

NORTH - EASTERN VOLCANO

GEOLOGY

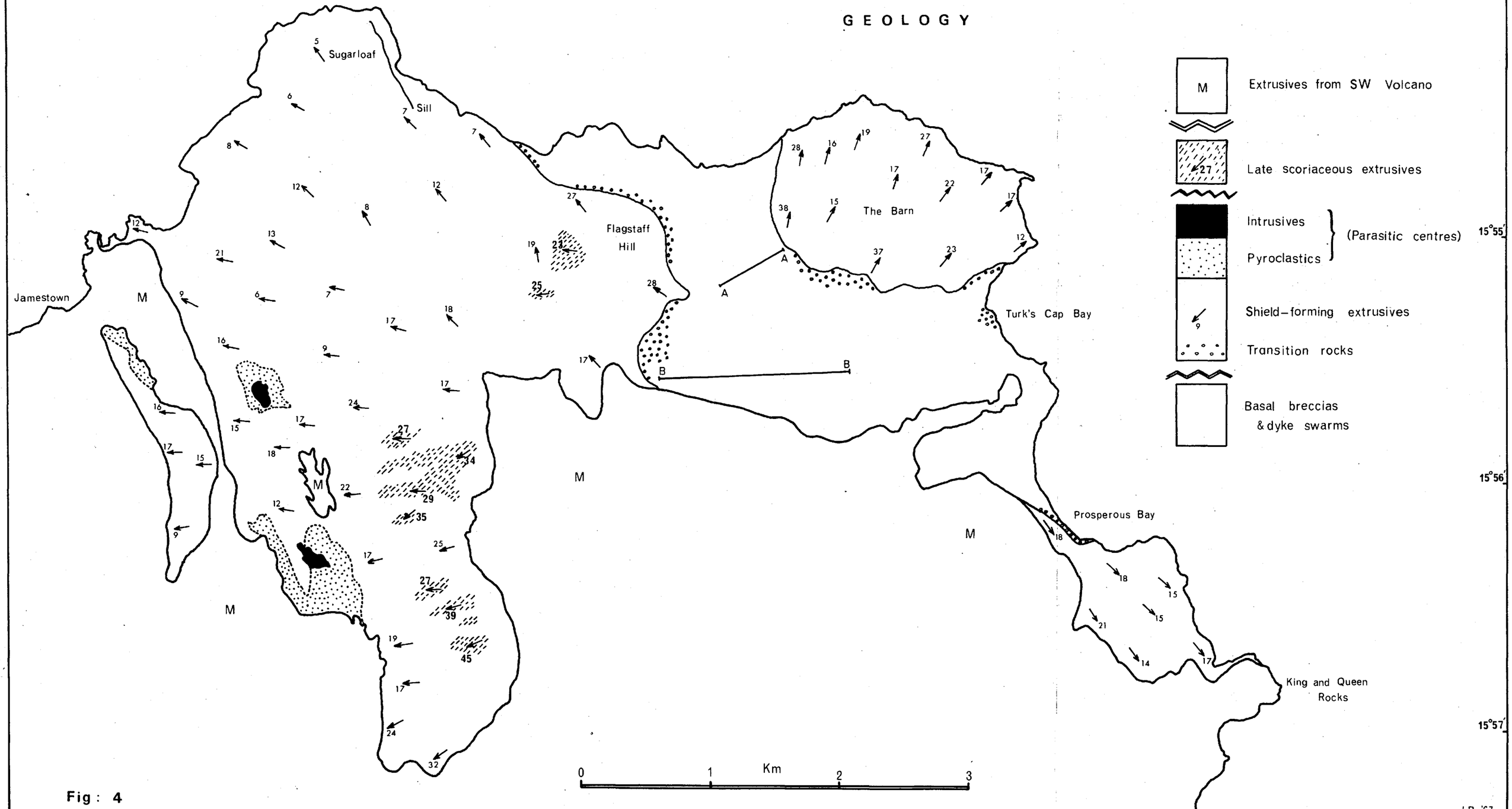

- M — Extrusives from SW Volcano
- 27 — Late scoriaceous extrusives
- Intrusives / Pyroclastics } (Parasitic centres)
- 9 — Shield-forming extrusives
- Transition rocks
- Basal breccias & dyke swarms

Fig : 4

IB '67

PLATE 1:

A: Typical basal breccia exposed in the main stream valley between The Barn and Turks Cap Ridge. Note the numerous thin, more or less regular dykes cutting the unsorted, unbedded breccias. Extensive secondary carbonate veining (typical of these parts of the north-eastern volcano) can be seen in the bottom left-hand corner of the photograph.

B: General view of the head of The Springs Valley between Turks Cap and Horse Point (Encl. 1). Intermediate flows from the SW volcano rest on an eroded surface cut into the basal breccias of the NE volcano. Note the high density of dykes cutting the breccias in a number of dominant directions, and the overall inaccessibility of the region. (Note also the highly altered nature of the overlying late flows especially in the middle and far distances.)

C: Sinuous, completely altered basic dykes (with glassy selvages) cutting ?pillow-lava within the basal breccias. Massive rock (top left) is a later dyke inclined at a small angle to the plane of the photograph.

Flagstaff, and possibly easterly in the valley at the seaward end of Knotty Ridge. Rock fragments are green, often with a serpentinous, greasy appearance, and are set in a matrix of finer yellow-green material. The whole mass is highly or completely altered and consists of chloritic materials and abundant calcite; quartz occurs very rarely. The general aspect of the breccias is unlike that of any other rocks occurring elsewhere on the island.

Although the south-western volcano is eroded deeply into an early, largely pyroclastic core, which has been subjected to a depth and period of burial comparable to that of the north-eastern volcano, there is no similarity between the two areas.

b. Petrography.

Specimens of the breccias were collected on the coast in Flagstaff Bay midway between The Barn and Flagstaff, and in the stream valley south of The Barn at an elevation of 180m. All of the rock fragments are basic with fine-grained basaltic or doleritic textures. Ferromagnesian minerals (augite and olivine), and groundmass material are largely or completely replaced by serpentine-chloritic minerals and calcite, plagioclase laths are frequently the only primary mineral preserved. Iron-titanium oxides, if preserved, frequently exhibit finely skeletal textures. The fragments are often vesicular (now infilled by calcite and chloritic materials) and original coarsely porphyritic varieties are recognizable. Two specimens exhibit normal basaltic texture, with largely altered euhedra of green diopsidic-augite and olivine in a fine-grained groundmass of augite, feldspar and equant opaques. Small rounded patches (2-5mm) with diffuse contacts are slightly coarser-grained and contain irregular feldspars, strongly titaniferous-augite and highly skeletal opaques.

Some specimens contain patches of very fine polycrystalline quartz and coarser-grained cross-cutting veins associated with blebs, spongy masses and rare fine veinlets of pyrite (and minor chalcopyrite). Both sulphides may occur within the quartz veins, but only pyrite occurs outside, its abundance and grain size decreasing away from the veins. The quartz and sulphides are believed to be of hydrothermal origin, and in these respects the highly altered chloritic rocks compare with those described from the Carlsberg Ridge by Cann and Vine (pp205-206, 1966).

Fragments from small areas of the breccias exhibit variable textures but there is no reason to believe that they are anything but contemporaneous fragments reflecting only their variable cooling histories. Similar wide textural variations have been observed in a basaltic pahoehoe flow and the breccia produced where it entered water (thin sections of material from a table-mountain in the Laugarvatn area, south-western Iceland, were kindly loaned by J.G. Jones).

A single block of limestone was found in situ in the main stream valley south of The Barn at an elevation of 170m. The block, although largely recrystallized, possibly as a result of adjacent dyke injection, retains contorted, banded structures believed to be of algal origin. No other comparable material was found on the island.

3. Transition Zone.

The transition zone is the name loosely applied to those rocks below the shield-forming subaerial extrusives and above the basal breccias (Fig. 4). These rocks are exposed in steep, inaccessible cliffs or valley sides, or are covered with detritus from the overlying shield-forming rocks. For these reasons they have been studied through field glasses.

The best exposures are in the south-east corner of The Barn, north of Prosperous Bay Beach, in Turks Cap Bay and in the north-east faces of Flagstaff Hill. Rocks of equivalent position are poorly exposed below the south-west face of The Barn and south-south-east of Flagstaff Hill. In this latter area the shield-forming rocks are highly altered and relationships are very obscure.

On the north-east side of Flagstaff Hill about 60m of red or purple-brown coarse angular breccias (to 30cm) underlie coarse subaerial pyroclastics. These breccias thin westerly, where a weak stratification becomes apparent, and consist largely of crystalline lithic fragments. Equivalent breccias may occur on the north-west side of The Barn, but if so they are thinner than those of Flagstaff and are largely obscured by detritus.

Below the south-west face of The Barn a local pyroclastic cone of medium to coarse, purple-red, scoria lies below the local level of shield-forming extrusives and has been included in the transition group.

In the south-east corner of The Barn normal basal breccias are overlain by nearly 100m of medium-grained yellow fragmental material containing less than 10% of sub-angular compact black basalt fragments up to 1.5m in diameter. Similar material is exposed overlying the basal breccias towards Prosperous Bay Beach, where it is overlain by over 30m of coarse boulder beds which extend up to the contact with scoriaceous, vesicular lavas. The boulder beds are only exposed for about 350m along the cliffs - northwards, the shield-forming flows rest directly on the yellow fragmental material. The black boulders average 1m in their maximum dimension and are set in a highly altered yellow matrix. Although poorly bedded they appear to dip south-easterly at

between 10-15° conformable with the overlying flows. The boulders exposed here are possibly the result of erosion of areas of the underlying yellow fragmental material, the large fragments being concentrated in detrital, muddy, scree-type deposits.

In the coast section of Turks Cap Bay a group of variable, essentially fragmental rocks have been included in the transition zone. They are totally unlike the basal breccias, are brown and yellow in colour and consist of rounded to sub-angular fragments generally of highly vesicular nature. Exposures are limited because of the numbers of dykes and cover by detrital deposits cemented by carbonate derived from the secondary mineralization of the area and correlation proved impossible. The rocks are geographically about 100m lower than equivalent rocks to north or south (cf. Fig. 4 with Encl. 1). The most probable interpretation, in view of the poor exposure, is that they represent a local 'valley' infilling eroded into be basal breccias.

At two exposures the material, a brown uniform agglomerate, strongly resembles the highly oxidized scoriaceous tops of subaerial flows. A more massive material forming the host rock for dykes close by consists of a heavy black basalt with an irregularly rounded surface. Both rocks are markedly feldsparphyric and could be related parts of a thick subaerial lava flow.

A very variable breccia nearly 100m away is made up of a wide variety of rounded to sub-angular rock types in a fine grained yellow-green matrix. Six fragments were taken from an area of approximately 1.5m square - these were:

(a) Highly oxidized vesicular fine-grained basalt.

(b) Fine-grained, completely altered, vesicular, weakly banded fragment consisting of green alteration

products, abundant opaque granules now largely replaced by sphene, and late granular quartz veins cutting the rock or replacing green materials infilling vesicles.

(c) Porphyritic feldspar - pyroxene - olivine - titanomagnetite basalt,

(d) Almost completely altered (chlorite and calcite) vesicular medium-grained basalt, with sub-skeletal oxides.

(e) Highly altered (calcite-rich), coarsely vesicular, microporphyritic feldsparphyric fine-grained basalt, containing apatite and very rare amphibole.

(f) Vesicular trachyte, with perfect trachytic texture. Ferromagnesian minerals are short, tabular, pleochroic aegirine and riebeckite-like mineral (pleochroic: blue - colourless, or blue-pale brown). A second brown amphibole may also be present. No other rock with a comparable texture has been found in the north-eastern volcano, and non of the other highly alkaline rocks anywhere on the island contain comparable ferromagnesian minerals.

Rocks of the transition zone, while not always closely related to the shield-forming rocks are of distinctly different origin to the basal breccias.

4. The Dyke Swarms.

The overwhelming impression of the basal rocks of the north-eastern volcano is of a chaos of innumerable dykes (Plate 1B). The concentration and regularity of the dykes increase in the area of Knotty Ridge, where parallel north-south lineations dominate the geology (Fig. 5a). Dyke counts along A-A and B-B of Fig. 4 revealed no country rocks, in spite of exposure being greater than 50%. More than 250 dykes were counted in the 500m of A-A, and nearly 800 in the 1.5km of B-B (Fig. 5b); the lowest elevation of A-A is just under 400m.

FIGURE 5:

5a: Distribution of dykes in the north-eastern volcano. Main boundaries as for Fig. 4.

South-west of dashed line R-R individual dykes are shown. North-east and east of R-R dyke distribution is shown by the trend of the lines, approximate concentration by its thickness. Those dykes without dip values are largely sub-vertical.

Inside dashed line e-e dyke intensity is so great that no country rock was seen; exposures of basal breccias increase markedly outside this line.

5b: Histogram showing dyke trends compiled from count along B-B of Fig. 4. The height of the columns is a linear measurement of thickness of dykes (not numbers) in a given direction. The scale is $\frac{1}{2}$ that of Fig. 9 constructed for dyke swarms in the south-western volcano.

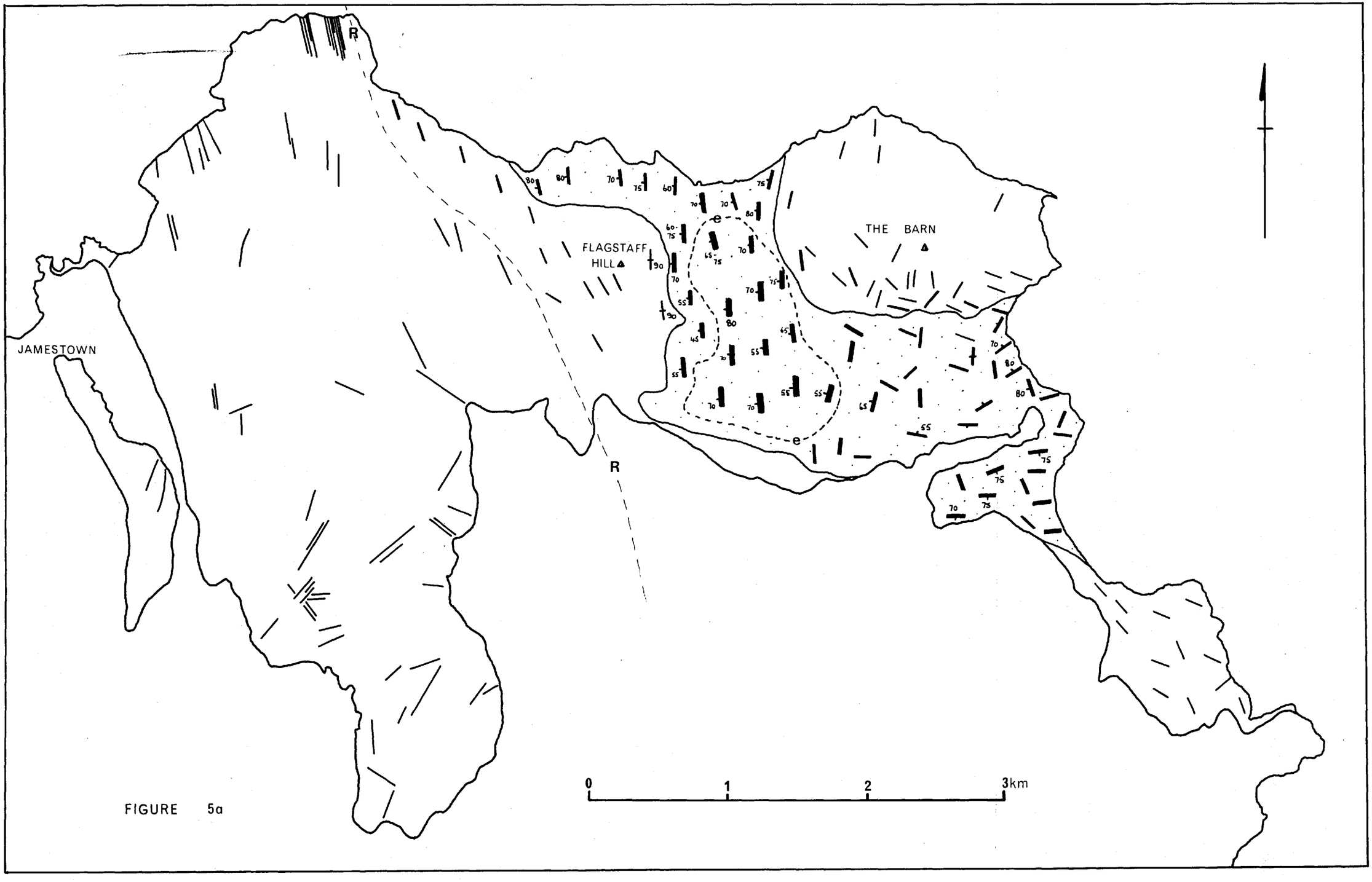

FIGURE 5a

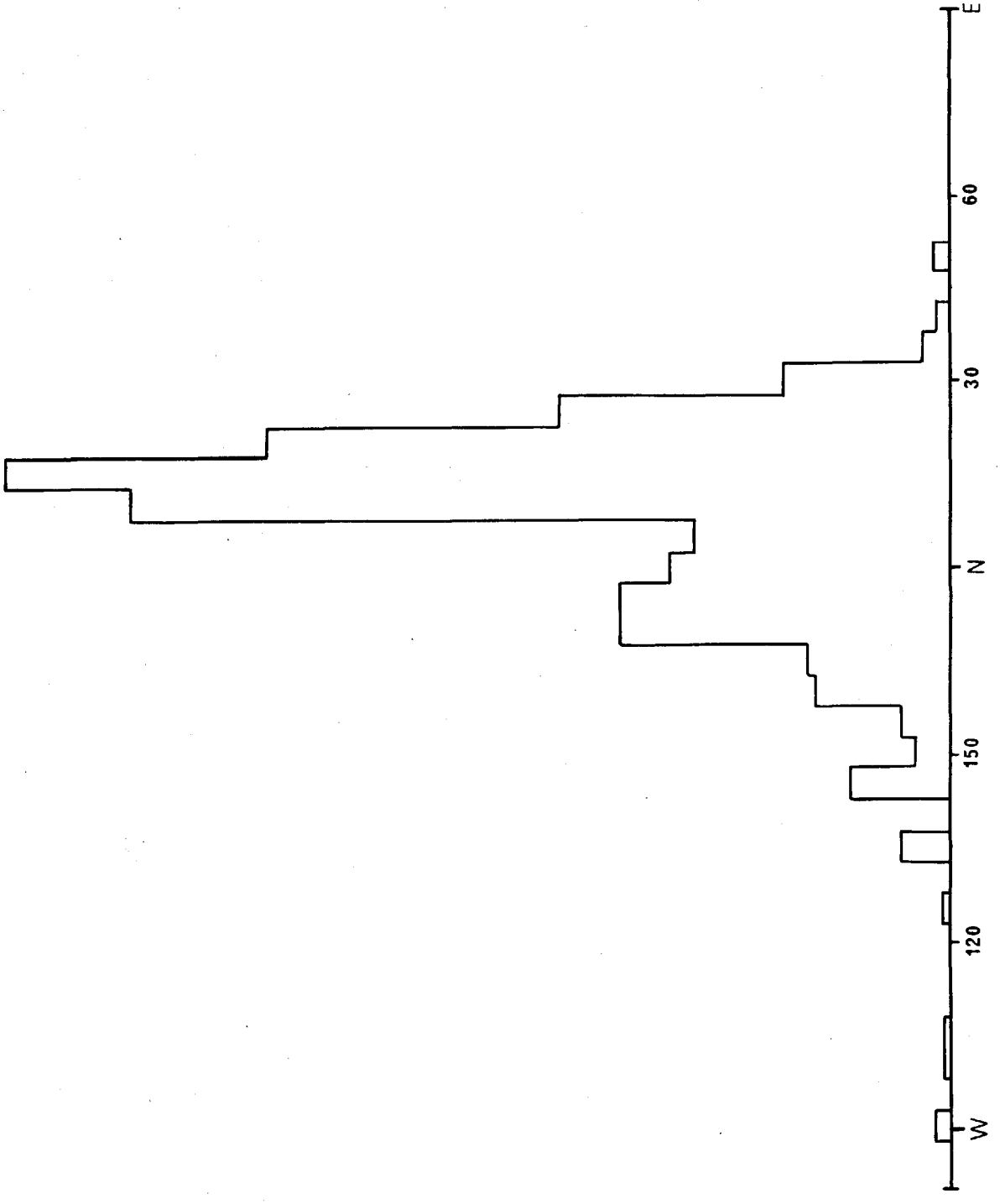

FIGURE 5b

Since the shield-forming extrusives are fed through fissures, it is not surprising to find the number of dykes decreasing with increasing elevation. This decrease is best seen in the extrusives on the south face of The Barn, but a similar type of decrease may well occur within the basal breccias. The most significant aspect of the vertical decrease in numbers of dykes is the very rapid reduction in numbers between the transition sone (or shield-forming rocks where the transition zone is not developed) and the basal breccias. This is best seen in the north-east face of Flagstaff Hill, and the north-west and south-west faces of The Barn (Plate 3): both areas are close to the maximum dyke concentration yet numbers of dykes below the boundaries shown in Fig. 4 are certainly more than ten times the numbers above the transition. This abrupt decrease is seen in all areas and is especially well marked at some distance from the Knotty Ridge dyke concentration.

Dykes are represented by a large variety of petrographic types but large numbers are altered to assemblages of chlorites + carbonate. Some of the dykes are doleritic, a texture virtually unknown to dykes in the south-western volcano. Only one dyke of intermediate composition was seen (1m thick); and one in which the groundmass is totally altered contains the only amphibole phenocrysts whithout reaction rims seen on the island. Highly porphyritic ankaramitic varieties occur (see Section III - 3b), but their numbers are less common than comparable varieties in the south-western volcano.

Dykes cutting the basal breccias belong to two distinct physical types: either they are regular and comparable to dykes seen elsewhere on the island, or they are thin, irregular, sinuous, highly altered with thin glassy (0.5-0.8cm wide) margins (Plate 1C). In many ways the dyke swarm of the

central area of the north-eastern volcano differs from the central swarm of the south-western shield:

(i) Although the north-eastern volcano is much smaller volumetrically, the number of dykes exposed in the central regions is far larger than in the south-western shield which is similarly deeply eroded. Very high dyke concentrations extend over an area slightly larger in the north-east than they do in the south-western volcano (Fig. 5a and Encl. 4).

(ii) Although a north-south trend is pronounced (near Knotty Ridge) and other trends are obvious (Fig. 5a), the dyke swarm lacks the marked regularity of that of the major shield. Cross-cutting relationships are far more numerous, and irregular sinuous dykes and bulbous, irregular apophyses, not uncommon in the north-east, are not seen in the south-western volcano.

(iii) In the south-western volcano the vertical decrease in the numbers of dykes is gradual - contours of the major swarm in Sandy Bay would probably present an elongate, domed surface in three dimensions. In the north-eastern volcano the number of dykes cutting the basal breccias is greater by a factor of more than ten than the numbers seen cutting the lowest levels of the shield-forming extrusives. Irregular sinuous dykes, abundant within the basal breccias, are not seen in the overlying rocks (Plate 1C).

(iv) A large number of the dykes cutting the basal breccias have glassy margins 0.5-0.8cm wide. No dyke with glassy margins was seen in the swarms of the south-western volcano, or in rocks above the breccias in the north-east.

(v) Dykes in both areas redden subaerial pyroclastics that they cut. No dyke has affected the colouration of the basal breccias, not even very thick dykes cutting dominantly fine material.

In the north-eastern volcano many of the more regular dykes, with dominant north-south orientation in the Knotty Ridge area, are believed to be feeder dykes for the shield-forming subaerial extrusives. It is believed that a systematic study of the dykes without glassy margins would show a more regular distribution pattern, more tightly concentrated about Knotty Ridge.

5. Stratigraphic Relationships and Origin of the Basal Breccias.

The contacts between the basal breccias and the overlying rocks are inaccessible or obscured by scree, and observations could only be made from a distance. In areas south of Flagstaff alteration of all rocks is intense and all contact relationships are obscured. Elsewhere, the following points apply to the 'contact':

(i) There is a very abrupt decrease in numbers of dykes above the basal breccias.

(ii) The entire appearance of the rocks changes; below, the rocks are overall brown and brown-yellow, above the contact, reds, purples and greys are typical. The chaotic jumble of the areas of basal breccias contrasts strongly with the regular nature of the overlying rocks.

(iii) Shield-forming rocks display a continuity with the 'transition rocks'. Dykes cutting these latter are no more numerous than in the shield-forming rocks.

(iv) The top surface of the basal breccias is regularly contoured except in one locality WNW of Flagstaff, where a 100m vertical contact is exposed and in Turks Cap Bay (by extrapolation only). The whole mass forms a "dome", elongate north-south, the radial dip of the contact rarely exceeding 20°.

The very abrupt decrease in numbers of dykes at the contact of the basal breccias with predominantly pyroclastics of the lower shield-forming rocks can only reasonably be interpreted as reflecting a major unconformity. The marked differences in lithology reflect a fundamental difference in origins of rocks above and below the unconformity.

The 'transition' rocks are certainly subaerial in part (e.g. the scoria cone in the SW face of The Barn, and the red and purple breccias beneath Flagstaff). The yellow fragmental rocks towards Prosperous Bay and in the south-east face of The Barn may be vitric tuffs of phreatic origin. The rocks described from Turk's Cap Bay may combine primary subaerial material with earlier fragments of basal breccias and intrusives (dykes and the trachyte) possibly derived in part by phreatic activity. These latter groups of 'transition' rocks probably reflect activity close to sea level.

The unique characteristics of the basal breccias, and in particular the widespread chloritic alteration believed to reflect the original presence of abundant glass, suggest that these rocks may be submarine in origin. This inference is strongly supported by the characteristics of the dykes which intrude them which with their glassy margins and absence of contact effects, would appear to have been emplaced in a saturated environment.

If the basal breccias are submarine, and the evidence strongly supports this, some explanation must account for their maximum elevation of 400m O.D.. The contact with overlying subaerial rocks is quite regular in exposed sections, all of which are sub-radial to the "dome" - i.e. the possibility of concentric topographic irregularities is not ruled out. This contact is an erosional unconformity, and while such regularity would not be expected of sub-aerial erosion,

the sub-aerial origin of the overlying shield suggests that this is a possibility.

The basal breccias have been uplifted through a vertical height of not less than 400m. While the high angles of dip of the shield in The Barn and near Flagstaff are readily explained as primary depositional features, the possibility of minor uplift of the breccias during formation of the sub-aerial shield cannot be completely ruled out. If there was uplift during this time it was by equivalent amounts over the whole volcano, as the dips of King and Queen Rocks are comparable to those in the north. The lack of information concerning the basal breccia/shield boundary makes definite interpretation of the time of uplift impossible. That the largest part of the uplift occurred before formation of the shield is believed to be a reasonable hypothesis.

6. The Shield-Forming Rocks.

The rocks forming the main shield of the north-eastern volcano are sub-aerial basaltic pyroclastics and lava flows. The bulk of the rocks have been extruded from a fissure system in the Knotty Ridge area, and parasitic activity is markedly subordinate. The volcano when complete would have formed a relatively steep sided shield, 15° on all sides except in the north-eastern quadrant where dips are approximately 10°, with a maximum diameter of about 9km and a maximum elevation of between 1200 and 1300m above sea-level. The shield was only moderately eroded before partial burial beneath the flanks of the south-western volcano. Before flooding by flows of the upper shield series however, a thickness of up to 600m of the shield had been removed in the central and southern areas.

At their maximum development the shield-forming extrusives attained a thickness of about 800m. The attitude of the flows exposed in the west side of Bunker's Hill suggests a possible slight movement of the centre of eruption with time in a northerly direction. The flows of Ruperts Hill and those to the north-west appear to rest on a marked disconformity which probably reflects this northerly shift. Numerous small-scale unconformities occur in the shield-forming rocks, but only one major erosional break is apparent in the succession. On the east side of Rupert's Valley, and west of Flagstaff Hill relic patches of basaltic agglomerate and scoriaceous flows rest at high angles on eroded surfaces of the underlying flows (Fig. 4).

In the area of The Barn and Flagstaff Hill the lowest shield-forming rocks are red, sub-aerial, more or less well bedded pyroclastics up to 100m thick. The scoria is coarse, and contains large bombs and numerous compact blocks. In the western face ofThe Barn blocks up to 3m across occur, but the pyroclastics are less coarse on Flagstaff Hill. Rare, very scoriaceous interbedded flows increase in abundance upwards in the succession, becoming more regular, somewhat less vesicular and scoriaceous, and eventually dominate the section. Widespread pyroclastics at equivalent levels in the Flagstaff Hill section are overall finer grained and have lower angles of dip than those of The Barn. This assymmetry probably reflects a combination of the early eruptive zone being closer to The Barn, and slight wind sorting. North-westerly away from this central area the thickness of the lowest, and later interbedded, pyroclastics decreases. Similarly in Prosperous Bay, only a few metres of scoria separate the 'boulder beds' from the early scoriaceous vesicular flows, and even this shows a south-easterly decrease in thickness. Interbedded pyroclastics in the lava pile at

Prosperous Bay Beach are markedly less abundant than near Flagstaff or even on Sugarloaf Hill.

The interpretation of the high angle dips of The Barn as the result of tilting (Daly, 1927) may have been based in part on the interpretation that the mass consisted largely of flows. Much of the lower succession however, consists of more or less well-bedded pyroclastics, and the interbedded thin scoriaceous flows retain the high angle of dip (approx. 30-35°). This may be compared with the late basaltic scoriaceous flows and agglomerates, exposed in Rupert's Valley, which dip regularly on an erosion surface at 30-40° (see above, and Fig. 4). However, higher in The Barn succession, with more numerous flows, the dip decreases fairly regularly to 12-15° at the top. The Barn is further complicated by the existence of patches of locally derived pyroclastics which add to the irregular appearance.

The present erosional configuration of the shield means that the higher levels of the succession are also the furthest from the centre. This accounts in part for the apparent increase in regularity of the flows, and decrease in amount of interbedded pyroclastics away from the central region. After the initial essentially explosive activity however, the eruptions became less violent, but many of the flows high in the succession are separated by a few centimetres of interbedded fine ash. In Rupert's Valley the top 350m of the succession exhibit a decrease in interbedded pyroclastic material with increasing height in the lava pile.

The lava flows are usually thin (1-4m) and vesicular, and almost invariably scoriaceous. The basal scoriaceous part of the flow is usually 10-20cm thick, but the scoriaceous top may constitute up to 50% of the flow thickness. In thick flows the scoriaceous top may be cut by lava dykes

and irregular apophyses from the more massive part of the flow. The interbedded pyroclastics are usually of well-bedded, fine basaltic lapilli.

In the valley south of Sugarloaf Hill the stream is cut for a distance of several hundred metres into a group of thin pahoehoe flow units, of fine-grained feldsparphyric basalt. The flow contains minute spherical vesicles and strongly orientated feldspars. In bulbous, entrail lava the vesicles are drawn out round the bulges, parallel to the flow direction. Ropes may develop on the bulges at right angles to the flow direction, and again the vesicles are drawn out in the direction of flow.

Petrographically the lavas are very variable; all major silicates and Fe-Ti oxides may exist as phenocrysts in porphyritic flows (see Section VI). In the head of Rupert's Valley (east side of Bunker's Hill) the number of porphyritic pyroxene-rich flows decreases upwards in the succession. Similar porphyritic flows occur higher up as single flows, but as singles flows or in isolated groups. Although ankaramitic dykes are encountered, very crystal-rich accumulate flows similar to those of the south-western volcano do not occur. High in this succession in the Jamestown area numerous trachybasaltic flows are recognizable by their purple sheen produced by flow oriented feldspars.

The relics of late basaltic rocks exposed in Rupert's Valley and west-north-west of Flagstaff (Fig. 4) are composed largely of coarse vesicular agglomerates interbedded with thin scoriaceous flows. The material is obviously very much later than the shield-forming series, but from its distribution little can be deduced about its original extent. It is possible that the patches are of local origin. In the Flagstaff area a number of dykes cutting through the shield-

forming rocks (Fig. 5a) could have readily served as feeders but the area of origin of other patches is more difficult to postulate. Several thin dykes of limited extent occur in the area, even onto the edge of Deadwood Plain, but a potential source in this latter area is obscured under a weathered relic cover of flows from the south-west. The eroded surfaces on which these basaltic, highly vesicular extrusives were deposited show that Rupert's Valley was already deeply incised, and they may well have infilled much of it, possibly blocking it in part to the late intermediate flows of the upper shield series. The existence of this early Rupert's Valley (a sub-radial valley to the south-western volcano) suggests that the south-western shield (main shield stage) was largely completed before the extrusion of the late north-eastern scoriaceous flows.

A single, presumably basaltic, sill is exposed in the cliffs north and east of Sugarloaf (Fig. 4). The sill, up to 5m thick, remains almost perfectly horizontal, is rarely stepped and may cut through flows even if the angular divergence is low.

7. Parasitic Activity.

Parasitic cinder cones are rare in the north-eastern volcano. The positions of exposed cones are shown in Enclosure 5 and their distribution, although irregular, shows an apparent grouping in the Bunker's Hill-Jamestown area, at high levels of the shield-forming flows. An arcuate double intrusion, not related to a parasitic cone, occurs at Prosperous Bay Beach and is described in Section IV.

Most of the cones consist of well-bedded, coarse scoria with larger fragments and frequently striated bombs (up to 1m) usually concentrated in distinct horizons.

Trachybasaltic intrusions and thick local lava flows, associated with two scoria cones on Bunker's Hill (Fig. 4), are described below.

i. The Bunker's Hill centre (Fig. 6).

The scoria cone rests on thin scoriaceous basaltic flows high in the succession of the north-eastern volcano, and is identical to the example described above. All of the ejected material is highly vesicular, the most vesicular bombs often containing olivine phenocrysts. Although much of the cone, especially the eastern side, has been eroded it is probably asymmetrical with finer material to the north-west.

The central part of the cone is composed largely of spatter and is now indurated, possibly as a result of the subsequent intrusion of an irregular fine-grained, purple, trachybasaltic mass through the side of the cone. Initially the cone fractured along a WSW-ENE radius, following the explosive removal of most of the western flank. Upwelling lava forced the fissure open within the limits of the cone (i.e. leaving the underlying flows unaffected) to a width of 50m (Fig. 6), the lava locally sending apophyses into the scoria. Whether or not this mass overflowed to any extent is knot known. The main mass of trachybasalt appears to have upwelled through the side of the cone sending a thick flow more than 1km to the north-west where it appears in an erosional 'window' in James Valley.

Two lava-tube infillings in the north-western flow from Bunker's stand out prominantly, in an area of considerable alteration, in the side of the ridge east of James Valley. The tubes appear to be more complex than those shown by Waters (p354, fig. 2, 1960) in having a lower portion with perfectly circular weak concentric joints superimposed on the stronger radial joints. (The Battery flow exhibits two lava

FIGURE 6:

Geology of the Bunker's Hill parasitic centre - for explanation see text. Note that the trachybasaltic intrusion is not coincident with the estimated centre of the scoria cone.

Figs. 1-4 are a schematic representation of the volcanic history.

1: Initial extrusion of trachybasaltic flow (hachured) from parasitic scoria cone (p) resting on basaltic flows of the north-eastern volcano (n).

2: Burial of partly eroded cone and flow by basalts of the south-western volcano (b).

3: NNW-SSE valley is eroded to expose part of cone before infilling by intermediate flows (i) of the upper shield series of the south-western volcano.

4: Present day schematic cross section showing relics of south-western flows.

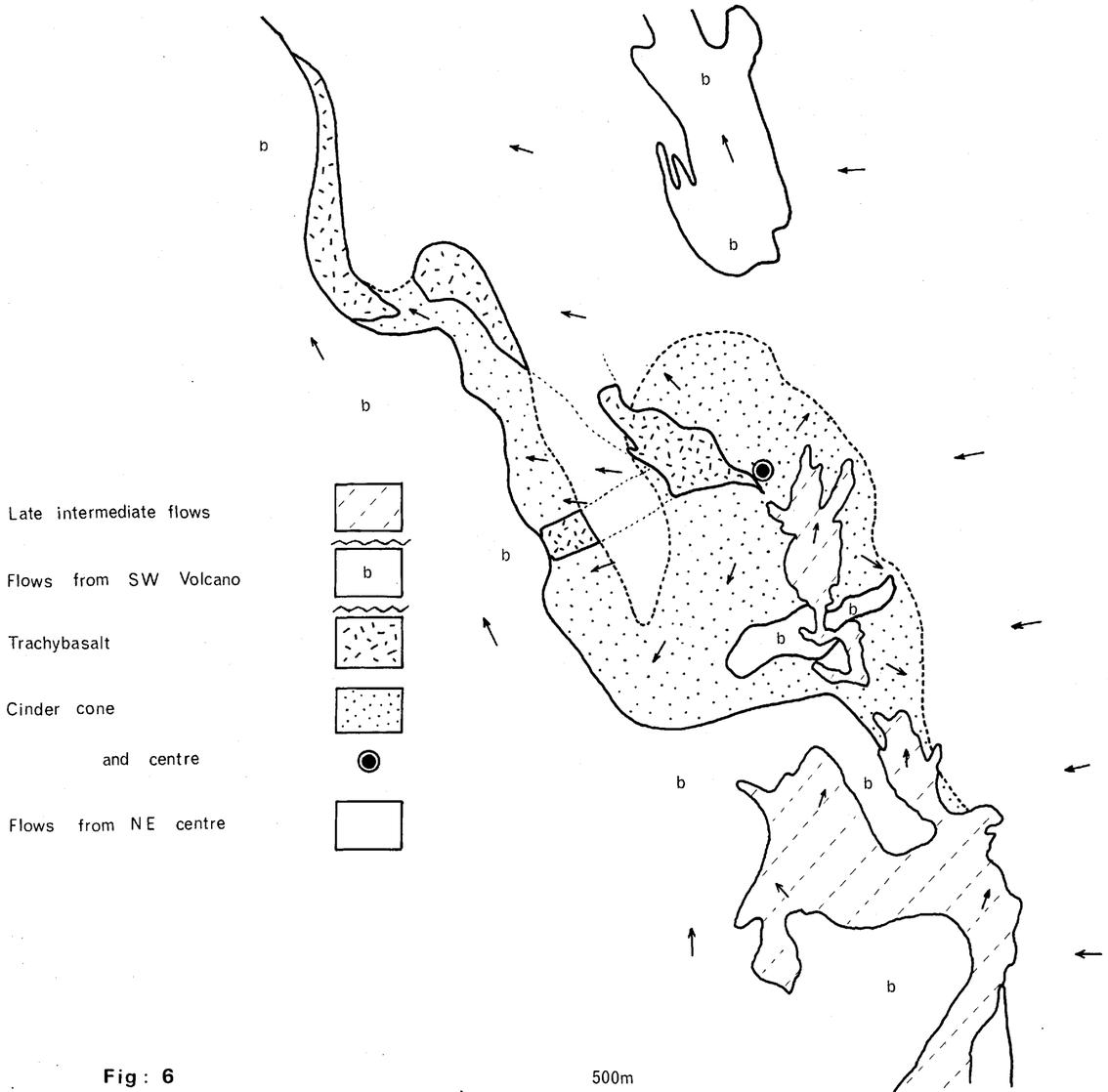
Late intermediate flows
Flows from SW Volcano
Trachybasalt
Cinder cone
and centre
Flows from NE centre
b
500m

Fig : 6

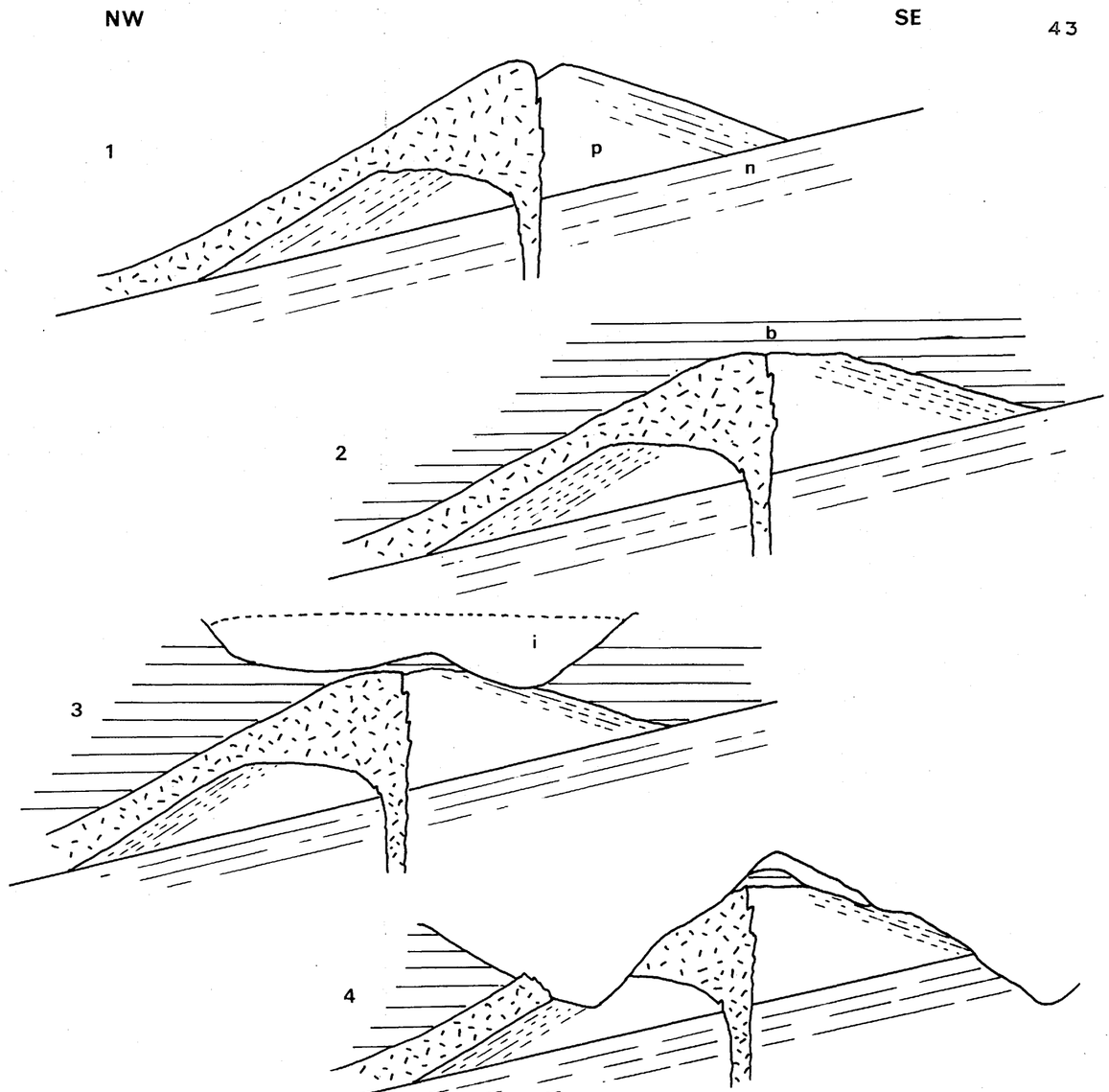
NW
SE
1
p
n
2
b
3
i
4

tube infillings similar to those described by Waters.) The massive tube infillings appear to have withstood alteration - the main part of the flow is largely altered, but may originally have been vesicular and composed of more than one unit.

The Bunker's Hill parasitic centre is later than the bulk of the north-eastern shield-forming lavas, is buried beneath flows from the south-western volcano (main shield series) (Fig. 6b), and is therefore older than the late extrusives of the north-east.

ii. The Battery centre.

The trachybasaltic parasitic centre of the Battery is almost the same size as the Bunker's Hill centre (Fig. 4). It is slightly older than the Bunker's mass, but still occurs in the upper levels of the shield-forming extrusives. The scoria is coarse throughout the cone (which is possibly a doublet) but bombs are quite rare. Several thin spatter flows from the main scoria centre are interbedded with the pyroclastics on the north-east side. The trachybasalt was intruded through the centre of the cone forming a vertical pipe nearly 200m x 100m in cross section. The pipe is irregular on the north-eastern side sending irregular apophyses into the cone - otherwise the contacts are sharply defined. The pipe broke the surface on the west side of the cone, following explosive removal of most of the side, and a flow about 30m thick and up to 250m across was extruded. The extent of the flow is unknown, since the cone and its products are buried initially beneath later shield-forming flows from the north-east, and then by flows from the south-western volcano.

SECTION III

THE SOUTH-WESTERN VOLCANO

1. Introduction

The geological history of this larger volcano is more complex than that of the north-eastern shield. The main dyke swarm of original feeder fissures is preserved in Sandy Bay, and a subsidiary dyke concentration is exposed in Manati Bay. Early products of rhythmic volcanism forming the Lower Shield are preserved in Sandy Bay and the south-west, under a thick sequence of basaltic and trachybasaltic flow groups (the Main Shield). The Upper Shield group, basaltic and later intermediate flows from a centre in the region of the Peaks, is separated from the main shield by a marked unconformity. Products of later local activity are exposed in the east of the island near Stone Tops. After cessation of major activity the shield was intruded by a number of highly alkaline dykes and parasitic masses. A group of local intermediate flows near White Hill may be of comparable age to these intrusions.

The south-western volcano has been divided into the following stratigraphic groups, the extents of which are shown in Fig. 7. (u denotes marked unconformity.)

Late intrusive activity
- u ---- u ------ u ---

East flank activity
-- u --- u ---

Intermediate flows
--- u ---

Upper Shield

Basaltic flows
-- u --- u --- u --

Main Shield

Lower Shield

FIGURE 7:

Main stratigraphic divisions of the south-western volcano. North-eastern shield lies inside the ticked line. Coarse stipple : Lower Shield; blank areas : Main Shield; U : Upper Shield; fine stipple : Eastern flank flows.

FIGURE 7

N
Jamestown
NORTH EASTERN VOLCANO
U
U
U
U
U
U
U
U
U
U
U
SANDY
BAY
Manati
Bay
Km
0
1
2
3

2. The Lower Shield

The oldest parts of the south-western volcano, exposed in the deeply dissected areas of Sandy Bay and the south-west, have been designated the Lower Shield. These rocks are exposed over an area of approximately 7 x 2km and attain a maximum topographic height of 550m at the south end of Hooper's Ridge (Plate 2). Because of widespread detrital cover, alteration, and difficulties of access, rocks forming these areas were believed to be almost entirely pyroclastic (Daly, 1927). The succession however, is represented by four groups of lava flows alternating with four groups of pyroclastics, individual groups being up to 300m thick. The complete succession in the lower shield is given below, and the distribution of the groups is shown in Enclosure 2 (Scale 1 : 7400).

Devil's Cap pyroclastics	
Devil's Hole breccias	
White Rock series	Upper flows (Fairyland pyroclastics) Upper pyroclastics Lower flows Lower pyroclastics
Man o' War flows	Upper basalts Lower porphyritic thick flows
Sandy Bay series	Very variable pyroclastics and some flows
Horse's Head flows	Porphyritic thick basalts Scoricaeous flows

The Sandy Bay series of pyroclastics presented considerable difficulties in interpretation and correlation. Although rocks of the White Rock series overstep the Sandy Bay series, the exact separation of the latter from the Upper pyroclastics is locally very obscure. The correlations of the rocks on the east side of Sandy Bay beneath White Hill are somewhat tentative because the important relationships in

PLATE 2:

Composite photograph of Sandy Bay from ridge below White Hill. Note highly irregular topography (and geology) of the central region and increasing regularity outwards. South-easterly dipping flows of the Horse's Head group are visible at left by Sandy Bay Beach (B) and Horse's Head (A). Compare with Enclosure 2.

C: Frightbus Rock breccia pipe.

D: Asses Ears, and towards camera, Man o' War Roost and southernmost main late highly alkaline dyke (onto foreground ridge).

E: Dyke relic of Lot's Wife (second major dyke).

F: Start of third (northern) major alkaline dyke and below it the area of The Gates of Chaos.

G: The regular flows at the top of the lower shield SSE of Hooper's Rock (I).

H: White Rocks (thick phonolitic-trachytic)dyke.

J: Regular flows at the top of the lower shield in the head of Broad Gut.

K: Lot, elongate nature due to view perpendicular to its elongation.

Note pronounced change in slope from skyline at G above regular topmost lower shield flows to position of thick hedge at extreme right - this denotes the start of the main shield series.

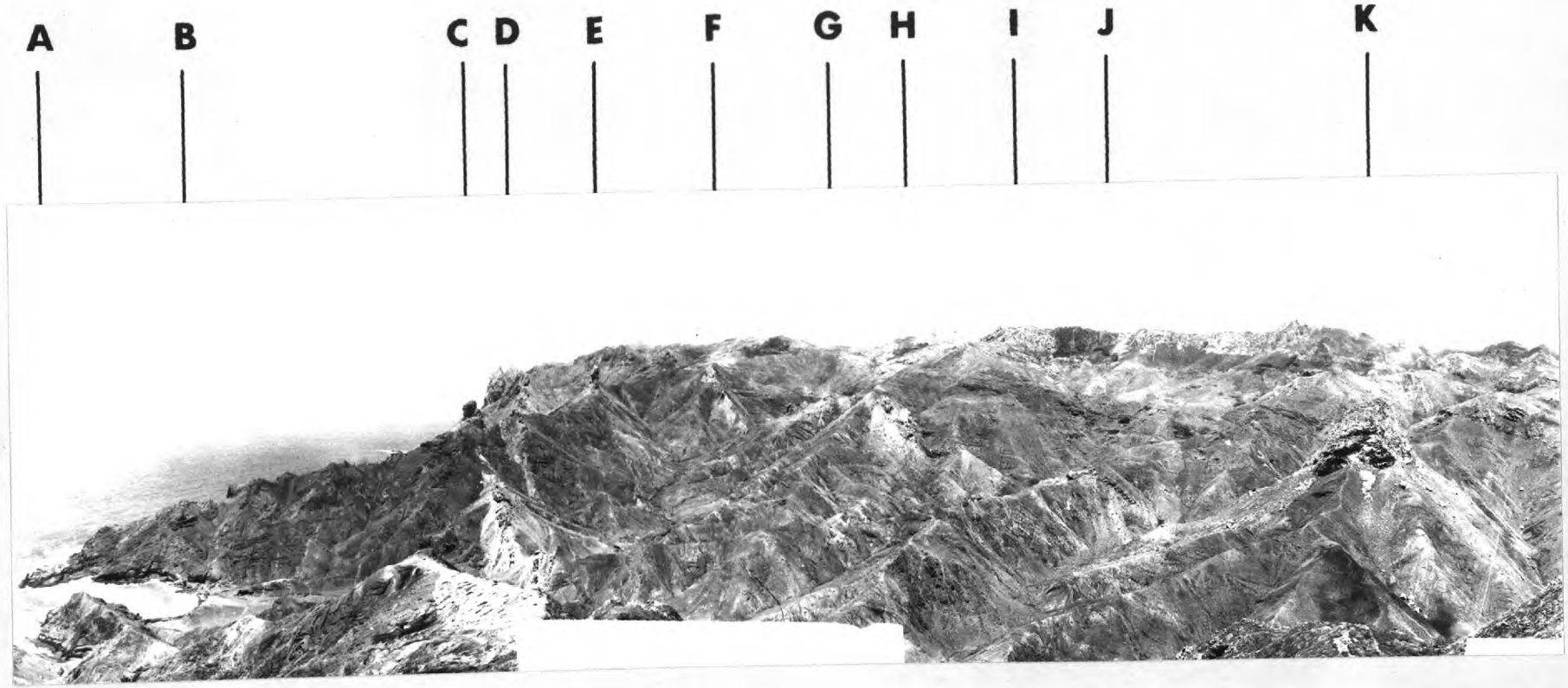

Plate 2

FIGURE 8:

Centres of effusive activity in the Lower Shield of the south-western volcano. Ellipsoidal zones are suggested extrusive centres for flow groups; various circles are estimated centres of scoria and tiff cones. Stippled pipes of Frightbus Rock and the Niggerhead are explained in the text.

LOWER SHIELD –

CENTRES OF ACTIVITY

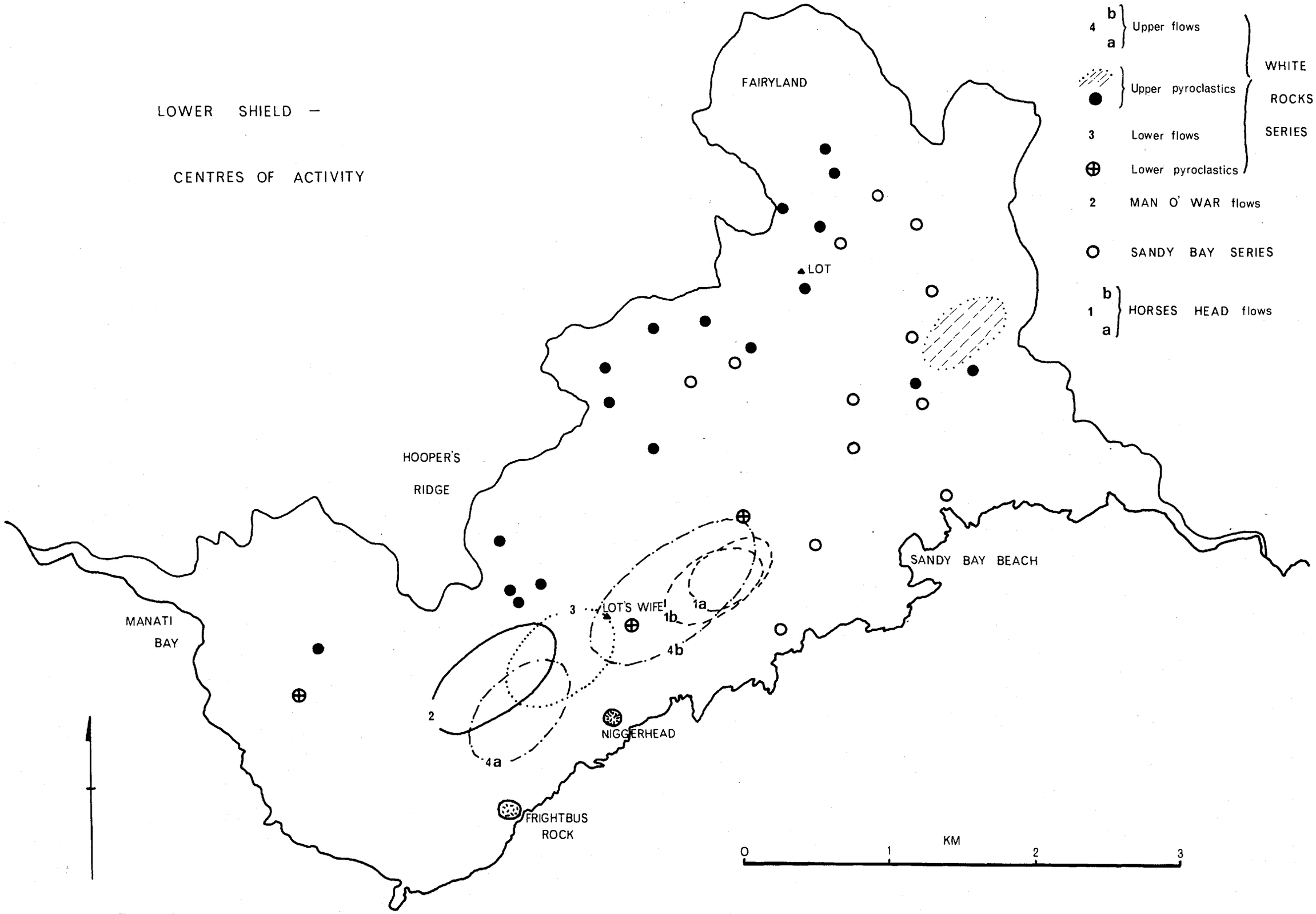

Fig : 8

the Riding Stones Hill area are obscured by the later intrusion.

The late, highly alkaline intrusive rocks have been included in Enclosure 2 to demonstrate their complexity at this larger scale.

a. Horse's Head flows.

The oldest exposed rocks of the south-west volcano consist of thin scoriaceous vesicular basalts. The rocks vary from fine-grained olivine basalts to porphyritic pyroxene-olivine basalts, and are more or less altered, with their vesicles containing zeolites. In the immediate region of Horse's Head the rocks, and the scenery are virtually identical to that part of the north-east shield exposed between Prosperous Bay Beach and the lower parts of King and Queen Rocks.

The vesicular flows are between 1 and 2m thick, but more massive porphyritic flows may be twice this value. East of Sandy Bay Beach the flows are more vesicular, and a higher proportion of the flow consists of scoriaceous material. Some thin ash bands occur, especially in the higher parts of the succession, and westwards their thickness increases slightly.

The upper, thick (up to 15m), black, porphyritic pyroxene-olivine basalts probably rest on an unconformable surface cut into the lower flows. Although these flows are principally developed along the coast to the west (towards the Chimney), they may have extended northwards into Broad Gut (Encl. 2), where some of the flows are highly porphyritic. Both groups of flows apparently originated from an area east of Lot's Wife (Fig. 8), close to where the maximum thickness is preserved to-day (160m mainly of the lower group). The flows probably formed a gently dipping "shield" elongate north-east - south-west.

b. The Sandy Bay series.

Pyroclastics of the Sandy Bay series are mainly products of a number of individual basaltic scoria cones, resting on a surface extensively eroded into the Horse's Head flows. Thin basaltic flows occur, especially in the east of Sandy Bay, and pyroclastics of wide extent occur in the higher parts of the series. Several of the individual cones are well preserved, but alteration in the area of Lot and Broad Gut has largely obscured relationships in the younger parts of the group.

Ejected material from 13 individual scoria cones has been detected; the centres of 9 may be reconstructed with some certainty, but the other 4 are badly eroded and only approximate centres are suggested (Fig. 8). The cones reflect variations of two types during their activity:

(i) Initial yellow, orange and red scoria becomes increasingly coarse upwards into red and purple material.

(ii) Initial coarse scoria becomes finer with time.

In most cases bombs of coarse spatter are restricted to distinct horizons; bombs are frequently spindled and very rarely exceed 0.5m in diameter. Pre-existing basaltic fragments were found in only one cone. Towards the tops of several of the cones, thin, highly scoriaceous spatter flows are developed. Vesicles in spatter flows and scoria fragments are frequently filled with zeolites.

In the north and north-west of the area a medium to coarse orange tuff horizon appears to have been of wide lateral extent, but no traces are found in the south and east.

North-west of Sandy Bay Beach, south-east of Lot, and along the whole eastern side of the exposure of the Sandy Bay series, thin, scoriaceous flows occur (Encl. 2). While certain thick flows may be of local origin, the attitudes of

the more extensive flows suggest they originated from an area near Lot's Wife. Normally only thin relics are preserved, except in the eastern wall, and groups of flows frequently overstep the scoria cones - especially south of Riding Stone Hill. These flows probably belong to one or both of the groups of the Upper Man o' War flows or Lower White Rocks flows, and have been included in Enclosure 2 with the Sandy Bay series because of the difficulty of identifying relics with specific groups. North-west of Sandy Bay Beach the flows are thin and scoriaceous, and locally may be porphyritic - this could equate them with the upper parts of the Man o' War flows. However, the elevation that the flows achieve in the east wall of Sandy Bay suggests closer correlation of these with the Lower White Rocks flow group (see below).

In Broad Gut an irregular porphyritic basaltic mass is intruded into the pyroclastics. The mass is about 100m across and over 500m long (Encl. 2); the contacts are sub-vertical, but the western contacts dip inwards at angles of 45°- 75° and in the north the roof is approximately horizontal.

Although the intrusion reddens the pyroclastics there is no sign of uplift. The mass is cut by approximately the same number of dykes that cut the host pyroclastics, so it is believed to be only slightly younger than them. The mass is of uncertain origin but may be associated with local expansion of a dyke (see also Section IV, 1a).

c. Man o' War flows.

Lower flows of this group are black, porphyritic, pyroxene-olivine basalts, ranging in thickness from less than 4m to more than 15m, with only thin scoriaceous tops and bottoms. The rocks are often very highly altered, initially forming a yellow-black friable material rich in pyroxene crystals, and eventually producing a yellow mud. West of the

Asses Ears this alteration is spheroidal, and relatively unaltered black spheroids, more than 4m in diameter, are preserved in thick masses of yellow clayey "sand". In Devil's Hole and around Frightbus Rock the flows are so intensely altered that until correlation was possible with the relics west of the Asses Ears and below Lot's Wife, the material was mapped as altered pyroclastics.

The upper lava flows preserved in Broad Gut and east of Lot's Wife, are usually thin, highly vesicular, and scoriaceous, contrasting markedly with their lower members. Many of them are porphyritic, but overall lighter in colour than the lower flows, although occasional very thick porphyritic flows do occur. Throughout the entire series the percentage of porphyritic olivine and pyroxene decreases slightly with time, but as a group the whole succession is markedly basic. Several thin ash horizons occur throughout both groups, and close to the original centre of activity coarse scoria fragments are commonly found, separating the thick porphyritic flows.

Most of the flows of this group originated from an elongate area around Blue Point (Fig. 8). Initially the lower groups formed a very flat "shield" (with dips of 3 - 8°), over 300m thick, apparently built outside the area of the earlier pyroclastic centres. As this "shield" grew the flows progressively overstepped the cones of the Sandy Bay series west of Horse's Head and may have extended eastwards across the eroded relics of the scoria cones. The upper, thinner flows were deflected northwards into the Broad Gut region but probably did not extend into the areas of scoria cones to the north-east. The upper flow group is mainly developed in the central and north-eastern areas. It is possible that the active zone of extrusion moved north-easterly causing the upper flows to bank dominantly on one flank of the lower shield.

The full extent of the shield at this time is unknown, but flows extend northerly into the Gates of Chaos (200m O.D.), and to the west many of the small islets around Speery are probably formed of rocks of this group. The Black Rocks are composed of a complex of basic dykes (one of which is more than 50m thick) trending north-west - south-east, with screens of these porphyritic basalts between them. From the reconstructed shape of the mass it is quite probable that the irregularity in the 50 fathom line south-west of Speery (Fig. 3) is a reflection of the development of these lower flows.

The later flows amount to a maximum of about 200m in total thickness. Largely developed on one flank they added little to the maximum height of the Man o' War "shield", but extended it by several kilometres over the Sandy Bay pyroclastics.

d. Beach trachybasalts.

A number of relic thick masses of basaltic and intermediate rocks are exposed in the vicinity of Sandy Bay Beach (Encl. 2). The masses are 15-60m thick, and exhibit broad sub-vertical joints, and laminar joints in units 0.5 - 1m thick parallel to the base of the unit. Flow texture in feldspars may be visible in hand specimen, and one flow locally exhibits tightly folded banding.

The rocks are variable petrochemically, and have originated from a number of separate sources. West of Horse's Head the flows are relatively regular and are believed to result from an irregular intrusive sheet breaking the surface. Some irregular, altered relic trachyandesitic flows from local dyke feeders are almost certainly later than the more regular flows. The mass south of Lot is a thick trachyandesite with its vertical feeder dyke preserved, and originally

almost certainly was intruded as a very high-level sheet. North and east of Sandy Bay Beach the rocks are trachybasaltic and basaltic flows with thin scoriaceous bases, their jointing suggesting local ponding of the lava.

All of the masses rest on more or less eroded surfaces cut into the Sandy Bay series and Horse's Head group. North-east of the Beach one relic may lie within the thin flows high in the Sandy Bay series, which have been tentatively correlated with the Lower White Rocks series. North-west of the Beach the flows overlie lavas equated with the Upper Man o' War group.

The masses are cut by dykes comparable in number to those cutting the underlying rocks. Almost certainly some of them are contemporaneous with the scoria cones of the Sandy Bay series, and are locally derived (cf. flows of the early High Hill centres, this section, 3c(i)). The others are very difficult to place in time, but are believed to have been extruded sporadically, later than the Sandy Bay series, infilling former valleys eroded into and through the cones. Flows of this type would have served to level off the topography of the Sandy Bay group, and may account in part for the regularity of distribution of overlying groups of extrusives.

e. The White Rocks series.

This complex series of extrusives is especially well exposed in the White Rocks area where the inter-relationships are most clear, but thick deposits occur from below White Hill in the east to west of Manati Bay (Encl. 2). The series is divided into four groups, the lower two of which form discrete pyroclastic and flow groups. The upper pyroclastic group is complex, locally containing lava flows. The upper flow group, like the lower flow group, is distinct, although products of local pyroclastic centres are represented at several localities.

(i) Lower pyroclastics.

Pyroclastics of this group form an excellent marker horizon from Manati Bay to Broad Gut. Scoria and fine ash appear to be products of one very large cone west of the Gates of Chaos, and two smaller cones near Lot's Wife, and on the north side of Devil's Hole (Fig. 8).

The main cone, originally between 300-400m high, is overall finer grained than other scoria cones. Early products were of purple-red basaltic scoria and some spatter, with bombs to 0.7m - however, the bulk of the cone was formed by orange lapilli, 1-2cm in diameter, and yellow ash. Scoria fragments to 20cm occur in discrete horizons up to 1m thick. The pyroclastics thin rapidly to a thickness of 2-3m, just over 1km west-south-west of the original vent.

Very little of the cone near Lot's Wife is exposed. Although much smaller than the main cone it is similarly composed of coarser early material and later fine yellow ash with thin scoria horizons. The cone north of Devil's Hole is composed of coarse red basaltic scoria and spatter, and is markedly asymmetrical, with finer material developed mainly in the north-west. Before burial under later lavas the cones were eroded mainly in the south, and the distribution of the products may reflect conditions of dominant south-east winds carrying the fine ash north-westerly, possibly with associated breaching of the cones in the south. Other later cones, notably High Knoll, reflect the strong influences of south-easterly winds in their morphology.

(ii) Lower flow group.

These flows everywhere rest on reddened pyroclastics of the lower group. The flows are thin (1-3m), regular, often highly scoriaceous and vesicular, and rich in secondary zeolites and carbonates. The flows are petrographically very

variable, but largely fine-grained. Feldsparphyric lavas are as common as porphyritic pyroxene-rich varieties. Pyroxene and olivine phenocrysts are smaller and less abundant than in typical porphyritic flows from underlying groups. Thin pyroclastic horizons separate many of the individual lavas.

The flows originated from a source area a little to the west of Lot's Wife (Fig. 8), and overstep the White Rocks cinder cones. They have a maximum thickness of more than 100m and extended the lower shield to the north and west. In the north-east they are banked up against pyroclastic centres of the Sandy Bay series, but it is probable that they extended through the eroded area of scoria cones on the east side of Sandy Bay (see above).

The island at the end of this stage of activity would have had a broad flattish shield-like form, with a less regular area of eroded scoria mounds and irregular flows in the north-eastern and central parts. The surface of the massive Man o' War flows in the south and south-west was little eroded, and provided a substantial area of high ground, preventing the extension of the White Rocks flows to this part of the early shield.

(iii) Upper pyroclastics.

Rocks of this group are exposed in an almost unbroken sequence in the ridges from Manati Bay to Lot and along the full length of the east side of Sandy Bay (Encl. 2). Most of the rocks are pyroclastics of local origin, and can be correlated with a number of scoria cones (Fig. 8). Groups of flows of limited extent occur in the headwaters of Broad Gut, and north-west of Lot's Wife; they become dominant south of White Hill. The scoria cones are all apparently basaltic and were frequently eroded before partial or complete burial by later adjacent cones and younger flows.

Smaller cones frequently show flattening of ejected blocks, a phenomenon seemingly restricted to smaller cones throughout the island. Larger cones are similar to those described in the Sandy Bay series, with layers of coarse bombs in overall finer scoria, with or without development of rare irregular spatter flows. An unusual character of the larger cones is the occurrence of rounded bombs (to 0.7m) with no associated sag into the finer matrix. These probably represent large ejected fragments that have rolled for variable distances down the cone. Original spindling may be preserved over parts of the rim, which is overall more compact than the central parts.

In spite of the incomplete exposure of the series the cones appear to be concentrated in a zone, elongate north-east - south-west, north of the centres of earlier activity (Fig. 8).

The higher levels of the sequence are characterized by orange and yellow pyroclastics of widespread extent. These are probably derived from several different centres, and may be of slightly different ages. In the south-west a coarse, bedded, orange scoria horizon thins easterly towards Lot's Wife. A second horizon east of Lot thins westerly and north-easterly. A fine, well bedded, orange lapilli tuff exposed in the east wall of Sandy Bay is probably continuous northwards under the Fairyland pyroclastics, and thickens and coarsens southwards into well bedded, cemented, coarse orange agglomerate.

Lava flows are developed within the upper pyroclastic group, but even the lowest flows rest on thin pyroclastics. The flows appear to infill valleys between scoria cones, and although locally quite thick they are of limited extent. In the east side of Sandy Bay the relationship of the mapped

equivalent of the upper pyroclastics to the material elsewhere is obscure. In the lower part of this section local coarse basaltic scoria cones rest on the flows described in the Sandy Bay series. These are overlain to the south by more regular pyroclastics. Coarse agglomerates overlie these and form much of the area south-east of Riding Stones Hill, the material thinning rapidly southwards. Above these pyroclastics are a series of well bedded scoriaceous units (about 1m or less thick) of highly vesicular olivine basalt which southwards appear to be equivalent to thin scoriaceous flows. Blocks of grey shimmering basalt or trachybasalt in the lower levels appear to be derived from the flows of the Sandy Bay series, or perhaps the Beach flows. The relationship of this material northwards is obscured by alteration and vegetation cover, but it is believed to be older than the Fairyland pyroclastics.

The distribution of these orange pyroclastics and the occurrence of highly scoriaceous flow units in the east wall of the Bay suggest that a distinct (probably) fissure centre was active during the late stages of this upper pyroclastic group. The probable location of this eruptive centre is shown in Figure 8, about 1km north of Sandy Bay Beach.

The Fairyland pyroclastics attain distinction because of their crystal tuffs, rich in perfectly euhedral augites up to 5cm long. Interpretation of the structure of Fairyland and the area to the east is complicated by vegetation cover and the inaccessibility of most of the cliff faces. The group is made up dominantly of coarse basaltic crystal rich agglomerates, possibly from more than one centre; these are best exposed in Coles Rock and in the valley north-east of Riding Stones Hill. The area is further complicated by the occurrence of a number of intermediate intrusive sheets.

One is shown in Enclosure 2, at Fairyland, and another occurs on the ridge 300m south. Others are exposed in Coles Rock, and in the cliffs to the east, and possibly in the south-eastern part of Rock Mount. It is possible that these last four sheets are in fact parts of one continuous arcuate system, curving from north of Lot through Fairyland to west of Riding Stones Hill. The sheets are on average 10-25m thick, and locally uplift the bedded agglomerate to angles of 60°. The highly indurated nature of the agglomerates may be in part due to these intrusions. The lack of interpretation of the structure of this area is greatly regretted.

(iv) Upper lava flows.

The upper flows are divisible into two groups of approximately equivalent thickness. The younger group originated from a source area north-east of the older centre (Fig. 8). The flows overstep the eroded surface of the upper pyroclastics and locally rest on the lower flow group of the White Rocks series (Encl. 2). Although minor valley infillings are obvious this surface is fairly regular, possibly reflecting a marked period of quiescence. Scoria cones are developed within the flow sequence, causing slight banking of the flows. These cones were partially eroded prior to the extrusion of later flows of the same group. Their importance is related to the development of the Devil's Hole and Devil's Cap fragmental rocks.

The flows throughout the group are thin, scoriaceous, vesicular basalts (and probably trachybasalts) with or without phenocrystal olivine and pyroxene - individual flows may be as little as 0.7m thick, of which 60-70% is scoriaceous material. Thin, fine-grained tuff horizons are frequently interbedded with the flows. In the most southerly part of this exposure irregular thin flows almost entirely of scoriaceous material are developed. The group has a maximum thickness of

150m (in Broad Gut), and served to smooth out the surface of the shield in the west and north. The flows were held back by the scoria cone complex of Fairyland in the north-east and the less eroded pyroclastics in the east and south-east.

f. (i) Devil's Hole breccias.

These highly altered fragmental deposits fill a saucer-shaped depression originally cut into the centre and south-west flank of the lower shield. The deposit is of composite origin, and varies in thickness from 10m to over 150m. The lowest parts are poorly sorted, very coarse angular breccias which thicken westwards. Locally the deposits contain rounded blocks in a thoroughly altered matrix of comimuted fragments. The rock fragments range from porphyritic olivine-pyroxene basalts to intermediate rocks, possibly with trachytic tendencies. In the east the blocks measure exceptionally up to 3m cubed. Comparison with later breccias suggests they are mainly of scree and detrital origin - certainly less angular blocks increase westerly (downslope). Occasionally a weak lamination is visible, especially to the west, and this increases in the upper part of the deposit. Several fine tuff horizons occur, and below Narrow Ridge irregular 'finger' flows may be developed; it is possible that the breccias are in part caused through local seismic activity. In the western exposures the deposits pass transitionally up into coarse agglomerates, containing lithic blocks up to 1m across. These in turn pass up transitionally into the Devil's Cap pyroclastics; in the east there is a distinct break between the lowest breccias and the overlying well bedded pyroclastics.

(ii) Devil's Cap pyroclastics.

The separation of these from the breccias is largely artificial when considering the deposits as a whole. The deposit, overall orange in colour, shows a progressive

decrease in grain size upwards from the coarsest of the breccias, through coarse agglomerates and tuffs to finer tuffs and ash bands. Lithic fragments include all rock types from porphyritic basalts to trachytes, and there is an apparent decrease in the numbers of intermediate rock types towards the top of the deposit. At Devil's Cap itself the tuff is medium-grained with scoria fragments to 2-3cm, but includes compact lithic fragments of trachyte up to 10cm across. Larger fragments are usually concentrated in layers and lenses, and finer material shows weak wind bedding. The material is largely altered to white or cream bands, which pass up into poorly bedded, finer, red and purple scoria; both types may contain olivine basalt fragments. This primary pale coloured tuff and scoria if not trachytic is almost certainly trachy-andesitic in composition. Rhythmically banded coarser scoria with olivine basalt fragments overlies this, but the uppermost material is a coarse compact lapilli tuff of uncertain composition (it is comparable in grain size, colours and texture to the altered pyroclastics associated with the Old Joan parasitic centres and may be trachybasaltic - see below).

These two fragmental groups are of limited extent in spite of their great local thickness. The local distribution of the breccias, which form a large part of the mass, can be explained, since they are largely detrital. The limited northward extent of the pyroclastics can be best explained if scoria cones within the Upper White Rocks series provided topographically high ground, thus largely restricting their northerly development.

The main interest of the deposits is the occurrence within it of quantities of intermediate and trachytic lithic material. The lithic fragments must have originally formed dykes or flows, but their stage of development is unknown. The occurrence of trachytes in the earliest breccias, the

mixed nature of lithic fragments within a single band, and the compact nature of the trachytes suggest that brecciation of a trachyte vent-dome is unlikely.

Frightbus Rock is the remnant of a coarse breccia vent infilling, south-south-east of the Asses Ears (Fig. 8, Encl. 2). Fragments in the breccia range from rounded to angular, from dust to more than 3m across. The pipe-like mass is almost completely altered to a muddy material, but the rock types certainly range from basalt to intermediate (altered cream coloured fragments may well be trachytic, but trachyandesites alter identically). Further east is a pipe of intermediate composition (the Niggerhead) which, although weakly brecciated at the margins, is essentially massive (Plate 12A).

The local development of the Devil's Hole breccias and Devil's Cap pyroclastics suggests that these two pipes could have acted as feeders for some of the material within the fragmental rocks. However large numbers of intermediate dykes occur throughout the central area as a whole. Certainly from the rocks exposed at present, no intermediate or trachytic extrusives are known earlier than these breccias and tuffs.

3. The Main Shield

The bulk of the Main Shield is made up of basaltic and trachybasaltic lavas from extrusive centres dominantly in Sandy Bay. The series may be divided into a number of groups visible in cliff sections, but impossible to map as specific units. Pyroclastic activity is markedly subordinate in terms of volume, but large numbers of parasitic scoria cones are exposed (Encl. 3).

a. Shield-forming activity.

The top of the Lower Shield was eroded prior to deposition of a fine-grained yellow crystal-tuff which marks the junction between these major divisions of the south-western volcano. This is the only unconformity in the south-west shield, where dykes are seen to terminate below younger rocks (west of Rock Mount). The early flows are thin, vesicular, scoriaceous basalts, overstepping the irregularly mantled surface. These are interbedded with fine to medium grained pyroclastic horizons. The flows pass rapidly upwards into a series of highly porphyritic pyroxene-olivine basalts, often more than 5m thick.

The flows, basalts and trachybasalts, are very variable petrographically, and show most of the flow structures exhibited by the flows of the north-eastern shield. Because of the transgressive nature of the lower flows of the main shield series, correlations around the rim of Sandy Bay proved impossible. North-west of Riding Stones Hill the lowest rocks are dominantly porphyritic basalts, but north of White Hill they are dominantly fine-grained. Porphyritic flows are quite common, but the percentage of pyroxene and olivine phenocrysts is lower than in the accumulate-type basalts of the lower shield and no typical black basalts are developed.

The flows all have scoriaceous tops, and thinner scoriaceous bottoms, with a more or less massive, often weakly vesicular central part. On average a 4m thick flow consists of 20cm of basal scoriaceous material, 2m of massive lava, and 1.8m of scoriaceous top. In cliff sections at Jamestown, Powell's Valley, Thompson's Valley, and Prosperous Bay and Rupert's Bay (in the north-eastern volcano) scoriaceous material forms an average of 50% of the flow thickness.

Locally nearly 70% of flows up to 3m thick is scoriaceous. The proportion of scoriaceous material may decrease slightly towards the central region, but no quantitative counts were made because of lack of extensive vertical sections. Only one flow group (approximately 10m thick) of thin pahoehoe flow units was seen, high in the succession west of Jamestown. Two beautifully preserved lava tubes were seen: on Ladder Hill 200m north-west of the Hospital, and at Half Moon Battery on the west side of Lemon Valley. These tubes are similar to those shown in Wentworth and Macdonald (Fig. 23, p46, 1953) with closely spaced concentric joints and a maximum outer diameter of between three and four metres.

Flows are very variable in thickness from less than 0.5m to nearly 70m where local ponding has occurred. In the ridges near High Peak several flows greater than 30m thick are exposed, and one tuff unit is nearly 40m thick. A large number of minor unconformities occur throughout the shield and the major flow groups seen in cliff sections are separated by more distinct breaks. The total thickness of lavas forming the succession preserved to-day is not less than 800m.

Even high in the succession tuffs of wide lateral extent are commonly interbedded with the flows. Certain of these tuff bands act as marker horizons which can often be traced for hundreds of meters. One of the tuff markers, from the central region, can be shown to coincide with flank activity at the parasitic centre of White Point, but no other horizons were correlated over any large distance. The tuffs are often developed at minor unconformities and more extensively at the breaks between flow groups (see above). The tuffs appear to have preceded the outpourings of lava, since they mantle the overlying erosion surface and their outcrop surfaces are rarely channelled prior to burial by later lava flows.

At Old Joan Hill in the west of the island two trachybasaltic flow domes and their feeders are preserved in the spectacular Man and Horse cliffs. The flat domes are stratigraphically about 550m above the base of the Main Shield series - they were eroded prior to covering by a distinctive thick, well bedded tuff, and later basaltic flows. The feeder dykes (three are visible) range from 10-30m in width, and flare slightly into the base of the domes. At least ten trachybasaltic flows were fed from the area of flow domes, and to the west rest on an irregular surface eroded into the underlying basaltic rocks. At one point an eroded coarse scoria cone lies within this junction. This distinctive flow group, over 100m thick in the cliffs at Tripe Bay, can be traced around into Thompson's Valley. The flows are of comparable age to two very thick trachybasalts (one is approximately 50m thick, though locally is ponded to 135m) which infilled a valley cut into basalts in approximately the present position of Thompson's Valley. These two flows appear to have emanated from the White Point area, but probably were also fed from the feeders of Old Joan Hill.

Several thick trachyandesite flows are exposed within the Main Shield succession. One flow, exposed in the cliffs 1.5km north of Gill Point, continues through Gill Point and forms Shore and George Islands 1km out to sea (Encl. 3). At Gill Point the flow is 125m thick, and 30m is preserved in George Island. Admittedly the flow has been channelled along a former broad valley, but its extent and thickness probably make it one of the most voluminous single flows on the island. A second flow, petrographically comparable, is exposed at about 500m O.D. in the head of Deep Valley, north of Long Range (Encl. 3). The flow is 60m thick here, and dips eastwards at about 6^{o}. The flow is about 1km wide, and rests on a thick orange tuff horizon, just as the

Gill Point flow does. It is quite possible, in terms of attitude, field relations, and petrography, that this is the same flow as that of Gill Point. The flow is not exposed in the Sandy Bay side of the main ridge, and it is possible that the flow is the product of flank eruption from the same source area as that of the upper shield flows.

At Headowain, north-west of High Peak, another trachyandesite flank flow is exposed. The flow is slightly more alkaline than the others (possibly trachytic) and thins out westerly. The flow is badly altered, but the jointing suggests a domed outline close to the vent, where small areas of poorly exposed scoria are preserved. The flow was originally quite broad, and rests relatively conformably on the underlying basalts. It is stratigraphically higher than the Old Joan trachybasalts, but its relation to the age of the Gill Point flow is unknown.

The latest flows of the main shield series are petrographically variable, scoriaceous basalts and trachybasalts, of variable thickness. The trachyandesite flows of the High Peak region may have originated from the central area, and may be placed within these uppermost parts of the Main Shield series. Although highly altered and much eroded, over 50m of trachyandesites are preserved, probably representing three flows.

The attitudes of the flows from the south-west volcano are influenced in the north and east by the north-eastern volcano. At King and Queen Rocks the lavas are diverted through nearly 90°, but the junction is much less obvious around Jamestown. It is difficult to reconstruct the relationships between the main shield series and the north-eastern shield with absolute certainty, because of cover by the extensive upper shield flows. The north-east shield

appears however, to have undergone only moderate erosion before its partial burial. The flanks were buried over 180° of arc (Encl. 3) and the maximum elevation attained by the main shield flows was probably about 600m O.D. west-south-west of Longwood. In Jamestown and Rupert's Valley the junction between the lavas of the two volcanoes is clear cut and regular (Plate 3B). Along the west side of Rupert's Valley the junction is marked by 3-10m of pyroclastics of unknown origin, but in James Valley, although tuffs are extensively developed between flows, the junction is a somewhat irregular surface, the underlying flows dipping westerly and the overlying flows dipping northwards.

b. Feeder dykes.

The feeder dykes for the extrusives of the lower and main shields are inseparable, and the swarms in Sandy Bay must be considered in terms of feeding both of these units. Since no flows in the lower shield appear to have emanated from Manati Bay, the local dyke concentration there is believed to represent a minor source area for flows of the main shield series. The concentration of feeder dykes of the south-west volcano are shown in Enclosure 4 - highly alkaline dykes of the late intrusive phase have been left out of the count ratios. The contoured areas represent the high density centres of dyke injection, the figures being ratios of total thickness of dykes to total thickness of all rocks in the count distances (average 100-200m). If the decimal point is removed the figure is in fact the average percentage of dykes in the area of individual dyke count.

The unusual asymmetry of the Manati Bay concentration is due to the steepness of the ridges to the north and east causing the decrease in the number of dykes with vertical height in the pile to become the dominant feature, not the

PLATE 3:

A: The Barn.

Thick, more or less regular mass of shield-forming extrusives of the north-eastern volcano. Sharp junction at base is unconformable boundary with basal breccias (and intense dyke swarms). Dykes are visible (and quite abundant) in this south face of The Barn, but compare with Plate 1B. Foreground and middle ridges are of highly altered upper shield flows. Note the general lack of vegetation and incipient gullying.

B: The regular nature of the contact between flows of the north-eastern volcano and overlying main shield flows of the south-west, extending from Rupert's Valley (left) round headland to below house nearly into James Valley. Minor unconformities in main shield series are visible. Prominent peak is parasitic centre of High Knoll. Ridge to right in far distance shows thick trachyandesite flow fed from the Saddle parasitic centre.

horizontal variation. However, the distribution in Manati Bay is unusual in that the direction of elongation of the dyke contours is 155°, whereas the dyke histograms have a maximum at about 125° (Fig. 9). This compares with the Sandy Bay dyke swarm, where the histogram constructed for two counts north-west - south-east across the area shows a maximum at about 35°, coincident with the dyke contour elongation (Fig. 9, Encl. 4).

Petrographically the dykes are as variable as the flows that they fed, and thicknesses vary from less than 10cm to more than 5m. Trachyandesitic dykes increase in number from north and south into the area of the Gates of Chaos (north of Lot's Wife). Variations in the distribution of trachybasaltic dykes were not observed because of their frequent similarity to fine-grained basaltic varieties.

Dykes are exposed throughout the south-west volcano (Encl. 4), and locally several may be clustered in relatively small areas. This is particularly noticeable in Powell's Valley and Deep Valley to the east. In Powell's Valley the dykes 1km from the sea dip north-westerly at 80°-85°, and at the seaward end the dip is 80°-85° south-easterly - in the central area the dykes are more or less vertical. No similar gross variation is seen in the main swarms, which maintain subvertical dips with a bias towards the north-west in Sandy Bay, and south-west in Manati Bay. In Manati Bay dykes frequently occur in groups of 4-7 (5-10m total thickness) and are separated from the next group by up to 15m of country rock. Dykes exposed in the flanks may be considered relatively younger than the dominant Sandy Bay swarms (the former generally cut flows fed by the latter) and for these "later" dykes an overall weak radial pattern is discernible (Encl. 4). Here Saint Helena differs from Tristan da Cunha and Gough Islands, where radial dyke swarms are obvious and there is no

FIGURE 9:

Histograms of traverses across the Sandy Bay (2) and Manati Bay (2) dyke swarms of the south-western volcano. Height of histogram is linear representation of dyke thicknesses summed at 5^{o} intervals from actual counts shown in lower diagrams. Choice of 5^{o} is largely responsible for double peaks.

a: SANDY BAY

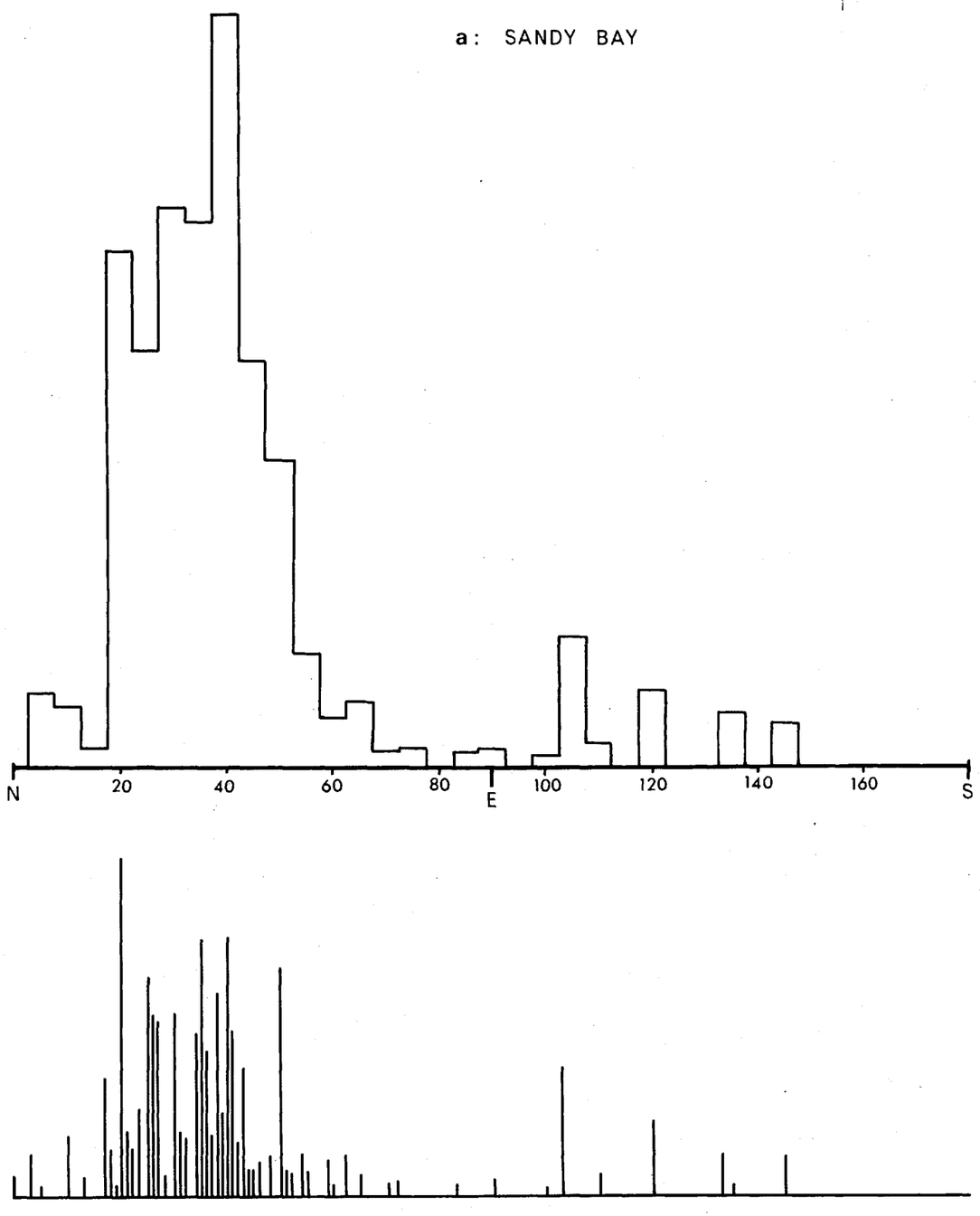

b: MANATI BAY

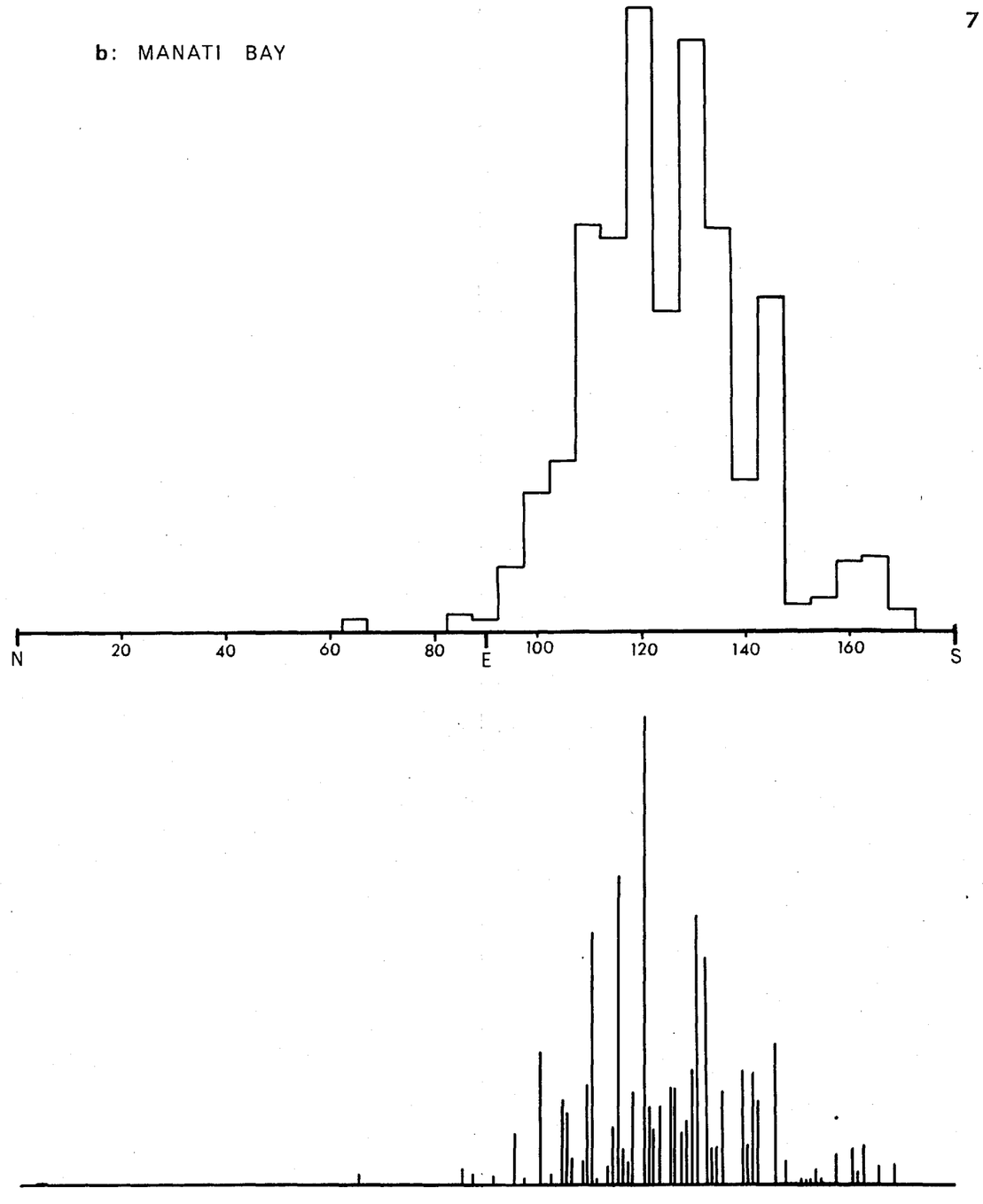

Fig: 9

evidence of pronounced linear swarms. The complete lack of dykes in the north-west, north, and north-east is probably real. The areas were extensively traversed along lines of excellent exposure, and only those dykes shown in Enclosure 4 were observed.

Cross-cutting relationships are seen in dykes throughout the island, but no distinct pattern is discernible. In Sandy Bay for instance dominant dykes at 020° will cut others at 055° or 140°, but less than 100m away the reverse cross-cutting relationships are seen. Although the greater numbers of dykes in any area follow a broad trend, and subordinate dyke directions are visible, there appears to be no systematic grouping of minor trends with time.

In several respects the basaltic dyke swarms on St. Helena resemble the well-documented examples from the Hawaiian group (see eg. Macdonald, 1965). The dykes appear largely tensional, with only very rare slight movement of rocks across the original fracture. In the central areas dykes locally form 35% or more of the exposure and more than 50% in the north-east volcano. Distensions of the exposed central parts of the volcanoes cannot be less than 2 or 2.5km in the north-eastern volcano and 0.75km in the south-western volcano (0.95km allowing for the late highly alkaline dykes). These figures compare with values of "not less than 0.75-1km" for the Hawaiian rift zones (Macdonald, 1965). The dominant NE-SW dyke swarm of the south-west volcano apparently accounts for the asymmetry of the volcano (island) in this direction. However, the dyke swarms differ from the Hawaiian examples in their gross morphology. Only one dominant dyke trend is developed for each volcano: north - south for the older, and north 35° east for the younger shield. There is no development of two major and one minor rift zones at 120° (Macdonald, 1965). The minor concentration of Manati Bay does lie however,

at an angle of approximately 110° to the main Sandy Bay swarm. The two swarms of the south-western volcano have distinct central maxima, and do not produce the major eruptive centre of the volcano at their point of intersection - this in fact is an area of relatively low dyke concentration (see Encl. 4). (This does not mean that intersection of dykes on two dominant trends has not been locally important, as for example in the formation of the Asses Ears.) Although certain close similarities are seen between St. Helenan and Hawaiian structures, these important differences should be carefully noted.

Several interesting structures are displayed by the dykes when cutting pyroclastics. Frequently the attitude of slightly inclined dykes changes by a few degrees across a basalt/pyroclastic junction - this is analogous to cleavage defraction between coarse and finer-grained sedimentary rocks. Thin dykes associated with small scoria cones are often irregular, and erosion of these centres may reveal an intricate "spider's web" structure consisting of sub-radial and rare sub-concentric dykes (good examples occur in the Sandy Bay pyroclastics). Thin dykes of limited extent are commonly more numerous close to scoria cones.

Vesicles show a decrease in number and an increase in size and irregularity towards the centres. In the late highly alkaline dykes this is very pronounced, one 15m dyke containing irregular (empty) cavities up to 1m in diameter. The central large vesicles are genuinely geometrically "central"; in a number of measured cases the centre of the vesicles coincided with the mid-point of the dyke, with a variation of less than 1.5%. Central vesicles are frequently infilled with secondary carbonates, and sulphides (pyrite, chalcopyrite) may be sufficiently enriched in dyke centres to be visible in hand specimen.

Structures of more specific interest shown by individual dykes are shown in Fig. 10. The curved basic dyke cutting the thick trachytic dyke (10a) is explained in relation to the development of curved jointing in other dykes (10b and 10c). Forceful injection of lava infills the curved fracture opened under tensional conditions (the thick dyke has 1-2cm carbonate infillings along joints parallel to its length). The unusual spheroidal jointing of the thick black porphyritic flows (Man o' War group) has resulted in a thin, very fluid dyke following the spheroidal outline (10d). The block in Fig. 10e, apparently quite separate from the mass as a whole, may also be related to spheroidal jointing. The example of one dyke meandering through another with similar orientation (Fig. 10f) is taken from the north-eastern volcano, and was not encountered in the south-west. Fig. 10g is a classic case of a younger dyke cut by an older one! Originally two narrow fissures (2a, 2b) opened in the country rock of thin basaltic flows and interbedded tuffs (at this locality the dominant tuff is 10m thick). The main 4.5m dyke (1) fractured only along one fissure (2b); intrusion of lava along 2a followed the irregular fracture in the tuff, forcing it away from the edge of the main dyke, and resulting in the dyke being turned back on itself (Fig. 10g, h). Dyke 2a must have broken through the thick dyke (1) at depth to allow for its appearance on the opposite side.

A number of dykes at topographically low levels in both volcanoes display structures (Plates 4, 5) interpreted as results of 'flowage differentiation' (Bhattacharji and Smith, 1964). The dykes are believed to be feeders for porphyritic flows rich in euhedral pyroxenes. The fluid magma, carrying quantities of crystals (pyroxene $>$ olivine), tends to concentrate larger crystals in larger quantities in the central parts of the dykes where the flow rate is a maximum.

FIGURE 10:

Structures shown by dykes; all but 10e, h shown in plan.

a: Alkaline dyke (P) cut by curved basaltic dyke (B) is explained in the text in relation to

b: flowage jointing patterns developed in intermediate dykes.

c: Development of weak prismatic joints at margins and slightly curved joints as a result of slight pre-consolidation movement.

d: Thin basalt dyke cutting thick spheroidally jointed porphyritic basalt (pbb). Dotted lines are joints in flow; lines in dyke show thin platey joints.

e: Vertical section of thin basaltic dyke cutting porphyritic basalt flow (pbb) with block of lava included in dyke. Shape of block may reflect a fragment broken along spheroidal joints.

f: Sinuous dyke (2) cutting earlier but unconsolidated thicker dyke (1). North-eastern volcano.

g: Thick early trachyandesite dyke (1) is cut by 2b and resists 2a (thin basaltic dykes). B-B' = line of section in h. Explanation in text.

h: View on B-B' in plane at 45° to horizontal inclined from top to bottom. Dashed lines in g and h close to dykes represent baked zones of host pyroclastics.

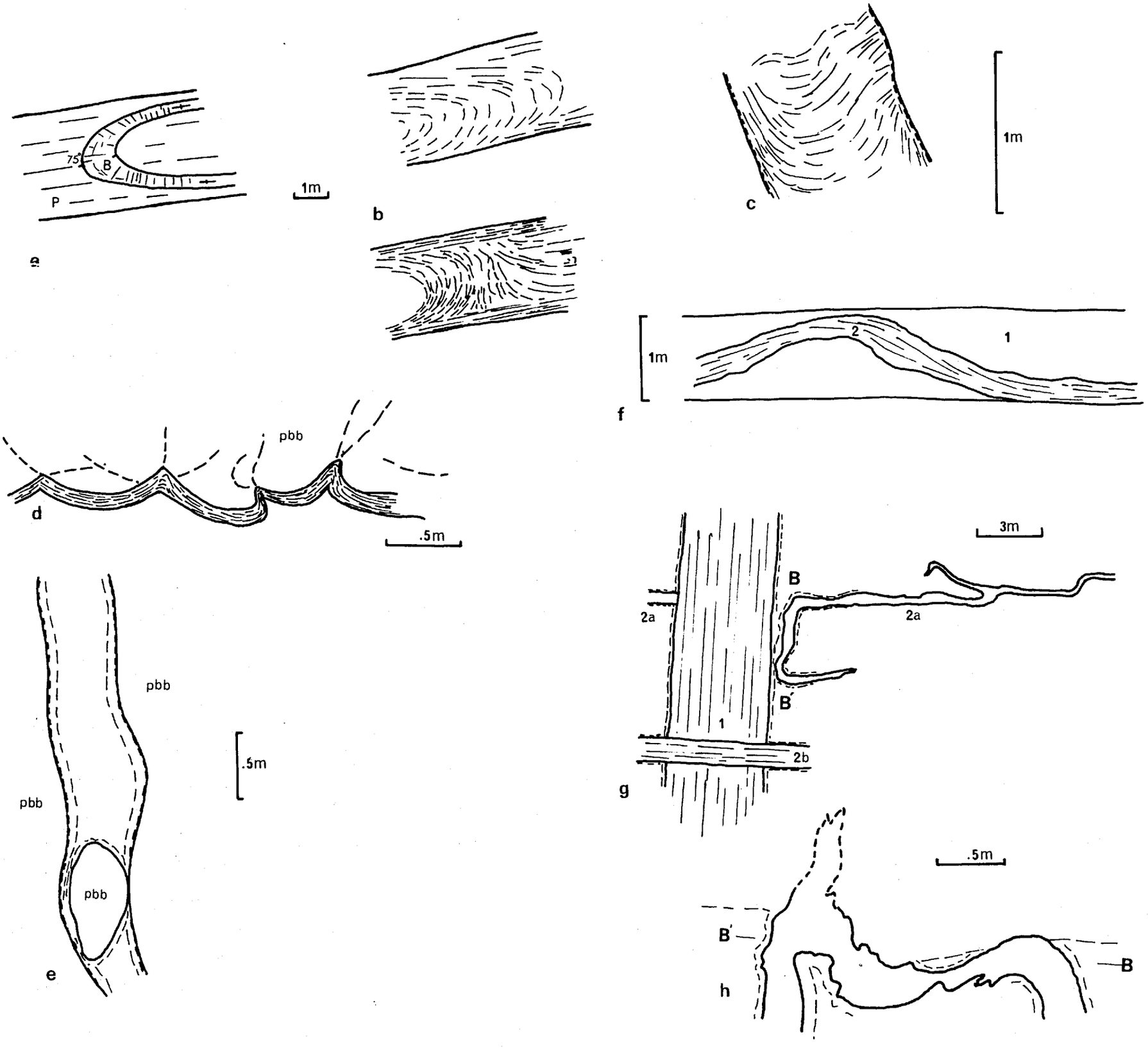
75°
B
P
1m
a
b
c
1m
1m
2
1
f
pbb
d
.5m
3m
B
2a
2a
B'
1
2b
g
pbb
pbb
pbb
.5m
e
.5m
B'
B
h

FIGURE 10

PLATE 4:

Porphyritic pyroxene-olivine basalt dyke - beach section 400m NW of Castle Rock, south-western volcano, lower shield.

A: Dyke, 1.35m wide shows marked central accumulation of euhedral pyroxene crystals. Plane of photograph vertical.

B: Right hand half of **A**. Note progressive overall increase in size and abundance of pyroxenes but obvious minor variations (shown also by slight variations in colour). This structure compares with experimentally produced 'dykes' - see Bhattacharji and Smith, Fig. 3c, p152 (1964).

C: Close up of the central part of the dyke. Euhedral black pyroxenes up to 2cm long and smaller olivines (much paler coloured) to 0.7cm across. Again note variations in crystal density and size distribution, although similar grain size crystals tend to occur in distinct zones. View in sub-horizontal (top) and sub-vertical (bottom).

PLATE 5:

Extreme cases of concentration of crystals at dyke centres by the process of 'flowage differentiation' (Bhattacharji and Smith, 1964).

A: Three dimensional view of 0.6m dyke, same locality as Plate 4. Note concentration of pyroxene (and olivine) into marked central portion, but also gradational increase in size towards the centre. Narrow 'banded' dyke margins are common and reflect only microscopic grain size variation or variation in abundance of minute vesicles.

B: Extreme case of type A with perfectly euhedral pyroxenes (1.7-2.0cm) and olivine (6-10mm) tightly concentrated in the central 23cm of a 0.50m dyke. Main valley between The Barn and Turks Cap. 'Banding' at margins again reflects variations in concentrations of small vesicles. Note overall slight increase in size of pyroxenes towards centre of dyke.

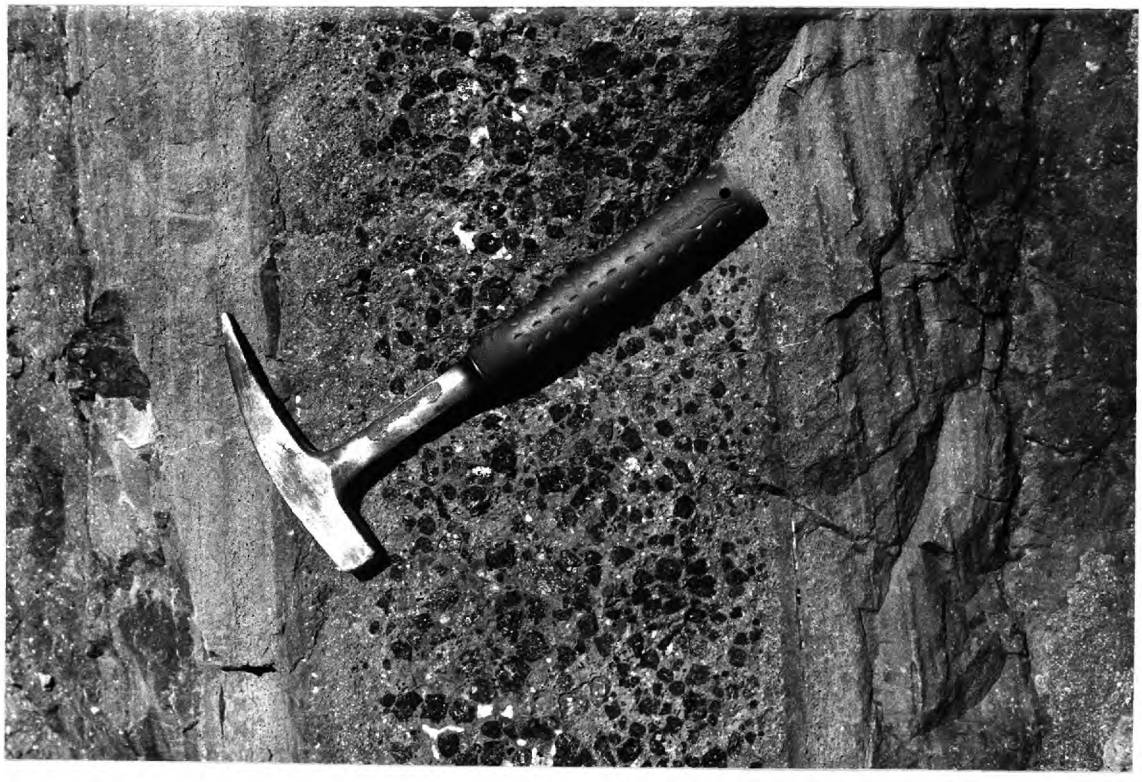

The increase in size and number of crystals is not absolutely regular as seen in the examples of Plate 4. In experiments simulating movement in crystal-rich dyke feeders, Bhattacharji and Smith have produced what may be a comparable texture (op. cit. p152, Fig. 3c) by stopping an upward moving "crystal" laden column and allowing partial settling of the crystals. The dyke here is very similar in having a pronounced central concentration of phenocrysts with minor fluctuations on either side (Plate 4). Plate 5a shows a dyke where the concentration of phenocrysts in the central part has resulted in an apparently multiple dyke. There is slight gradation in phenocryst grain size across the mass, and the planar "units" may reflect an increased degree in settling out of material, or a marked change in velocity gradient. In Plate 5b, an extreme case is shown. The dykes showing these very pronounced central accumulations occur at elevations greater than 170m (up to 370m) in the north-east volcano, and were not seen in the south-western volcano. The dykes are always thin, and the boundaries between crystal-rich and crystal-impoverished zones are sharp. The dykes are believed to be equivalent to the dykes of Plate 4 at higher levels (cf. Bhattacharji and Smith, p152, Fig. 3d). The velocity gradient is very marked in the central part of the dykes, and when flow stops, because of the thinness of the dyke, cooling is rapid allowing a minimum of settling out of the pyroxenes. Single euhedra up to 3cm are not unusual, and one dyke in the north-eastern volcano contained a single augite 7.5cm long, enclosing a number of rounded olivines, each greater than 1.0cm in diameter.

c. Parasitic activity.

A large number of scoria cones were built up on the flanks of the south-western volcano during growth of the main shield (Encl. 5). They range in size from small, fine-grained, yellow tuff cones to very large, red-purple, coarse scoria

cones, originally over 300m high. A number of the parasitic cones are associated with alkaline intrusions, and a few have extruded intermediate flows. In almost all cases the intrusions and flows are very significantly younger than the cones with which they are associated.

The cones are very similar to those described from the north-eastern volcano with good bedding, and bombs and coarse scoria fragments concentrated into distinct horizons. Irregular highly scoriaceous flows are rarely developed, and only in the late stages of the cone formation. Several of the large cones are products of more than one centre, but single-vent cones predominate. The cones are occasionally asymmetric with finer material extending to the north-west. This almost certainly reflects dominance of south-easterly winds - the dominant Trade winds of the present.

The great majority of the cones are buried beneath undoubted flows of the main shield series, but several rest on the latest flows of this group. A number of deeply eroded cones are partly buried beneath flows of the Upper Shield (Encl. 3), and it is possible that a number have been totally eroded from the flanks of the south-western volcano. However, exposure on the island is sufficiently good (as a result of the numerous sub-radiate valleys) that the distribution of scoria cones shown in Enclosure 5 may be accepted as an approximation to the real distribution. In a number of areas groups of scoria cones and local dyke concentrations are coincident (e.g. High Knoll, High Hill). However, large numbers of dykes are not related to parasitic cones and large numbers of cones are not visibly related to dykes. It was suggested above that certain groups of scoria cones in the Lower Shield were orientated approximately parallel to the dominant NE-SW dyke swarms. From a study of Enclosure 5 it would be tempting to suggest, for example, that the NW-SE

grouping of scoria cones near High Hill is similarly related to the local dyke concentrations. The dykes in this area however, trend approximately N-S (Encl. 4), and direct correlation of the cones with the radial dyke pattern tentatively proposed for late dykes of the south-western volcano is impossible. Whilst scoria cones are undoubtedly related to "fissures" connecting them to the underlying magma source, it would be inaccurate to suggest that the parasitic cones on St. Helena are situated along dominant radii or other "lineaments".

(i) The High Hill scoria cones.

Exposure in the steep north side of Old Woman's Valley reveals products of six explosive centres. The High Hill area has been a centre of parasitic activity intermittently during the build up of much of the Main Shield. The distribution of the pyroclastic cones is shown in Fig. 11. The combined thicknesses of scoria from the first 5 centres is nearly 300m in the valley side, but cones have individually attained this height at their maximum development (Encl. 5).

Centre 1 (well bedded coarse orange scoria) rests directly on flows of the main shield series. Its original height of approximately 400m was greatly reduced by erosion prior to the build up of Centre 2.

Centre 2 (coarse or very coarse brown-orange scoria) was originally nearly 400m high and almost completely buried the relics of Centre 1. Two thick trachybasaltic flows were extruded from this cone, one late in the centre's activity, the second after cessation of explosive activity.

Centre 3 (coarse orange scoria grading up into late fine yellow tuff with the top 5m very rich in bombs) is separated from the scoria of Centre 1 by at least one flow of the main shield series. The scoria buried the remainder

FIGURE 11:

Geological map of scoria cone activity in vicinity of High Hill (712m O.D.).

Products of six centres numbered 1-6; 1 = oldest, 6 = youngest. MSF = basaltic flows of the main shield series.

Stippled areas = trachybasaltic flows from Centre 2. Dashed areas are trachybasaltic flows possibly of local (Centre 6) origin.

Compare with Enclosures 3 and 5 for relationship to volcano as a whole and location of cone centres. Geometry of arcuate sheet and High Hill trachyte given in Figs. 20 and 24.

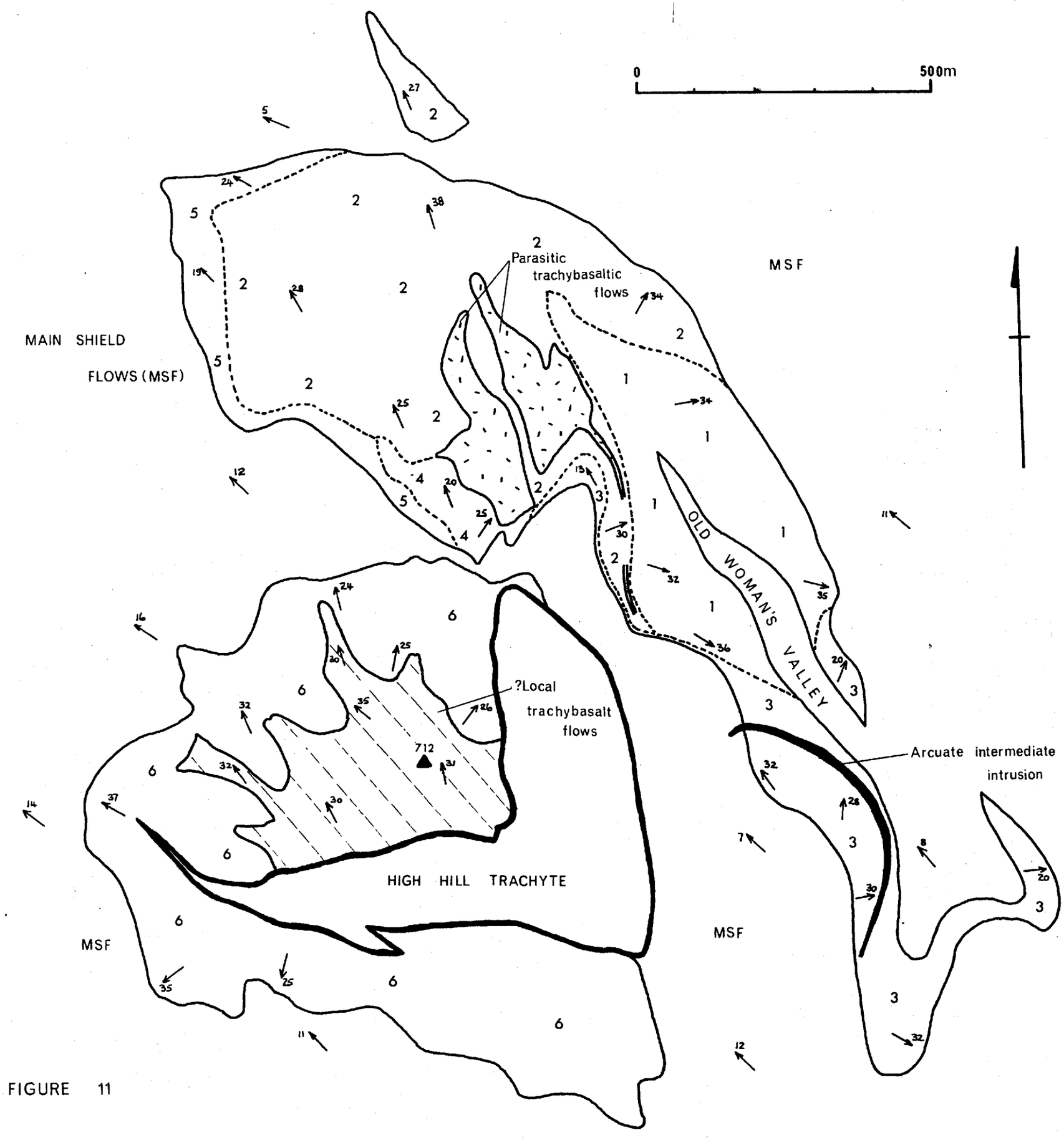
0
500m
MAIN SHIELD
FLOWS (MSF)
Parasitic
trachybasaltic
flows
MSF
OLD WOMAN'S VALLEY
?Local
trachybasalt
flows
712
HIGH HILL TRACHYTE
Arcuate intermediate
intrusion
MSF
MSF

FIGURE 11

of Centre 1 and the latest tuff mantled the eroded cones to the north-west.

Centre 4 (coarse orange-red scoria) rests on a marked erosional surface cut especially deeply into the Centre 2 scoria. Although coarse the scoria mantles the irregularly eroded surface.

Centre 5 (pale yellow medium-grained scoria grading up into a very fine yellow tuff, which thickens markedly to the west, containing rounded bombs up to 1.5m diameter) was apparently a very important source east of the present High Hill. Comparable tuffs are exposed nearly 2km south in Thompson's Valley where they overlie relics of two coarse scoria cones (Encls. 3 and 5), one of which is associated with a thick trachybasaltic flow. The relationship between these latter cones and the High Hill group of cones is uncertain, but they are almost certainly of comparable age (similarly the tuff cone opposite Egg Island shown in Encls. 3 and 5).

Overlying flows of the main shield series rest with no apparent break on the tuff of Centre 5, and the entire area of scoria cones was buried before late renewed explosive activity formed the late coarse scoria cone of High Hill itself (Centre 6 in Fig. 11). The intrusion into this cone occurred some two million years later and is described in Section IV.

(ii) The Blue Point area.

A complex group of local intrusive and extrusive rocks is exposed in the steep sides of the ridge south from Hooper's Rock to Blue Point (Fig. 12). The scoria cone of the Blue Point area rests on a surface eroded into the Devil's Cap pyroclastics, and the intrusions are later than the formation of this cone. Several distinct groups of intrusives

FIGURE 12:

Geology of the Blue Point area.

Dotted areas : Blue Point scoria.

Dashed areas : Blue Point trachyandesite flows.

Blank area inside dashed line is Devil's Cap fragmental rocks.

Intrusive rocks:

F = Frightbus Rock intermediate breccia pipe.

P_1 = Asses Ears phonolite.

P_2 = Man o' War Roost phonolite.

Hachured areas : trachyandesitic sheet of Narrow Ridge area.

B : basaltic sub-horizontal sheet.

D : basaltic irregular 'cone' sheet (see Section IV).

G : intermediate irregular sheet.

T_1, T_2 : trachytic laccolithic intrusions, possibly related.

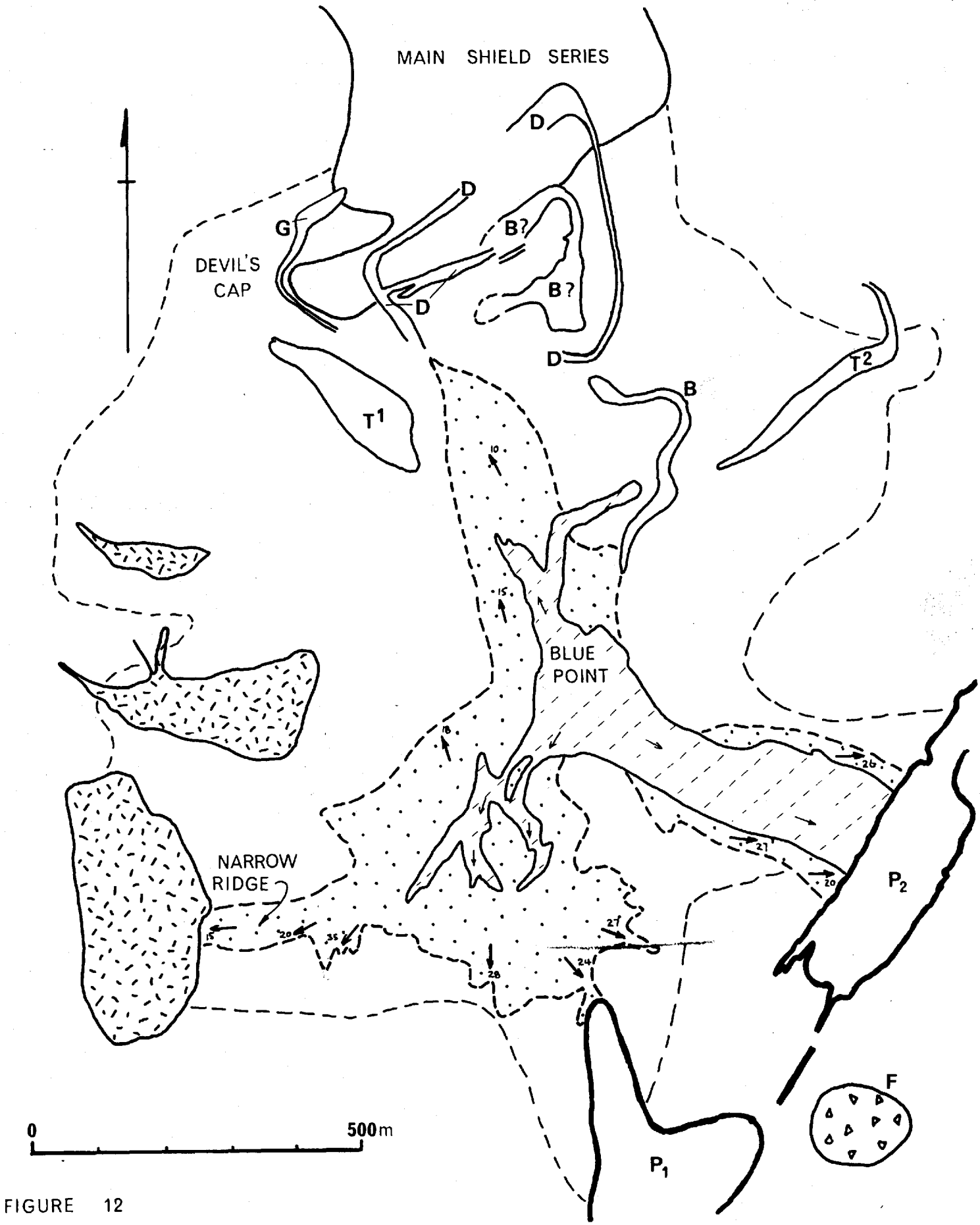
MAIN SHIELD SERIES
DEVIL'S CAP
G
D
D
B?
B?
D
D
T1
T2
B
BLUE POINT
NARROW RIDGE
P2
P1
F
0
500m

FIGURE 12

are exposed but exact time relationships are uncertain. Although no rocks overlie the Blue Point extrusives they are cut by numbers of dykes equivalent to numbers cutting the immediately underlying rocks, and parasitic activity is believed to have occurred during the growth of the main shield.

The main cone is centred about 300m south-west of Blue Point (Fig. 12), and is composed of dominantly coarse scoria with spindled bombs and flattened spatter fragments up to 1.2m across. Finer ash horizons occur throughout the highly eroded cone, and irregular spatter flows are poorly developed close to the original vent. Fragments of olivine basalt are rarely found and the scoria is red, purple and brown, comparable to basaltic scoria elsewhere on the island. Material to the north may have originated from a separate smaller vent on the flanks of the basaltic cone, and rests with only minor discordance on the Devil's Cap pyroclastics. This material is finer and contains flow banded fragments. The alteration, to blue, white and pale purple material, closely resembles that developed high in the High Knoll cone and suggests that it is also probably trachybasaltic.

The completed Blue Point (double) cone was eroded before renewed explosive activity destroyed parts of the eastern flank. These deposits consist largely of redistributed basaltic (and trachybasaltic?) scoria and are preserved only in the south-east. Following the explosive activity trachyandesite flows were extruded from a "feeder" area over 200m north-east of the original basaltic cone centre, but possibly coincident with the centre of this very latest explosive activity. The "feeder" area consists of irregular stringers and thin dykes which permeate the scoria. The trachyandesite flowed mainly to the south-west and south-east but minor relics are preserved to the north (Fig. 12). In the south-west the flow has been largely eroded but from the

distribution of the relics must have been at least 20m thick. The main flow preserved forms the south-east ridge leading to Man o' War Roost where it is still 100m thick (Plate 6A). Weak columnar jointing is developed in the central parts, and closely spaced vertical sheet joints are locally developed parallel to the flow direction in the upper parts of the flow. The trachyandesite is truncated sharply by the phonolite dyke of Man o' War Roost, although mixed breccias of the two rock types are preserved. Adjacent to the phonolite the trachyandesite is completely altered. The alteration throughout the flow has produced extraordinary spheroidal patterns in red and green which compare closely with the colours developed locally in the White Point and White Hill trachyandesites. A 4m dyke cutting the scoria and "feeder" area at Blue Point breaks up into a series of irregular stringers. The structure is similar to that shown by dykes cutting incompetent altered material (cf. the laterite horizon of the Antrim basalts), and the centre was presumably highly altered (?hydrothermally) after extrusion of the trachyandesites.

A number of later intrusive masses are exposed north of Blue Point and are partly explained in Figure 13. The thick vertical trachyandesitic mass of Narrow Ridge (truncating the scoria cone) is believed to continue into the two irregular masses to the north. The masses appear to be local extensions of a major north-south sheet. The basaltic sheet (Fig. 13 "B") rests almost concordantly within the Devil's Cap pyroclastics. The irregular basaltic sheet (D, explained in Section IV.) has probably cut the sheet "B". The trachytic intrusions (T1 and T2) may be related to each other, both are thich (T1 = 35m, T2 = 25m), flat-lying, petrographically similar, and outcrop at equivalent elevations on the two sides of the ridge (Fig. 13). The sheet (G) cutting the pyroclastics at Devil's Cap is altered, but is intermediate in

composition. In the north its contact is discordant, cutting the bedded tuff nearly at right angles, but the sheet swings round into a concordant sub-horizontal attitude to the south. On the south side of the ridge it disappears in an area of thick vegetation and cannot be traced further.

4. The Upper Shield.

The south-western volcano had probably attained a height of approximately 1400m above sea level at the end of the formation of the Main Shield (estimated by extrapolating the shield flows back into the central area - this agrees completely with Daly's estimate). The north-eastern volcano although already eroded from a comparable height, may still have risen nearly 1000m above sea level. A period of prolonged erosion followed cessation of activity in the south-west. The most highly eroded area was in the north-east and east where a broad depression was carved into the flanks of the two shields. Minor sub-radiate valleys were also eroded but were less pronounced than their present day equivalents. The unconformity is well exposed in the north-east cliffs (Plate 7) and in other rare exposures, but inland the exact distribution of the Upper Shield rocks is often confused by alteration and vegetation (see Fig. 7, and Encl. 3). It is the upper rocks of this group that were interpreted as 'Late feldspathic lavas' by Darwin, Oliver and Melliss (op. cit.).

The Upper Shield extrusives can be divided into two groups separated by an unconformity; an earlier sequence of thick basaltic flows and a later group of thick intermediate flows. The distribution of the two groups is shown in Enclosure 3. Inland the later trachyandesites are distinguished by their green colour when fresh and characteristic orange weathering, but the basaltic flows are often indistinguishable from the Main Shield lavas. From their present

PLATE 6:

A: View of the lower shield extrusives and later rocks between Lot's Wife (right) and Frightbus Rock (extreme left). Foreground is in nearly horizontal thick flows of the Man o' War group, cut by numerous thin dykes. Triple 'peaks' right of Frightbus are the phonolitic intrusions of the Asses Ears and Man o' War Roost (note multiple dykes intruding the main phonolite). Between camera and Asses Ears is the intermediate pipe of The Niggerhead. Note two major highly alkaline dykes : one from Asses Ears, through Man o' War Roost to Lot's Wife, and the second below The Niggerhead extending to below Lot's Wife. The thick weakly columnar-jointed flow forming skyline (centre) is the trachyandesite flow from the Blue Point parasitic centre (high point).

B: Seaward end of Fisher's Valley cut into flows of the upper shield series. The top four flows are trachyandesites, lower flows are basalts. The apparently thick flow (top left) is over-thickened top trachyandesite which has poured over a cliff into the 'proto Fisher's Valley'. The flat area is the edge of Prosperous Bay Plain. Height of left hand side of photograph approximately 300m.

PLATE 7:

Composite view from King and Queen Rocks (B) to the SE corner of The Barn (L). Relationships of both volcanoes and upper shield series are beautifully laid out.

A: Extreme southerly limit of the shield-forming rocks of the north-eastern volcano.

C: Prosperous Bay Signal Station.

D: Unconformity: upper shield series on main shield of south-western volcano.

E: Unconformity: main shield series (SW)on shield of NE - both unconformably overlain by upper shield series.

F: Prosperous Bay Beach - head of Fisher's Valley.

G: Holdfast Tom.

H: Latest trachyandesite overthickened in Bryan's Rock below Horse Point.

I: Turks Cap and ridge of upper shield trachyandesites.

J: Main valley eroded into basal breccias.

K: (Skyline) Knotty Ridge.

Note the chaotic appearance of the basal breccias (north-eastern volcano) and dykes extending throughout its exposure.

Plate 7

distribution the flows forming the Upper Shield appear to have originated largely from an area close to The Peaks (Encl. 3).

a. Lower basalts.

At their maximum development eight thick basaltic flows are exposed in the seaward end of Fisher's Valley. The flows irrespective of thickness are remarkably flat-topped (Plate 7); single flows may extend for nearly 2km along the strike and the flow top remains virtually horizontal throughout. Individual flows are on average about 15m thick with fairly well developed columnar (rarely slightly curved) and weak horizontal jointing (Plate 6B). The flows have scoriaceous bases and probably similar tops, although these are usually obscured by detritus. Fine-grained reddened tuff horizons separate several of the flows.

Flows belonging to this group extend as far as the Stone Tops area where they appear to rest virtually conformably on flows of the main shield series. They are preserved inland as erosional relics in this highly altered area, and are greatly obscured by highly altered later trachyandesites.

In the high ground on the Sandy Bay side of the central peaks, relic flows are exposed which are believed to belong in part to these lower basalts. They dip at low angles into Sandy Bay and demonstrate that erosion had already started to open up that area. Unfortunately the whole of the Peaks area above 600m is almost 100% vegetated with flax and indigenous vegetation, and relationships in the area are very obscure.

b. Intermediate flows.

These flows are of widespread occurrence in the north and east of the island and originally covered an area

greater than that covered by the lower basalts. Four flows are developed in Fisher's Valley (seaward end) but only the upper three are developed at Turk's Cap (Plate 7), and in the inland areas only one flow is usually seen at any given locality. The flows are trachyandesites each of which probably had an average thickness of 30-35m.

In hand specimen the trachyandesites are green and shimmering as a result of well developed orientation of the feldspars. The degree of parallel orientation (and development of poikilitic pyroxene as seen in thin section) increases away from the source area. The flows weather to a characteristic orange clayey material, individual spheroids being preserved as almost perfect thin discoids reflecting the original tabular joint pattern of the flows.

Above Prosperous Bay Beach and south towards Gill Point the top flow has plunged over cliffs originally 100m or more high cut into the underlying members of the upper shield series (Plate 6B). This same flow infills an erosional depression at Horse Point, its 120m thickness forming the impressive cliff of Bryan's Rock (Plate 7). In much of the area inland from the cliffs only a metre or less of the trachyandesites is preserved as a "smear" on broad valley sides originally cut into lower basalts. From their present distribution and the intense erosion they have undergone it is obvious that these trachyandesites were volumetrically some of the largest individual flows.

Structures cutting the flow south of Woody Ridge are similar to ones cutting the thick trachyandesite of Headwain and the White Point intrusion. Breccia "dykes" from 2-20cm wide cut the trachyandesites with a constant linear trend. The vertical "dykes", in all cases now completely altered, contain angular to sub-angular basic and intermediate

fragments ranging in size from 3cm down into the comminuted matrix. The contact with the host flow is sharp, but the base of the flow is not exposed. It is suggested that the ground surface upon which the flow was deposited was water-logged and this underlying material was brecciated by the explosive action of entrapped water and driven upwards along cooling joints in the flow (or intrusion). A structure believed to be related is found beneath several intermediate flows. The scoriaceous base of these flows frequently contains basic and relatively compact intermediate fragments which are believed to be produced by small steam explosions beneath the advancing flow front. The only flow in which spiracles were developed in the base had a mixed rock fragmental base to it (Plate 8A, cf. Waters, 1960, Plate 2 no. 2).

Relic patches of a thick (at least 35m) porphyritic olivine-pyroxene basalt occur at several widespread stratigraphically high localities. The flow is preserved south and east of Diana's Peak, on Long Range, and relics are seen north of Stiches Ridge and possibly north of Riding Stones Hill. Patches of the flow occur north of Scotland and the capping of Thompson's Hill may be of this flow. Although the rock is of uncertain age, field and K-Ar evidence suggest it could belong to the Upper Shield although its position in the sequence is unknown (Baker et al, 1967).

No evidence of the feeder dykes to the lower basalts is exposed in their suggested source area. However, a very thick (up to 30m) dyke of intermediate composition strikes north-south, east of Sheep Knoll, and another just west of the Knoll strikes ENE-WSW (Encl. 4 and Fig. 18).

PLATE 8:

A: Base of intermediate flow at White Point, overlying more or less well-bedded tuffs. Flow base is fragmented on left (possibly by steam explosion) and scoriaceous to right (alteration produces the different colours). Top is scoriaceous (fragmental in the sense as used in the text). Note spiracle in centre, curving down slope (Hammer handle bottom right).

B: Honeycomb weathering of homogeneous (Bencoolen) trachyandesite flow at Boxwood Hill.

5. East Flank Activity.

Three groups of flows, of local development, later than the intermediate flows of the Upper Shield, are exposed in the Bencoolen - Stone Tops area (Fig. 13). The Upper Shield flows beneath, and east of, Bencoolen are banked around an originally large (300m) scoria cone. The trachyandesite flows must have completely buried its eroded remnants. Resting on the trachyandesites are several basaltic flow units which may have filled a slight depression east of the original cone (Fig. 13). An area about 1000m across was updomed slightly by the intrusion of an arcuate intermediate sheet exposed in the sides of Sharks Valley (Plate 17). The Bencoolen flow group and possibly the Stone Tops flow domes were later than this updoming.

a. The Stone Tops.

Great and Little Stone Tops are the eroded remnants of two multiple trachytic flow domes. They rest on a relatively flat surface weakly eroded into the lower basalts of the Upper Shield. Great Stone Top is associated with three arcuate sheets one of which at least served as a feeder (Plate 10); the structure of these sheets is described in Section IV.

Great Stone Top is the older of the domes and is composed of four or five thick flows (Plate 9A, Fig. 13), the lowest of which appears as a flat sheet, over 100m thick, in the sides of Sharks Valley (Plate 10). The second (flow II) is distinctly separate from the oldest flow, but the latest flows, although distinct away from the central region, appear to have cooled as a single unit with flow II in the central area (Plate 10, Fig. 13).

The Little Stone Top trachyte dome, composed of at least two and possibly five flow units (Plate 9B), was extruded in part onto the second flow of Great Stone Top (Fig. 13).

FIGURE 13:

Geology of the Bencoolen-Stone Tops area.

MSF = Main Shield flows

Dotted areas = basaltic scoria cone

u = Upper Shield basalts

t = Upper Shield trachyandesites

Dashed areas = (?local) basaltic flows

Black = arcuate trachytic intrusions.

Note bending of basaltic flows by Rough Rock trachyte and also the Sharks Valley trachyandesite arcuate sheets.

Stone Tops flow domes shown blank.

Successive flows of Great Stone Top : I-IVb. Short lines (ticked) denote dominant joints.

TA = Bencoolen trachyandesites and feeder dyke, recognizable flow units a-d visible on Boxwood Hill.

Plain arrows are flow directions in trachytes and trachyandesites.

See also Plates 9 and 10.

Geology of the Stone Tops - Bencoolen area

Figure 13

PLATE 9:

The Bencoolen-Stone Tops area.

A: Composite view from Bencoolen (left) across Sharks Valley past Little Stone Top (highly altered) to Great Stone Top (right centre). Prosperous Bay Plain in distance left of Bencoolen.

Note thick composite nature of both Stone Tops (cf. 9B and Fig. 13). Early flow from Little Stone Top visible in front of Great Stone Top.

View taken from Boxwood Hill.

B: View looking inland from Great Stone Top. Highly altered trachyte of Little Stone Top and (Bencoolen) multiple trachyandesite of Boxwood Hill (centre) extending round the Stone Tops (Fig. 13). Valley in middle ground (centre) is partly cut into basalts of the upper shield series.

On the skyline: regular basaltic flows of the main shield and hillocks of Long Range (left) and gradual ascent to thickly vegetated central high ground (Diana's Peak). Series of ridges and hillocks towards Levelwood and on right, highly altered upper shield series basalts and trachyandesites east of Woody Ridge, and to Longwood in extreme distance.

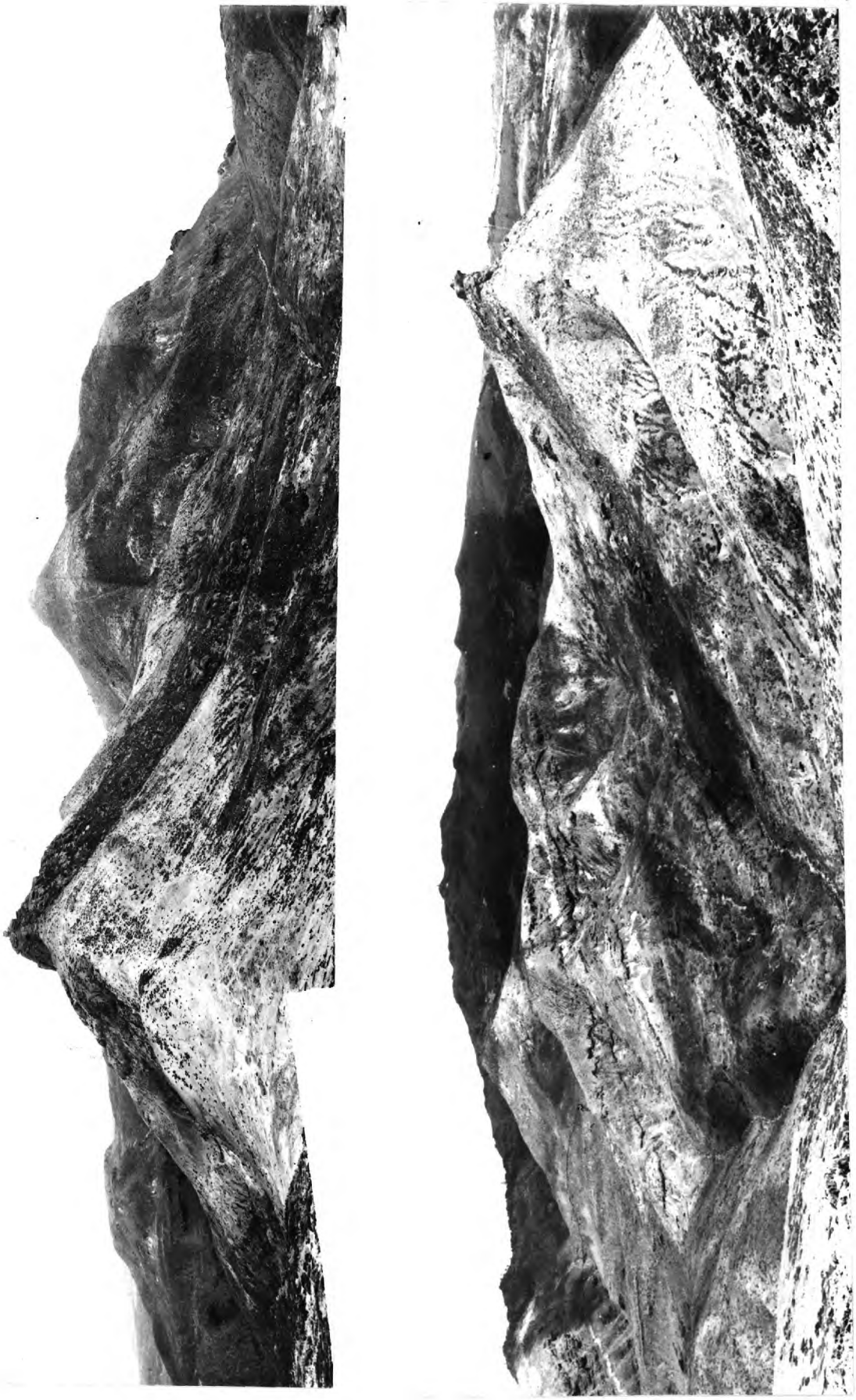

PLATE 10:

Great Stone Top.

A: North face exposed in Sharks Valley. Regular basaltic flows of main shield series are unconformably overlain by thicker (4-5) basalts of the upper shield series (right fore-ground is basaltic scoria cone east of Bencoolen). Flat-lying lowest trachyte sheet and overlying one extend towards Little Stone Top (later). Note curved jointing in seaward face of top of flow dome (The Lion) and the inclined cone-like sheet feeder. This view demonstrates the cylindrical jointing of the rather obscure Little Stone Top mass.

B: East face showing inclined cone-like arcuate "feeder" to the flow dome (i.e. post flow I). Note slight bowing of basalts within arc under the trachyte, and the apparently undisturbed nature of the central block of basalts. The central of the three sheets of Fig. 16 is just visible near the right hand side of the major arcuate sheet. Compare cooling joints left of the highest point with Plate 9A where at least two individual flow units are visible (III and IVa of Fig. 13).

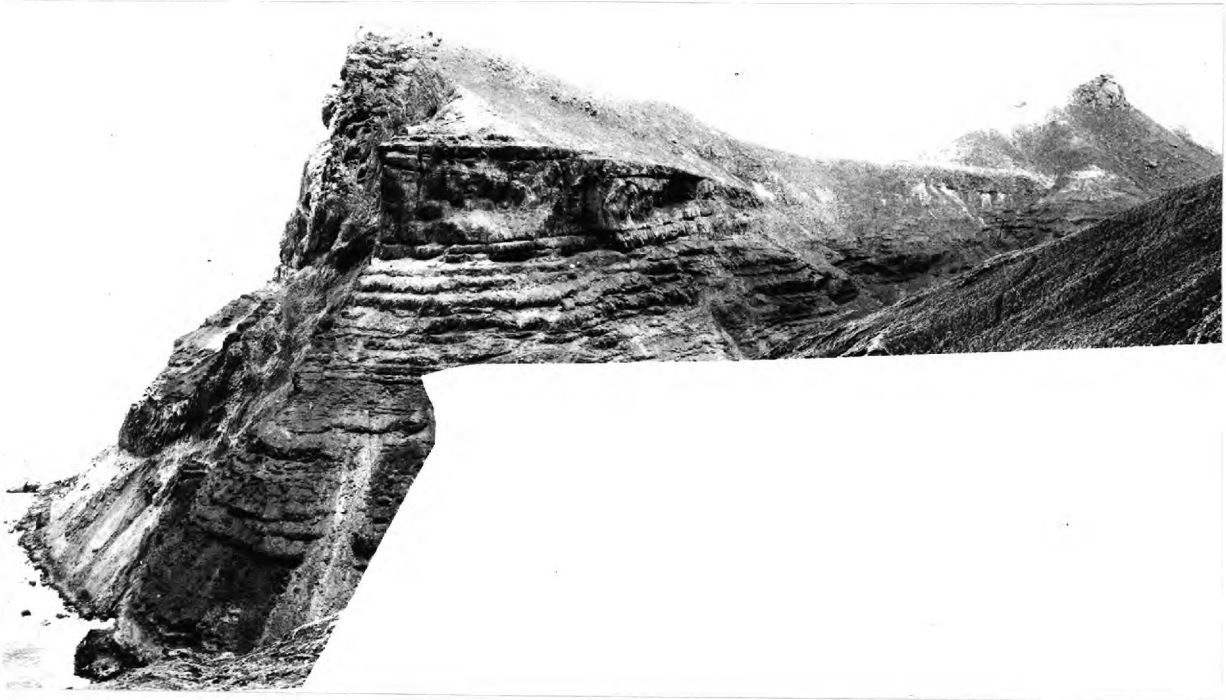

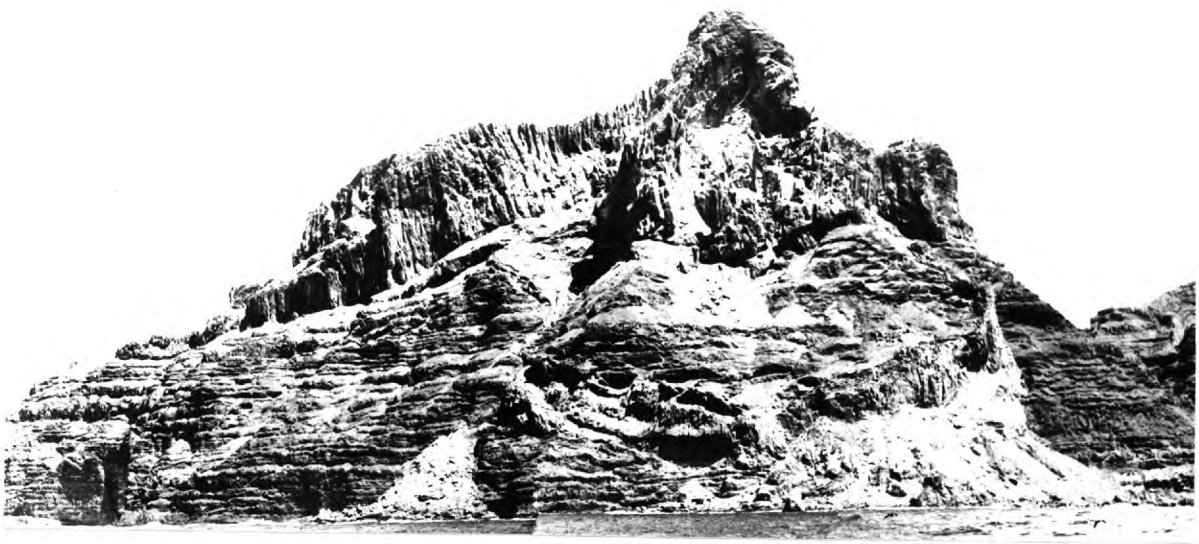

Although one major flow dips south-easterly the composite structure of the dome is obliterated by intense alteration. How much of the dome has been eroded away is unknown, but the cylindrical jointing in Plate 9B may result from the cooling of a thick viscous mass.

The bases of the flows resting on basalts contain angular to sub-angular fragments of the scoriaceous basalts and are themselves fragmented up to 2m above the base. The lowest of the Little Stone Top flows retains structures suggesting that it was flow banded prior to its intense alteration.

The trachytic intrusion of Rough Rock (see Section IV) is probably of the same age as the Stone Tops. It is certainly older than the Bencoolen flows since the intrusion has updomed a small area, round and over which the Bencoolen trachyandesites flowed, and which may have also served as a slight barrier to the Great Stone Top flows (Fig. 13).

b. The Bencoolen flow.

The latest extrusives in the east of the island are very distinctive trachyandesites forming the long low ridge of Bencoolen and Boxwood Hill to its south west. The flows are fed through a single fissure (Fig. 13 and Plate 17) and were probably extruded in a short space of time. Bencoolen may have largely cooled as a single mass but in the north-eastern side close to the feeder there is evidence of six distinct units. At Boxwood Hill five separate units are superimposed (Plate 9B) although only four are shown in Figure 13.

The present distribution of the Bencoolen trachyandesites clearly shows that Sharks Valley did not exist when they were extruded. After completion of the Main Shield a broad shallow depression eroded between Stone Tops and Prosperous Bay Plain was infilled by the lower basalts of the

Upper Shield. Erosion cut shallow valleys into these flows and the area as a whole was 'smoothed out' by the Upper Shield trachyandesites. Intrusion of the arcuate trachyandesite sheet (Fig. 13) and the associated local updoming produced an inland dipping slope east of the present Bencoolen (Fig. 13). The Bencoolen trachyandesite feeder dyke probably broke through the slope close to its highest point and lava was initially extruded mainly to the west, i.e. inland. The topography was responsible for the asymmetry of Bencoolen (35m thick to the east and 75m thick to the north and south-west) and the unusual distribution of these trachyandesites in general. The flows travelled south-westerly partly burying the west flank of the topographically high Little Stone Top dome, and are preserved in Boxwood Hill. From here an off-shoot flowed down a small valley to the south (now eroded away), with the main lava streams turning south-easterly following the dip of the eroded flank of the Main Shield to cover much of the area uplifted by the Rough Rock intrusion (Fig. 13).

On the south-west side of Boxwood Hill the trachy-andesite is completely altered and displays honeycomb weather-ing, the only example seen on the island (Plate 8B).

6. Late Intrusive Activity.

The south-western volcano is intruded by a number of highly alkaline dykes and parasitic bodies. Potassium-argon absolute age determinations (Baker, et al, 1967) have shown that they belong to an intrusive episode later than shield-forming activity (Fig. 14). Two intermediate flows emanating from older parasitic scoria cones are believed to belong to this major intrusive episode. A large number of the individual intrusive masses are arcuate and are discussed in Section IV; only the dykes and the individual centres of the Saddle and

FIGURE 14:

Radiometric ages (from Baker, Gale and Simons, 1967).

In the NE volcano 679 and 145 are from the bottom and top of the shield-forming extrusives; 678 is a dyke cutting flow 679.

In the SW volcano : 785 is from the Horse's Head flows and 792 is one of the Beach trachybasalts of the lower shield; 179 is one of the lowest flows of the main shield and 78 (believed to be an anomalous date) is from the top.

794, and 803 are from the lower basalts of the upper shield; 844 is the extensive porphyritic basalt of uncertain age in the upper shield; TC is from the trachy-andesites of Turk's Cap.

105 and 111 are from Great and Little Stone Tops respectively.

The intrusions are placed in groups related to their maximum age on field relationships:

746 (High Knoll) cuts the main shield; 281, 290, 313, 358 are from phonolitic dykes of Sandy Bay; 414 and 443 are from Riding Stones Hill; 683 is from Lot. The oldest rocks that these are seen to cut are older than 179.

88 (High Hill), 121 (Wild Cattle Pound), and 661 (White Hill East) all cut flows of the main shield series.

The grouping of the late highly alkaline intrusive rocks is striking.

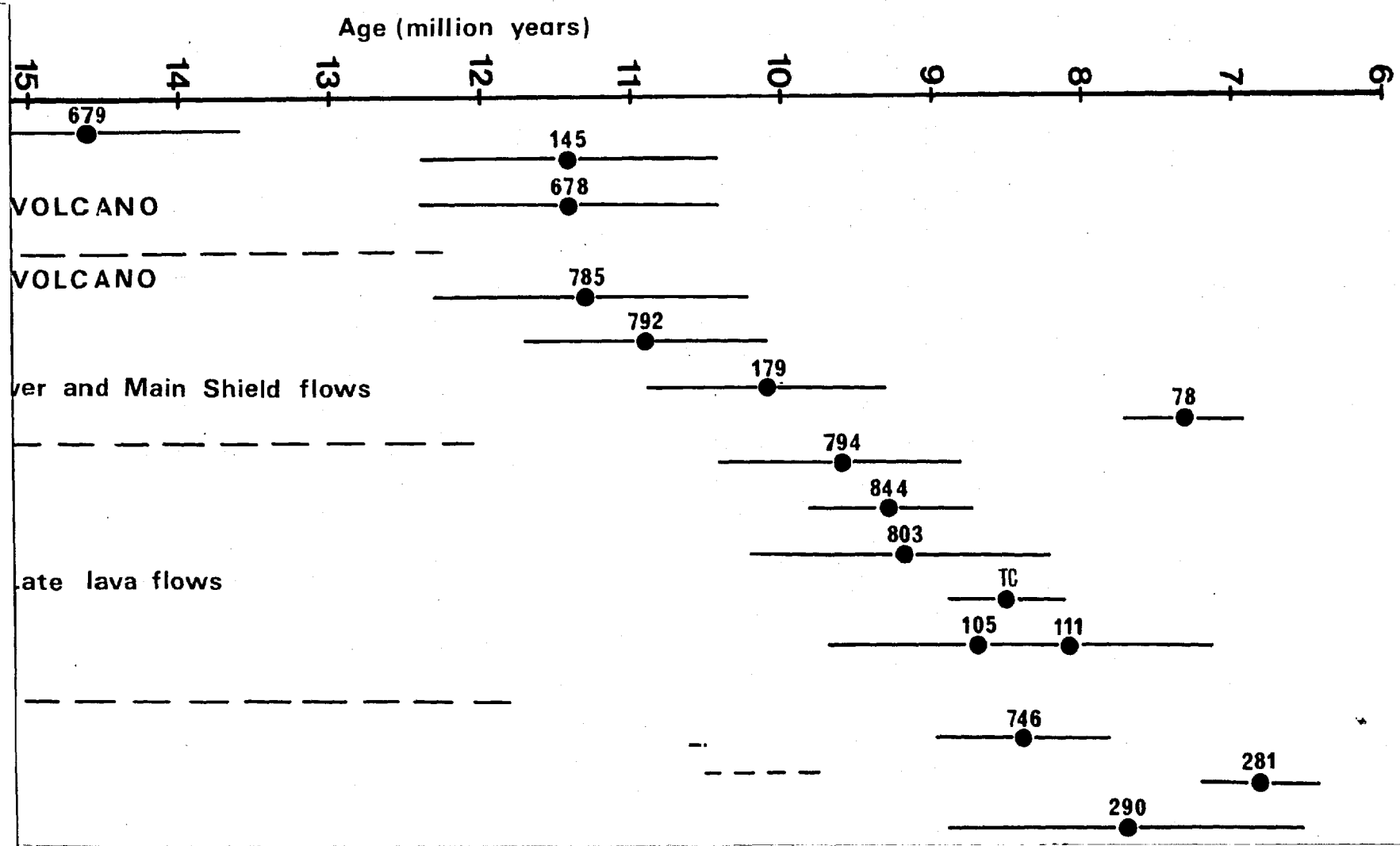
Age (million years)
15
14
13
12
11
10
9
8
7
6
679
145
678
VOLCANO
VOLCANO
785
792
179
ver and Main Shield flows
78
794
844
803
ate lava flows
TC
105
111
746
281
290

High Knoll, and the trachyandesite flows of White Hill will be discussed here. The chemical variations shown by these late intrusives will be discussed below (see also Baker, in press).

Some local activity occurred later than, or during, this intrusive episode. Castle Rock is cut by six thin (0.8-1.2m) vertical basaltic dykes. Another 5m trachytic dyke at Lot's Wife's Ponds is cut by a 0.6m basaltic dyke of almost identical petrography to those cutting Castle Rock. The irregular, highly altered Castle Rock sheet is itself bounded in the north-east by a thick fresh phonolite which may represent the latest intrusion in this area.

a. The alkaline dykes.

The distribution of the later alkaline dykes has been included in Enclosure 2; one thick and several thin dykes in Powell's Valley are included in Enclosure 4. The maximum development of these late dykes is in Sandy Bay and shows close correlation with the maximum concentration of earlier basaltic feeder dykes (cf. Encl. 2 and 4). There are three major dykes which form prominent lines of grey crags and scree across the multi-coloured basaltic products of the Lower Shield. The dykes extend for nearly 7km along the strike but they are never continuous for more than 800-1000m. They are frequently arranged en echelon and locally these offsets are related to thick (approximately 100m) horizontal, sill-like extensions (e.g. White Rocks). The pipes of Lot and Speery Island, and possibly Sheep Knoll, lying along two of these dykes, and the local extensions (vertical not sill-like) of the Asses Ears and Lot's Wife, may have actually broken the surface (see Plates 2, 6, 11, 13; Encl. 2).

The major dykes average 15-25m in thickness but may be extended to over 100m in Man o' War Roost, the Asses Ears

PLATE 11:

Phonolitic-trachyte pipe of Lot.

A: North-western face (height approx. 100m from ridge crest). Note irregular sinuous jointing of bottom right (developed close to chilled edge) and blocky, even rare columns of bulk of the mass.

On skyline left are the Peaks; immediately to the right is Sheep Knoll (?pipe) and ridge leading to White Hill (i.e. forming the eastern edge of Sandy Bay). The pinnacle just below the ridge is Partridge Rock - a locally extended basaltic dyke.

B: From the south-west - the most impressive view, near face is 200m high. Note alkaline dyke on line with the mass. The irregular, deeply dissected rocks of the lower shield are typical of Sandy Bay - numbers of dykes are obvious but larger numbers blend in with the thin detrital cover. Mt. Actaeon is the small peak (to the right of the tree) on extreme right. In 'hollow' below the Peaks the phonolitic-trachyte mass of Riding Stones Hill is visible.

PLATE 12:

Perfectly cylindrical trachyandesite pipe of The Niggerhead, from Man o' War Roost (note alkaline dyke in foreground), showing rather irregular sub-horizontal jointing. Completely altered material surrounding the pipe was originally thick basaltic flows of the Man o' War group.

Light patches beyond the Niggerhead are of wind blown calcareous sand (see Appendix). Note wave-cut platform (and dykes) extending along this windward coast.

Flows forming distant headland are from the Horses Head group.

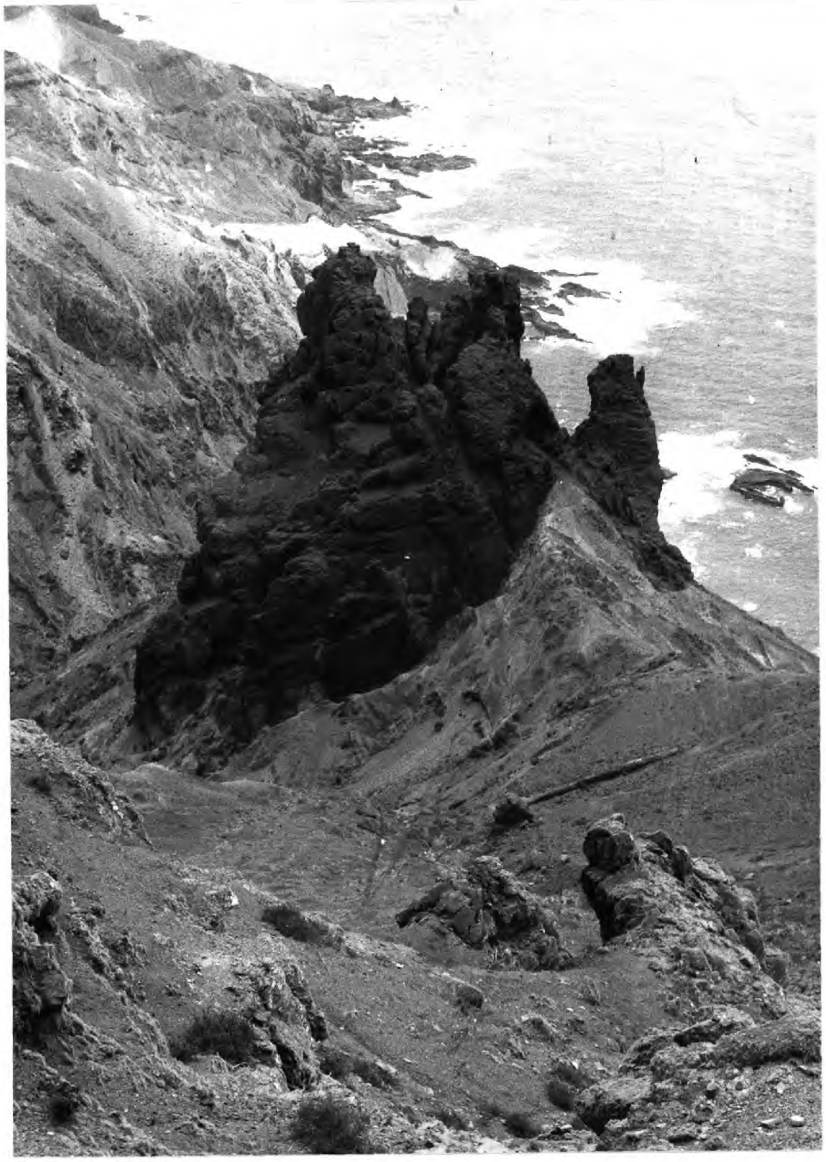

PLATE 13:

A: Highly alkaline guano-covered elongate pipe of Speery Island. Scale of photograph is difficult to visualize: the island is about 160m high, and the photograph is taken from ridge at 560m O.D. Sandy-looking material with black 'peak' is altered Man o' War flows. Island on right is Lower Black Rock (Man o' War flows as screens between thick NW-SE basaltic dykes). Island left of Speery is also a dyke ?alkaline) probably related to Castle Rock dyke.

B: Jointing (radiating, fan-like, columns) in western and south-western face of Speery Island. Extreme left is phonolitic-trachyte dyke of Castle Rock, and to right is a thin dyke adjacent to Speery (just visible in A).

C: Phonolitic-trachyte (?pipe-like mass) of White Hill East - White Hill off to right on skyline. Note jointing, blocky, irregular columns, and thin dyke cutting the mass. Light coloured altered areas on ridge are trachyandesitic flows of the White Hill area (see also Section VIII) their feeder dykes are not obvious in the photograph. Rock mass, right foreground is part of the Powell's Valley Hill intrusion.

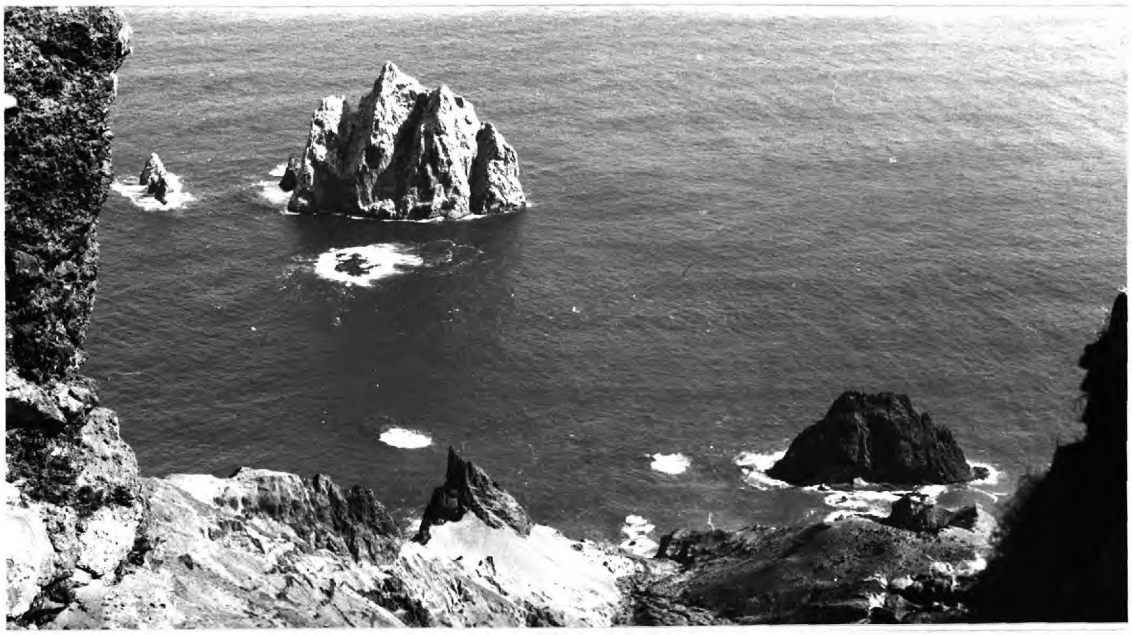

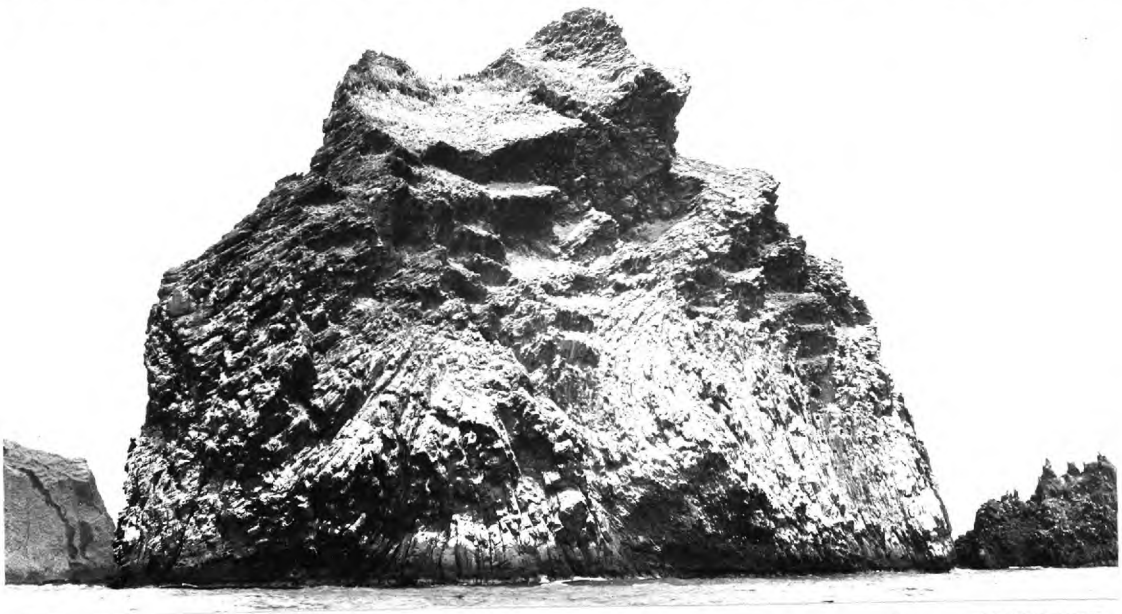

and Lot's Wife. The minor dykes may be 10m thick but are usually less. All of the dykes are sub-vertical, the northern one of the three major dykes dipping south-easterly at angles down to 75°, the southern two are less regular but are rarely more than 5° off vertical.

The dykes and extensions frequently exhibit thin chilled margins (especially well seen in the Asses Ears), and locally the Man o' War Roost and Lot's Wife masses are brecciated. Man o' War Roost is the only mass which shows evidence of multiple intrusion, with thin (1m or less) dykes cutting through the main mass (Plate 6A). Whereas the contacts with the country rocks are usually sharp the Man o' War Roost mass is characterized along both contacts by mixed breccias up to 5m thick of country rock + phonolite fragments. The actual phonolite dyke mass is locally brecciated in situ for thicknesses of 5-50m.

The Asses Ears mass in part resembles Man o' War Roost with a rounded north-eastern contact (Encl. 2; Fig. 12). Its southern margin is controlled by a phonolite dyke which becomes sheet-like (dipping 40° to the south-east) to the south-west and is again vertical in Castle Rock. The northern Ear appears to have a vertical contact but in the east a horizontal step several metres wide is developed. It is possible that the mass owes its irregular shape to intrusion at the intersection of two fissures. Thick north-south trending intermediate and alkaline dykes certainly occur north of Castle Rock and form the Narrow Ridge mass (Fig. 13). However, the mass appears to represent one single cooling unit and not a double injection (Plate 20B).

The phonolites are frequently altered at the contacts and exhibit two unusual textures, "spotting" and veining (Plate 14). The veining is primary and consists of local concentrations of aegirine ± alkali feldspar (see also Section VI).

PLATE 14:

Spotted phonolites, marginal rocks of the Man o' War Roost phonolite. There is no visible mineralogical control for the spots - even for the zoned and banded ones (some of which even form cubes). The veins are visible mineralogically and are explained in the text - they appear to be related only to marginal facies of this intrusion and also the Asses Ears.

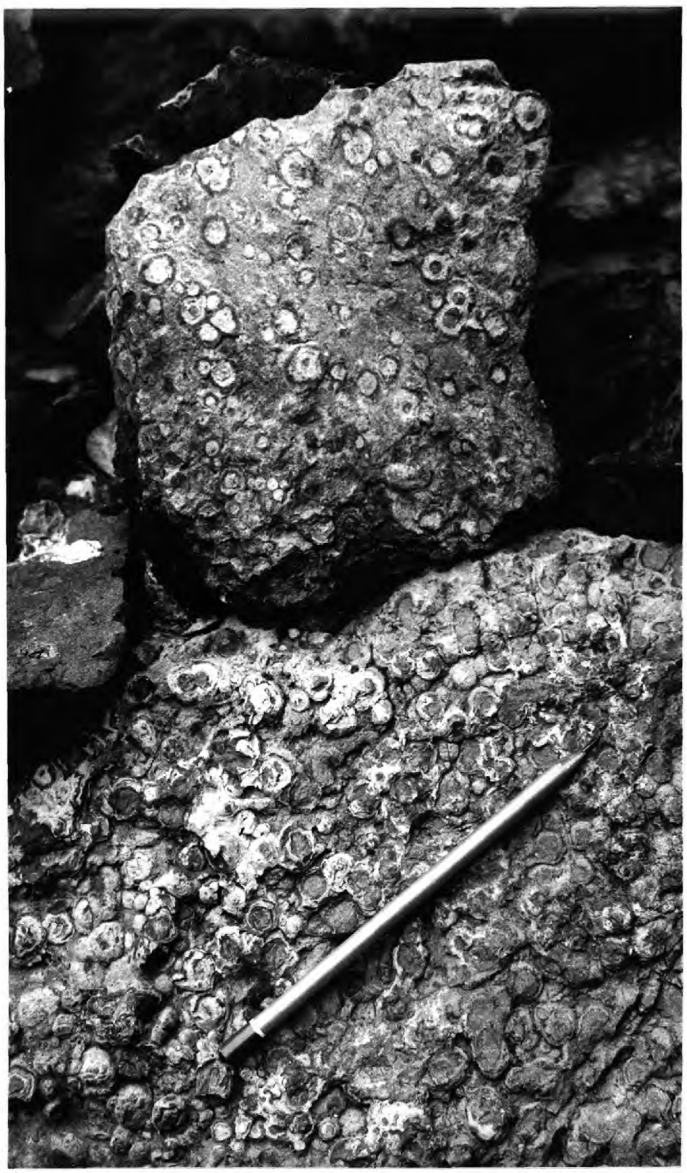

The "spots" in thin section show no mineralogical variation to the host rock, and are merely areas which have altered less than the enclosing rock.

Jointing may form at right angles to the sides of the dykes or may be distinctly irregular. Both Lot's Wife and Man o' War Roost have well developed columnar joints which are curved (Plate 6A). The thinner dykes, 5m or less, may develop closely spaced laminar jointing, and for this reason are usually altered. However, dykes less than 3m thick (down to 30cm) usually exhibit evenly spaced joints perpendicular to the contacts.

The dykes are occasionally slightly vesicular, small (1-5mm) vesicles are concentrated into bands parallel to the sides and large irregular ones develop in the geometric centre (see above: III,3b). The large central vesicles provide some very beautiful secondary carbonates.

Where the rocks on each side of the dyke can be correlated there is no evidence of vertical movement, and although the country rocks may be reddened, except in the rare cases of brecciation, they are not disturbed. The alkaline dykes therefore appear to result from the infilling of dominantly tensional fissures without extensive forceful injection.

b. Miscellaneous alkaline masses.

The alkaline intrusions in Thompson's Valley (Rush Knoll), 100m north of Sheep Knoll, and 500m east of White Hill are of uncertain origin (Encl. 3). From partial exposure and jointing the Rush Knoll mass appears to be a steep sided laccolithic body circular in plan with a diameter of about 240m and maximum thickness of not less than 65m. Overlying relic flows are gently domed above its domed vesicular roof. This vesicular zone has a maximum thickness of 6-7m and a virtually horizontal base suggesting an origin by the

accumulation of volatiles after emplacement. Similar textural variants are found in the flat parts of the roofs of the Powell's Valley Hill and Riding Stones Hill intrusions. In all cases these vesicular zones are very highly altered.

The intrusion north of Sheep Knoll appears to be a vertical pipe-like mass approximately 100m in maximum diameter with a slight north-south elongation. The mass is almost completely altered and locally is rich in xenolithic olivine basalt fragments.

The steep-sided mass east of White Hill (Plate 13) was recognized by Daly (p70, 1927), however, his suggested "phonolite" to the south is a locally thickened olivine basalt lava flow. The area is highly altered and contacts are not exposed but the form and jointing of the alkaline mass suggest that it may be an extended 'pipe'-like intrusion, similar to Sheep Knoll.

c. The Saddle parasitic centre.

The huge basaltic scoria cone near The Saddle was buried after only limited erosion, beneath flows high in the main shield series. These covering flows were already eroded before a trachyandesitic vertical sided intrusion broke through the cone about 300m north of the original centre and extruded a thick flow (Encl. 3). The original 'pipe' is about 300m in maximum diameter at the present level of erosion, and the flow, although badly eroded, must have originally filled a valley cut into the basalts which buried the cone. Even now the flow is greater than 70m thick. Although too altered for analysis the flow and intrusion, from their mineralogy, would fit into the pattern of systematic variation in composition of intrusions outwards from Sandy Bay (see below).

d. High Knoll.

The High Knoll parasitic centre still forms a topographic high south-west of Jamestown. The centre is composed of a basaltic-trachybasaltic double scoria cone intruded by an irregular trachybasaltic mass. The cones coalesced after initial independent activity and are composed of medium-grained scoria and rare bombs. One bomb measuring 5 x 1.2 x $>$ 1.2m retained sufficient heat after impact to redden the overlying scoria. The cones are asymmetric as a result of wind sorting, the finer material being distributed to the north-west. The central high parts of the cones consist of coarse agglomerate and rare spatter flows - the whole being highly altered to a soft, but resilient, homogeneous material formerly quarried for building blocks.

The elongate trachybasaltic intrusion (Encl. 3) is vertically sided and slightly off-centre. In the immediate area, and south, of the High Knoll Fort, apophyses intrude the scoria cone, and locally a sub-horizontal roof is preserved under coarse scoria. The intrusion is partly dyke controlled and to the north is a narrow, almost vertically sided mass with at least one dyke-like off-shoot. The east side of the intrusion displays broad curving sheet joints, similar to those in the near-vertical south-west side of Riding Stones Hill (Section IV). The intrusion broke through the north side of the cone and continued to the north-west as a thick multiple flow consisting locally of a number of units with scoriaceous bases. The flow on the north-west cliff tops is slightly more alkaline than the intrusion itself (this is quite common, see for example Thorarinsson, 1950; Vlodavetz, 1959) and is interpreted in the light of tapping a differentiated magma chamber to increasingly basic levels as the eruption continued (Baker, in press).

The High Knoll and Saddle intrusions have been included here because they may be related to the late alkaline intrusive episode. The High Knoll mass has a similar absolute age (Baker, et al, 1967); the Saddle flow is very much later than the cone; and chemically both masses agree with the progressive variation in the composition of the intrusive rocks.

The late intrusions and the late flow of the Saddle demonstrate one of the characteristics of St. Helenan parasitic activity: intrusions associated with parasitic scoria cones are much later than their 'host' cone. Many of the cones were buried under thick sequences of lavas before the intrusions were emplaced, and K-Ar ages suggest that the time interval between the explosive and the intrusive activities at an individual parasitic cone hase been from 1-3 million years.

e. Trachyandesites of the White Hill area.

A number of trachyandesitic dykes and flows are exposed south and east of White Hill (Encl. 3). The area is highly altered and trachyandesites are readily distinguishable because of their characteristic alteration. About 12 dykes (1-1.5m thick) with constant trend at 60° are concentrated into an area 650m by approximately 1000m (perpendicular and parallel to the strike respectively). The lavas originally flowed over an irregular topography, cut into rocks of the Main Shield, and are preserved up to 1km away from their suggested feeder zone. Trachyandesitic dykes of this local group cut the phonolitic-trachyte intrusions of Powell's Valley Hill and east of White Hill (Plate 13C).

Two thick (total 125m) trachybasaltic flows form the summit of Sandy Bay Barn, an elongate ridge 2km south-south-east of White Hill (Encl. 3). Relic patches of these flows

are preserved on the steep cliff faces forming the seaward end of the ridge. These lavas appear to have flowed along a small valley (now forming the topographic high of Sandy Bay Barn) and plunged over less precipitous cliffs (than now) to the south and south-east. A thick trachyte dyke (7-15m), also trending 60°, extends up to the unconformable base of the trachybasaltic flows.

The thick trachytic dyke and the alkaline intrusions east and north-east of White Hill belong to the late highly alkaline intrusive phase. The trachyandesites of White Hill, and the trachybasalt of Sandy Bay Barn, are later than these intrusions (the trachybasalts apparently the latest). This suggests too, that they are younger than the east flank activity of the Bencoolen - Stone Tops area.

A further discussion of these lavas and their possible relationships to the late intrusive phase is included in Section VIII where the geochemistry of these intrusions is discussed.

SECTION IV

ARCUATE INTRUSIONS

1. Field Occurrence.

Cone sheets and ring dykes were first described from Scotland early this century; since then they have been extensively described from all over the world. Most of these arcuate intrusions have diameters of several kilometres, and many are greater than ten kilometres across. The central block of a ring dyke system, however, may be as little as one kilometre in diameter (Richey and Thomas, 1930; Jacobson et al, 1958), and Hawaiian pit craters (Wentworth and Macdonald, 1953) have diameters at the surface of a few hundred metres or less.

On St. Helena a number of arcuate intrusive masses are exposed, which, with one exception, have outer diameters of less than 1000m. The intrusions are of three distinct types:

a. Irregular basic sheets dipping inwards at high angles.
b. Inclined cone-like sheets dipping inwards towards an inclined axis.
c. Large trachytic intrusions with near-vertical sides and infilled roof cavities.

In the first part of this section the forms and field relationships of these types of intrusion are described. In the second part the possible mechanisms of their formation are discussed. A small appendix has been added to describe the geology adjacent to one intrusion (White Point) where its

complexity would detract from the main theme of this section.

a. Steeply inward dipping basic sheets.

The only two examples of these structures known on the island lie 300m and 1300m south of Hooper's Rock. Neither example is visibly associated with a parasitic centre, and little is known of their age, except that they are younger than the lowest flows of the Main Shield series. Both occur in highly altered areas, and relatively fresh material is restricted to relic spheroidal blocks. Petrographically the smaller basaltic mass (716) is distinctive in thin section, containing spectacular poikilitic titan-augite. The larger mass (715) is of weakly porphyritic basalt with phenocrystal olivine, titanaugite and plagioclase.

The variations in attitude of the intrusions are shown in Fig. 15. The 715 sheet maintains a thickness of 7.5m along the vertical eastern exposure, but this increases in the north and west to about 15m. The western part is not seen in direct continuation with the better exposed eastern part, but the structure appears to form an entity. The 716 sheets are more variable in thickness, the central value of 5-7m increasing to nearly 20m in the north and south (Fig. 15b).

The contacts between the sheets and country rock at both localities are sharply defined and non-brecciated; the margins of the intrusions are chilled. The apparent correlation of two flat-lying basaltic sheets intruding the Devil's Cap pyroclastics (Fig. 12 "B") suggests a 20m uplift of the block enclosed within the 715 sheet.

Intense alteration and thick vegetation have obscured certain critical details of the 716 intrusives. The dip of the flows within the arcuate sheet appears to be

FIGURE 15:

Basic intrusive sheets with high angle inward dips.

a: Poorly exposed sheets on ridge south of Hooper's Rock due east of Devil's Cap (cf. Fig. 12). Exposure may be considered in a horizontal plane.

b: Very small scale arcuate sheets, due south of Hooper's Rock. Topography slopes regularly from west to east through a vertical height of 130m. Note increased dip of basalts inside the 'cone.

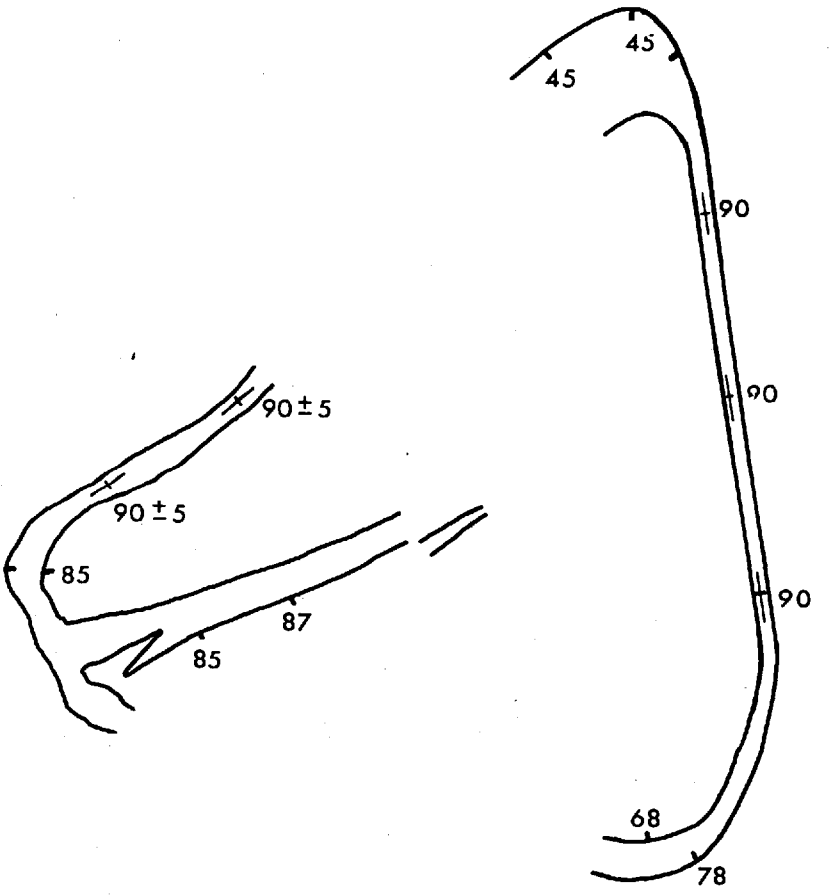

a (715)

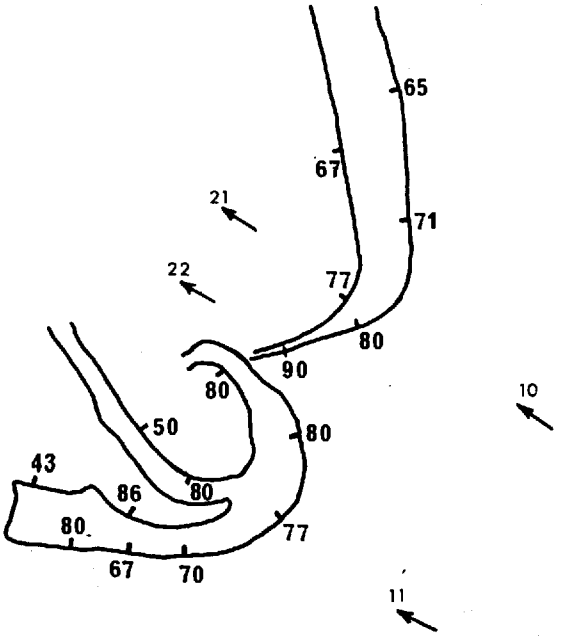

b (716)

FIGURE 15

slightly greater than the dip outside (20° and 10° respectively). There is however, no distinct change in the attitude of the lavas higher up the side of the ridge, and the variation may reflect minor tilting. The attitudes of the lavas forming Hooper's Ridge do show slight variations south from Hooper's Rock, and it is possible that the Ridge area as a whole has been gently bowed, independent of the tilting inside the sheet. In the south-western extremity, in the side of Hooper's Ridge, there is no vertical displacement of pyroclastics across the sheet, and there is no visible disturbance at the contacts. The intrusion stops abruptly beneath a thick sequence of lavas, but a thin band of pyroclastics separates the intrusion from the lavas. The intrusion shows no evidence for breaking the original ground surface, and is not mantled by the pyroclastics. This type of relationship may be compared with Fig. 10g (the dykes are cutting the same pyroclastic horizon) and the basaltic intrusion into the Sandy Bay pyroclastics (Section III, 2b). In all cases field evidence strongly suggests that the intrusions are younger than the overlying massive lavas:

(i) Pyroclastics above and at the sides of the intrusions are 'baked' by a comparable amount.

(ii) The overlying thin pyroclastics are not mantling the 'intrusion'.

(iii) The overlying thin pyroclastics are not updomed, brecciated, or in any way disturbed.

(iv) The lavas rest conformably on the pyroclastics and are not affected by the intrusions.

The structures therefore appear to represent intrusion into a cavity opened in pyroclastics underlying an undisturbed thickness of lava flows. The relationships described above may be produced under conditions allowing an initial tensional

fracture to form in incoherent* pyroclastics and then open by gradual intrusion of lava. Slip within the pyroclastics may relieve the stress conditions to such an extent that the overlying more massive lava sequence is virtually undisturbed by the process.

From the small scale nature, irregular attitudes, and relationships to the country rock, of these arcuate intrusions (715, 716), their mechanism of formation appears to be dependent upon tensional conditions at high level in the volcano.

b. Inclined cone-like sheets.

Four of the eight intrusions of this type are closely associated with formerly large scoria cones. In all localities where these sheets have been recognized the exposed section has been at right angles to the symmetry plane of the fracture. Plate 10B displays the typical shape of these intrusions, which are usually more than 200m in maximum cross-section. Two much smaller arcuate intrusions however, are believed to be structurally related. The locations, sizes and rock types of these eight intrusions are given in Table 1.

The arcuate fracture dips inwards at a low angle in the central area, and at the sides the inward dip increases markedly (Plate 10B). The amount of 'closure' of the fracture - i.e. the maximum observed dip at the sides - decreases with increasing diameter (Table 1). The Prosperous Bay Beach arc (Plate 15A) is almost completely circular, as is that of Tripe Bay (Plate 15B). The Great Stone Top "feeder" turns through more than 90^{o} on the northern side (Plate 10B), as does the sheet of Rough Rock and possibly High Hill (Plate 16). The Shark's Valley and Thompson's Valley fractures show an

*Sub-aerial pyroclastics weather easily and rapidly to alteration products rich in clay minerals.

Location	Rock type	Associated with scoria cone	Completene of arc
Prosperous Bay Beach	Basalt	No	300°(360°?
Tripe Bay North	Trachyandesite	?	270°(360°?
Sandy Bay Beach	Trachybasalt ?Trachyandesite	Yes	205°
Rough Rock	Trachyte	No	approx 200
Great Stone Top	Trachyte	No	210°
High Hill	?Trachybasalt	Yes	195°
Thompson's Valley	Trachytic	Yes	100°(180°?
Sharks Valley	Trachyandesite	Yes	115°

TABLE 1.

Maximum thickness (T)* (metres)	Maximum diameter (D) (metres)	Ratio T:D	Minimum dip*	Depth of section below ground surface at formation (metres)
3.5	24	1:7	10-15°	? > 500
35	145	1:4	< 15°	≥ 300
11	230	1:20	25°	
50(modified?)	250	1:5	low	300
60	360	1:6	15°	250
20	350	1:17	10-15°	
12	525(780?)	1:44	10-15°	
30	665	1:22	20°	175

* Maximum thickness and minimum dip usually occur in the topographically lowest part of the exposed sheet.

increase in dip, but remain much more open than their smaller equivalents. The smaller masses are relatively thick compared to those with larger diameters (cf. for example the intrusions of Shark's Valley and Great Stone Top).

Although the rock types infilling the fractures show a complete range from basalt to phonolitic-trachyte, all of the intrusions display well-developed columnar jointing where the angle of dip is low (Plates 10B, 16). This jointing may change to more or less regular sheet jointing parallel to the fracture sides in more steeply dipping parts.

The Prosperous Bay Beach mass is unusual in that the original fracture infilling is of medium-grained basalt (carrying small phenocrysts dominantly of plagioclase) while the central part of the mass is of highly porphyritic pyroxene-olivine basalt. The later inner intrusion apparently forced out the block of basaltic flows originally contained within the fracture and reheated but did not damage the original sheet. The trends of later basaltic dykes which cut the intrusions, or approach it closely, should be studied in Plate 15A.

The material inside the arc of Tripe Bay, resembling cemented basaltic agglomerate through field glasses, was not positively identified (Plate 15B). If the material is agglomerate, it may be derived from a scoria cone which is completely buried beneath the flows of the cliff. If this interpretation is correct the material inside the arcuate intrusion must have moved seawards in relation to the cliff as a whole.

The intrusions of Rough Rock (seen only from a boat) and Shark's Valley are associated with local tilting in the adjacent rocks (see Plate 17). The Shark's Valley fracture appears to die out upwards at both ends (Fig. 13,

PLATE 15:

A: The tiny (25m diameter) Prosperous Bay Beach basaltic inclined cone-like sheet. Note closely-spaced prismatic joints perpendicular to contacts throughout the exposure.

Note jointing of central, later porphyritic basalt, and the curvature of later dykes within the intrusion and one outside on the right which possibly followed a fracture developed at the same time as, and concentric to, the main arcuate fracture.

B: Trachyandesitic inclined cone-like intrusion north of Tripe Bay. Again note prismatic jointing at lower levels and modified in left hand side (cf. Plate 10A). Material inside the sheet is unidentified. Central one third of cliffs shows trachybasalts from the Old Joan centre, overlain by regular, thinner flows at high levels of the main shield series.

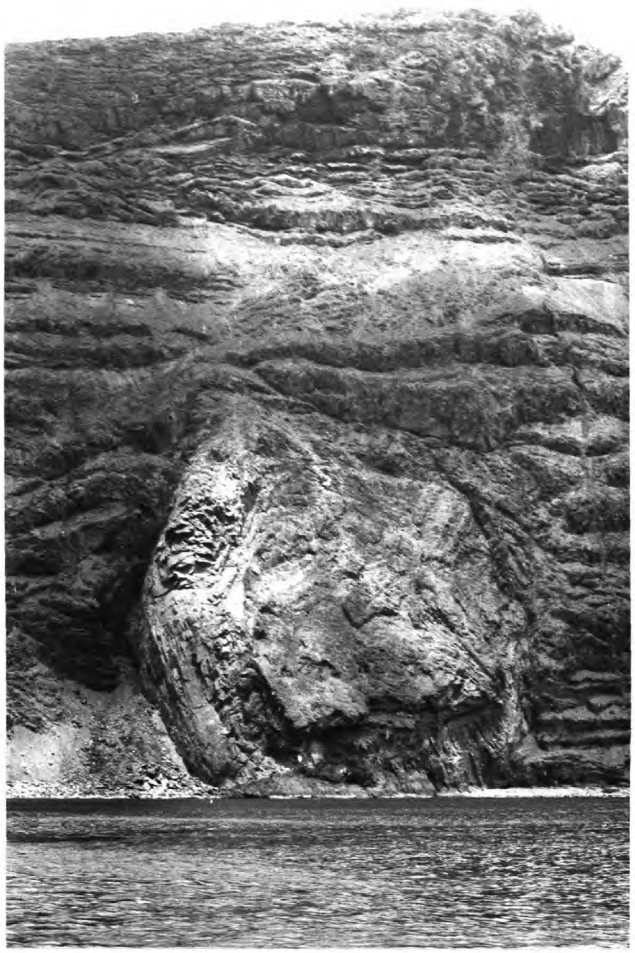

PLATE 16:

Inclined cone-like sheet below High Hill (see Plate 19). Note the excellent prismatic jointing in the thick, lower, parts becoming less distinct upwards. The sharp contact above the sheet is between basalts of the main shield series and the underlying basaltic scoria cone of Centre 3 of the High Hill parasitic group.

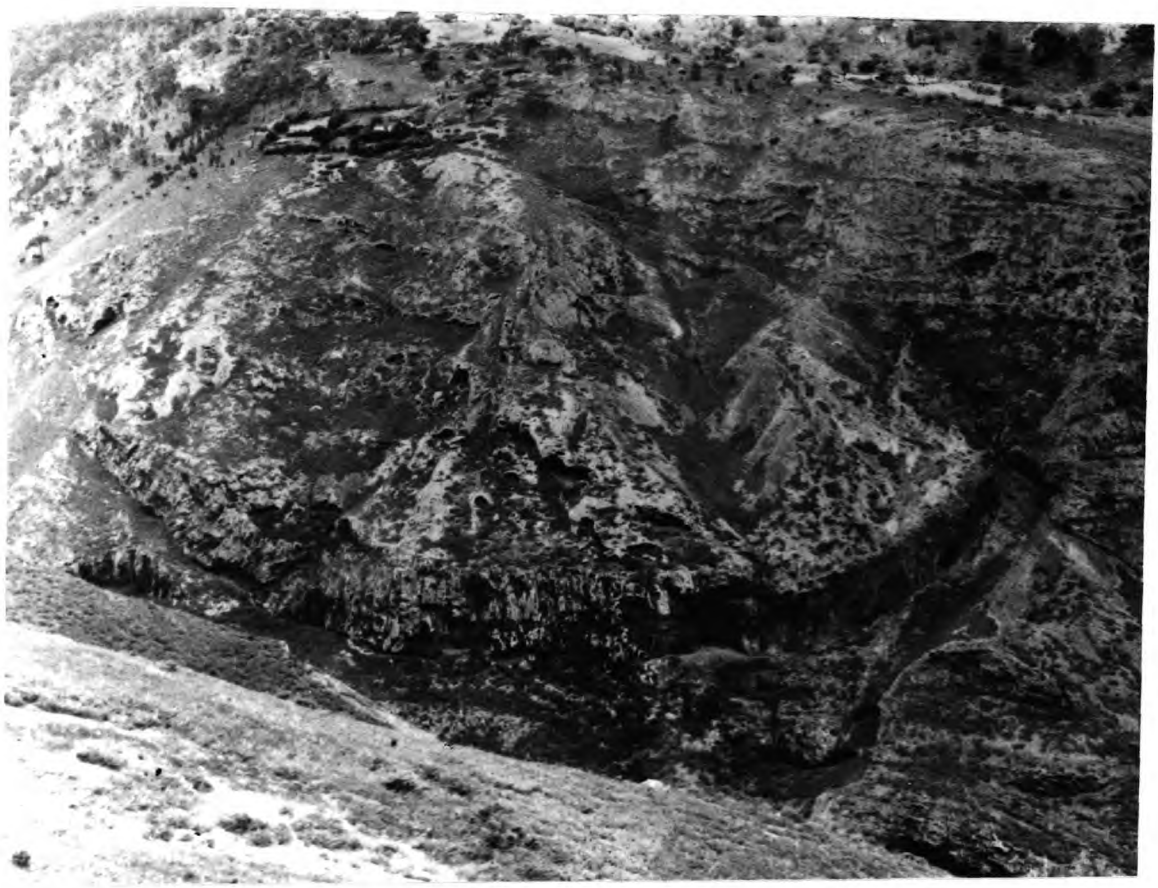

PLATE 17:

Composite view of Sharks Valley and Bencoolen, from col between Little and Great Stone Tops (left and right foreground).

Regular, thicker, columnar jointed basalts and early trachyandesites of the upper shield series rest on basaltic flows of the main shield.

A: Highly altered upper shield flows between Longwood Plain and Horse Point.

B: Flagstaff Hill (north-eastern volcano) and slightly to right Knotty Ridge.

C: Western end of The Barn.

Arcuate cone-like sheet extending from D to H in the valley side cuts scoria cone G and upper shield flows updoming the overlying trachyandesites (D and G) and the later (?local) basalts (I).

F: Trachyandesite feeder dyke, continuing down to left, of Bencoolen (C to E) flow group, which initially flowed inland and south round Little Stone Top (left) because of doming by the arcuate sheet.

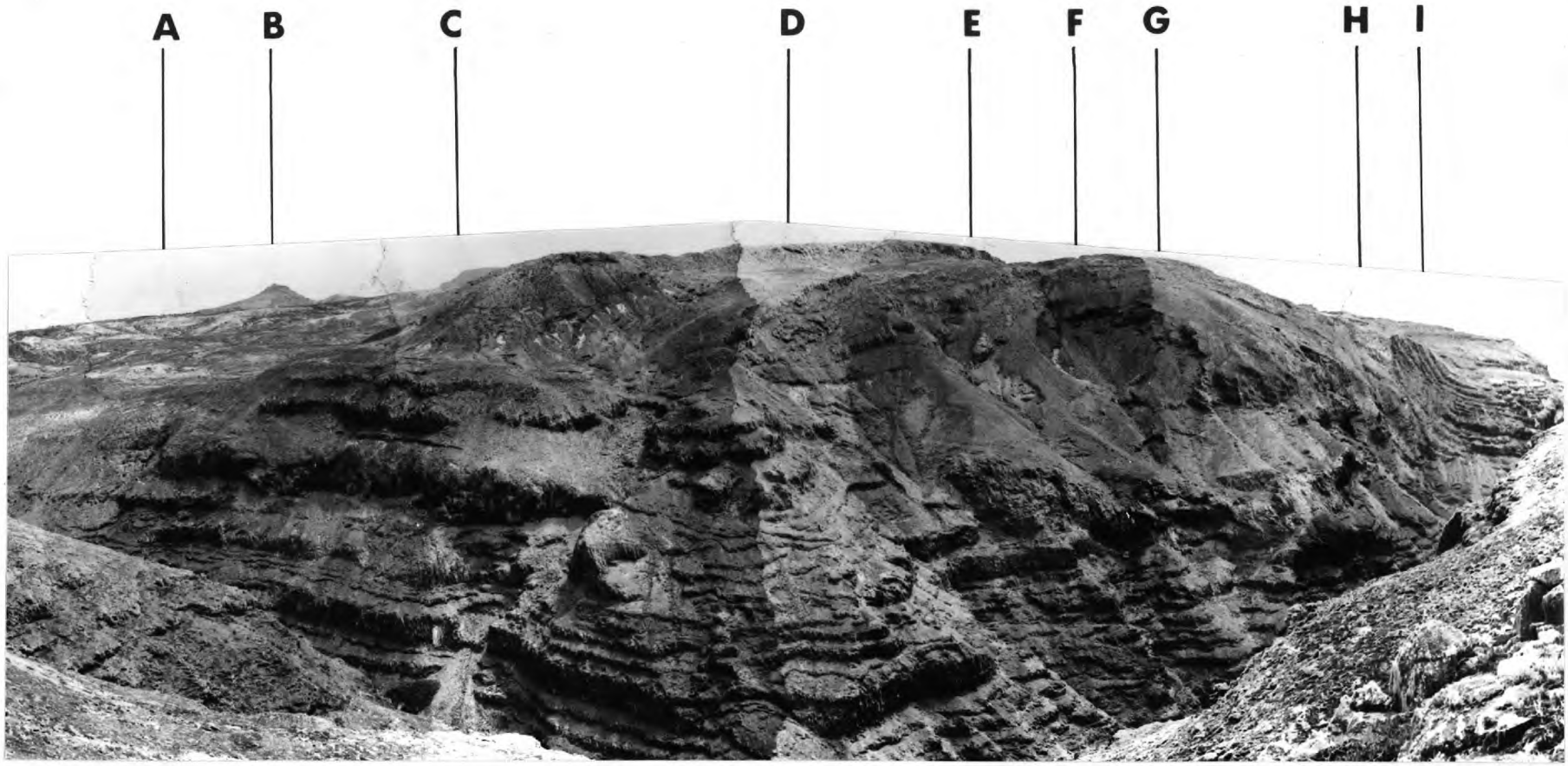

Plate 17

Plate 17), and the area inside and above the intrusion has been uplifted. The uplift of the flows at the edges is calculated at 30m, which is equal to the maximum thickness of the intrusive sheet. The entire block of country rock appears to have been uplifted as a unit by the injection of trachy-andesite into the fracture. The geometry of the fracture leads to the almost horizontal base being opened most (30m), and the steeply inward dipping sides being opened least ($<$1m). The bending of lava flows to steep angles in a short horizontal distance is a not uncommon feature in areas associated with local intrusions (see for example Gibson et al, Fig. 16, p30, 1966). It is probable that the structure associated with the Sharks Valley intrusion represents two distinct processes. First, an initial build up of local stress was abruptly released fracturing the rocks along a sharply defined arcuate fracture. Secondly, ensuing gradual injection of magma infilled the fracture, uplifted the overlying block of country rock and plastically deformed those rocks lying immediately above the terminations of the fracture.

At the smaller Rough Rock intrusion processes similar to those suggested for the Sharks Valley sheet appear to have gone a step further. The initial intrusion of lava into the fracture caused the adjacent basalts to bend through 55°. Continued intrusion of lava then appears to have extended the fracture forcing it to cut through the initially tilted basalts. The lowest parts of the arcuate mass are bulbous and less regular than other masses, which led Daly (1927, p54) to call it a "chonolith". However, there appears to be another trachytic sheet, above the more obvious arcuate mass, concordantly intruding the overlying basalts and its relation to the main arcuate sheet is unknown.

The arcuate intrusion of Great Stone Top is probably the most impressive of these fractures because of its

FIGURE 16:

Arcuate trachytic sheets associated with the Great Stone Top flow dome. Figures show dips of contacts, dash denoting direction. Western arc is a nearly perfect inclined cone-like intrusion (Plate 10); the other two somewhat irregular masses are explained in the text.

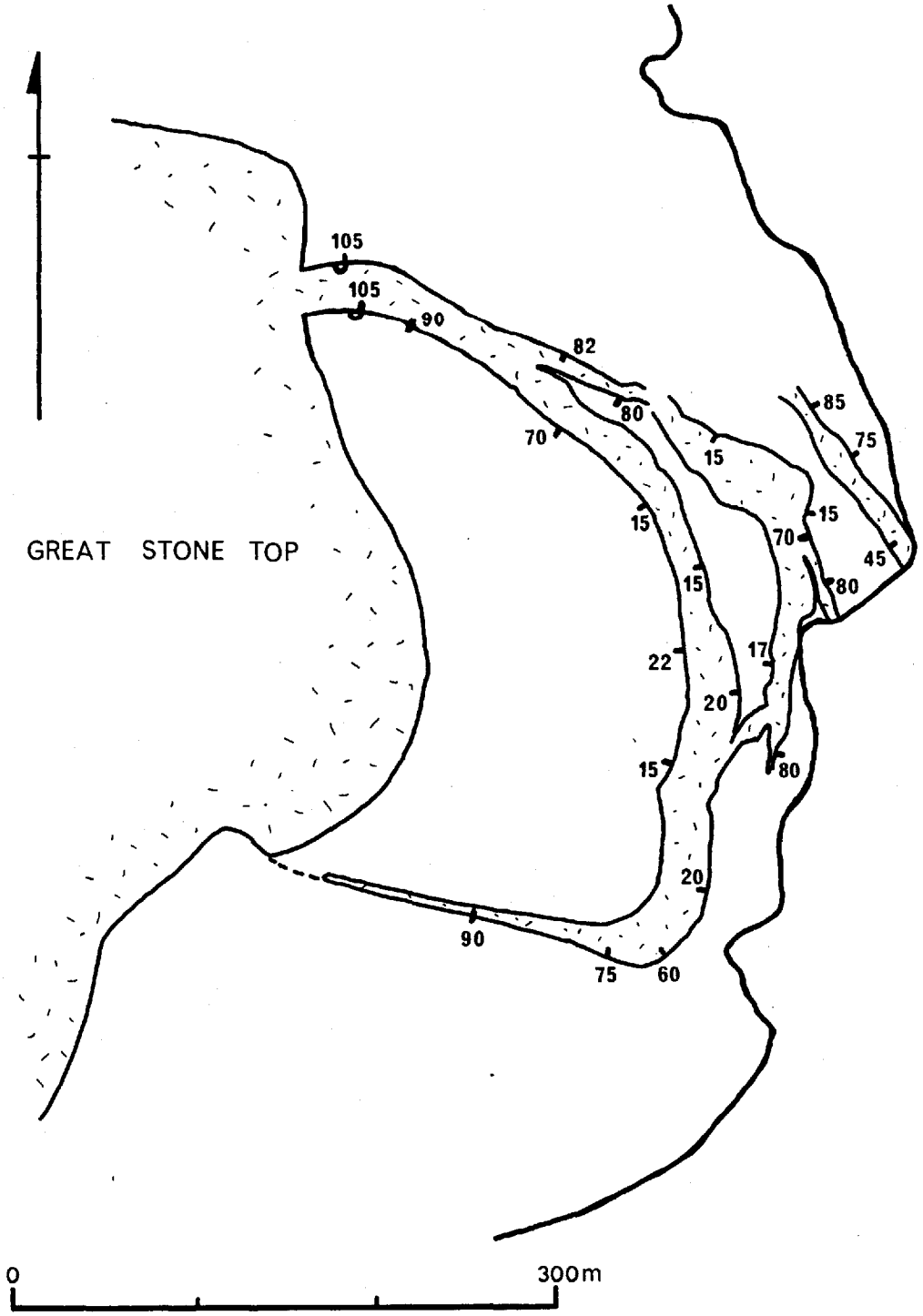
GREAT STONE TOP
105
105
90
82
80
70
15
85
75
15
70
15
45
80
15
22
17
20
15
80
20
90
75
60
0
300m

FIGURE 16

exposure in an almost sheer 500m cliff face (Plate 10B). The intrusion is unique on the island in that it actually fed at least one of the massive Great Stone Top flows. This obvious intrusion is only the most perfectly developed of three arcuate sheets, the attitudes of which are shown in Fig. 16. The eastern sheet dips easterly at moderate to high angles. The central sheet, although somewhat irregular, dips partly to the east at high angles and partly to the west at low angles. These two components are similar to those of the eastern sheet, and the low angle part of the main arcuate intrusion (Fig. 16). The high angle intrusions are thin (less than 10m), and appear to be only locally opened and infilled by magma.

The movement of the block inside the main Great Stone Top fracture relative to the basalts outside is obscure. From the attitude of the base of the flow dome it is thought that the central mass has moved down-dip (seawards) and upwards to allow the intrusion of 60m of trachyte. The weight of the overlying thick pile of trachytes may have assisted this movement by increasing the load on the "heel" of the slipping block (the basalts underlying the trachytes are bowed gently downwards, Plate 10B).

c. Steep-sided roofed arcuate masses.

Five intrusions of this type have been recognized on St. Helena, and their localities and dimensions are given in Table 2. All of the intrusions except White Point are of comparable age being formed after cessation of shield-building activity of the south-western volcano (see above). The White Point mass is believed to be older than the others because of its complete alteration, its unusual mineralogy and its possible relationship to the Thompson's Valley flow (Section III). Although High Hill and White Point are closely

Location	Maximum dimensions exposed (m)	Degree of curvature exposed	Thickness of roof cavity (m)	Associated with earlier scoria cone	Uplift of country rocks (m)
Hooper's Rock	590 (circular)	210°	60 (or less)	?	<50
Powell's Valley Hill	450 x ?730	160°	>15	No	None apparent
White Point	345 x 580	355°	35 (or less)	Yes	approx. 65
High Hill	750 (?circular)	180°	40-approx 80	Yes	slight
Riding Stones Hill	900 x 1070	210°	Max. approx 110	Probably	None exposed

TABLE 2

associated with large scoria cones, the direct correlation of Riding Stones and Hooper's Rock is impossible because of the present state of erosion. Powell's Valley Hill appears to be unrelated to any former scoria centre.

Contacts of these intrusions demonstrate that they have steeply inclined sides which may dip outwards or inwards at angles rarely more than 10° off vertical. The intrusions have roofs which are regularly inclined at low angles to the horizontal. The transition from side to roof, where actually exposed, is obvious and forms either a gradual curve (Riding Stones Hill) or a sharp angle (Hooper's Rock). Primary joints are well developed and are usually parallel to the exposed contacts and flow oriented tabular feldspars (see especially Figs. 17 and 22). Because of the lack of good exposures of the contacts the primary joints were mapped to give as close approximation as possible to the original forms of the intrusions. Calculations of the thickness of the roof cavity of the intrusions are largely based on these relationships. In exposures which cut through the side and roof of an intrusion, the position where the joints change from high to low angle was usually taken as the approximate position of the base of the roof cavity.

(i) Hooper's Rock

The outer contacts of the sides dip outwards at angles of about 80°. The basalts within 300m of the contacts on the northern and north-eastern sides, and those overlying the roof cavity, have been uplifted and tilted to angles of 25-40°. On the other sides of the intrusion and more than 300m away to the north-east the country rocks are totally unaffected.

Jointing (Fig. 17) close to the sides forms broadly spaced high angle sheets (1-3m apart), but near the top is in

FIGURE 17:

Phonolitic-trachyte roofed intrusion of Hooper's Rock. Lines denote primary jointing (single bar) and flow orientation of alkali feldspars (double bar).

Dashed line indicates position of change from sub-vertical joints of the side to flat-lying joints of the roof cavity.

Two sections are at half the scale of the plan - vertical and horizontal scales approximately equal. Note the absence of updoming in SE and SW.

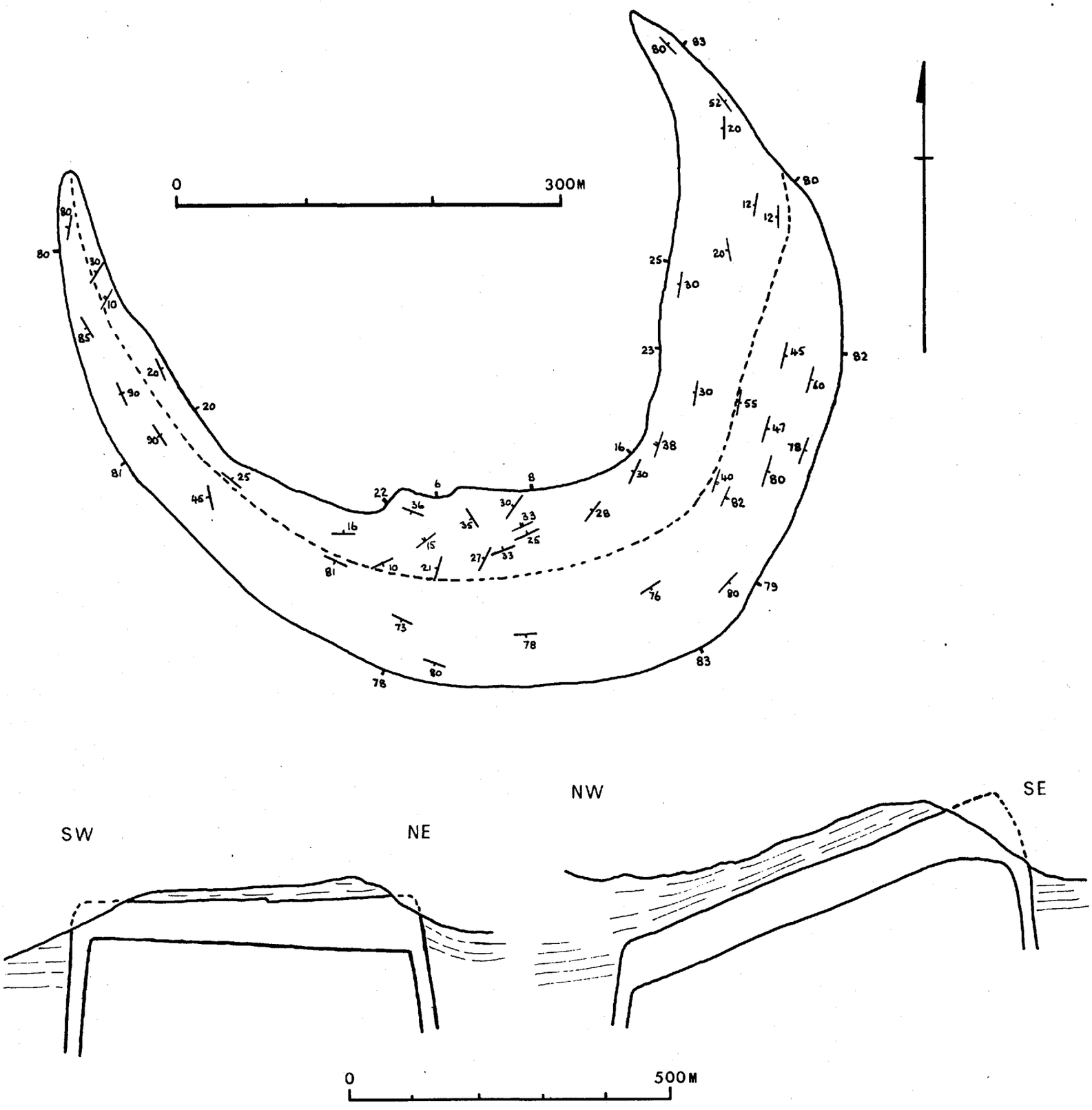

FIGURE 17

thinner sheets (less than 0.5m), parallel to the roof, dipping north-westerly at about 25°. The change in attitude of the joints is abrupt (cf. Riding Stones Hill) and occurs at slightly variable heights below the roof-top on the eastern side (Fig. 17). Although elsewhere the orientation of joints and feldspars is closely parallel, at the side/roof transition the orientations of the feldspars show a gradual change over a vertical height of 10-15m.

The roof of the intrusion is smooth and concordant with the overlying flows and pyroclastics, but is stepped (3m) at one point. The immediately overlying tuff is baked for 25cm above the mass, but minor colouration extends upwards for 1m.

The variation in the jointing in the western "prong" (Fig. 17) suggests that along this side the high angle "ring dyke" may be 15m thick. Theoretically the collapse of a block bounded by a ring fracture dipping outwards at an angle z° will provide a side opening dependent on the distance (T) through which the block drops. The horizontal apparent thickness of the "ring dyke" will therefore be: T cot z°. The change in the attitude of the jointing in the eroded sides and roof of Hooper's Rock suggests that the roof cavity is about 60m thick. If the side fracture dips outwards at 80°, collapse of a central block through 60m will theoretically open an annular side cavity with a horizontal apparent thickness of just over 10m (60 cot 80°).

Hooper's Rock is unusual in that it has outward dipping sides associated with (minor) uplift of the adjacent country rock. In other examples uplift is typically associated with vertical or slightly inward dipping fractures. The irregularities in the structures however, make positive comparisons difficult.

(ii) Powell's Valley Hill.

The Powell's Valley Hill intrusion is a poorly exposed, almost completely altered trachytic mass (Fig. 18). The roof is flat-lying and dips to the north-east at angles less than 10°. The north-west contact dips outwards at a high angle, and the attitude of the jointing in the valley sides suggests that this outward dip is uniform round the exposed parts of the intrusion. Nothing is known of the thickness of the roof cavity or of the steep arcuate sides.

The Sheep Knoll mass, 600m to the north, appears to be controlled on its north-west side by a dyke. From the exposed outline of the Powell's Valley Hill body it is conceivable that the two masses are related, lying on a single "ring" fracture. A north-south elongation of the arcuate fracture could result from collapse in an area already cut by major north-south dykes (Fig. 18). If Sheep Knoll is controlled by the Powell's Valley arcuate fracture, then it is later than the main collapse block, extending even now over 200m above the roof top. However the existence of the pipe-like masses north of Sheep Knoll and east of White Hill (Fig. 18) could lead to the interpretation that all of the masses are governed by a north-south zone of weakness, the Sheep Knoll mass being modified by intrusion alongside an earlier resistant dyke.

(iii) White Point.

At the present levels of erosion the White Point intrusion is the most complex of the arcuate bodies (Figs. 19 and 26). The mass as a whole is quite well exposed, 100% altered, and is the only arcuate intrusion which can be traced through 360° of an arc.

On the western side up to 350m away from the intrusion the basalts into which the mass is intruded are

FIGURE 18:

Intrusions north and east of White Hill.

1: Pipe-like mass north of
2: Sheep Knoll, also pipe-like.
3: Powell's Valley Hill with attitudes of jointing and contacts.
4: White Hill East (Plate 13C) phonolitic-trachyte, possibly also pipe-like.
5: Possible hypothetical line of arcuate fracture of Powell's Valley Hill collapse feature.

Flat roof of 3 is at 430m, road at 'b' at 480m, and 1 at 650m above sea level.

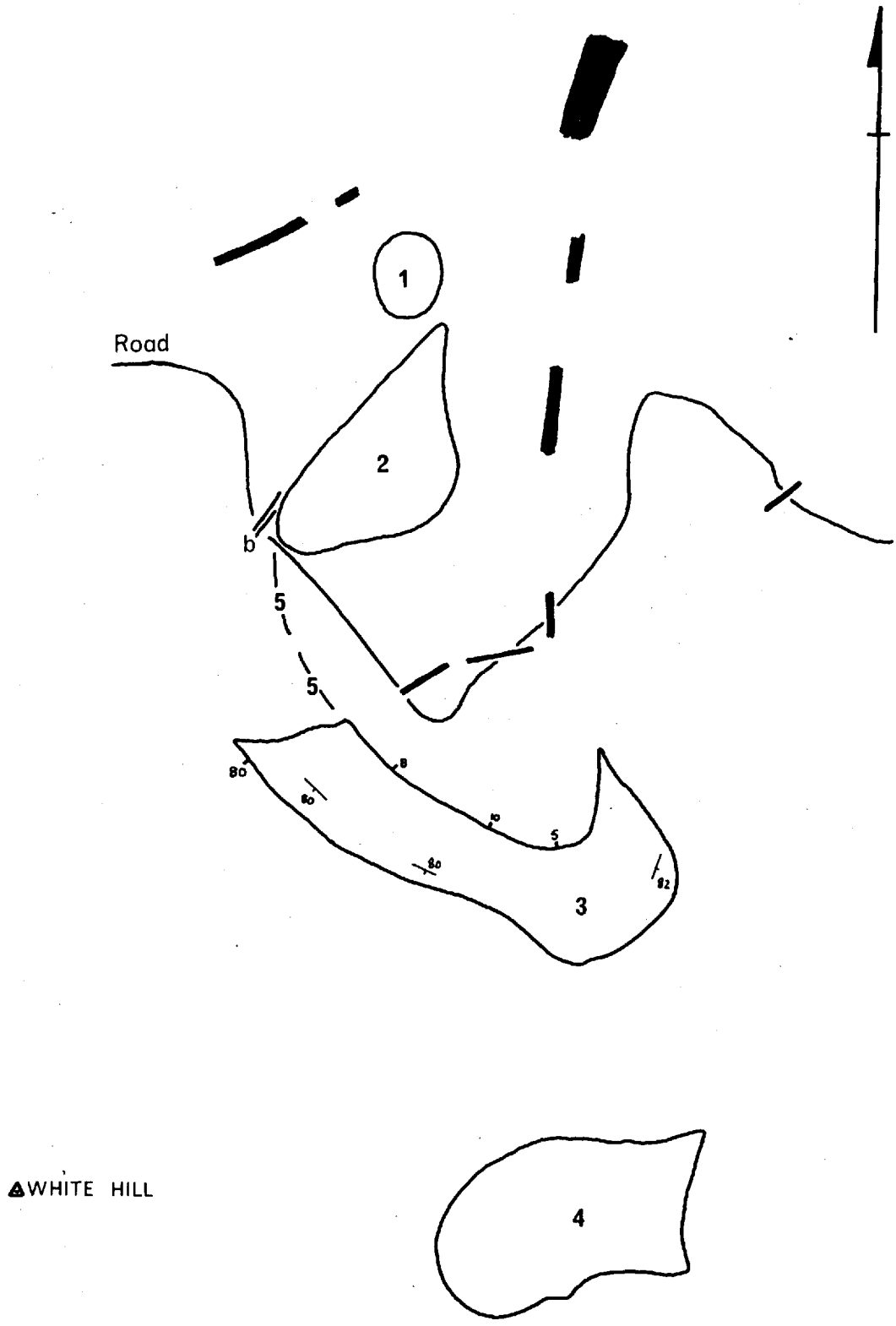

FIGURE 18 .

FIGURE 19:

White Point trachyandesitic roofed intrusion, showing attitude of jointing and contacts - note variations along eastern side. Dotted areas are zones of brecciation (see Plate 18). Dashed lines are basic-trachyandesitic breccia dyklets explained in text (Section III, 4b).

X = basaltic roof relics

Sections at half scale of plan; vertical and horizontal scales approximately equal.

Continuation of arcuate fracture and development of "sills" caused by continued high magmatic pressure (see Fig. 25, 5).

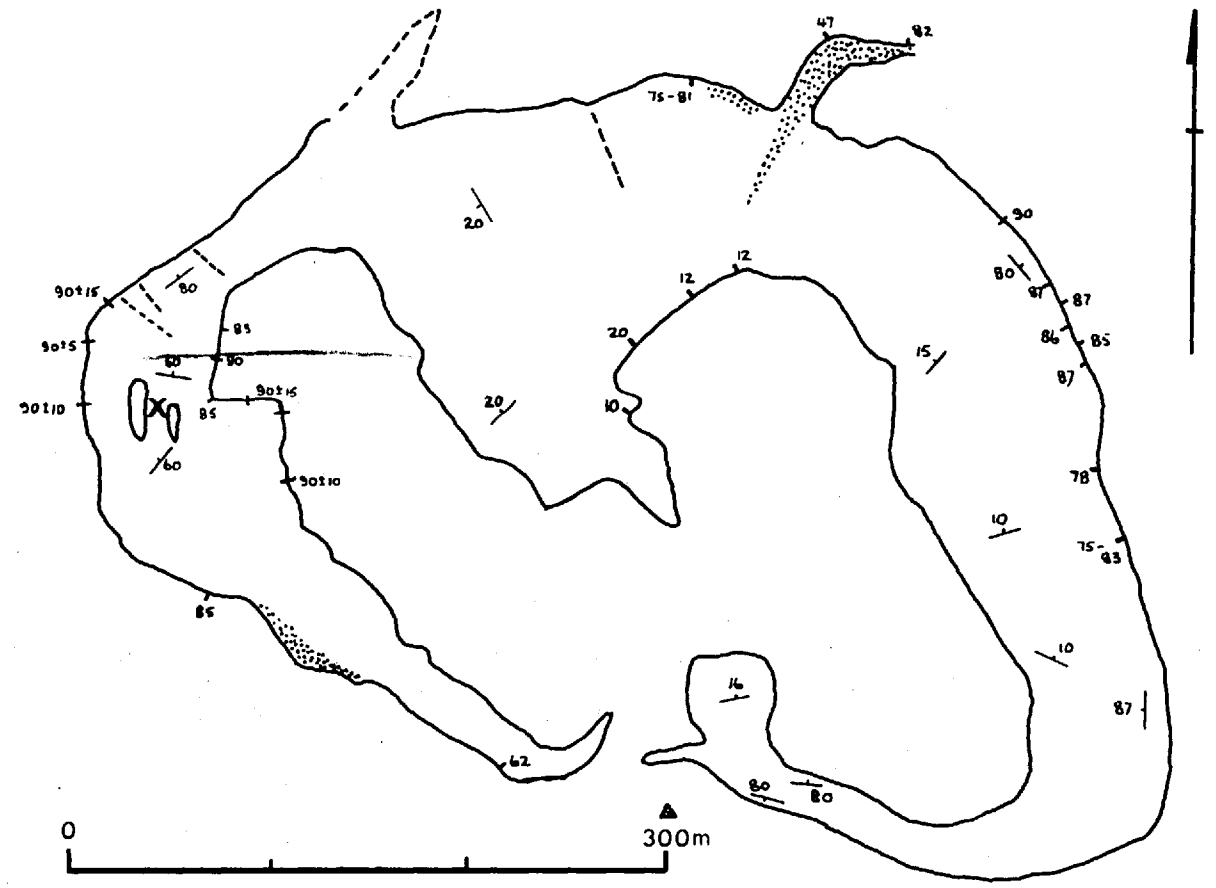

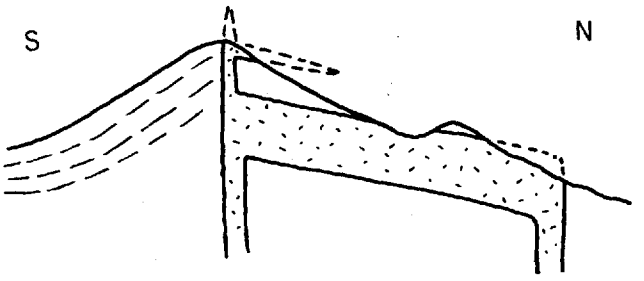

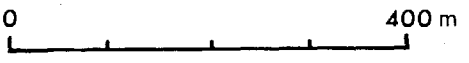

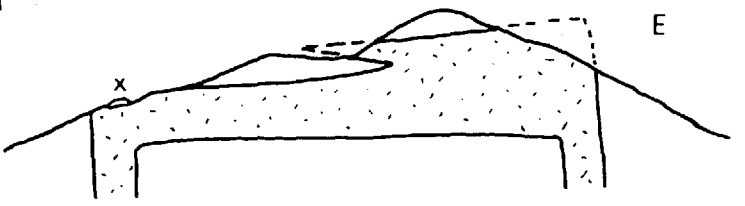

FIGURE 19

oversteepened and locally are vertical. The tilting stops abruptly, and within less than 50m the attitude of the flows changes from 40° to the west-south-west, back to the regional dip of 10° to the north-west (Fig. 26).

The contacts are rarely exposed for more than a metre in vertical section, but appear to be more variable than those of other intrusions. The outer contacts round most of the body are within 5-10° of vertical (Fig. 19). Slightly more of the measured contacts have an inward dip component, and at one locality on the south-west side the contacts dip inwards at 62°. The roof of the collapse cavity dips regularly to the north-west at about 20°, but the top of the intrusion is complicated by at least two sill-like off-shoots (Fig. 19).

Although both contacts of the north-western corner of the intrusion are locally sub-vertical, two sub-horizontal relic patches of country rock rest on the trachyandesite (Fig. 19"X"). These measure 3 x 10 x ?m and 7 x 25 ?m and may represent former roof cappings, preserved as a result of stepped movements of the bounding fracture. The outer contact south-east of this locality, and the northern extremity of the intrusion, are extensively brecciated (Plate 18, Fig. 19). The breccias consist of more or less angular, large platey fragments of trachyandesite, and appear to result from fragmentation of parts of an earlier consolidated ring intrusion caught up in a later trachyandesitic pulse (see below).

(iv) High Hill.

The trachytic intrusion of High Hill is the most impressive of these larger masses, with sheer cliffs up to 170m high (Plate 19). The mass is formed by three intrusions, two along arcuate fractures and a later one along a linear fracture. The relation of the intrusion to the country rocks

PLATE 18:

Brecciated margins of White Point trachy-andesite.

A: Angular-tabular breccia along western contact possibly related to continuation of arcuate fracture after consolidation of earlier intrusion (see text).

B: Northern margin, brecciated area within intrusion which continues into breccia dyke and mass of Fig. 26 (indexed 8 on map).

Note sub-angular to sub-rounded edges and continuous gradation in size of fragments (originally irregularly vesicular with altered secondary mineral infillings).

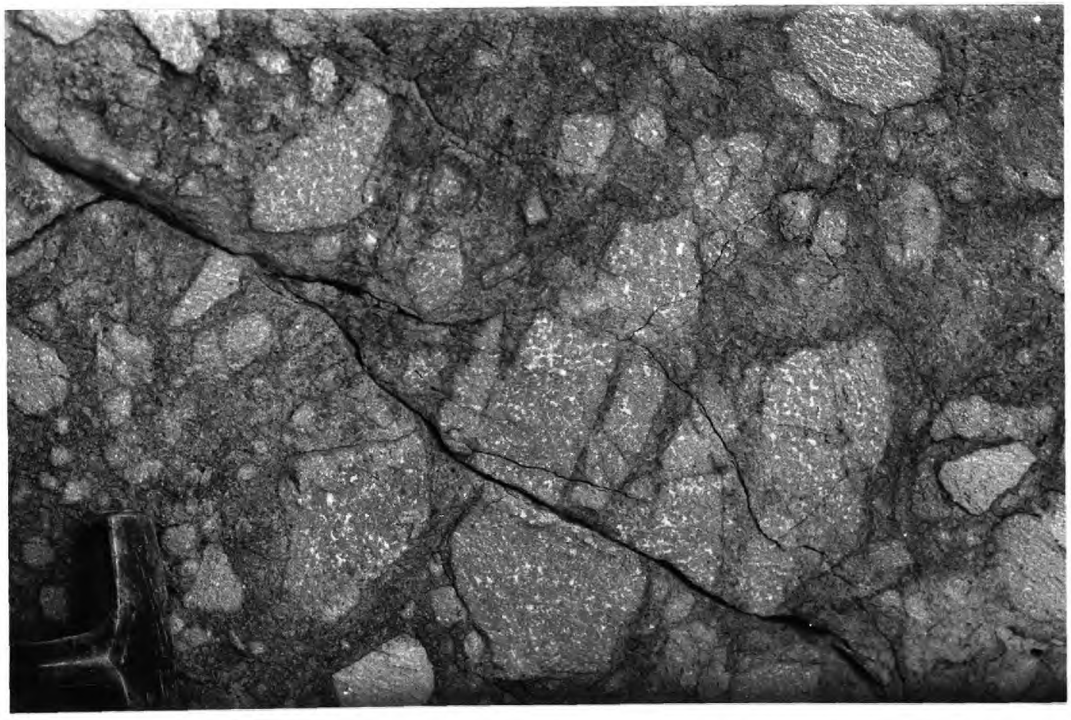

FIGURE 20:

Multiple trachytic roofed intrusion of High Hill, showing dominant jointing - flow orientation of feldspars shown by double bar.

"X" : two scoriaceous screens explained in the text.
b : order of emplacement of intrusions
1 : initial high angle "ring" body with roof cavity
2 : second concentric arcuate intrusion
3 : final N-S dyke-controlled mass (Plate 20A).

Sections are drawn at $\frac{2}{3}$ scale, through summit of High Hill.

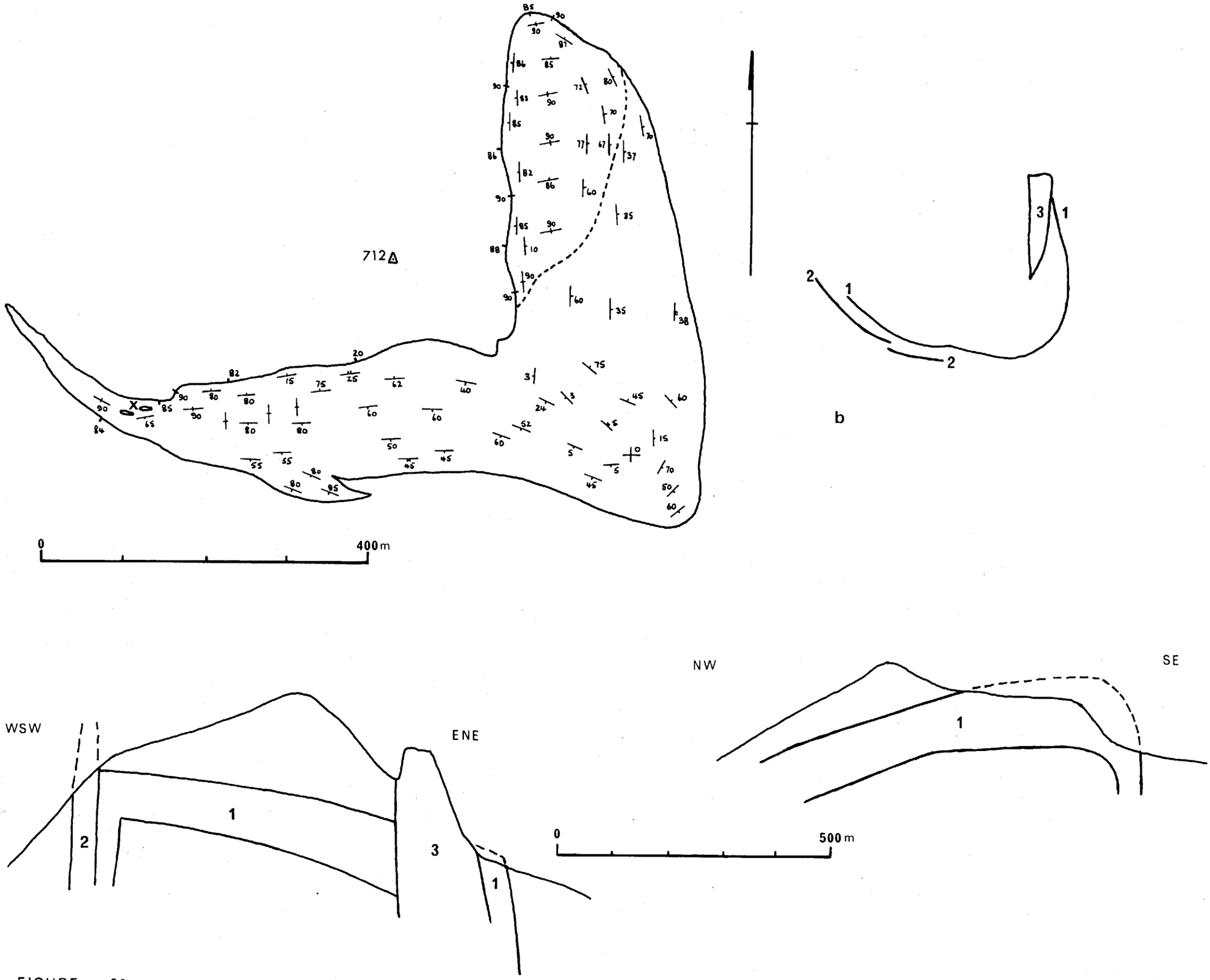

FIGURE 20

PLATE 19:

Composite view of High Hill and area. Central ridge (locally = Spyglass) separates Swanley Valley from Old Woman's Valley.

Early scoria cones of High Hill area, extending from beyond A to G, interdigitated in part with the main shield flows and were eventually buried completely beneath them with the regular contact well exposed from E to G. Compare with Fig. 11.

A: Inclined cone-like sheet (Plate 16).

B: White Point.

C: Rounded jointing of roof/side of intrusion 1 of High Hill trachyte.

D: Steep sided north ridge - intrusion 3 of High Hill trachyte.

E: Summit of High Hill; scoriaceous trachybasaltic (?local) flows resting on scoria cone (Centre 6, Fig. 11).

F: Limit of scoria of Centre 6 - main High Hill scoria cone - and some main shield flows overlying it.

H: Thompson's Valley Island.

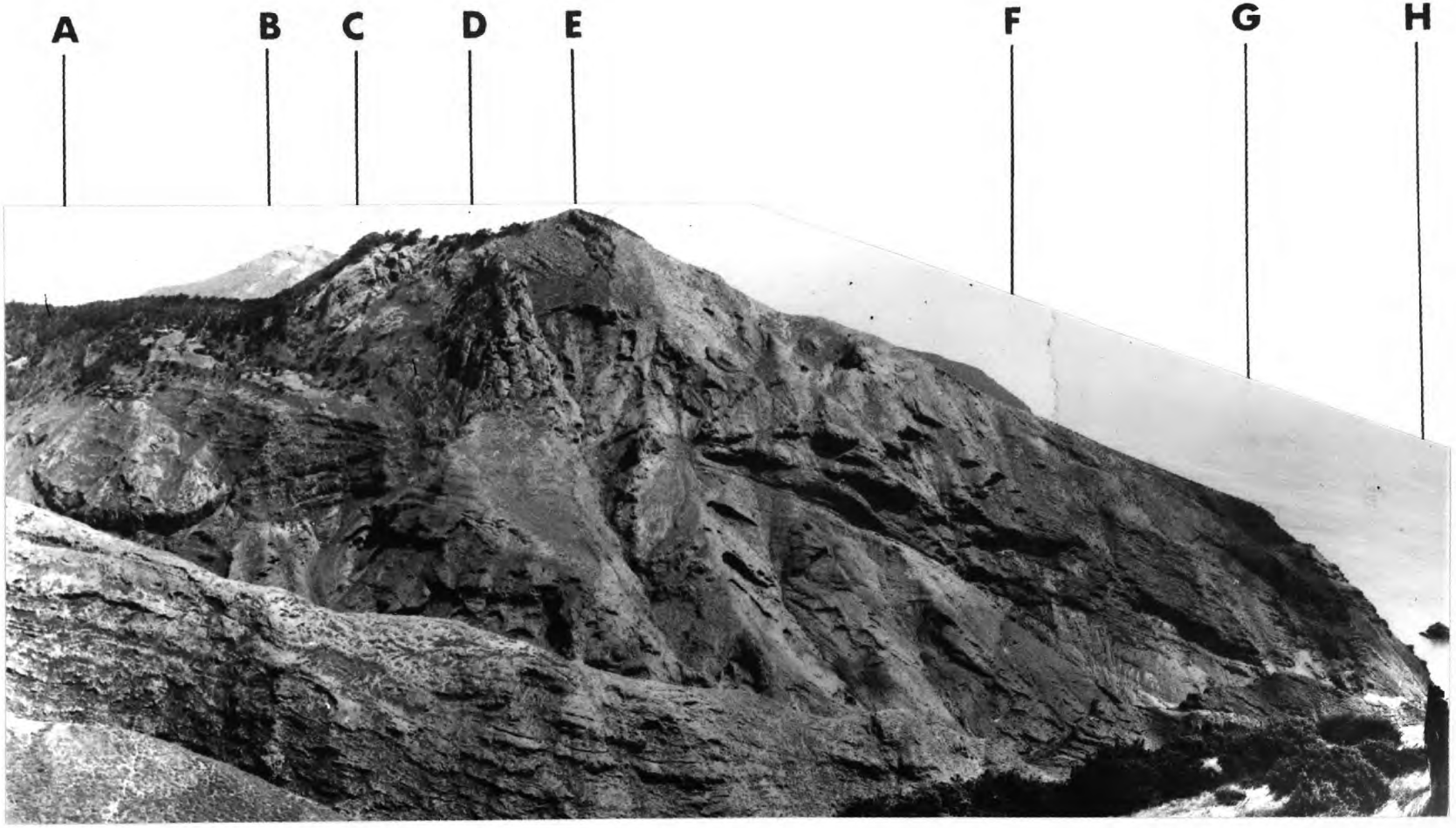

Plate 19

'167

is shown in Fig. 11, and a more detailed diagram of jointing and contact relations is given in Fig. 20.

The High Hill intrusion shows little evidence of uplift of the adjacent rocks. The dip of 35° of the highly scoriaceous and vesicular flows forming the summit is largely due to original attitude of deposition - however, a tilt of 10° may be inferred from flows immediately adjacent to the western edge of the body.

The gradual curve of jointing in the east and north-east outer parts suggests that the roof in these areas is domed rather than flat (cf. east of Riding Stones Hill, Plate 21). However, the sharp break in jointing along the southern cliff suggests an angular, 'wall/roof' relationship. These variations undoubtedly reflect changes in lithology and attitude of bedding in the overlying scoria and scoriaceous lava flows and result in its variable estimated thickness (Table 2). In the south and south-east, the attitude of the jointing suggests a cavity thickness of under 40m, but the gradual curve along the eastern side suggests that 80m would not be too high.

A second minor arcuate intrusion is believed to form the outer contact of the intrusion in the south-west, apparently concentric with the earlier arcuate mass. Evidence for this is taken from the unusual outline along the south-west contact and from the occurrence of two screens of country rock caught up in the near-vertical intrusion (Fig. 20"X"). Both masses, aligned parallel to the intrusion contacts, are about ten metres long, and from three to five metres across, and are composed of scoriaceous lava fragments (cf. flows of Fig. 11). An irregular zone in the adjacent (higher) trachyte is slightly brecciated, and its orientation suggests that it may be related to the roof of the early intrusion.

PLATE 20:

A: Jointing in the north ridge (intrusion 3) of the High Hill trachyte. Joints are dominantly sub-perpendicular to the length of the ridge; note slight curvature. Compare view in Plate 19 showing sheets (with some curvature at top) sub-parallel to the length; and the rounded north end (see text), and also Plate 21B.

B: Asses Ears from the north, looking along the length of the northern Ear (cf. Plate 6). Dominant tabular joints, developing into columnar joints on the western side of the southern Ear. Note continuity of structure along whole of the western (right hand) side; and outward sloping columns on both sides.

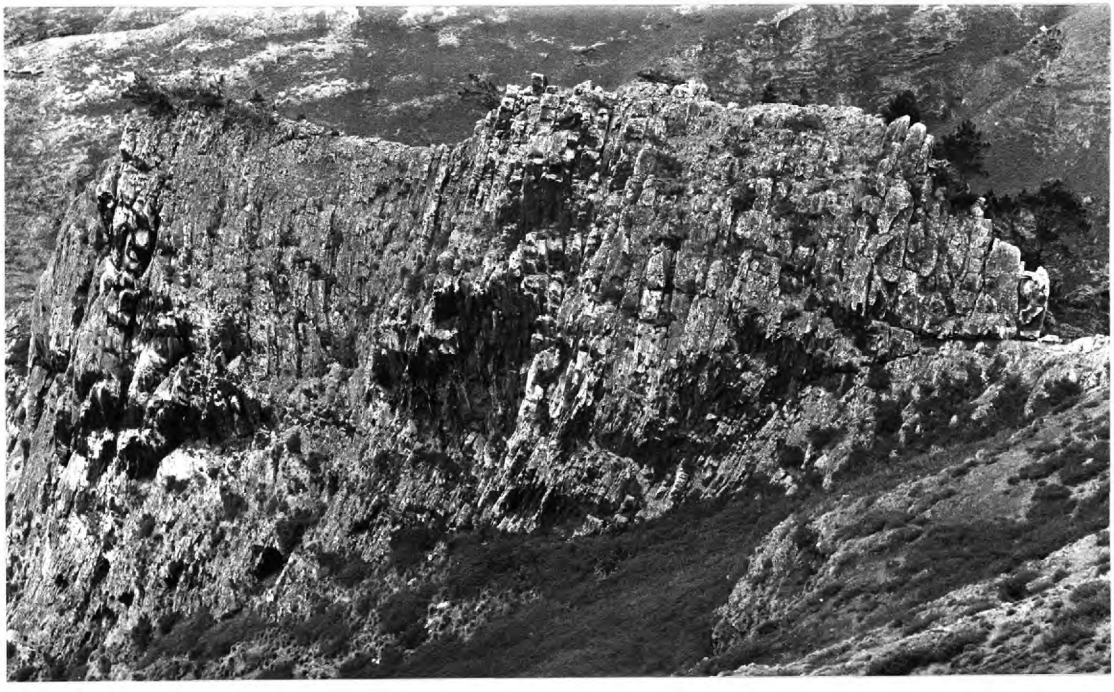

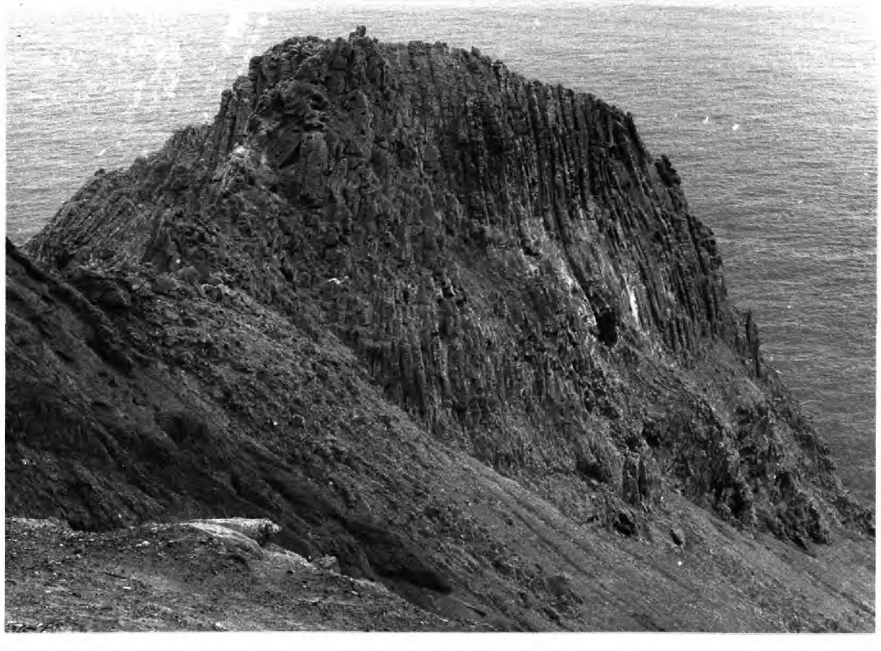

The jointing of the sheer-sided northern ridge is almost vertical, orientated in two sets parallel and dominantly perpendicular to the ridge (Fig. 20). The sudden change from the broad curved jointing of the eastern side of the main intrusion contrasts markedly with the abrupt cliff of the north ridge (Plate 19). Plate 20 shows the similarity between this part of the intrusion and the jointing displayed by the Asses Ear phonolite dyke extension. The contact of the north end of the ridge is chilled, weakly brecciated, and curved in plan; this compares very closely with the east side of the southern Asses Ear and the western extremity of Man o' War Roost (Encl. 2). This sub-vertical extremity of the High Hill intrusion is believed to be later than the arcuate intrusions, and is controlled by a north-south fracture (cf. north-south dykes in Encl. 4). The proposed sequence of intrusions is shown in Fig. 20b.

(v) Riding Stones Hill

The Riding Stones - Chapel Rock intrusion is the largest arcuate body on the island (Fig. 21). The north-east - south-west elongation, the straight south-east contact, and the thin dyke east of Chapel Rock clearly demonstrate some control of the arcuate fracture by the earlier NE-SW dyke swarm of Sandy Bay.

The intrusion is unusual in that the roof has been completely removed in the south-west, and the top of the central block is exposed (Plate 21). The material, highly altered porphyritic scoriaceous flows, agglomerates, and finer pyroclastics, cannot be accurately equated with material outside the mass. It is certainly not comparable with the Fairyland pyroclastics or the overlying lava flows (as exposed on Scott's Hill), but could be equated with the White Rocks upper pyroclastics as exposed in the east wall of Sandy Bay.

FIGURE 21:

Largest arcuate roofed intrusion - phonolitic-trachyte of Riding Stones-Chapel Rock. Jointing and contacts shown as in earlier figures.

Black lines are trachytic dykes associated with the western edge of the intrusion; those south of Virgin Hall are related to the main high angle outward-dipping arcuate fracture.

Compare this plan with the photographs of Plate 21.

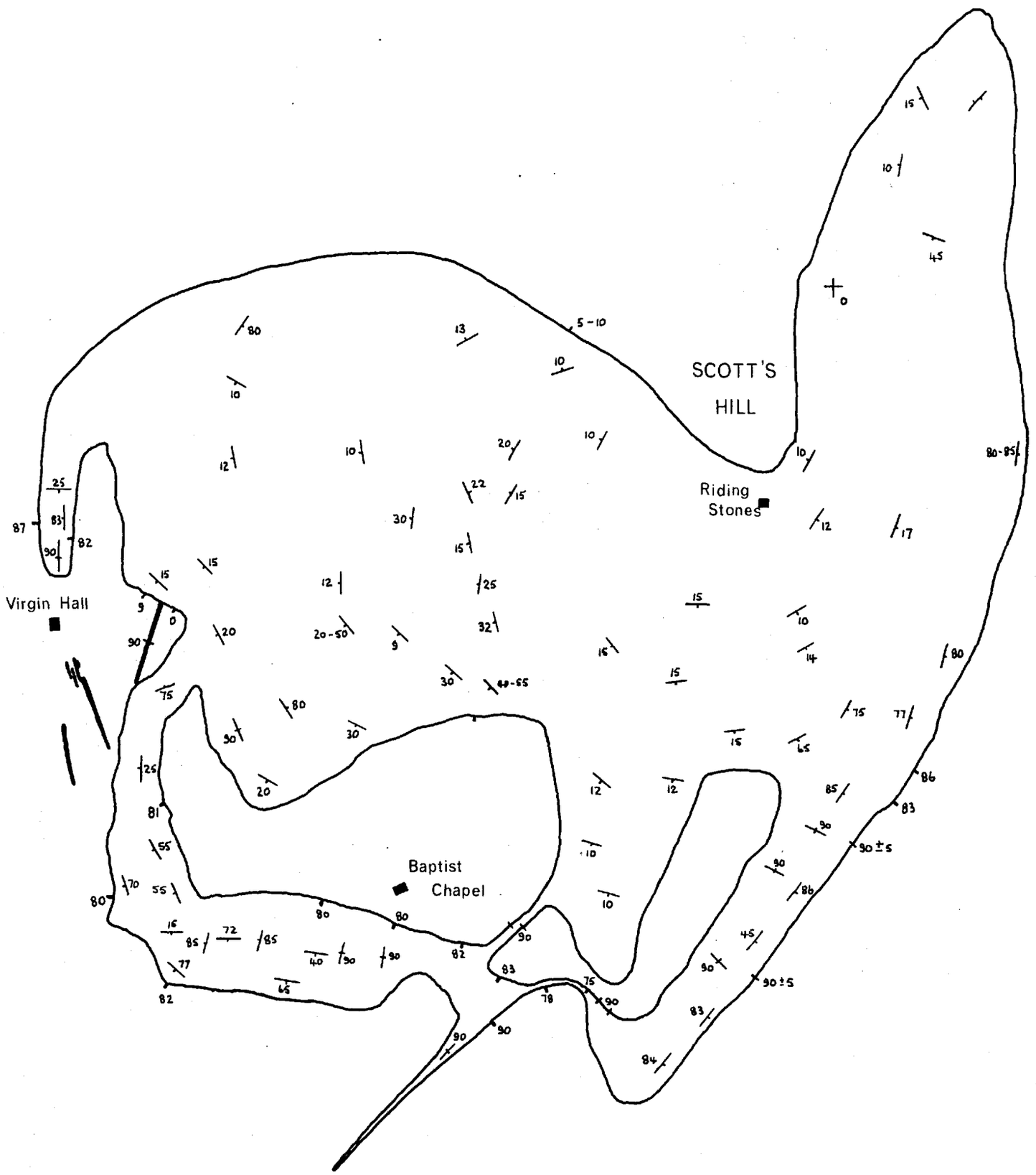
SCOTT'S
HILL
Riding
Stones
Virgin Hall
Baptist
Chapel
5-10
80-85
0
500M

FIGURE 21

PLATE 21:

Riding Stones Hill phonolitic-trachyte steep-sided, roofed intrusion.

A: From the east. Left hand side is Chapel Rock, part of "ring" dyke. Roof is on right (note curve of jointing from bottom right hand side); highly altered central block between and to right of the hair-pin bends in path,

B: From the south. The apparent 'high' on the left is Chapel Rock; clump of trees (centre) is at Riding Stones House on the end of Scott's Hill. Note steep outward dipping sheet joints parallel to the contacts on the right hand (SE) side, weak vertical joints in thickest part of the infilled roof cavity and the rather blocky jointing in the exposed part of the Chapel Rock mass.

A number of dykes cutting the material inside the fracture stop abruptly at the contacts with the trachyte. The material inside the "ring" and under the roof is highly zeolitized, as are the rocks adjacent to the high angle sides. Although the rocks of the Sandy Bay series are usually zeolitized, the abundance of secondary minerals does appear to increase within the confines of, and adjacent to, the major intrusion.

Jointing in the mass is shown in Fig. 21, and the pronounced vertical set perpendicular to the contacts of Chapel Rock should be compared with the curved joints of the roof at the east side (Plate 21). The contacts are largely sub-vertical - in the west and south-west they dip outwards at angles of 82-83°, but along the eastern contact they are vertical ±10°. There appears to be some variation with height in the eastern cliffs; at the base the chilled margin apparently dips inwards at 80-82°, but 100m higher the dip is 80-82° outwards. The flat-lying, broadly-spaced joints within the infilled roof cavity vary systematically throughout the exposure (Fig.21).

There is no evidence for updoming of the surrounding rocks - the flows on top of the intrusion are virtually horizontal. The maximum width of the infilled arcuate fracture, however, is greater than a theoretical value for straightforward collapse. Chemically there is strong evidence that the mass was intruded as one pulse, and the roof cavity filling was subsequently differentiated slightly in situ (see below, Section VII and VIII).

One final intrusion deserves description because it demonstrates the close relationship existing between a restricted sub-vertical intrusion and broad, flat-lying sheets. The trachybasaltic mass is exposed in vertical and part-

FIGURE 22:

Irregular trachybasaltic intrusion near Sandy Bay Beach (SBB) west of Horses Head (HH), with elliptical "feeder".

Height of cliff section at 'd' is 220m. Jointing shown schematically in A; hachuring = irregular; dashes = planar.

1: Horses Head flows; 2: Sandy Bay pyroclastics; 3: Man o' War flows; 4: Intermediate arcuate inclined "conical"sheet.

b, d, g, j = points of reference for plan and cliff section.

P = Old Picquet House

Q = position from which sketch section was made.

circle = estimated centre of large scoria cone

In the plan view, B, the cliff face is drawn with its slope less steep than its true value - consequently the shape appears even more unusual.

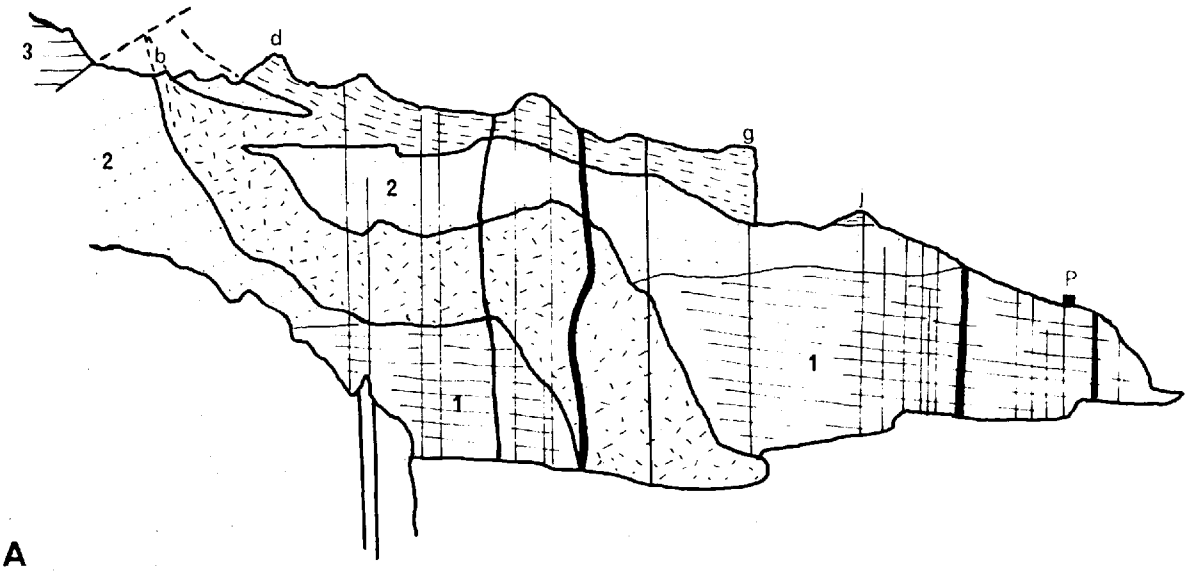

A

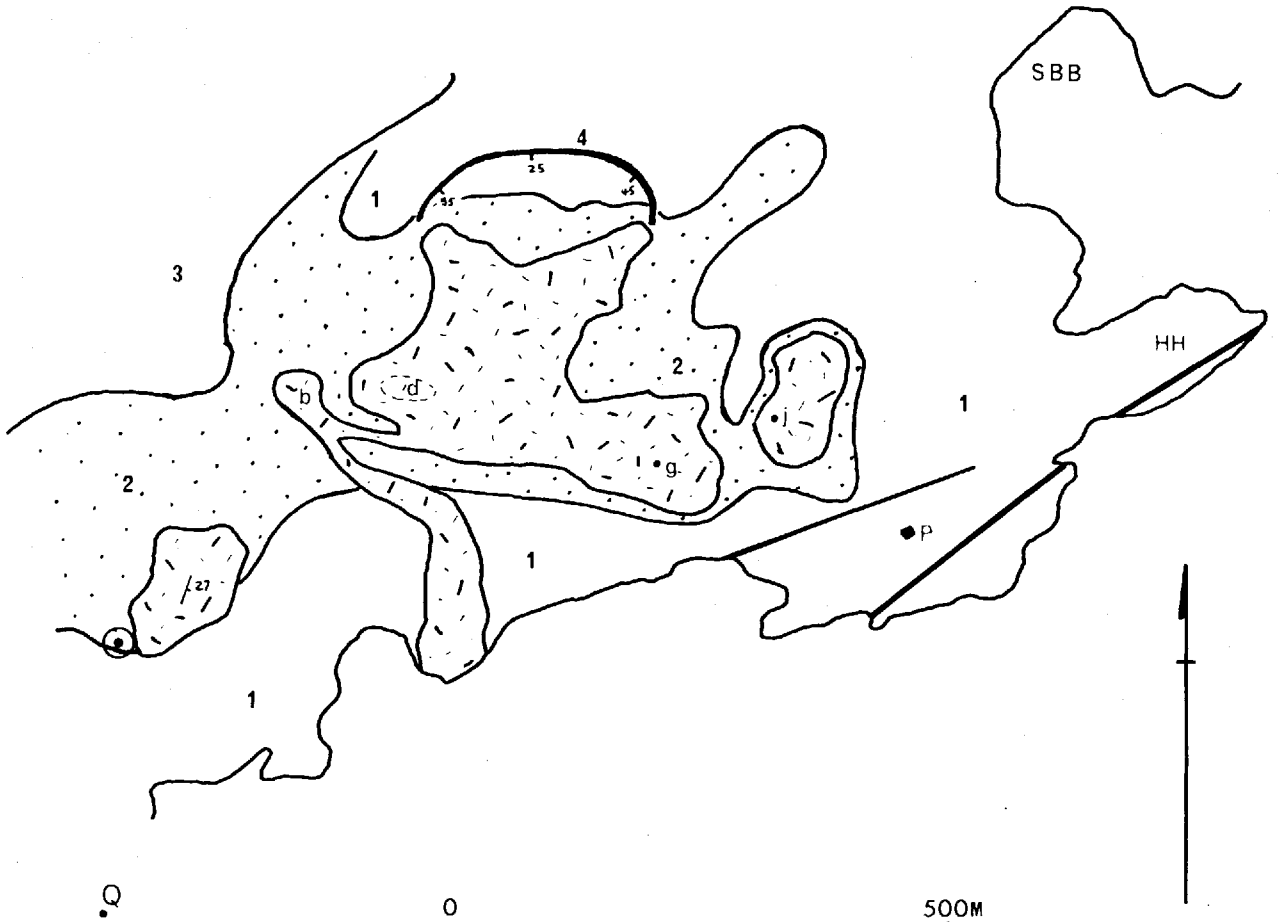

B

Q

0 500M

FIGURE 22

horizontal section in the cliff face 1km west of Horses Head near Sandy Bay Beach.

The intrusion may be related to a former large scoria cone (Fig. 22b), products of which form the top 100m of the cliff section. An irregular pipe-like mass (75m x ≥75m), inclined at 70° to the horizontal, cuts through the underlying lavas and turns sharply through nearly 90° in the scoria to form a curved, flat-lying sheet (Fig. 22a). At the cliff top the sheet turns sharply back on itself, forming an almost horizontal continuation, which probably broke surface on the north side of the ridge. This overlying sub-horizontal sheet possibly represents another related curved fracture infilled by lava from the lower sheet after deflection at the contact with an overlying thick lava sequence (Fig. 22a). Both of the flat-lying sheets have lateral dimensions greater than 400m, and thicknesses of approximately 50m, compared with the 'pipe' with dimensions of less than 100m.

2. Geometry and Formation of Arcuate Structures.

A mathematical treatment of the very complex stress conditions in the rocks surrounding a body of fluid magma was first attempted by Anderson in his classic interpretation of the formation of cone-sheets and ring-dykes (Bailey et al, 1924; Anderson, 1936). Anderson assumed somewhat simplified conditions in a "homogeneous isotropic and infinite solid", with a point pressure source and horizontal ground surface. More complex solutions offered by Garson (1959) and Robson and Barr (1964) have assumed non-point pressure sources, in non-homogeneously stressed country rocks.

Garson (1959) deduced that the magma-body ("pluton") responsible for the complex system of dykes of the Tundulu ring structures was a flat lens with a convex upper surface.

Robson and Barr (1964), in theoretical considerations have assumed that the magma-body has a small radius compared to its depth below the ground surface. Their stress distribution is that produced by "an infinitely long cylinder containing a fluid in an infinite solid subjected to inhomogeneous stresses". In both of these analyses the body responsible for creating the stress systems leading to fracture was at a depth of several kilometres.

Macdonald (discussion to Robson and Barr, 1964) pointed out that arcuate fractures occur in Hawaii with diameters of a few hundred metres or less, and suggested that very high level cupolas of magma are responsible for the collapse which produces the pit-craters (Macdonald, 1965, p321, 331-332). Similarly the small scale of the arcuate fractures on St. Helena strongly suggests that their source of origin is at shallow depths, in some instances only a few hundred metres below the original ground surface. In such circumstances the orientation of the ground free surface will play a major role in determining the shape of the fracture. Clearly the solutions of Anderson (1936), Garson (1959), and Robson and Barr(1964), which postulate a horizontal surface and a magma source of variable shape and depth, must be applied with great caution. However, it is possible to interpret the forms and stress conditions of some of the St. Helena intrusions by modifying the published solutions of Garson.

The three types of arcuate fractures occurring on St. Helena are never seen inter-related. The proposed mechanisms of formation can therefore be discussed separately.

a. Irregular, steeply inward-dipping basic sheets.

Intrusion of a laccolith-like body of magma into the gently dipping flanks of a volcano may cause broad, gentle doming of the overlying rocks. If the intruded mass covers

an appreciable area in relation to its depth, local irregularities in the roof will produce local stress conditions which become potential areas for the development of tensional fractures. Similarly, a small lens of magma will serve as an individual centre for the development of local fractures. If the pressure applied by the magma is sufficiently high, tensional fractures can open in the overlying rocks, and continuing high pressure allows magma to rise up along them. The fractures produced by this source of limited areal extent will be inward-dipping, and if pressure is uniformly applied they will be symmetrical about a vertical axis. The theoretical shape of these fractures in depth is dependent upon the boundary conditions initially assumed. In the analyses of Anderson, Garson, and Robson and Barr, the inward dip of the fractures essentially decreases with proximity to the source.

Intrusions believed to be of this type on St. Helena are not associated with parasitic scoria cones and are developed in the flanks of the shield dipping regularly at approximately 10°. It is therefore permissible to accept a plane, near-horizontal boundary surface, and a stress system similar to that proposed by Garson (p319, fig. 5, 1959) and reproduced in Fig. 23A. The irregularities in the examples described above (715 and 716, Fig. 15) may be caused by minor asymmetry of the stress field as a result of the ground surface dipping at 10°, and local inhomogeneities of stress and lithology. There appears to be no justification in proposing an upward pressure source appreciably inclined from the vertical.

The 715 and 716 intrusive sheets are believed to result from an upward pressure exerted on the roof of flat-lying laccolithic bodies of magma intruded to a high level in the volcanic structure. Although of different composition,

FIGURE 23:

A: Trajectories of maximum shear (solid lines) and tensional stresses (dashed lines) in elastic solid bounded by horizontal plane due to uniform upward pressure on a circular area within the solid. (From Garson, 1959, Fig. 5, p319).

B: Suggested slip line field showing trajectories of tensional (dashed) and maximum shear stresses (solid) in a rigid, perfectly plastic isotropic solid, bounded by a horizontal plane, due to uniform inclined pressure on a point, or very restricted, source area within the solid.

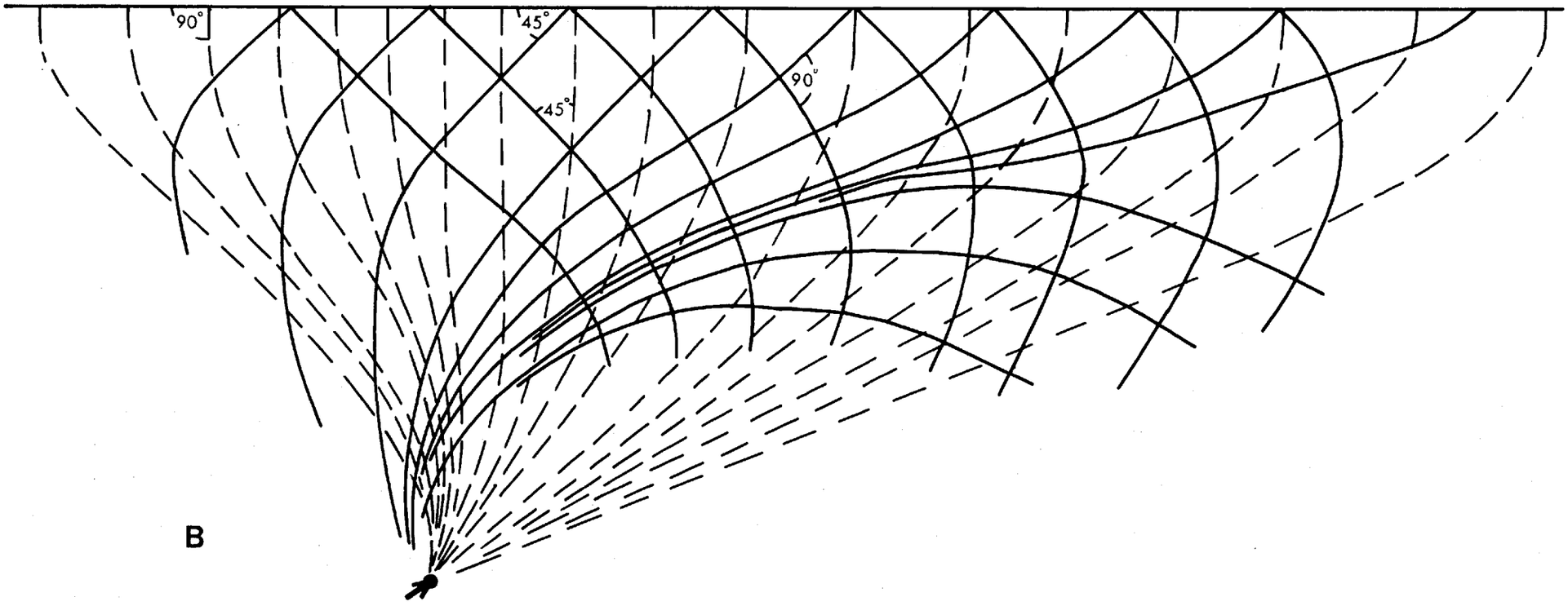

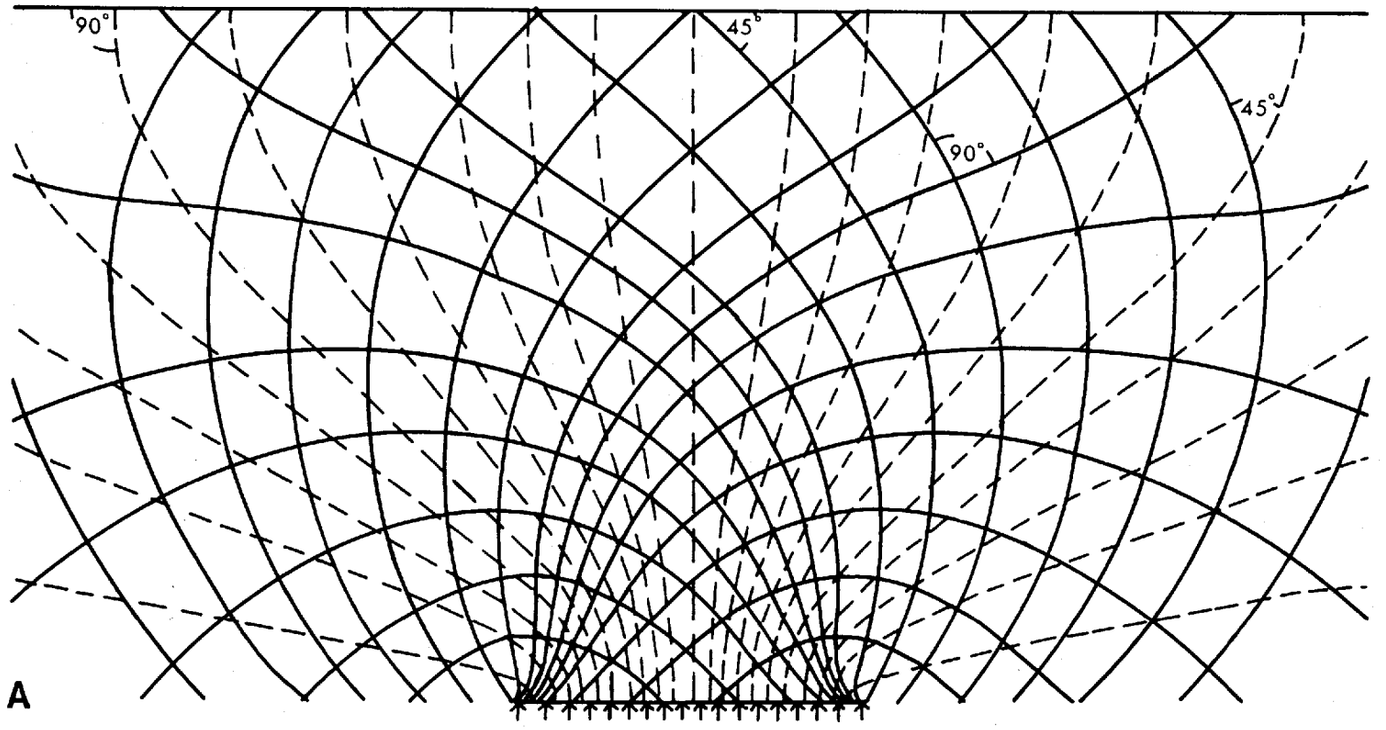

Fig : 23

the trachytic "laccolith" of Devil's Cap (Section III, Fig. 13) may provide an example of a similar type of intrusion. The irregularities in the curvature of the exposed fractures, especially in the 716 mass, strongly suggest that the fractures are curved in a vertical plane. The nature of this curvature is beyond the scope of this study.

In order to estimate an approximate depth of the fracture source the exposed dips around the fractures have been extrapolated linearly downwards and the area of intersection taken as the maximum depth of action of this pressure source. Dips greater than 80° have not been used in the calculations because of the possibility of this value decreasing relatively rapidly below the present level of exposure. The depths of the point of action of the pressure sources are estimated at less than 300m (for 716) and 400m (for 715) below their present level of exposure. These results give estimated depths of the pressure source of approximately 500-600m below the volcano surface at the time of formation of the basic sheets.

b. Inclined cone-like sheets.

The variable geometric relationships of intrusions of this type were given in the first part of this Section. The small sheets (diameter < 150m) form almost closed arcs, and large intrusions demonstrate that outward movement of the block inside the fracture has occurred. The fracture surface therefore opens outwards, i.e. away from the origin, and in this respect is "cone-like". Reconstruction of the original ground surface for intrusions of known age (Sharks Valley, Rough Rock, Tripe Bay, Great Stone Tops, Sandy Bay) demonstrates that it was not more than 10° off-horizontal, and in some cases (Sharks Valley and Great Stone Tops) was inclined at about three degrees. The depth of the exposed sections

below the ground surface at the time of formation of the fractures can be calculated quite accurately for a number of the sheets (Table 1). The variations in these values suggest that the cross-sectional diameter of the fracture decreases with increasing depth below the free surface at the time of formation. This decrease in diameter is interpreted as reflecting increasing proximity of the source of pressure (and presumably the source of magma which infilled the fracture). The fracture near the source therefore approximates closely to a surface of revolution, and with increasing distance from the source (and decreasing depth below the surface) the fracture opens and the degree of closure of the sides decreases (Fig. 24). The attitudes of the lowest parts of the sheets however, remain relatively constant, with low angle inward dips.

The following features are common to all intrusions of this type:

(i) The fracture is bilaterally symmetrical about a near-vertical plane.

(ii) The fractures are developed with similar geometries in both scoria and lava sequences, or combinations of the two rock types.

(iii) Fractures show no evidence of deflection when cutting piles of lavas, even where the angular divergence between fracture and flow is very small.

(iv) The intrusions are chilled at their margins, and the adjacent country rocks show no evidence of brecciation.

A possible three dimensional model can therefore be envisaged for the variations in shape of the fracture. If the physical conditions relating to the country rocks and the

FIGURE 24:

Inclined arcuate cone-like intrusions.

h, i, j = hypothetical cross-sections of tensional fractures from a stress field proposed in Fig. 23B. Possible decrease in stress away from the source accounts for the dying out of fractures in 'i' and 'j'.

St. Helena examples are shown for comparison; sections are drawn as nearly as possible at right angles to the fractures and to the symmetry plane. All are at the same scale - the very small size of the Prosperous Bay Beach mass is quite extraordinary (see also Plate 15A).

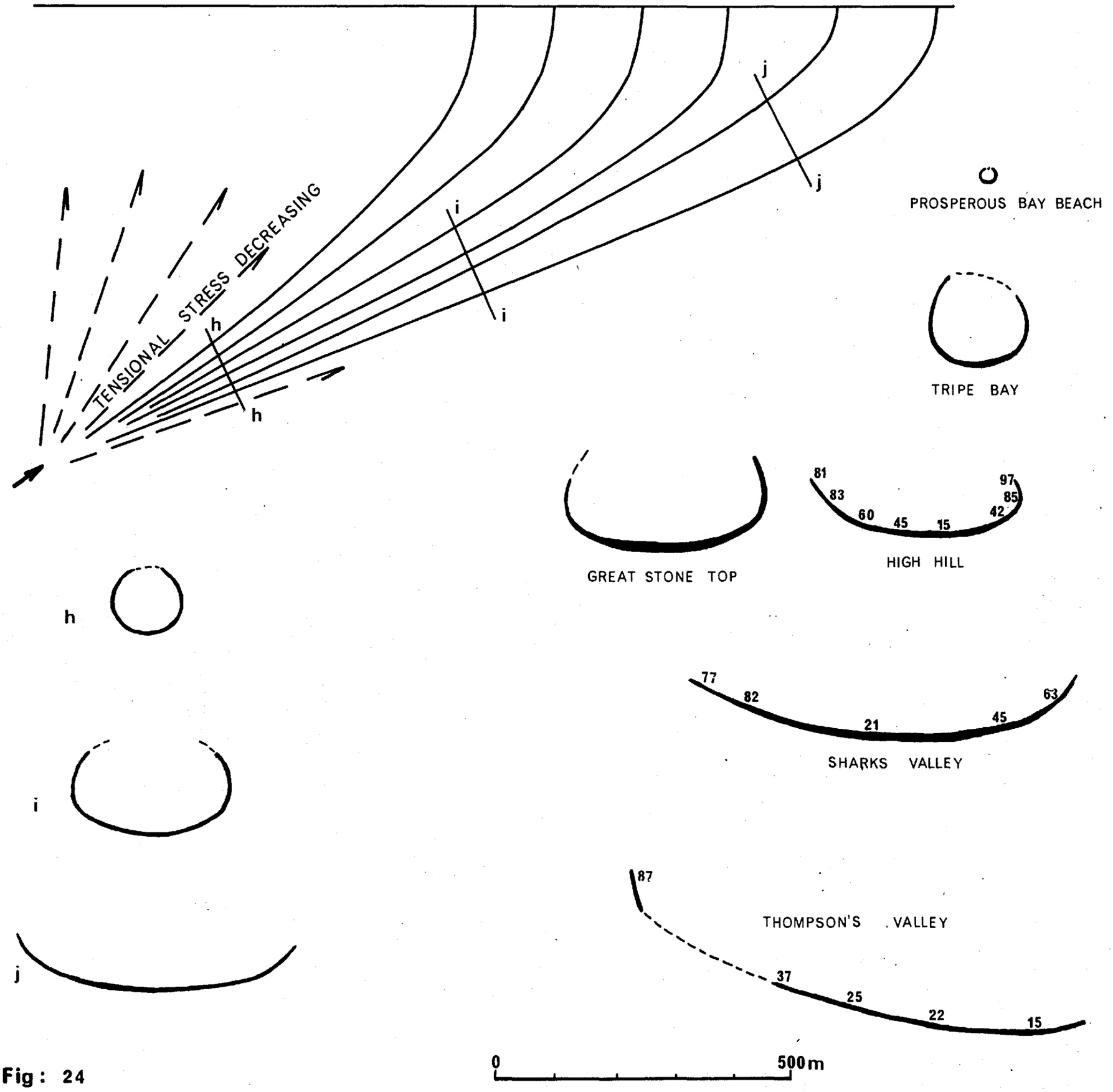
TENSIONAL STRESS DECREASING
h
h
i
i
j
j
PROSPEROUS BAY BEACH
TRIPE BAY
GREAT STONE TOP
81
83
60
45
15
42
85
97
HIGH HILL
h
i
j
77
82
21
45
63
SHARKS VALLEY
87
37
25
22
15
THOMPSON'S VALLEY
0
500m

Fig : 24

pressure source can be estimated, then from these combined data it should be possible to establish a stress field responsible for their formation. The free boundary surface is very nearly horizontal, and the pressure source is inclined, and probably very restricted, perhaps "pipe"-like - to a first approximation it may be considered an inclined point source. From (ii) and (iii) it is reasonable to assume that at the time of failure the country rocks behaved as isotropic materials. Subsequent deformation resulting in bending of basaltic lavas may be plastic (see above). A stress field has been constructed for an inclined point source and horizontal free surface based on the slip-line field theory described in Johnson and Mellor (p159, 1962). The conditions of application of this theory are defined as "non-homogeneous plane-strain deformation of a rigid, perfectly plastic isotropic solid." While these conditions are idealizations, their application as an approximation to the solution of the geometry of these structures is believed to be valid. A diagram showing the trajectories of tensional and maximum shearing stresses in this proposed system is given in Fig. 23b. The inclined cone-like sheets are believed to represent infilled tensional fractures. In three dimensions the fractures will not be given by rotating a particular line in Fig. 23b about the inclined "pressure axis". This would be possible about a vertical axis, but the "pressure axis" is not a true axis of symmetry. Near the source the fracture approximates to a surface of revolution, and it is likely that further away the surfaces are approximately elliptical, with their long axes at right angles to the "pressure axis", parallel to the free ground surface. The variable shape of the sheets as exposed on St. Helena demonstrates this ellipticity with increasing diameter of the fracture. Just as the maximum shearing stresses decrease away from the source (see for example

Anderson p143, 1936; Garson p321, 1959) so do the tensional stresses (Fig. 24). This may therefore explain the dying out of the fractures at the sides with increasing diameter (i.e. increasing distance from the pressure source) as shown in Fig. 24.

These cone-like sheets on St. Helena therefore may be seen as inclined equivalents of true "cone-sheets". The St. Helena examples are tighter cones, are slightly "flattened", show a variety of rock types (especially highly differentiated types), and do not form "swarms", but they are tensional fractures, dip inwards at high angles towards the pressure source, and allow outward movement of the central block with infilling and opening.

The exact relationship of the locally developed sheets at Great Stone Top (Fig. 16; and possibly that related to the Thompson's Valley sheet - Fig. 26, indexed 5 and 5a) to the inclined "cone-like" sheets is rather obscure. They may represent locally opened shear fractures (theoretically inclined at 45° to tensional fractures) especially in the case of the Thompson's Valley sheet (see below). The Great Stone Top sheets are complicated by having part of a second inclined 'cone' developed lower than the more perfect one (see above). The lack of development of related minor sheets at other sites does not allow interpretation of their full significance.

c. Steep-sided roofed intrusions.

Four intrusions of this type belong to the late, highly alkaline intrusive phase described in Section III. The geometry of the White Point mass is so similar that all five may be considered in terms of the same basic stress conditions.

In a large body of magma (the late high-level magma chamber) minor irregularities in the roof become potential sites for stress concentrations. Each of these areas may therefore be considered as an individual pressure source, possibly as a lens of magma, convex upwards, similar to that proposed for the larger Tundulu ring structure (Garson, 1959). High magmatic pressure results in the production of high angle shear fractures as shown in Fig. 23A, and is believed to initiate a sequence of events shown schematically in Fig. 25. Formation of the ring fracture temporarily releases stress, allowing the enclosed block to drop fractionally along a gently-domed tensional fracture, which may be locally modified by the attitude of the overlying country rocks. This roof cavity will be opened by two processes, either by dropping of the enclosed block into the chamber, or by intrusion of magma under high magmatic pressure into the fractures and forceful updoming of the over lying rocks. The Powell's Valley Hill body appears to be an example of the former, White Point an example of the latter. Hooper's Rock may combine both processes, initial injection under high pressure domed the overlying rocks, and with lowering of magmatic pressure the enclosed block dropped slightly to open the roof cavity further. The White Point intrusion appears to have formed under very high magmatic pressure; after initial updoming of the overlying lavas the ring fracture was continued to extend above the former roof cavity along the southern and western sides (Fig. 19).

All of the arcuate intrusions of this type were developed high in the volcanic structure - the roofs can be shown to have been only a few hundred metres below the original ground surface. The diameters of the "ring" fractures are less than 1000m, and in the case of Riding Stones Hill the central enclosed block has apparently behaved as a "single"

FIGURE 25:

Hypothetical formation of the steep-sided roofed intrusions on St. Helena. Vertical and horizontal scales approximately equivalent.

1: Initiation of near vertical "ring" fracture above lensoid pressure source; and development of sub-horizontal cross-fracture.

2: Initial slight downward movement of block and injection of magma from underlying chamber into openings.

3: Continued injection of magma if block drops under its own weight into a chamber at low pressure.

4: High magmatic pressure allows no sinking of block but opens roof cavity by updoming overlying and adjacent country rocks.

5: Very high magmatic pressure updomes overlying country rock and extends arcuate fracture upwards (± formation of sub-horizontal "sills"). High pressure permits no sinking of original fault block.

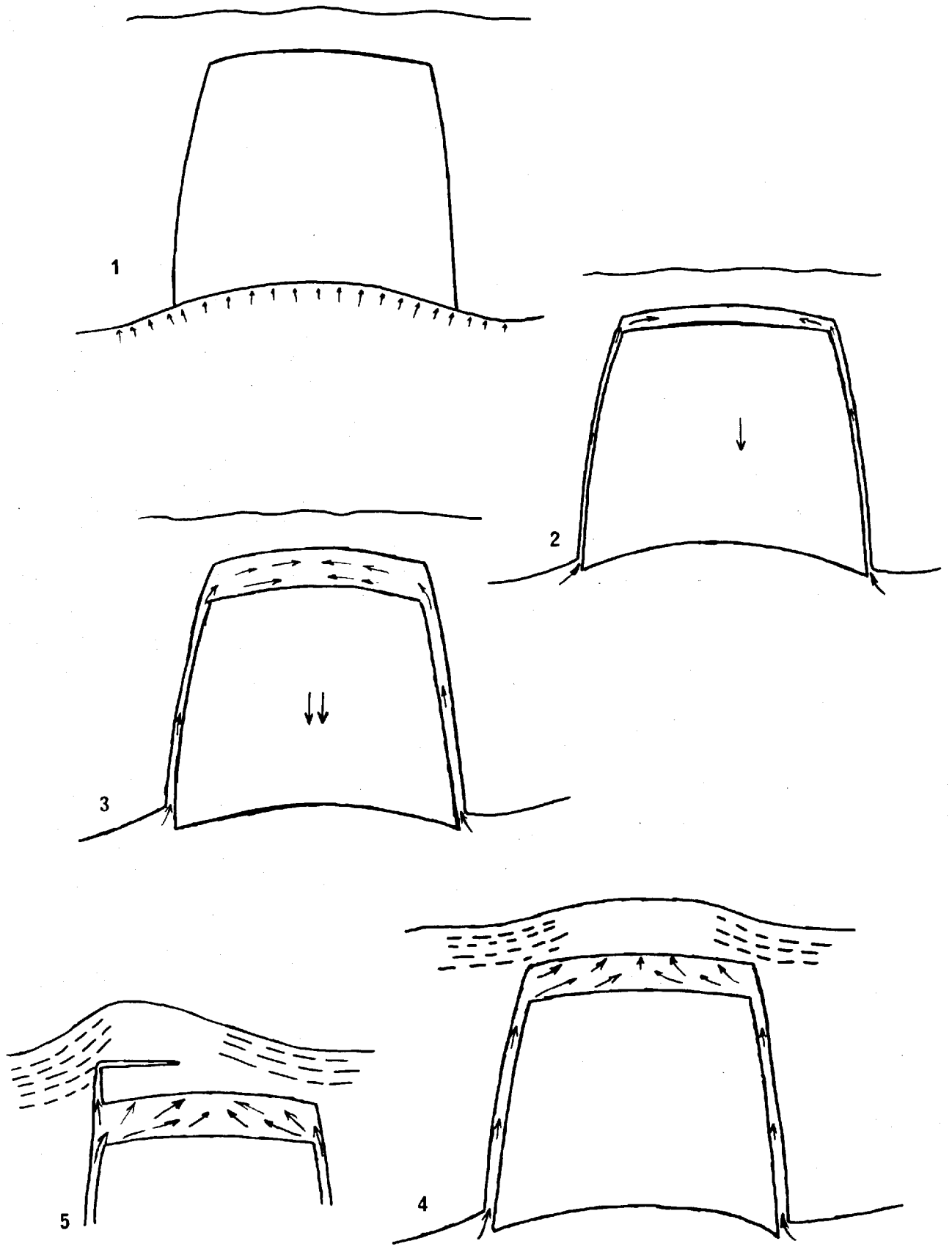

Fig : 25

unit. If the geometry of the stress trajectories shown in Fig. 23A is realistic, then, considering the above points, it is suggested the pressure sources responsible for the fractures are within two, or at the most three, kilometres of the volcano surface. The geochemical variation of these intrusions is so regular that the roof of the main chamber is believed to be broadly and gently domed (Baker, in press). Although local minor irregularities are developed, the roof of the magma chamber as a whole will similarly be only two, or at the outside three, kilometres below the volcano surface.

d. Summary.

Arcuate intrusions exposed at high levels in the volcano were produced under three sets of stress conditions originating high in the volcanic pile. Two types of arcuate sheets, with maximum diameters of less than 1km, are believed to be infilled tensional fractures. Steeply inward-dipping basic sheets are believed to be formed above a laccolithic body of magma intruded into the volcanic pile less than 1km below the surface. The inclined cone-like sheets are believed to be related to inclined pressure sources acting on very restricted areas ('points') at a depth in the order of 500m.

Larger highly alkaline steep-sided roofed intrusions are produced by injection of magma into a near-vertical 'ring' shear fracture bounding a 'cylinder' of country rock. Low magmatic pressure allows the block to drop, thereby opening the roof cavity by collapse. High magmatic pressure results in opening of the roof cavity by updoming the overlying rocks, the enclosed block remaining virtually in place. Pressures developed on domed (convex upwards) areas of a magma chamber roof lying at a depth of about 2km are believed to be responsible for the formation of these intrusions.

The geology of the White Point Area.

The geology of the complex White Point parasitic centre and the intrusive rocks in the upper reaches of Thompson's Valley, to the east, is shown in Fig. 26. Initial explosive activity built up a coarse crystal-rich (pyroxene) scoria cone from which was extruded a single thick basaltic flow. Renewed explosive activity built up a scoria and tuff cone centred 300m to the north. Products of this cone show characteristic asymmetry, with finer material carried considerable distances (2km) to the north-west. The scoria cones were subsequently buried by a thick sequence of basaltic flows of the main shield series, before emplacement of any of the intrusions.

The Thompson's Valley arcuate sheet (Thompson's Valley "sill", Daly, 1927, p51) consists of a rock type unusual even for the White Point area. Two small relics of identical rock occur between Wild Cattle Pound and White Point (Fig. 26). All of the exposures are badly altered. The rock is a fine-grained trachyte, rich in small, invariably rounded, weakly vesicular 'xenoliths' of trachytic material, with finely acicular, almost hair-like feldspars. In the accessible southern end of the Thompson's Valley sheet, the xenoliths are of equivalent size, vesicularity and abundance to those in the smaller bodies further south. Of the smaller bodies, the northern one is inclined concordantly, with a dip of 20° to the north-east, within the pyroclastics, and the sinuous southern mass appears to be sub-vertical. If these two are related to the main Thompson's Valley intrusion, and their unique petrography strongly suggests this, their unusual attitudes can be explained by assuming the vertical one to be the direct continuation of the main fracture, and the concordant mass to be a related shear fracture of limited development. The gap in the exposure is explained if both the

FIGURE 26:

Geology of the White Point parasitic centre and adjacent area.

MSF = main shield basalts

1: Crystal-rich pyroclastics of White Point Centre 1.

1a: Thick flow from Centre 1

2: Orange (?in part trachytic) pyroclastics of White Point Centre 2.

TVF: Thick trachybasalt flow of same age as Old Joan trachybasalts, possibly fed from White Point area (see Section III, 3).

3: Pyroclastics from large scoria centre NE of White Point.

4: Scoria from cone originally SW of Rush Knoll trachytic "laccolith" (6).

WP: White Point trachyandesite roofed intrusion.

5: Xenolithic trachyte arcuate cone-like sheet of Thompson's Valley, and probable continuations (5a); northern one dips at low angle to north-east.

7: Trachyte intrusion of uncertain origin forming cliffs west of Wild Cattle Pound (WCP).

7a: Trachytic mass possibly related to 7; eastern lobe is sub-horizontal, western part has sub-vertical contacts where exposed.

8: Coarse trachyandesite breccias related to, and later than, White Point main intrusion.

Note abrupt change in dip of Main Shield basalts SW of White Point and lack of updoming to north (and probably through east to SE).


THOMPSON'S VALLEY
MSF
TVF
WP
WCP
WHITE POINT
MSF
MSF
1
1a
2
3
4
5
5a
6
7
7a
8
0
500
1000m

Fig : 26

Wild Cattle Pound mass and the unusual breccias are later, and cut out the sheet (Fig. 26).

A thin, near vertical, intrusive breccia extends from the north-eastern corner of the White Point intrusion to north of the Wild Cattle Pound trachyte (Fig. 26, '8' and '7'). The 'dyke'-like breccia (1-5m in average thickness) actually cuts the White Point intrusion for a distance of 20-25m (see Fig. 19). North of Wild Cattle Pound the mass flares out, still with sub-vertical contacts, to a width of more than 35m. Further east exposures are very limited but the mass appears to be relatively flat-lying, and a possible continuation is exposed 200m east of Wild Cattle Pound (Fig. 26). The breccia consists of blocks of weakly vesicular, altered, trachyandesite, ranging in size from 25cm downwards into the comminuted matrix (Plate 18). It is tentatively suggested that the mass represents a gas-brecciated irregular arcuate intrusion, and a related sheet-like off-shoot, later than the main White Point body.

The structure of the Wild Cattle Pound trachyte is not understood (Fig. 26). The mass is apparently related to the late sequence of highly alkaline intrusions, and chemically is closer to the Rush Knoll mass than to the White Point trachyandesite. About 150m east of the mass another irregular trachytic intrusive is poorly exposed - the two may be related (Fig. 26). Although the area is badly altered the Wild Cattle Pound mass is not seen to disturb the attitudes of the adjacent pyroclastics, is much fresher than the White Point mass, and has, at least in part, a sub-vertical western contact. The intrusion in some respects resembles the basaltic body exposed in Broad Gut (Section III, 2b) and may be related to a north-south dyke. Because of the relationship to the White Point pyroclastics it is thought to be an essentially tensional feature, possibly related to a small elongate collapse. The

small intrusion to the east, which is possibly related, does not contradict this interpretation.

The complicated picture of extrusive and intrusive activity of widely differing types over long periods of time at White Point is similar to that of the Blue Point and High Hill parasitic centres. Complex parasitic centres, with histories of spasmodic activity over very long periods of time, are a striking feature of the south-western volcano on St. Helena.

SECTION V

CLASSIFICATION

1. Introduction.

The most obvious feature of the volcanic rocks of St. Helena (Sections VI and VII) is their gradational nature. Texturally, petrographically, mineralogically and chemically there are no obvious breaks at which to draw clean boundaries of classification. Yet a classification is important as a means of transmitting information of a general nature; specific information may be transmitted by detailed petrographical and geochemical descriptions.

The extreme members of the series, basalts and phonolites, are readily separated. There is considerably more difficulty with the intermediate members. It is with the classification of these intermediate rocks that the greater part of this Section is concerned.

As a whole the rocks form a weakly undersaturated series, and none of the problems associated with nomenclature of strongly feldspathoidal lavas is encountered. Modal nepheline first appears in the phonolitic-trachytes; normative nepheline in the basaltic and intermediate rocks is usually 5% or less, although some rocks contain up to 9%.

2. Basaltic Rocks.

The highly porphyritic basalts with more than 30-40% phenocrysts invariably contain a greater percentage of pyroxene than olivine (approximately 3 : 1). Modal feldspar constitutes less than 30% of the rock, so they are picrite-

basalts of ankaramitic type according to the classification of Macdonald (1949). Although olivine is abundant in the St. Helena rocks the term 'ankaramite' is used alone as originally applied by Lacroix (1916) for rocks of this type with dominant pyroxene.

Macdonald and Katsura (1964) have convincingly argued the retention of the term 'olivine basalt' for all basalts containing significant modal olivine. The St. Helena basalts contain appreciable olivine, are undoubtedly alkaline (Fig. 30) and contain 5% or less normative nepheline - the rocks are therefore alkali olivine basalts. If the 5% limit on normative nepheline content is to mark the alkali basalt/basanitoid division (Macdonald and Katsura, p85, 1964) then three rocks, 737, 706 and 786 (Section VII, Table 7) would fall into the basanitoid group (5.1%, 5.4%, 9.1%, ne). The term basanitoid is not used however, because the degree of undersaturation of the St. Helenan basaltic rocks as a group is not considered sufficiently great that it should be "over-stressed". The potential importance of the single analysis with 9% ne should not be overlooked, but unless its significance is outstanding, the introduction of basanitoid is unnecessary.

A further point in favour of retaining alkali basalt for all of the St. Helena basalts is the problem of classification of the basic intermediates, several of which contain between 5% and 8% normative nepheline. The classification used here would necessitate using "trachybasanitoid" for these rocks. The term trachybasalt leads to such extensive argument (see below) that "trachybasanitoid" (even if aesthetically acceptable) would provoke discussion far in excess of its value.

3. Intermediate Rocks.

Tilley and Muir (1964) have distinguished two series of intermediate rocks in the oceanic alkali olivine basalt - trachyte series, dependent upon the dominance of either K_2O or Na_2O in the alkalis. The series established exclude strongly undersaturated members; the sodic rocks of Hawaii and the Hebridean province are contrasted with the more potassic rocks of Gough Island and the Tristan da Cunha group. For the potassic series the sequence is: olivine basalt - trachybasalt - tristanite - trachyte; for the sodic series: olivine basalt - hawaiite - mugearite - benmoreite - trachyte. The specific terms benmoreite and tristanite were introduced for those intermediate rocks falling in the minimum frequency group of Chayes (1963b), which is given by the limits: $53 < SiO_2 < 57$; $3 < CaO < 6$; $5\frac{1}{4} < FeO + Fe_2O_3 < 8\frac{1}{2}$; $65 < D.I. < 75$ (all figures quoted in weight percent, D.I. = differentiation index of Thornton and Tuttle, 1960).

The petrography of the intermediate rocks has been described in Section VI. Many of these rocks are very fine-grained, but with a powerful microscope it is possible to determine optically the composition of groundmass feldspars. Even the rocks classified as basalts with abundant olivine and pyroxene, have extensively zoned groundmass feldspars. In the intermediate rocks this zoning is extreme. Using published curves the plagioclase composition may be determined out to a zone where lamellar twinning ceases, but the orthoclase in solid solution cannot be estimated, and frequently zoning is relatively continuous from calcic andesine to alkali feldspar. The estimation of 'modal feldspar' composition therefore becomes impossible. Similarly, because of the ternary nature and zonation of the feldspars, the term 'normative plagioclase' frequently used in rigid classifications is open to misuse.

Textures and groundmass optical determinations may be useful in classifying these rocks, but a large number of mistakes would be made in a classification based solely on petrographic criteria. Because of this fine grain-size, the "ternary" aspect of the feldspars and the very considerable zoning, it is more realistic to classify the rocks on a basis of their chemistry.

Harker (1904, pp263-266) first described mugearite as a basaltic rock with oligoclase as the dominant feldspar, but with subordinate orthoclase. Certain of his 'basic mugearites' (pp267-268) contained oligoclase-andesine. Macdonald (1949) named the Hawaiian equivalents of these rocks: andesine-andesites and oligoclase-andesites. Walker (1952) demonstrated the very marked similarity between the Scottish mugearites and Hawaiian and other oligoclase-basalts. He proposed the abandonment of the term oligoclase-andesite of Macdonald(1949), and defined mugearite essentially on textural terms. An oligoclase-basalt was any rock chemically comparable to mugearite but lacking the fluidal texture of the feldspars (Walker, 1952). Wells (1954) maintained that mugearite was a textural term, and that the rocks were oligoclase-basalts: if the trachytic texture was pronounced and the rock was otherwise similar to the Druim na Criche (type) specimen, then the rocks were "oligoclase-basalts of Mugeary type". Macdonald (1960) reintroduced the term hawaiite (originally proposed by Iddings, 1913) for andesine-bearing basaltic rocks, because of opposition to his suggestion (1957) to call them andesine basalts. Muir and Tilley (1961), in a very detailed study of mugearitic rocks, firmly retained the terms hawaiite and mugearite on mineralogical and chemical grounds. Rocks were described by them however as "mugearite-trachytes" and one as "mugearite basalt (comparable to hawaiite except for its much lower potash content". Tilley

and Muir (1964) completed the assemblage by introducing benmoreite as an intermediate between mugearite and trachyte, and tristanite between trachybasalt and trachyte, hence removing the terms "mugearite-trachyte" and "trachyandesite".

The two trends proposed by Tilley and Muir (1964) are shown in a plot of Na_2O : K_2O (Fig. 27). The potassic trend is that of Gough Island (LeMaitre, 1962), and the sodic trend that of the Hawaiian alkali rocks (Macdonald and Katsura, 1964). Also shown are the plots for the Tristan da Cunha group (Baker, et al, 1964) and St. Helena (this study). Fig. 28 shows similar plots for Ascension, Heard Island, Madeira, Principe, and Teneriffe (references in Fig. description), together with the plots of Hawaii, Gough, St. Helena and Tristan da Cunha. Analyses from Ascension and Principe have been plotted on Fig. 28 to demonstrate the scatter of analyses from these two islands. The best fit trend lines of each of the islands do tend to fall into two groups and some of the scatter of the Ascension and Principe rocks may be due to the several different analysts resonsible. There is nevertheless some overlap when the envelopes of individual islands are considered. The Hebridean intermediate rocks quoted in Muir and Tilley (1961, Table 4, anals. 1, 2, 7-11), and rocks upon which the sodic group of the double system of nomenclature is based (Tilley and Muir, 1964) show considerable scatter (Fig. 29). One analysis lies on the Tristan trend, two plot between the trends, and three lie far below the Hawaiian trend. The type mugearite lies very close to the Hawaiian trend. The two analyses lying between the trend lines (Fig. 29, 6 and 7) are the 'type' benmoreites of Tilley and Muir (1964, Table 1, anals. 4 and 5). Nockolds' (1954) average nepheline latite and Dunne's (1941) feldspathoidal intermediate from Tristan (reclassified by Tilley and Muir as leucite-tristanites, Table 2, anals. 2 and 3, 1964) plot so close to the type benmoreites

FIGURE 27:

Soda-potash variation for Gough Island: G (LeMaitre, 1962); Hawaiian alkali rocks : Ha (Macdonald and Katsura, 1964); St. Helena : SH (this study); Tristan da Cunha group : T (Baker, et al, 1964). Envelopes of analyses of islands except Hawaii are shown.

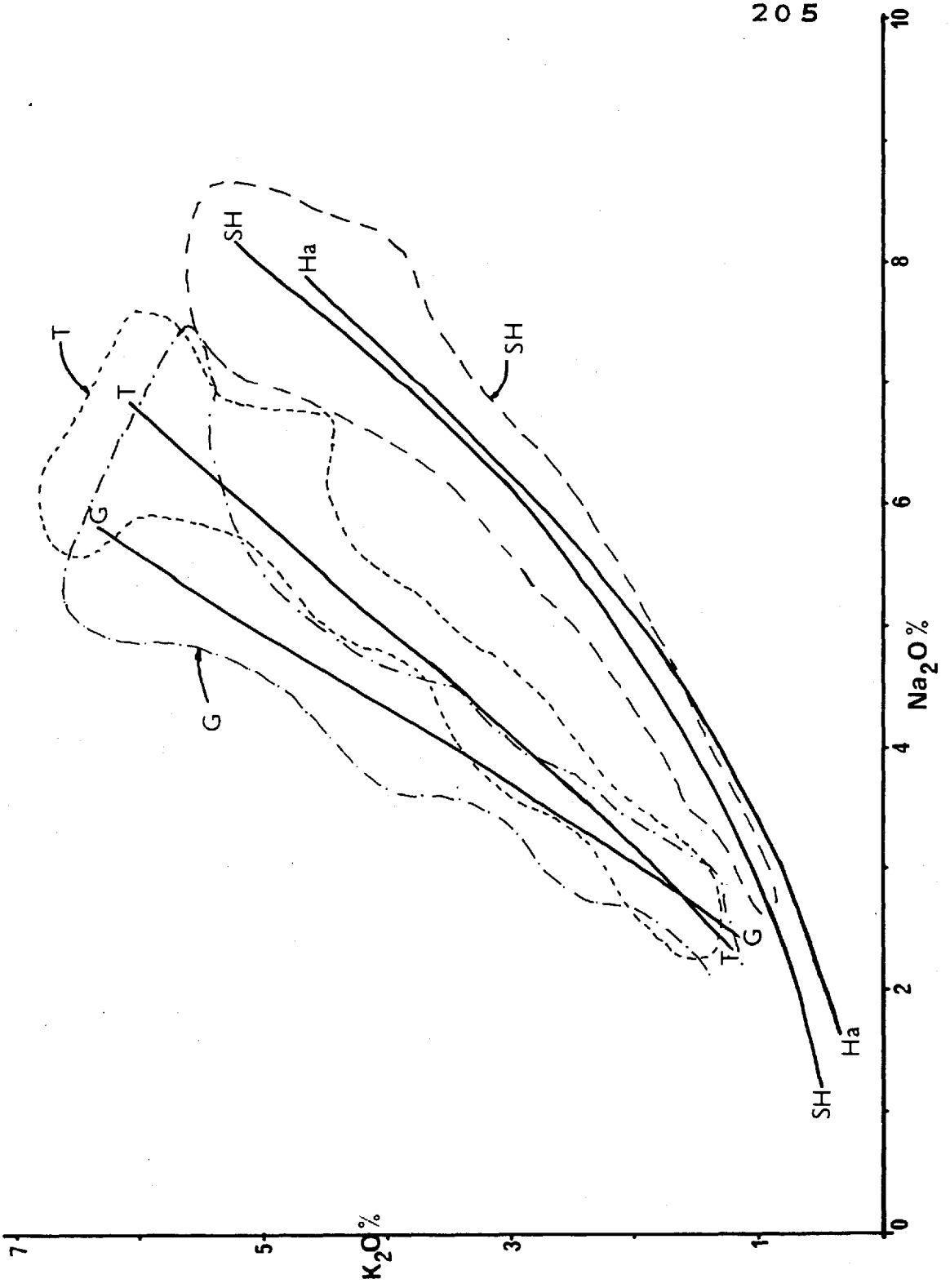

FIGURE 27

FIGURE 28:

Soda-potash variation diagram for Ascension: + (Daly, 1925); Gough Island : G (LeMaitre, 1962); Hawaii : Ha (Macdonald and Katsura, 1964); Heard Island : H (Tyrell, 1937); St. Helena : SH (this study); Tenerife : Te (W.I. Ridley and M.J. Abbott, unpublished data, personal communication); Tristan da Cunha group : T (Baker, et al, 1964).

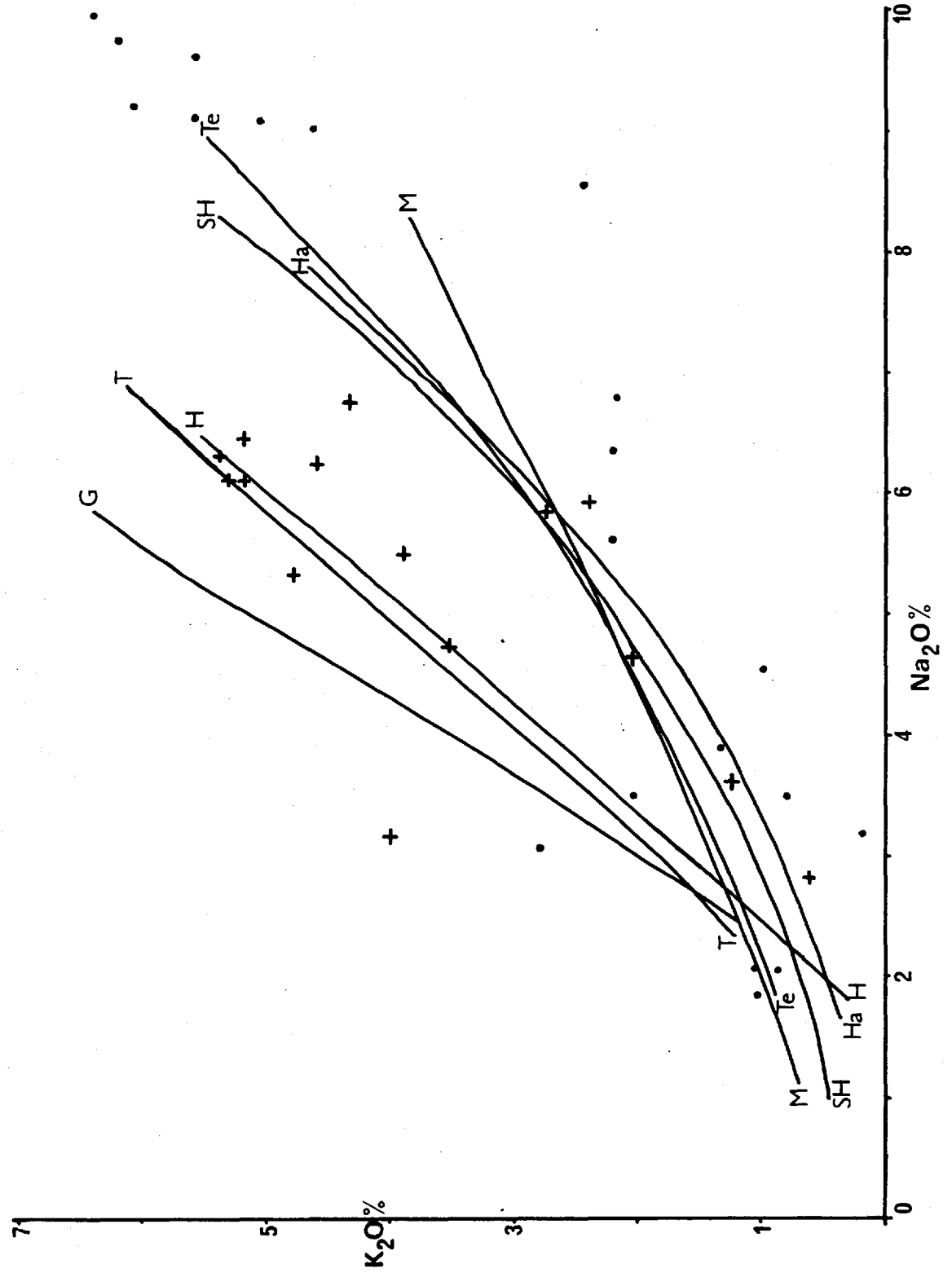

FIGURE 28

FIGURE 29:

Soda-potash variation of selected intermediate rocks compared to the Gough Island (G), Hawaiian alkali (Ha), and Tristan group (T) trends (see Fig. 27).

\+ : Hebridean rocks (Muir and Tilley, 1961).

1 : Average Gough trachyandesite (3) (LeMaitre, Table 10, 1962).

2 : Average Tristan group trachyandesite (9) (Baker, et al, Table 8, 1964).

3 : Average St. Helena trachyandesite (12) (this study).

4 : Average "feldspathoidal tristanite" (16) (nepheline latite, Table 10, Nockolds, 1954).

5 : "Leucite tristanite", Tristan da Cunha (Dunne, 1941, in Baker et al, Table 6, 1964).

6 : "Benmoreite", Ben More horizon, Mull; and

7 : "Benmoreite", Totardor, Skye (Muir and Tilley, Table 4, 1961).

8 : "Trachytes trending towards mugearite", Hawaii

9 : (Macdonald and Katsura, Tables 3 and 6, 1964).

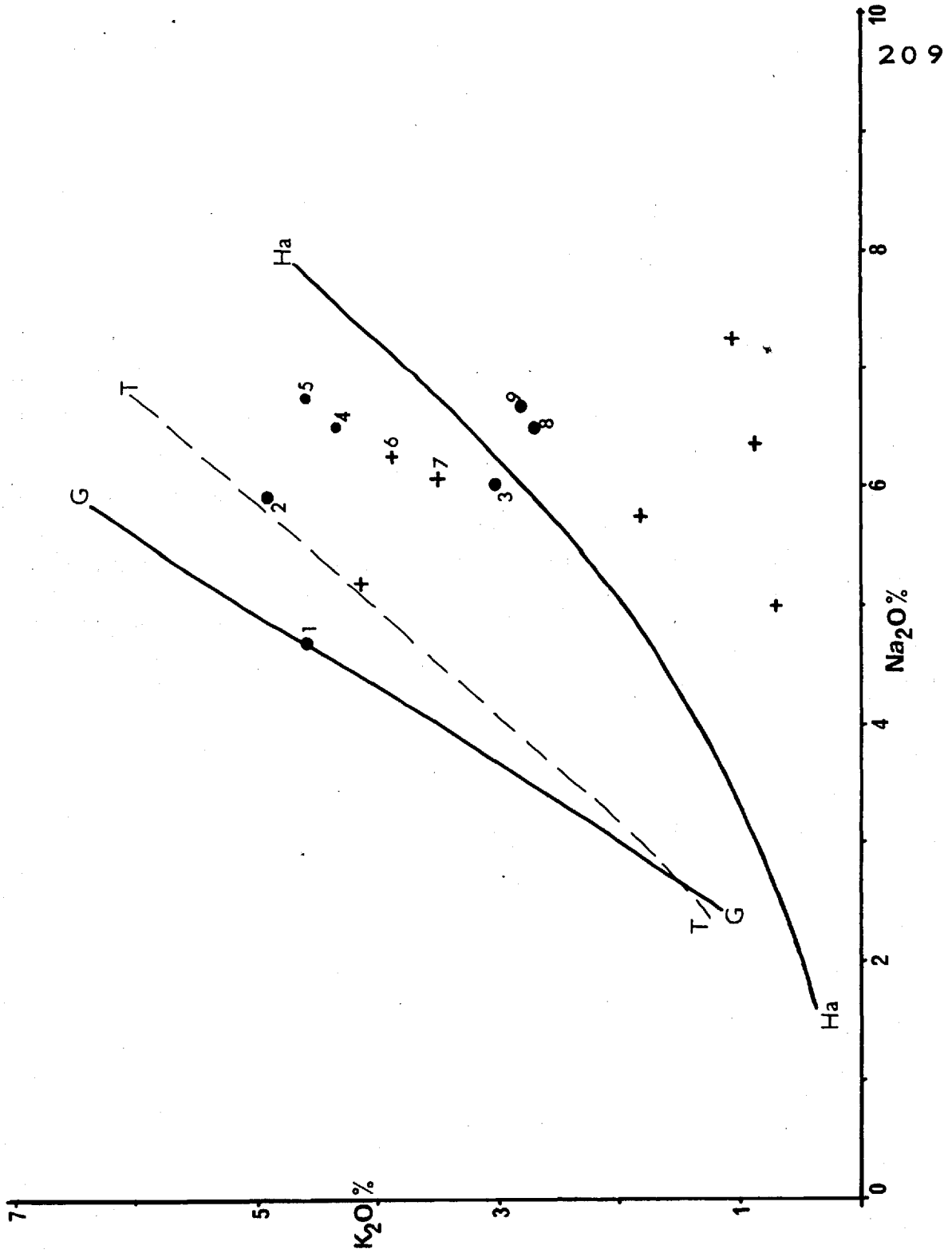

FIGURE 29

(Fig. 29, 4 and 5) that the four analyses could be taken to lie on a trend line similar (but intermediate) to those drawn for the sodic Hawaiian and the potassic Gough Island trends (Fig. 29).

The terms tristanite and benmoreite are defined for rocks which do not display marked undersaturation (Tilley and Muir, 1964). The intermediate rocks of Tristan da Cunha are undersaturated, the average trachyandesite containing 10.4% normative nepheline, whereas the Nightingale, Inaccessible and Gough Island "trachyandesites" all contain less than 5% normative nepheline. Since the variation diagrams of Tilley and Muir (1964) are plotted on data from the Gough Island rocks a logical name for an intermediate, if two trends are to be established, would be "goughite", not tristanite.

With all of these points in mind, it is suggested that the existing nomenclature, based on two series dependent on soda : potash ratio, is only of limited use. Any system which is to be of widespread application should be one to which the prefixes 'potassic' or 'sodic' can be affixed if the dominance of either is sufficiently marked.

The existing nomenclature for these intermediate rocks uses group names taken from Hawaii, Mull, Skye and Tristan da Cunha. The transitional and gradational nature of the alkali olivine basalt - trachyte assemblages from the vast majority of oceanic islands is strongly stressed by all workers, a fact not at all apparent in existing complex nomenclature. It is for this reason that LeMaitre (1962) and Baker, et al (1964) have used the broad terms "trachybasalt", "trachyandesite", for the intermediate rocks of Gough Island and the Tristan group, although the terms are defined between limits specified for each island (see LeMaitre, 1962, p1311).

In spite of the confusion surrounding the terms trachybasalt and trachyandesite, the names express the intermediate transitional nature of the rocks in question. The term trachybasalt was recommended for general use by the Committee on British Petrographic Nomenclature (Mineral. Mag. 19, p144, 1921) for "intermediate potash-rich rocks containing basic plagioclase together with orthoclase", in which connotation it has been retained by Tilley and Muir (1964).

The andesine-andesites and oligoclase-andesites of Hawaii (Macdonald, 1949) were reclassified by him as andesine basalts and mugearites (1957) and hawaiites and mugearites (1960). He stressed (1960) the difference between oceanic alkali intermediate rocks and continental andesites. Although from the published chemistry and mineralogy these rocks are obviously very different, confusion has developed because of lack of "careful reading of the description" (Macdonald, p172, 1960). Because of this misinterpretation their marked differences must be accentuated, and distinctive names be sought (op. cit. para. 2, p173). If the differences in oceanic and continental andesites need to be stressed in order to eliminate misinterpretation by the cursory reader, then for this very reason the breaking up of the oceanic intermediate rocks into hawaiite and mugearite not only detracts from their transitional nature but implies a distinctness not at all in keeping with their petrography, chemistry or occurrence. Even the subdivision of the series into andesine- or oligoclase-bearing groups presents difficulties. Rocks described by Daly (1911, pp297-301) and Cross (1915, pp30-31), petrographically similar to St. Helenan lavas, are placed by Macdonald (1960, p173) into his group of hawaiites. Modally Daly's 'andesitic basalt' (pp297-298) contains plagioclase with cores of An_{50}, a thin shell of oligoclase (An_{30}) and a thinner outer shell of more acid oligoclase or orthoclase. Groundmass

feldspar consists of zoned plagioclase with a greater development of acid shells and possibly an outer zone of alkali feldspar. His "trachydolerite" (pp299-301) has groundmass plagioclase of An_{50} and interstitial orthoclase; labradorite micro-phenocrysts have an outer shell of alkali feldspar. The total alkali feldspar in the rock is not more than 15% by weight. Cross's rocks (1915, pp30-31) both contain andesine, or andesine-oligoclase laths, with modal nepheline and orthoclase. Analyses of these rocks are shown in Table 3, together with the average Hawaiite and mugearite (Macdonald and Katsura, table 10, 1964). Although the rocks from Haleakala (Cross, 1915) are more undersaturated than the average Hawaiian intermediates, they compare closely with the average 'mugearite' (if anything, one is slightly more alkaline) and not with the hawaiites. Hawaiites in Macdonald and Katsura's work (1964) on the Hawaiian lavas are very varied in their chemical properties. They range in differentiation index from 33.9 (Table 2, anal. 10) to 56.6 (Table 4, anal. 9), although of the eight analyses five have values between 39.6 and 50.5. Their total alkalis range from 4.32% to 7.58%, the above five however, containing between 4.90% and 6.66%. The normative plagioclase (calculating Or as Na-free) is andesine in all cases.

For a given percentage of total alkalis between similar limits of silica composition, saturated to mildly undersaturated rocks will give a norm dependent on the soda : potash ratio. If K_2O is high the rock norm will be rich in orthoclase with a coexisting calcic plagioclase - if Na_2O is high there will be less orthoclase and a dominant sodic plagioclase. From consideration of analyses from islands with soda : potash ratios less extreme than those of Gough and Hawaii, and because of the transitional nature of the oceanic intermediate alkali rock series, it is proposed to use the term trachybasalt for those intermediate rocks called trachy-

	1	2	3	4	5	6
SiO_2	49.73	50.92	48.60	51.90	49.55	51.26
TiO_2	3.05	2.55	3.16	2.57	2.09	2.57
Al_2O_3	16.39	17.59	16.49	16.65	17.78	16.74
Fe_2O_3	7.58	3.80	4.19	4.25	4.65	2.92
FeO	3.98	6.69	7.40	6.17	5.89	7.11
MnO	0.23	0.20	0.18	0.21	0.28	0.23
MgO	4.06	3.90	4.70	3.56	2.49	2.80
CaO	7.17	6.97	7.79	6.30	7.01	6.61
Na_2O	4.12	4.28	4.43	5.22	6.12	5.86
K_2O	1.93	1.86	1.60	2.01	2.29	2.25
P_2O_5	0.84	0.40	0.69	0.93	1.10	0.81
H_2O	1.35	1.14			0.63	0.68
Rest	0.10				0.18	0.19
Total	100.53	100.30			100.06	100.03
$Na_2O:K_2O$	2.1	2.3	2.8	2.6	2.7	2.6
q	1.86*					
or	11.12	11.12	9.45	11.68	13.34	12.79
ab	34.58	36.16	35.11	44.01	34.58	38.25
an	20.85	23.35	20.57	16.12	15.01	12.79
ne			1.14		9.09	6.25
D.I.	47.56	47.28	45.69	55.69	57.01	57.29

*(Almost certainly due to the Fe_2O_3:FeO ratio.)

1: "Andesitic basalt", Mauna Kea (Daly, p298, 1911).

2: "Trachydolerite", Mauna Kea (Daly, p301, 1911).

3: Average Hawaiian hawaiite (Macdonald and Katsura, p124, 1964).

4: Average Hawaiian mugearite (Macdonald and Katsura, p124, 1964).

5: } "Essexitic andesites" or "trachyandesites", Haleakala,
6: } (Cross, p31, 1915).

TABLE 3.

basalts, hawaiites and mugearites by Macdonald (1960) and Tilley and Muir (1964). Certainly the total alkalis for both groups are comparable and this is a prime consideration in the oceanic alkali rocks. Sodic and potassic may be used as prefixes to trachybasalt if the dominance of one or other is sufficiently marked.

That oceanic rocks equivalent to andesites exist under different names cannot be discredited (Macdonald, 1960); similarly trachytes exist. Trachyandesite is therefore quite legitimately an intermediate rock lying between these two. The Chayes minimum frequency limits were taken by Tilley and Muir (1964) to define the limits for benmoreite and tristanite, and these limits are taken here to define trachyandesites. Any intermediate rock of the oceanic alkali basalt-trachyte series which chemically falls inside three of Chayes four minimum frequency parameters may be called a trachyandesite. Rocks in fact called "trachyandesites" by LeMaitre (1962) and Baker et al (1964) fall more completely into Chayes' minimum frequency group than do the tristanites and benmoreites specifically named on the basis of these limits by Tilley and Muir (1964) (see Table 4 below). Analyses of eight trachyandesites (as defined here) from St. Helena are averaged in Table 4, Column 3, and Column 4 includes four similar rocks but with two parameters outside Chayes limits. Nockolds' (1954) average nepheline latite ("leucite-tristanite" of Tilley and Muir, 1964), two benmoreites (including the 'type' rock) and two "trachytes tending towards mugearites" from Hawaii are included for comparison (see also Fig. 29). Although the St. Helena alkali trend is very close to that of Hawaii, the average trachyandesite is much closer in terms of silica and differentiation index to those of Tristan and Gough (and Nockolds' average nepheline-latite), presumably as a result of the slight undersaturation.

	1	2	3	4	5	6	7	8	9
SiO_2	55.4	54.9	55.0	55.1	53.0	55.8	58.6	58.3	58.0
CaO	4.6	5.7	3.9	3.8	5.3	3.2	2.9	3.0	3.3
$FeO+Fe_2O_3$	7.4	5.7	8.8	9.0	6.1	9.1	8.0	7.1	6.6
D.I.	66.0	69.7	68.0	67.3	67.9	73.4	74.5	74.3	73.6

1: Average (3) "trachyandesite", Gough Island (LeMaitre, Table 10, 1962).

2: Average (9) "trachyandesite", Tristan da Cunha group (Baker et al, p531, 1964).

3: Average (8) trachyandesite, St. Helena.

4: Average (12) trachyandesite, St. Helena (4 rocks included with 2 parameters outside Chayes' limits, but in all other ways similar to the other 8 specimens).

5: Average nepheline latite (Nockolds, p1024, 1954).

6: "Benmoreite", E of Kinloch Hotel, Mull (Tilley and Muir, Table 1, 1964).

7: "Benmoreite", Totardor, Skye (Tilley and Muir, Table 1, 1964).

8: } "Trachytes trending toward mugearites", Hawaii (Macdonald
9: } and Katsura, Table 3, anal. 18; Table 6, anal. 27, 1964).

TABLE 4

The limits of trachybasalt would be given by trachyandesite at one end, and basalts at the other (less than 10% normative orthoclase and groundmass plagioclase cores more calcic than An_{50}). For these intermediate rocks of Gough, St. Helena and the Tristan group the lower differentiation index limit is about 40; for hawaiites from Hawaii, the lowest D.I. is 33.9 although most are greater than 40 (Macdonald and Katsura, 1964). It is impossible to define the limits of the alkali olivine basalt - trachyte series on any one criterion, but rocks with a D.I. of less than about 40 will probably fall into the system of basaltic nomenclature.

4. Highly Alkaline Rocks.

Rocks with differentiation indices usually greater than 75 have been called trachytes, phonolitic-trachytes and phonolites. All of the rocks occur as intrusives with the exception of two closely associated flow domes (The Stone Tops). The intrusive rocks belong to a major late intrusive phase and it has proved difficult to "pigeon-hole" many of them because of their almost perfectly transitional nature.

The flow domes contain up to 10% normative nepheline, but modally lack the minute hexagonal euhedra characteristic of the intrusions. Instead, the interstitial material and parts of the groundmass consist of analcite, or zeolites, and is of uncertain origin. The rocks usually exhibit modal plagioclase cores to the feldspar laths and have a relatively high content of normative anorthite. For these reasons these rocks have been designated trachytes. Intrusions which have similar mineralogy and/or chemistry to the flow domes, or lack modal nepheline are also termed trachytes.

Many of the intrusions contain up to 5% modal and normative nepheline. Several of the dykes however, in the

central areas of Sandy Bay, contain more than 10% modal nepheline and up to 16% in the norm. These rocks are markedly undersaturated and are justifiably called phonolites. The rocks which are less undersaturated, less alkaline, and contain only a small amount of modal nepheline have been called phonolitic-trachytes. Although rigid classifications would require 5% or 10% limitations on modal or normative constituents the name is used broadly and demonstrates the transitional characters of the felsic rocks as a whole.

SECTION VI

PETROGRAPHY

1. Petrography of the volcanic rocks.

Transmitted light studies were made with a Zeiss Ultraphot II binocular microscope, and reflected light identification of the opaque phases was carried out by S.E. Haggerty, using a Reichert Zetapan reflecting microscope. Both instruments are capable of high resolution with magnifications up to x 1600. Optical properties of individual minerals were studied using a Leitz-Wetzlar 4-axis universal stage attached to a Swift monocular microscope; refractive indices were measured by the conventional immersion method. Olivine compositions with greater than 30 mol per cent fayalite were determined using the X-ray method of Jambor and Smith (1964).

The mineralogies of the various rock types are summarized in Table 5. Throughout this Section analyzed rocks are described using their collection number (1 to 847) as in the chemical abalyses and norms presented in Tables 6-12 of Section VII.

Alteration products after olivine have been studied in detail with S.E. Haggerty, and the results published as work separate from the bulk of this thesis (Haggerty and Baker; Baker and Haggerty, 1967). Here they will be referred to under broad groupings as used in these publications.

TABLE 5

Rock type	(Micro)phenocrysts		Groundmass	
	Common	Rare	Common	Rare
Ankaramites and highly porphyritic basalts	Pyroxene Olivine	Plagioclase Titanomagnetite	Pyroxene Titanomagnetite Plagioclase ± Olivine	Alkali-feldspar
Olivine basalts	Olivine Plagioclase	Pyroxene Titanomagnetite	Plagioclase Pyroxene Titanomagnetite Olivine ± Ilmenite	Alkali-feldspar Biotite Apatite
Trachybasalts	Olivine Titanomagnetite Plagioclase	Apatite	Plagioclase Pyroxene Titanomagnetite ± Ilmenite Alkali-feldspar	Olivine Biotite Apatite
Trachyandesites	Plagioclase Olivine Titanomagnetite	Pseudomorphs after amphibole Apatite	Plagioclase Alkali-feldspar Titanomagnetite Pyroxene Apatite	

Trachytes (extrusive)		Olivine	Alkali-feldspar	
		Titanomagnetite	Plagioclase	
		(Amphibole)	Aegirine-augite	
		Apatite	Titanomagnetite	
<u>Intrusive rocks</u>				
Trachytes		Olivine	Alkali-feldspar	Apatite
		Titanomagnetite	Aegirine-augite	?Nepheline
			Titanomagnetite	
			Plagioclase	
Phonolitic-trachytes	Alkali-feldspar	Aegirine-augite	Alkali-feldspar	Aegirine
		Amphibole psuedomorphs	Aegirine-augite	Cossyrite
		Olivine	Titanomagnetite	
			Nepheline	
Phonolites	Alkali-feldspar	Amphibole pseudomorphs	Alkali-feldspar	Cossyrite
			Aegirine-augite	
			Nepheline	
			Titanomagnetite	
			Aegirine	

a. Ankaramites and highly porphyritic olivine basalts (Table 6).

Ankaramites with phenocrystal pyroxene greatly in excess of olivine (3:1 or 2:1) are especially abundant in the lower shield of the south-western volcano, and occur more rarely in the north-east. The rocks have a black or dark-grey fine-grained matrix enclosing numerous black euhedral pyroxenes(up to 20mm) and rounded, frequently "iddingsitized" yellow-green olivines (up to 8mm). Phenocrysts may form over 60% of the rock, but the most porphyritic rocks analyzed contained ~50% (804) and ~40% (785). Plagioclases are usually present in subordinate amounts, and rare titano-magnetite phenocrysts occur in 679. Composite phenocrysts of plagioclase, pyroxene + plagioclase ± olivine, and pyroxene + olivine + titanomagnetite may occur.

In thin section the pyroxenes are non-pleochroic pale yellow-brown, or rarely pale pink-brown. Although they frequently form perfect euhedra, some appear to be broken fragments (844); they usually display a sieve-texture, enclosing patches of groundmass (Plate 22A). The outer zones, or zones nearest the enclosed sieve patches, are usually darker brown or purple. The pyroxenes have a moderate 2V (53°-54°), positive sign, high extinction (43°-46°), and β = 1.707 (804) to 1.686 (179).

These optics indicate that the pyroxenes are augites, usually with sufficient Ti to produce the purple colouration; the pale grey-green ill-defined cores in some ankaramites may be diopsidic-augites. The zoning suggests that after extrusion the crystallizing pyroxene is much richer in Ti than the early crystallizing phase.

Olivine phenocrysts are colourless, slightly rounded or euhedral (844), show variable development of the

(010) cleavage and may be partly enclosed by pyroxenes. Optical properties (2V very high, negative; β = 1.694 - 1.696) indicate compositions of Fa_{20-23} in all of the rocks.

Plagioclase phenocrysts (cores: An_{80-67}) occur singly or in small clots, are usually strongly normally zoned, and may include zones of inclusions and corrosion traces. Minor oscillatory zoning is rare, e.g. from core to rim:

$$An_{80} \rightarrow An_{68}/An_{73} \rightarrow An_{68}/An_{73} \rightarrow An_{66} \rightarrow An_{60}$$
$$An_{78}/An_{64}/An_{75}/An_{72} \rightarrow An_{71} \rightarrow An_{74} \rightarrow An_{66}$$

The intergranular groundmass consists of multiply twinned plagioclase laths, granules of pale brown or neutral pyroxene and titanomagnetite (frequently of two generations), and interstitial alkali feldspar. The plagioclases (An_{61-67}) are more or less strongly zoned out towards andesine. The alkali feldspar is present in all specimens, its proportion increasing slightly from 804 (D.I. = 13.3) to 679 (D.I. = 31.6). In 844 it forms irregular patches often consisting of large single "crystals", with characteristic curved extinction.

The porphyritic flows frequently contain spinels (of Cr,Al, Fe types) as small euhedral inclusions in olivines or as discrete 'microphenocrystal' grains invariably rimmed by titanomagnetite with minute silicate inclusions. Spinels also occur in some finer-grained basalts, but only as small inclusions within olivines, never as discrete microphenocrysts.

b. Olivine basalts (Table 7).

The olivine basalts are fine-grained, compact, grey-green, purple-grey, or dark grey rocks, occasionally with a slight shimmer parallel to the flow oriented plagioclases.

PLATE 22:

A: Sieve pyroxene in alkali olivine basalt (179). Note included small olivine (extreme left of crystal), and very slight fluxional orientation of plagioclase laths round the phenocryst. Pyroxene is 2.3mm across; magnification x30. Crossed Nicols.

B: "Spongy" homogeneous titanomagnetite in fine-grained basalt (830). Microphenocryst is 0.7mm long; magnification x100. Plane polarized light.

C: Alkali feldspar patch in basalt (737). Note polycrystalline nature and relatively coarse grain size. Field of photograph: 1.4 x 2.3mm; magnification x55. Crossed Nicols.

D: Corroded feldspar phenocrysts in Bencoolen trachyandesite flow (828). Note thickness of corrosion rim and the degree of zoning in the core. Field: 2.5 x 3.5mm; magnification x30. Crossed Nicols.

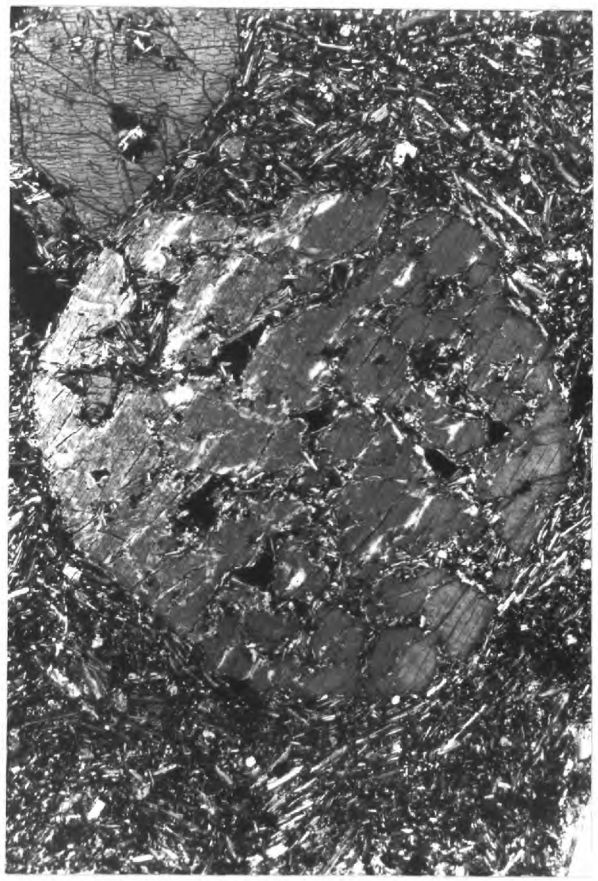

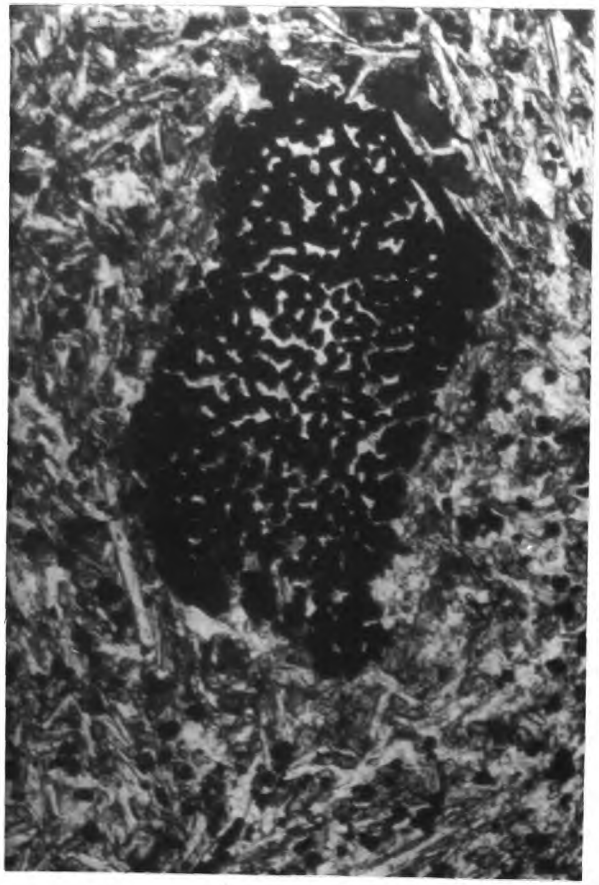

Phenocrysts are uncommon to absent, although microphenocrysts may be abundant.

The (micro)phenocrysts vary considerably, olivine is almost ubiquitous and plagioclase may be dominant or totally absent, titanomagnetite is a little more common than the very rare pyroxene, and may display a "spongy" texture (Plate 22B). Two very fine-grained basalts (747 and 201) contain single large corroded olivines penetrated by 'fingers' of groundmass. Their 2V is nearly 90^{o} and they are optically positive indicating a composition more forsteritic than Fa_{15} - they are believed to be xenocrysts.

Plagioclase (micro)phenocrysts (An_{74-60}) are zoned out to An_{54-52}, and sharply rimmed by untwinned plagioclase (probably oligoclase). Colourless, unzoned olivines (Fa_{23-29}) may be rounded, euhedral, or rarely elongate parallel to the c-axis and often display (010) cleavage. Minor alteration to "iddingsite" or green phyllosilicates is not uncommon.

Phenocrysts of augite are non-pleochroic pale-brown or pale yellow-neutral. They have a moderate 2V (48^{o}-50^{o}) are optically positive with extinction of 42^{o}, sometimes decreasing very slightly at the rim. Large phenocrysts usually display sieve-texture, and patchy, weakly undulose extinction.

The groundmass of pyroxene granules, Fe-Ti oxides, plagioclase laths and rarely olivines, displays a fluidal intergranular texture. The plagioclases (An_{64-55}) are strongly zoned (to An_{35-30}) and multiply-twinned on Carlsbad, albite, pericline and, very rarely, Baveno laws. In some rocks (especially 706 and 834) a thick outer zone of untwinned plagioclase, probably oligoclase (R.I. $\geqslant$ C.B.), is developed. A large number of groundmass plagioclases display

polysynthetic twinning at both ends of the laths but have an untwinned centre; the laths rarely appear 'bent'. In basalts with Differentiation Index greater than 36 (786, 809, 830, 834) twinning in groundmass plagioclase is indistinct or absent, extinction angle variations, however, suggest continuous compositional variation.

The small, rounded groundmass pyroxenes are very pale neutral-brown or neutral-green in colour. In 716 (an intrusive sheet) fine-grained (0.1-0.2mm) plagioclase laths, titanomagnetites, and subhedral olivines (Fa_{29}) are set in large poikilitic patches (to 4.5mm) of deep purple-pink titanaugite with purple margins. Optically the non-pleochroic titanaugite is comparable to phenocyrstal pyroxenes with $2V = 48^{o}$, and positive sign; the high R.I. (δ = 1.720) may be a result of the high titanium content.

Oxides occur in two or more generations, the titanomagnetite (micro)phenocrysts may be skeletal with broad "arrowhead" outgrowths from the corners of a small central cube. Rocks either contain no ilmenite or approximately equal proportions of ilmenite and titanomagnetite as equant granules. In 226 small late patches of alkali feldspar and biotite are surrounded by a discontinuous rim of tiny titanomagnetites. An indistinct banding in some basalts, and trachybasalts, results from the distribution of oxides into bands with large, less abundant grains, and bands packed with very tiny granules.

Many basalts contain small "droplets" of sulphides (pyrite $>$ chalcopyrite $>$ pyrrhotite) which are usually included in oxides but rarely occur in olivines and pyroxenes.

Abundant alkali feldspar ($2V = 30^{o}$-55^{o}) occurs as polycrystalline patches (Plate 22C) displaying irregular grain boundaries and curved extinction, as truly interstitial

material, or as vesicle linings. In all cases it contains numerous fine hair-like, colourless crystals, probably of apatite.

Biotite (2V approx. 10^{o}, negative; Z = fox-red to pink-orange, Y = yellow-brown, X = colourless or very pale pink-neutral) occurs interstitially or associated with the alkali feldspar-rich patches. The sheets frequently contain numerous colourless, weakly birefringent silicates, and locally may partially enclose olivines. The distinctive pink colours in the pleochroim strongly suggest an appreciable Ti content.

c. Trachybasalts (Table 8).

The trachybasalts are fine-grained rocks in shades of dark-grey, grey-green or purple-grey with a sheen developed parallel to the flow oriented feldspars (except in minor intrusions).

Microphenocrysts are not uncommon with olivine > titanomagnetite > plagioclase, frequently all occurring together. Pyroxene never occurs outside the groundmass, but in two flows (723, 85) is weakly poikilitic. The groundmass consists of fluxionally arranged feldspar laths, granular pyroxene, oxides, and rarely olivine with abundant interstitial alkali feldspar and biotite. 'Microphenocrystal' apatite occurs, but more usually is included as acicular crystals in alkali feldspars.

The neutral or pale straw-yellow olivines (Fa_{31-46}) are frequently altered to "iddingsite". They are frequently elongate parallel to the c-axis with length : width ratios up to 10 : 1. Microphenocrysts of homogeneous titanomagnetite are usually sub-skeletal as in the basalts, although rarely 'spongy' phenocrysts may occur. The twinned plagioclase may be strongly normally zoned (37, 277, 521) from cores

of An_{68-59} to oligoclase, and in some instances alkali feldspar. Other microphenocrysts with calcic labradorite cores (747, 201, 744, 438) are only weakly zoned before a sharp rim of very sodic feldspar.

The groundmass plagioclasesare strongly zoned from cores as calcic as An_{66} (499), An_{63} (744), An_{59} (792, 723) or An_{58} (277, 521), to sodic plagioclases and/or alkali feldspars. Albite twinning becomes diffuse and disappears at a composition of about An_{30}. Polysynthetic twinning is often of the type developed only at opposite ends of the lath, and Carlsbad twins are uncommon or absent. Untwinned plagioclase with R.I. just greater than Balsam has 2V close to 90^{o} and is optically negative with straight extinction ($\pm$ 2^{o}) on (010). The outermost zone of the feldspars is a thin clear rim of alkali feldspar with extinction varying progressively across it. The groundmass pyroxene is colourless, pale-green or rarely purple-brown (499, 201). In most of the rocks it occurs as slightly elongate granules with extinction = 43^{o}.

Fe-Ti oxides usually of two generations are abundant in the groundmass of all trachybasalts. Equant and lath-shaped grains occur in 499, but in the polished sections studied ilmenite occurs only rarely in 37 and is absent in the other rocks, where the oxides are homogeneous titanomagnetites ($\pm$ development of maghemite).

In the more basic trachybasalts alkali feldspar occurs dominantly as rims to plagioclase laths, but in the more alkaline rocks it occurs interstitially, often concentrated in particularly rich patches containing abundant hair-like apatites. In 438 distinctive large patches of alkali feldspar consist of single 'crystals' with undulose extinction.

Biotite, optically similar to that found in the basalts, occurs interstitially, in tiny flakes concentrated

near oxide grains (744) or more usually in patches rich in alkali feldspar.

Microphenocrysts of apatite (277, 782, 438) containing oriented inclusions (of ?rutile) may be associated with titanomagnetite microphenocrysts.

Traces of green phyllosilicates occur in the groundmass of a few rocks and traces of carbonate were seen in 744. A completely clear, nearly isotropic mineral with R.I. very much lower than Balsam and birefringence = 0.001, infilling minute vesicles in 277 is probably analcite.

The dyke 782 may represent a mixed rock with phenocrysts of olivine, amphibole, plagioclase, titanomagnetite and apatite, in a groundmass of plagioclase, elongate olivines, minute pyroxene granules, two generations of homogeneous titanomagnetite, alkali feldspar and biotite. Olivine occurs as corroded crystals or euhedra with $2V = 90^{o}$ (Fa_{15}), and good (010) cleavage. Plagioclases are corroded with cores more sodic than the thick outer zone (on extinction variations); many are completely untwinned with 2V approximately 90^{o}. Titanomagnetite phenocrysts are corroded or embayed. The amphibole (Z = dark brown to fox-red; X = yellow-brown) has an unbroken reaction rim of ilmenite and titanomagnetite set in sub-poikilitic, colourless pyroxene and twinned plagioclase (Plate 23A). Tiny relic amphiboles are distinctly paler than unaffected crystals. The groundmass plagioclases are strongly and apparently normally zoned (increasingly sodic outwards), and are set in very abundant interstitial alkali feldspar.

d. Trachyandesites (Table 9).

The trachyandesite flows (except 828) are medium-grained, green shimmering rocks with excellent flow oriented feldspars. The intrusions (218, 845, 323, 671) also display

this shimmer but 218 is highly altered and oxidized, 845 is very fine-grained grey-green, and 323 is oxidized to brown-grey. The Bencoolen flow (828) is a coarse-grained, completely oxidized purple-brown or purple-grey rock, and so rough to the touch that it would readily fit the original classification of "trachyte".

Phenocrysts are very rare and are either feldspars (822, 828, 704) or embayed titanomagnetites (664). Microphenocrysts are of feldspars and/or olivine, and less commonly of titanomagnetite or oxide/silicate pseudomorphs after amphibole (161 is the only analyzed rock of this type). Pyroxene never occurs as microphenocrysts, but in a number of rocks is markedly poikilitic.

The flows of wide lateral extent, the dyke (845) and two intrusions (323, 671) are similar petrographically, with straw-yellow subhedral olivines, equant homogeneous titanomagnetites and zoned feldspar laths set in a fine-grained matrix of flow oriented feldspars, one or two generations of titanomagnetites, poikilitic green aegirine-augite and irregular alkali feldspars. Olivines, subhedral not elongate, in a number of rocks are partly rimmed by overgrowths of the pyroxene and may enclose rounded titanomagnetites. In 613 up to three olivines (Fa_{69}) may occur in clusters with apatite and titanomagnetite microphenocrysts. Alteration of olivine is either of the high temperature variety resulting in an 'opaque' rim, or is of intermediate or low temperature type resulting in the breakdown to green phyllosilicates. Olivines overgrown by pyroxene are protected and show only intermediate and low temperature alteration.

Plagioclase microphenocrysts are continuously zoned from homogeneous cores of An_{56-48} (599, 613, 486) or An_{46-42} (704, 664) through increasingly sodic plagioclase

to a thick rim of untwinned alkali feldspar. In the groundmass, plagioclases display prominent Carlsbad twins with diffuse albite and rarely pericline sets.

The pyroxene is weakly to moderately pleochroic (increasing with increasing differentiation index), with: X = medium to bright green; Y = yellow-green to pale brown-green; Z = pale yellow-green to pale grey-green. Poikilitic patches, 2-3mm across, may be elongate parallel to the feldspar orientation. The pyroxene is optically positive with a moderate 2V (about 60°) and extinction from 41°-44°. Zoning may be weakly developed with slightly greener margins with extinction up to 7° lower than the cores, probably reflecting minor increases in soda-content of the aegirine-augite. Pyroxene prisms may include numerous oxide grains (704).

The opaque minerals, although more or less deuterically oxidized (Watkins and Haggerty, 1967), were originally homogeneous titanomagnetites; discrete ilmenite is rare or absent.

Alkali feldspar forms interstitial patches, with undulatory extinction and diffuse crystal boundaries, often concentrated into distinct areas. More rarely individual "crystals" are developed with an equivalent grain size to the microphenocrysts. Clear acicular apatites may be included in the feldspar, but frequently euhedral microphenocrysts occur discretely or associated with titanomagnetites or olivines. These apatites are packed with minute, oriented rods (?rutile) increasing in number towards the rim and appear pale pink and weakly pleochroic.

The 218 intrusion is badly altered - veins of green chloritic material traverse the groundmass and vesicles may contain goethite. Original titanomagnetites of two

generations are oxidized and contain metailmenite with minor replacement by hematite. The rock is medium-grained with tabular zoned plagioclases, completely altered olivine, granular pyroxene and small apatite euhedra set in a felted mass of feldspars containing discrete "crystals" of alkali feldspar with 2V of about 40°. Recognizable ferromagnesian minerals are aegirine-augite (extinction = 43°), rare biotite (X = colourless; Y = pale yellow-brown; Z = red-brown or pale chocolate-brown), and a highly birefringent amphibole with moderate pleochroism (X = pale green-brown or medium green; and Z = medium brown-green or dark green-brown), 2V close to 90° and extinction greater than 20°.

Specimen 161 is a relic flow petrographically similar to flows known to originate from parasitic centres. Mineralogically it is comparable to other trachyandesites with microphenocrysts of rare zoned plagioclase (core = An_{53}) but also abundant pseudomorphs after amphibole (Plate 23B). The pseudomorphs are prismatic, with a six-sided basal section, and consist of Fe-Ti oxide granules and subordinate colourless or pale green pyroxene, and rarely a second colourless silicate (birefringence = 0.004).

In thin section 822 and 828 flows (see Section III, 5b) are extraordinary, with phenocrysts of plagioclase and anorthoclase and microphenocrysts of neutral-yellow olivine (Fa_{41}), and pink inclusion-rich apatite (828), set in a mass of alkali feldspar, plagioclase, two generations of titanomagnetite, abundant acicular apatites and granular to subpoikilitic pyroxene. In 828 where oxidation is extreme (original titanomagnetite pseudomorphed by rutile, titanohematite and pseudobrookite) olivines are completely altered (at high temperature) to virtually opaque areas of iron oxides and highly reddened silicates.

PLATE 23:

All in plain polarized light.

A: Amphibole xenocryst with complete reaction rim of granular titanomagnetite and ilmenite (782). Note breakdown apparently concentrated along the cleavages producing oxides and pyroxene. Xenocryst : 1.1 x 1.6mm; magnification x50.

B: Titanomagnetite > pyroxene clots in trachyandesite (161). Original euhedral amphibole outline is preserved, and oriented parallel to the fluxional feldspars. Field: 0.75 x 1.1mm; magnification x100.

C: Complete breakdown of amphiboles to clots with titanomagnetite >> pyroxene in trachyte flow (109). Note the distortion of original pseudomorphs with drawing out parallel to the feldspars during flowage. Field: 3 x 4mm; magnification x25.

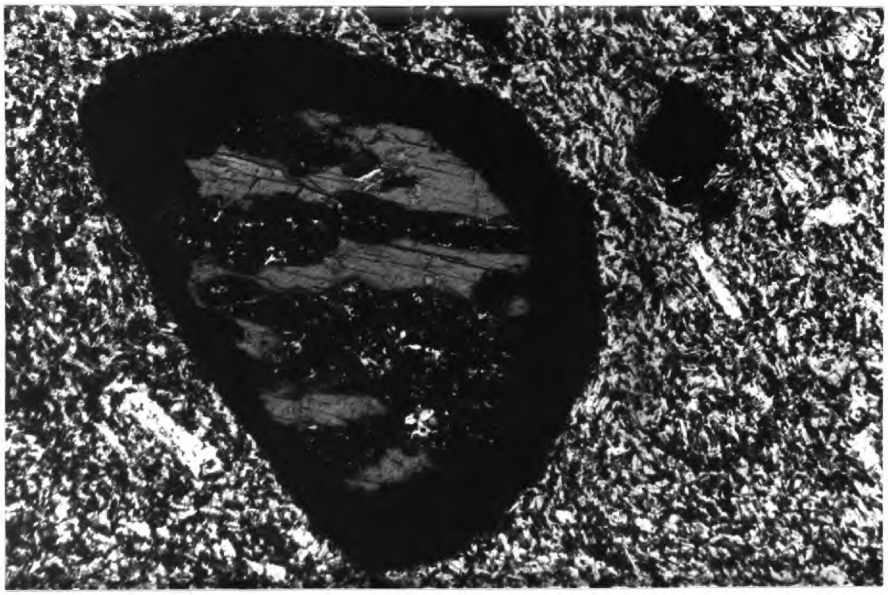

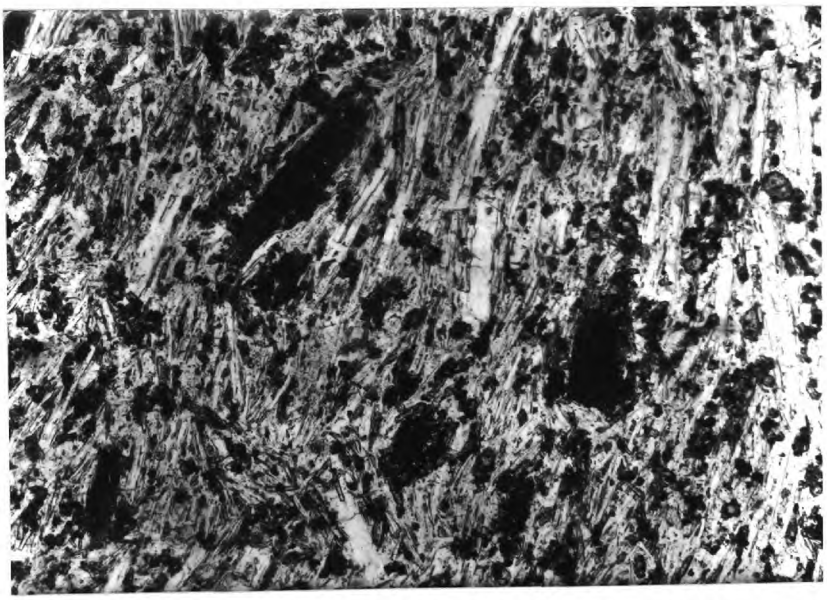

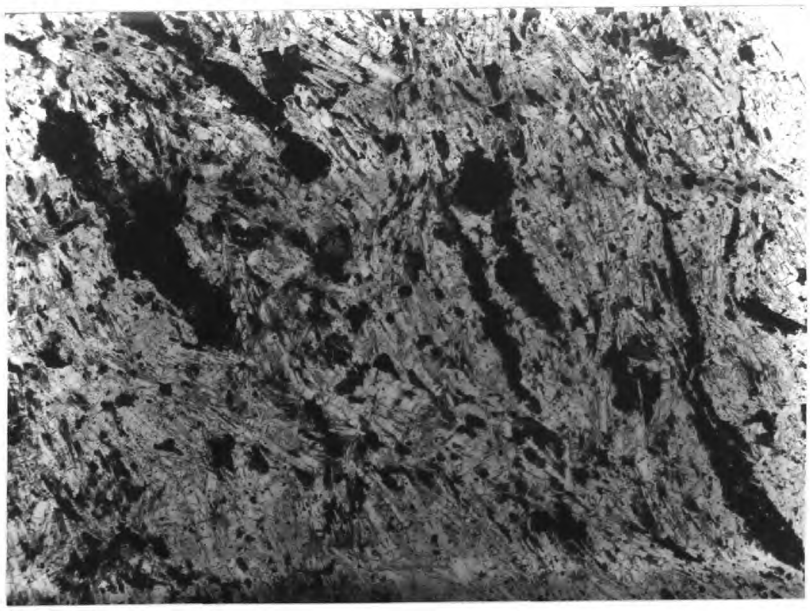

The tabular phenocrysts contain a zone of extensive corrosion which may extend through half the width of the crystal (Plate 22D). Compositionally the phenocryst cores are either anorthoclase (2V from $< 35^{\circ}$ to $> 45^{\circ}$) or plagioclase (An_{54}). Anorthoclases show very fine diffuse lamellar, or rarely cross-hatch, twinning and are corroded with an outer rim of plagioclase zoned outwards from sodic to calcic and back to sodic, sometimes with an alkali feldspar rim. The labradorite/andesine phenocrysts show albite twinning and are zoned out to the corrosion zone of untwinned oligoclase separated sharply from the thick rim continuously zoned from andesine (albite twinned) through untwinned oligoclase to alkali feldspar.

The groundmass feldspar forms very strongly zoned more or less equant crystals, of andesine (An_{47-39}) or alkali feldspar. Plagioclases become increasingly sodic with outer zones of untwinned oligoclase and/or alkali feldspar. Two generations of homogeneous titanomagnetites are totally unaltered in 822, and rare pyrite droplets are visible. The pyroxene (only preserved in 822) is a pale clear green (weakly pleochroic to pale yellow-green) aegirine-augite (2V moderate, + ve, extinction 42°) partly enclosing the olivines.

e. Trachytes (early, and flow domes (Table 10).

The early trachytes, 745a and 763, are petrographically similar to the alkali-rich trachyandesites (704, 664), with feldspar laths zoned from a core of untwinned or very diffusely twinned (Carlsbad-Albite) plagioclase, to alkali feldspar. Discrete tabular alkali feldspars are also present. The optically positive pyroxene (2V about 70°) is pleochroic (X = bright green, Y = bright yellow-green, Z = yellow-brown) and may be zoned out to a darker green rim,

with extinction of 42° changing to 30° at the rim. In 745a, minute subhedra of pleochroic, yellow-brown to bright green, very highly birefringent pyroxene also occur, with tiny flakes of biotite (Z = orange brown, Y or X = colourless) and euhedral apatites. Both rocks contain analcite (birefringence to 0.002) occurring interstitially or in vesicles - whether its origin is deuteric or secondary is unknown.

The trachytic flows (824, 108, 109, 111; and the "feeder" 831) contain microphenocrysts of olivine, titanomagnetite, oxide/pyroxene pseudomorphs after amphibole, and apatites, in a groundmass of fluxional feldspars, granular pyroxene, titanomagnetite and interstitial alkali-feldspar. The olivine (Fa_{70}), partly altered to green phyllosilicates, is quite deeply coloured in shades of yellow, and larger euhedra may be mantled by an overgrowth of later pyroxene. The olivines in 108 and 109 have been oxidized at higher temperatures together with the Fe-Ti oxides, and in thin section appear largely opaque.

The pyroxene, pleochroic in shades of bright green and bright yellow-green, is an aegirine-augite (optically + ve, with high 2V and extinction 41-43°) frequently containing abundant small titanomagnetites. In the pleochroic schemes it is similar to that of the intermediate rocks, with $X > Y \geq Z$, but occasionally grains with $X = Z > Y$ are encountered.

The feldspars have very variable properties. Some laths retain plagioclase cores, either with vague Carlsbad-Albite twinning (An_{38-34}) or untwinned (2V approx. 90°, optically - ve), which zone outwards to alkali feldspar. Discrete laths of alkali feldspar are abundant, some with 2V = 30-40° may show cross-hatch twinning, and some have lower birefringence (lamellar twinning diffuse to absent) and 2V from less than 5° to about 20°. Interstitial patches

of alkali feldspar with irregular boundaries show characteristic undulose extinction. Analcite (824, 108, 109, 831, 111), two zeolites (831, 111) and rarely traces of calcite (109) occur interstitially or in vesicles, forming up to 5% of the rock (calcite $< 1\%$). The analcite is earlier than the zeolites and the carbonate, but whether it is of deuteric or secondary origin is uncertain.

Small apatites may be enclosed in titanomagnetite microphenocrysts or pseudomorphs after amphibole, and larger crystals rich in fine rod-like inclusions may reach microphenocrystal size.

In 108, 109 and 111 microphenocrystal clots of granular titanomagnetite, pyroxene, optically identical to that of the host rock, and an unidentified silicate are pseudomorphic after amphibole (Plate 23C). The pyroxene : oxide ratio is approximately 1 : 1. In 108 'cores' of the pseudomorphs consist of fine titanomagnetites so densely packed that they appear opaque in transmitted light. In these cases the rim consists either of granular pyroxene + titanomagnetite, or 3-4 larger pyroxene crystals with only rare oxide grains.

f. Late intrusive trachytes and phonolitic-trachytes (Tables 11-12).

In hand specimen these green or grey rocks are fine or medium-grained, rarely phenocrystal, usually with pronounced flow orientation of the feldspars. Individual intrusions may show an increase in grain size in from the very fine-grained margins.

In thin section the dyke 751 consists of a very fine-grained mass of zoned plagioclase (cores An_{30-40}) and alkali feldspar laths (2V approx. 30°), with interstitial alkali feldspar. Aegirine-augite (extinction = 41°, optically

+ ve) occurs in poikilitic grains elongated parallel to the feldspars. Small patches of three or four pyroxene 'crystals' may be separated by areas impoverished in ferromagnesian minerals. Titanomagnetites and rarely phyllosilicate pseudomorphs after olivine make up the remainder of the rock.

The fine-grained High Hill trachyte (87, 259, 468) consists of a fluxional mass of zoned feldspars (largely alkali but some with oligoclase/sodic andesine cores), microphenocrysts of yellow olivine, rare titanomagnetite, and granular to sub-poikilitic pyroxene in an interstitial mass of titanomagnetite and alkali feldspar. The alkali feldspar, rarely with fine cross-hatch twinning, has 2V of 45-55°, negative sign, undulose extinction and may be distinctly zoned, although extinction on (010) may only vary by 2-3°.

The green pyroxene is weakly pleochroic, optically positive with high 2V (70-80°), and birefringence $\geq$ 0.030. Rarely pyroxenes are packed with small titanomagnetite granules. Minute colourless hexagonal or rectangular inclusions in the more poikilitic aegirine-augites may be small nephelines.

Analcite occurs interstitially and in 468 in part replaces the interstitial alkali feldspar.

In the phonolitic-trachytes the rare olivines may be embayed and are strongly coloured deep yellow or even pale brown. In 662 the olivine is pure fayalite (X-ray determination).

The pyroxene varies from subhedral prisms through ragged anhedra to sub-poikilitic patches with decreasing grain size. It may be simply twinned (not necessarily on (001) or (100)) and the green colouration is frequently patchy. Rims of crystals are usually darker in colour, with lower extinction and higher birefringence (121, 846). Optical data is very difficult to obtain from the pyroxenes of the

phonolitic-trachytes. The crystals are progressively zoned outwards and interference figures are diffuse - 2V is certainly very large but the optic sign is uncertain (232, 452) - cores occasionally give a recognizable optic axis figure, with 2V of about 80° and a + ve sign (421). The pyroxenes are pleochroic with X = medium green, Y = pale green, and Z = yellow-green, but zone outwards to darker green rims sometimes pleochroic to a strong yellow (almost orange-yellow). Extinction angles of the cores vary from 38-42°), but in the outermost zones may be as low as 8° (452). From the scanty optical data the pyroxene is probably an intermediate aegirine-augite. In more alkaline intrusions the outermost pyroxene zones, and rare tiny discrete grains, are very pale, clear green (pleochroic to pale yellow-neutral) with very high birefringence ($>$ 0.045) and extinction of 4-2° (682, 167). This zoning reflects increasing aegirine content and pale-coloured varieties must be compositionally very close to aegirine.

Untwinned alkali feldspar microphenocrysts have 2V close to 30°, crystals with Carlsbad and diffuse lamellar twinning have 2V = 40-50° (662, 846), and with cross-hatch twinning 2V varies from 30-50° (121). Laths with twinned cores frequently have untwinned rims. Alkali feldspar microphenocrysts may enclose subhedra of dark green pyroxene. In more alkaline rocks they are tabular and rarely elongate. Hair-like lamellar, and more rarely cross-hatch, twinning is developed but single Carlsbad twins are most common; 2V ranges from about 20° to over 40°. Physically the crystals are often composite with a 'wheatsheaf' structure developed, as many as 6-8 individuals may be intergrown in this manner.

Opaques occur as scattered small rounded grains of homogeneous titanomagnetite. Microphenocrystal grains may occur but a single fine-grained phase is most common.

Small nepheline euhedra may be rimmed by ragged fibres of pyroxene at right angles to the crystal boundaries (662, 121, 846), but in more alkaline rocks occur in the groundmass or enclosed in poikilitic aegirine-augite. They may be altered to low birefringent fibrous zeolites or a yellow isotropic polycrystalline material. When unaltered they have a birefringence of up to 0.004.

Cossyrite (421, ?395) occurs as minute sub-poikilitic patches pleochroic under strong illumination from smoky-brown to medium chocolate-brown.

Pseudomorphs after original euhedral amphibole consist of dominant titanomagnetite grains, pale green highly birefringent aegirine-augite and a very low birefringent silicate (232). In 167 titanomagnetite is very dominant and the pseudomorphs are dragged out and curved round feldspars - i.e. the amphibole had completely broken down before complete consolidation of the intrusion. These pseudomorphs are absent in 421, 415, 452, 682, and 395.

g. Phonolites (Table 12).

Phonolites occur as late dykes in the central part of the south-western volcano, and in hand specimen are grey or green, fine to medium grained, with or without obvious oriented feldspars.

Specimen 281 is the most undersaturated of the rocks and is the most beautiful in thin section (Plate 24A). Alkali feldspar laths, anhedral pyroxene 'prisms' and nepheline euhedra are set in a very fine-grained groundmass of alkali feldspar, nephelines, pyroxene and rare rounded titanomagnetites. Large elongate alkali feldspars ($2V = 25\text{-}30^{\circ}$) have a single Carlsbad twin and rarely display hair-like lamellar twinning. True cross-hatch twinning is apparently

PLATE 24:

A: Phonolite texture of specimen 281. Alkali feldspars and nepheline, with irregular anhedral aegirine-augite/aegirine in very fine groundmass of the same minerals. Magnification x30. Plane polarized light.

B: Zoned alkali feldspar phenocryst in phonolite (11). Note 'polycrystalline' core: fine lamellar and weak cross-hatch twinning, and thin rim of untwinned feldspar. Length of phenocryst: 3.5mm; magnification x35. Crossed Nicols.

C: Gabbroic xenolith from basaltic dyke (821). Note sieve-pyroxene; distorted albite twinning in plagioclase; sutured contacts; complete phyllosilicate alteration of olivine. Crystals top and bottom right are both pyroxenes. Field: 3.3 x 5.0mm; magnification x25. Crossed Nicols.

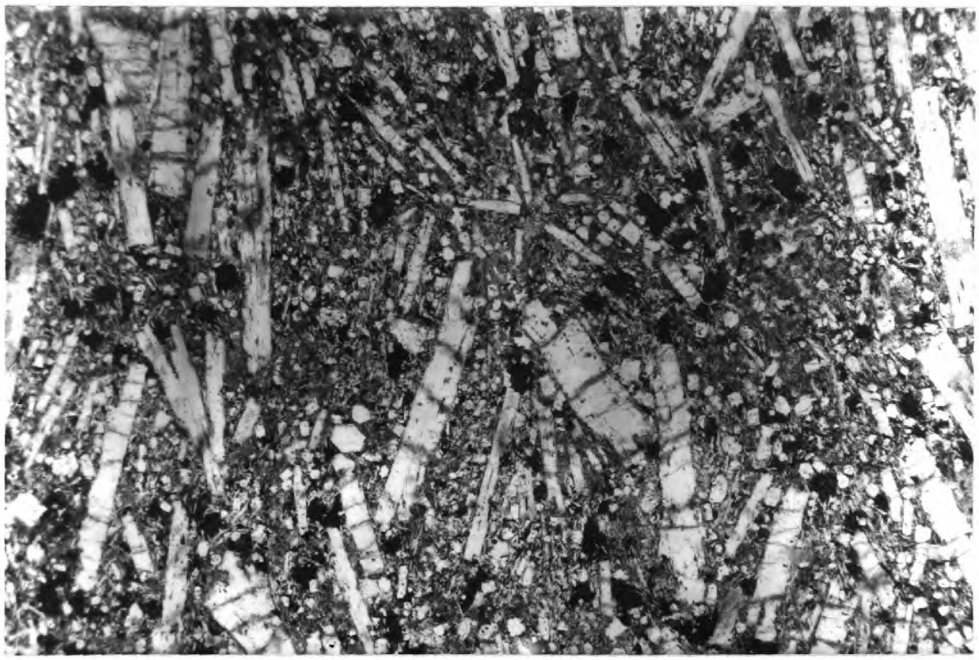

absent but the pericline set may develop without the albite lamellae. Nephelines make up about 15% of the rock, and locally nearly 20% - very small euhedra may be included in the pyroxene, but the majority are independent. The nephelines (up to 0.15mm) contain zones of included 'prisms', oriented tangentially, with equivalent R.I. and slightly higher birefringence (nepheline = 0.005). The aegirine-augite cores, pleochroic from deep green to yellow, are optically - ve, with very large 2V and extinction of 37°. They may have a thick, sharply defined outer zone of pale yellow-green, weakly pleochroic aegirine with extinction varying from 7-2°. Birefringence of the aegirine (2V approx. 60-70°), which may also occur as discrete sub-poikilitic patches in areas rich in interlocking alkali feldspars, is from 0.050 to 0.055.

The very fine-grained phonolites contain tabular microphenocrysts of alkali feldspar (379, 319) in a fluxional mass of feldspar laths, mossy (379, 628) or granular (319) pyroxene, nepheline euhedra (approx. 10-12%) and relatively rare titanomagnetite granules; alkali feldspar microphenocrysts have a variable 2V from 20° to 40°. In the slightly coarser-grained specimen 11 a single complex, large (5mm) alkali feldspar phenocryst (2V = 20-25°) is seen (Plate 24B).

The green pyroxene is more poikilitic where the feldspars form sharp laths - irregular areas of interstitial alkali feldspar are associated with anhedral paler coloured pyroxene. Sub-poikilitic cossyrite (pleochroism red-brown to pale brown-green) may form a rim to titanomagnetite granules (628, 379, 11). All four rocks are traversed by linear 'veins' of finely polycrystalline alkali feldspar and granular green pyroxene and titanomagnetite. Analcite occurs in 319 as small blebs, and in 379 in irregular interstitial patches.

In thin section 290 is a very striking rock with predominant stout alkali feldspar prisms set in a fine-grained groundmass with beautiful bright green (pleochroic to yellow) poikilitic aegirine-augite enclosing tiny nephelines. The pyroxene is zoned out to a colourless aegirine, extinction decreasing from 36° to 2°, birefringence increasing to greater than 0.40, and the optic sign remaining negative throughout. Sporadic titanomagnetites may be rimmed, more or less completely, by strongly pleochroic cossyrite (deep red-brown or red-brown, to dark green-brown or medium olive-green) or aegirine(-augite), but the two are never seen together. Alkali feldspars show a range in 2V from 25° to about 50°; invariably a clear untwinned outer rim is present.

Texturally 403 resembles 682 although alkali feldspar phenocrysts (5-6mm) are abundant and the subhedral pyroxene is very deep green. The groundmass consists of pale yellow-green, highly birefringent granular pyroxene, alkali feldspar laths, rare titanomagnetite and euhedral nephelines. Pyroxene and titanomagnetite, pseudomorphic after amphibole, may be associated with polycrystalline feldspar phenocrysts. The coarsely granular pyroxene is optically similar to that in the host rock (although pleochroism may be stronger with: X = deep green, Y = medium green-yellow, Z = rich yellow or yellow-brown; rare twins on (100); extinction 27°). One feldspar phenocryst encloses an amphibole (pleochroism: yellow-brown to very deep green-brown) with a thick opaque reaction rim, which in turn is rimmed incompletely by granular green pyroxene.

The alkali feldspar phenocrysts were analyzed by W.I. Ridley of this Department and are of anothoclase very close to sanidine: Ab = 65.6, Or = 34.1, An = 2.7; recalc. to 100% as: Ab = 64.1; Or = 33.3; An = 2.6.

Specimen 403 also contains small rounded 'xenoliths' texturally comparable to, but finer-grained than, 281 (nepheline up to 20%).

h. Summary of petrographic variations.

Throughout the whole rock series there is a striking petrographic continuity. The variations may summarized, from ankaramites to phonolites.

i. Alkali feldspar, present in all rocks, increase progressively in abundance; the first distinct laths appear in the trachyandesites.

ii. Plagioclases are normally zoned in all rocks, become increasingly sodic into the trachytes, and disappear as recognizable discrete phases in the phonolitic-trachytes.

iii. Nephelines appear in the trachytes and increase in abundance and size.

iv. Phenocrystal pyroxene occurs only in ankaramites and basalts.

v. Compositionally, pyroxenes vary from (titan)-augites through aegirine-augites to, rarely, aegirine.

vi. Olivines decrease in number and increase in their fayalite content, disappearing in the phonolitic-trachytes.

vii. Interstitial biotite is present in basalts and trachybasalts.

viii. Fe-Ti oxides are predominantly titanomagnetites; ilmenite occurs in some basalts and trachybasalts.

ix. Cossyrite occurs in only six analyzed rocks (4 phonolites and 2 phonolitic-trachytes).

x. Pseudomorphs, of pyroxene + titanomagnetite ± ilmenite ± subordinate silicate, after amphibole occur from trachybasalts to phonolites. All states of breakdown are represented, from thin rims on the amphibole, to coarsely granular clots of pyroxene and Fe-Ti oxides in all proportions.

2. Petrography of the "xenoliths".

The term xenolith is used here for all polycrystalline materials not formerly extruded from the volcano, or crystallized from the rock in which they are now included. Xenoliths were so rare that they were specifically sought out and all collected specimens were sectioned.

a. Plagioclase clots.

The four xenoliths of this type (less than 1.5cm across), occurring in basalts and trachybasalts contain plagioclase (An_{74}-An_{56}) with a thin corroded rim (An_{45}) rich in inclusions of groundmass, zoned out continuously to untwinned feldspar. Large numbers of euhedral pink apatite prisms rich in orientated inclusions are included in, or associated with, the plagioclases.

b. Sodic feldspar clot.

One large clot (6cm) in the base of the Bencoolen trachyandesite, consists of a granular mass of variable grain-size untwinned alkali feldspars and sodic plagioclases (up to 1.5cm), some of which show minor distortion. At the contact with the host rock the feldspars are corroded, and the rim is packed with highly oxidized inclusions; the appearance is identical to similar rims shown by discrete 'phenocrysts' in the trachyandesite flow (Plate 22D).

c. Gabbroic xenoliths.

Two thick doleritic dykes in the north-eastern volcano contain abundant rounded xenoliths (up to 8cm) of fine-grained gabbro (average approx. 2mm), with pleochroic purple-brown titanaugite, altered olivine, plagioclase and titanomagnetite (Plate 24C). The titanaugite is slightly zoned, and is most highly coloured (purple) when it occurs 'interstitially' between plagioclases. The plagioclases (An_{78} zoned to less calcic rims) are frequently rounded and may be bent, with evidence of 'pressure' lamellar twinning. Large plagioclases, enclosed in pyroxenes with sieve-texture, may enclose stumpy, inclusion-free apatites. Biotote occurs as rare pleochroic flakes (Z = deep fox-red, X = very pale pink-orange, 2V about 5^{o}, optically negative). Titanomagnetites occur enclosed in sieve-pyroxenes, or as oriented small rectangular grains in plagioclases.

A coarser gabbroic xenolith (3cm), in an olivine-pyroxene basalt flow in the south-western volcano, consists of large neutral unzoned pyroxenes (6mm), rare pseudomorphs after irregularly rounded, reheated olivines (2mm), and rounded, complexly twinned interlocking plagioclases (An_{85}-An_{78}) (1mm), zoned slightly to more sodic rims. Fe-Ti oxides are absent except as "dust" in rare rectangular corrosion blocks in plagioclases.

d. Amphibole-bearing xenoliths.

All xenoliths with amphibole as a major phase occur in the late intrusions of the south-western volcano. Their distribution is shown in Fig.49 in Section VIII.

Thin sections, electron-microprobe polished sections and, rarely, polished sections for the reflecting microscope have been made. The coarse-grained varieties are so rare and so small, that little systematic optical data has been

attempted until the xenoliths can be studied using the microprobe.

i. Feldspar-rich, coarse xenoliths.

Feldspars (alkali and sodic plagioclase) constitute more than 90% of the two small (2cm) xenoliths. Small, slightly elongate amphiboles (pleochroic in shades of brown) occur between interlocking feldspar grains, and may be associated with minute clear euhedral apatites. There is no visible reaction rim with the host phonolite.

ii. Coarse-grained varieties.

Four xenoliths of this type, the largest measuring 2.2 x 1.0 x 0.9cm, may be described in two groups, divided on their percentage of amphibole. The first type (236, 369) has a granular 'gabbroic' texture without groundmass, with average grain size 1-2mm, and consists of pyroxene, amphibole, olivine, (biotite), opaque oxides, alkali feldspars, plagioclase and abundant acicular apatites (to 0.8mm).

In 236 the pyroxenes, rarely twinned on (100), are non-pleochroic pale pink-neutral with 2V approximately 35-45°, positive sign, extinction of 43-44°, and maximum birefringence of about 0.030. They are surrounded by orientated overgrowths of amphibole, (close to which the pyroxene becomes pale green, slightly pleochroic to pale yellow-green). The pyroxene-amphibole contacts are sharp but often irregular and all stages of replacement by amphibole are visible, from thin rims to complete pseudomorphs, isolated pyroxene fragments remaining in optical continuity throughout (Plate 25A). The amphibole (extinction 16°) is strongly coloured, dark red-brown to nearly black, and pleochroic to bright yellow-brown. The amphibole itself breaks down to granular Fe-Ti oxides and sub-poikilitic (to the ore) green pyroxene, the thickness of this reaction increases with proximity to the

PLATE 25:

A: Monzonitic xenolith (236). Cores of pyroxene with overgrowth of amphibole itself breaking down to pyroxene + oxides at, and close to, the host rock contact. Note inclusions of feldspar and titanomagnetite in the larger pyroxene - amphibole crystal. There is no coarsening of grain-size of the host rock at the xenolith contact. Note the abundant thin prisms of apatite (bottom). Field: 2.7 x 4.0mm; magnification x35. Plane polarized light.

B: (Syeno-)gabbroic xenolith (369). Amphibole is rimming or replacing pyroxene which has exsolution plates on (100) and (010). Note also amphibole rims to titanomagnetite (bottom). Very abundant apatites especially in, or associated with, opaques. Note coarser grain-size of host rock adjacent to the xenolith, and breakdown of xenolith ferromagnesians to granular pyroxene and Fe-Ti oxides. Field: 2.7 x 4.0mm; magnification x35. Plane polarized light.

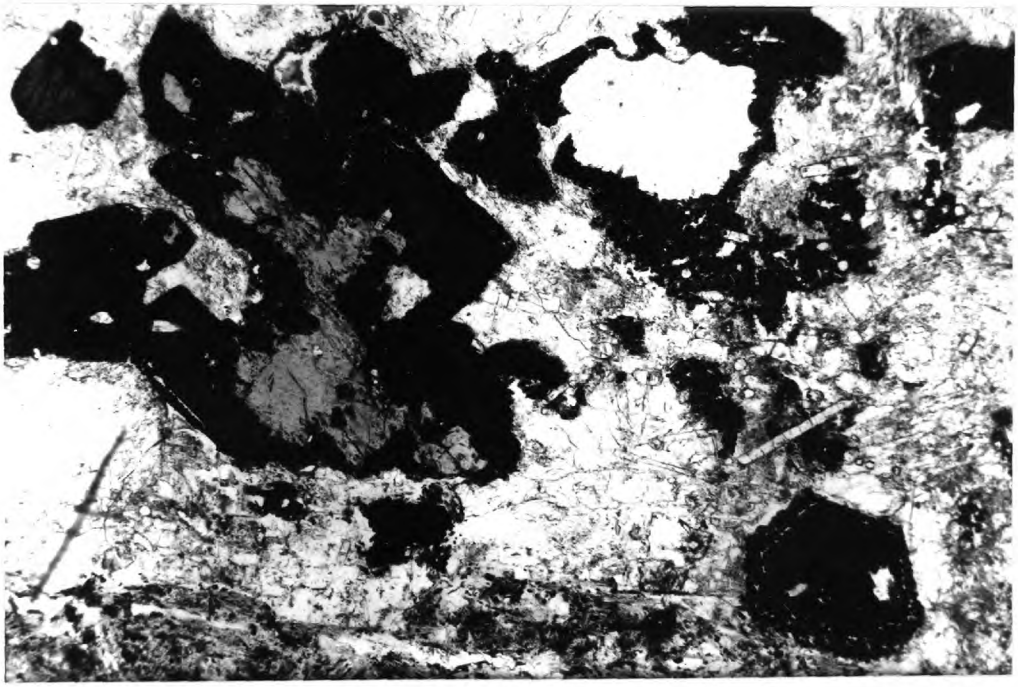

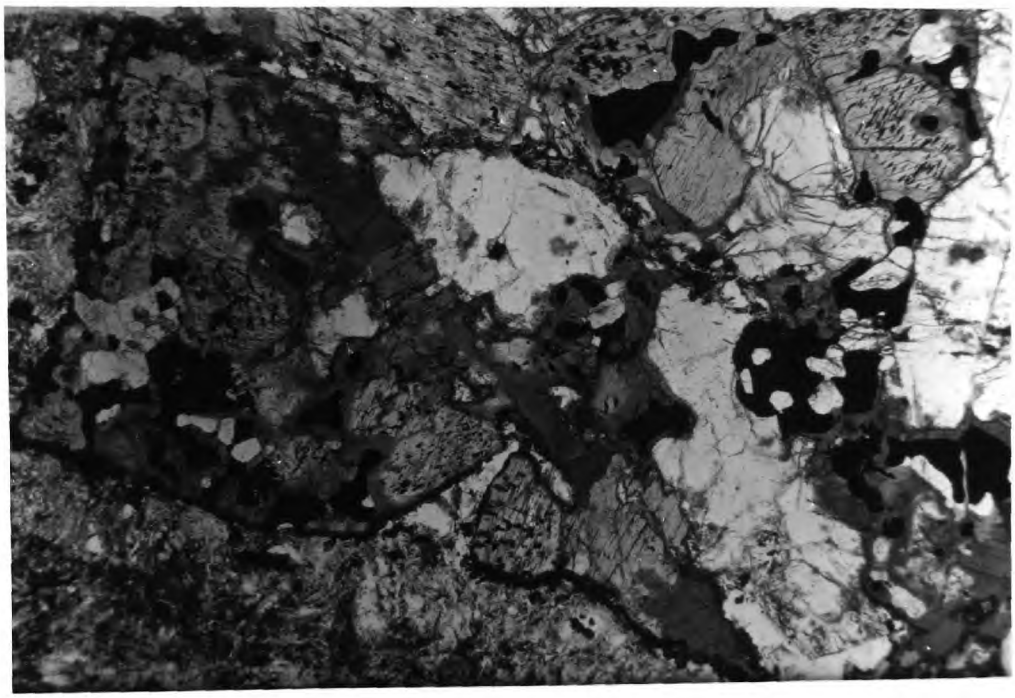

edge of the xenolith (Plate 25A). With very small original amphiboles the rim pyroxene may be in optical continuity throughout as a single 'crystal', and amphibole relics in this rim remain in optical continuity with the main crystal. At the xenolith/host boundary the green pyroxene may be developed as thin bladed crystals in parallel orientation approximately perpendicular to the amphibole boundary. The colour of the pyroxene developed by this reaction increases from colourless-neutral near the amphibole outwards to green comparable to the colour of the host rock pyroxene.

The slightly more abundant alkali feldspars may exhibit fine lamellar (or rarely cross-hatch) twinning and 2V ranges from about 20° to 50°. The plagioclases (oligoclase/andesine) with distinct albite twinning may be zoned out to a thick rim of untwinned plagioclase $\pm$ alkali feldspar.

Specimen 369 (1cm across) is a coarser-grained xenolith with feldspars to 2.5mm, consisting of pyroxene, amphibole, Fe-Ti oxides, biotite, olivine, plagioclase and apatite. The host rock adjacent to the xenolith is coarser grained than the rock as a whole, and is depleted in ferromagnesian minerals; the xenolith displays a thin discontinuous reaction rim.

The pyroxene is pale pink, faintly pleochroic to pale yellow-neutral, with $2V = 60^{\circ}$ or less, positive sign, extinction 43° and birefringence not less than 0.030. It is packed with oriented inclusions, exsolved on (010) and (100), of thin equant plates in a non-pleochroic deep shade of 'ox-blood' (Plate 25B). The pyroxene has a thin continuous rim, or is patchily replaced by, amphibole more or less oriented on (010) and (100) (Plate 25B). Opaque grains enclosed in pyroxenes may be rimmed by amphibole.

The amphibole has a strong body colour, with pleochroism in shades of brown, brown-green and olive-green. Cleavage is poorly developed but extinction may be as high as 27^{o}, 2V is approximately 80^{o} to 85^{o} with a negative sign. At the host rock contact it is rimmed by locally oriented deep green aegirine-augite and rare fragments of a more aegirine-rich pyroxene. The smaller grains of amphibole become green to green-brown (and the extinction angle increases) before actually breaking down to pyroxene. In the replacement of the pyroxene by amphibole the oriented inclusions are taken chemically into the latter so no trace remains.

Flakes of biotite (pleochroic: fox-red - orange-brown - very pale pink-yellow, 2V approx. 0^{o}, optically - ve) occur between the large feldspars. Several rounded olivines are highly oxidized to red materials with black rims and cracks, but one is completely unaltered and with 2V = $80-85^{o}$ (optically - ve) would have a composition of approximately Fa_{30}. Where adjacent to plagioclases the olivines are also rimmed by amphibole.

The plagioclases (An_{60}) display sharp lamellar twins often of the discontinuous variety with visible bending. Small rounded grains may be included in other plagioclases or may have a thin rim of amphibole round them. Alkali feldspar was not positively identified, and the rock is technically a gabbro, whereas 236 is a monzonite on the monzonite/syenite boundary.

Of the other two xenoliths specimen 733 (just over 2cm across) consists of one large (14mm) amphibole, and two large plagioclase crystals (An_{43}), poikilitically enclosing numerous rounded pyroxene grains (0.8-1.5mm), and rare rectangular opaques (Plate 26A). The amphibole appears

PLATE 26:

A: Xenolith with amphibole poikilitically enclosing unoriented rounded titaniferous pyroxenes (733). Note no coarsening of host rock at boundary, and breakdown of amphibole to a thin rim of granular pyroxenes and titanomagnetite. Field: 3.2 x 4.7mm; magnification x30. Plane polarized light.

B: Xenolith of kaersutitic (?) amphibole with enclosed small relic pyroxenes (732). The xenolith amphibole is converted to a brilliant green ?ferrohastingsite adjacent to the host. Note that host rock is coarser grained and depleted in ferromagnesian minerals at the xenolith rim. Small xenolithic amphiboles virtually completely converted to second amphibole. The kaersutitic amphibole may break down to granular pyroxene + titanomagnetite adjacent to the host rock if the second amphibole is absent, extreme right centre. Field: 2.7 x 4.0mm; magnification x35. Plane polarized light.

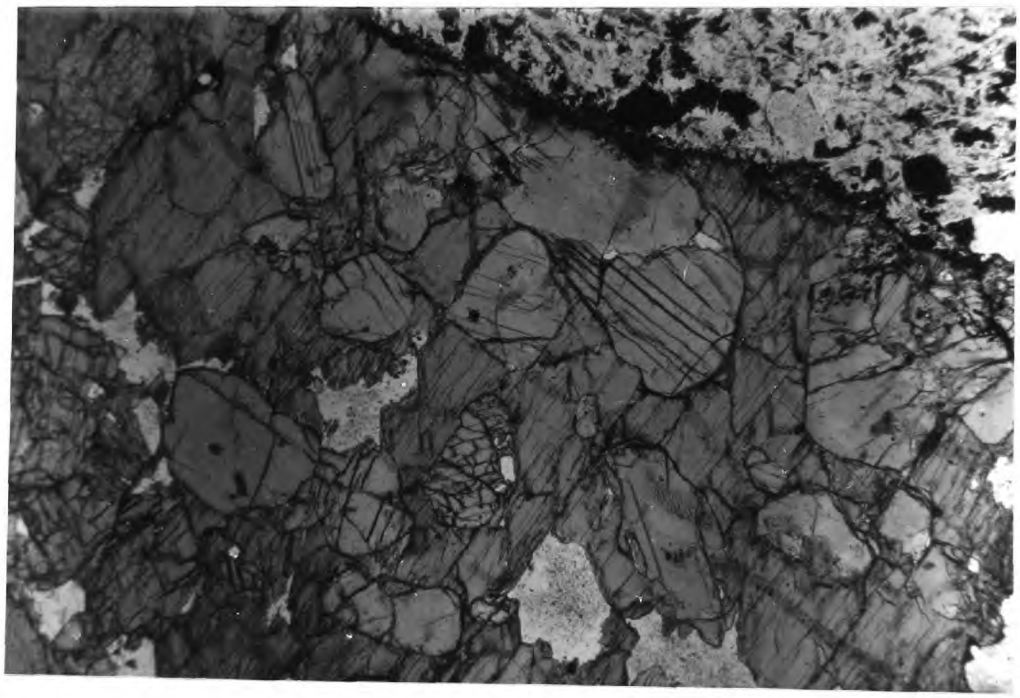

completely homogeneous (pleochroic from rich red-brown to honey-yellow), is length fast with birefringence greater than 0.035, and β = 1.696.

The rounded pyroxenes (unoriented relative to each other and the host minerals), often twinned on (100) and either (101) or (011), are pink with irregular variations in the intensity of the colour. Optically the pyroxene has 2V from about 37° to about 57°, positive sign, extinction of 41°, birefringence of 0.023 and β = 1.707. Relics of a highly oxidized material are preserved as rounded granules in pyroxenes or as irregular patches in amphibole - ?olivine.

At the xenolith/host rock boundary both pyroxene and amphibole break down to a granular green pyroxene plus Fe-Ti oxides. Xenolith pyroxene initially turns colourless and becomes increasingly green with proximity to the host rock.

In 732 the amphibole constitutes over 85% of the xenolith (1.3cm), individual crystals being up to 7mm across. The amphibole is strongly pleochroic (X = deep fox red-brown; Y = pale pink-brown; Z = very pale pink-neutral), with 2V approximately 80-85° and uncertain optical sign; extinction is not less than 21°. Small bent flakes of mica (Z = orange-brown; Y = very pale yellow-pink) form aggregates in interstices between amphibole grains.

Numerous sub-rounded opaques and clear apatite euhedra rich in fluid inclusions, may be included in amphiboles (large), or occur along crystal boundaries (small). One zoned feldspar with lamellar twinning has a moderate to high 2V and is optically negative (?andesine). Small rounded pale pink to colourless pyroxenes may be remnants after resorption by amphibole; their 2V appears to be high with positive sign; extinction is not less than 31°.

At the xenolith rim a coarser-grained variety of the host rock, with sub-perpendicular alkali feldspar laths, may be 2.5mm wide. Small isotropic cubes of a clear mineral also occur in this rim and may constitute 20% by volume. The amphibole turns green at the host rock contact (Plate26B) with an exceedingly thin (even x1600) transition zone). This second amphibole is pleochroic (X = deep green-brown or very deep olive-green; Y = very dark green or brown-olive green; Z = rich yellow-green), with 2V close to 0° and negative optic sign. The colour increases slightly outwards and extinction increases by as much as 12°. A very thin rim on this green amphibole has an extinction of $3\text{-}6^{\circ}$ and may be an aegirine-rich pyroxene - its green colour is sufficiently strong to obscure the birefringence. Fragments of amphibole surrounded by host rock have a thick green rim (amphibole) and their brown colour and pleochroism gradually disappear with increasing reaction, eventually producing an aggregate of green amphibole.

From the optical data it is impossible to determine whether the amphibole is a kaersutite or a basaltic hornblende. The difference in X, Y and Z absorption, lack of dominant pink colouration, and low R.I. suggest that it is perhaps an intermediate variety. The amphibole with strong green body colour produced by reaction with the host phonolite could be a ferrohastingsite. Reaction relationships between titanaugites, kaersutite, titan-biotite and ferrohastingsite described by Aoki (1959) from the Iki Islands, Japan, show a number of close similarities to material described above.

The second type of xenolith (av. approx. 4 x 2 x 2cm, but up to 8 x 3.5 x 1.3cm), is black, with acicular amphiboles and more or less rounded abundant vesicles infilled with secondary minerals. The contacts with the phonolites appear sharp although usually irregular. The xenoliths may be

PLATE 27:

All in plane polarized light.

A: Typical xenolith with acicular amphiboles (770). Note variation in grain-size of amphiboles, abundant vesicles, small plagioclase 'phenocryst' (top centre). One crystal of cluster below centre of main amphibole is biotite. Amphibole is 3.8mm long; magnification x30.

B: Amphiboles with finely acicular growth at crystal terminations (339). Note dark (green) rim to crystal (brown), even more pronounced in top right where acicular terminations are completely green. Main crystal is 1.14mm long; magnification x70.

C: Very fine acicular amphibole growth in xenolith close to a vesicle (315). Each group of crystals is in optical continuity. Field: 0.28 x 0.42mm; magnification x290.

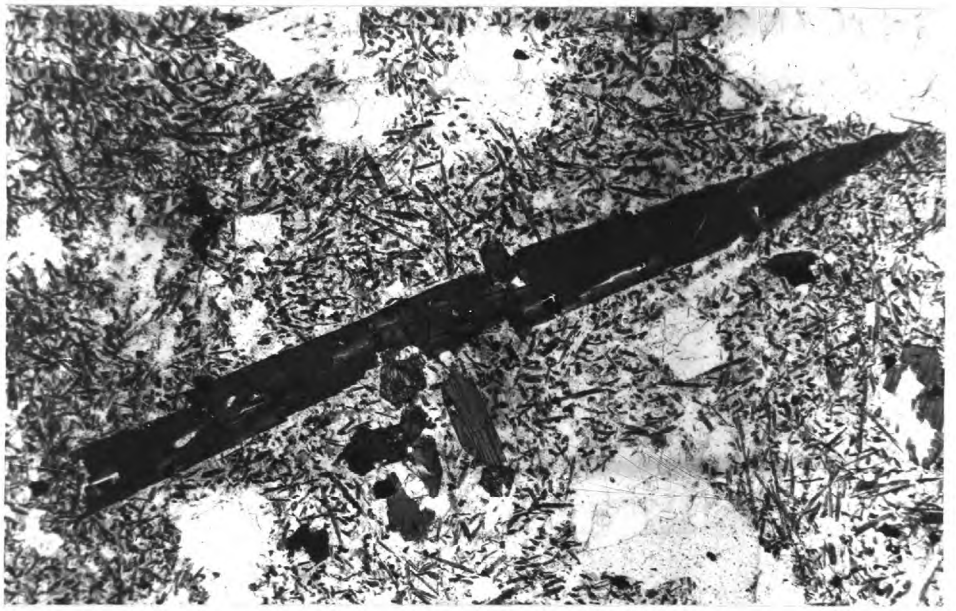

orientated parallel to the fluxional host rock feldspars, and the irregular sinuous contacts suggest plasticity at their time of incorporation in the dykes.

The xenoliths probably originally consisted of a monzonitic assemblage: amphibole, biotite, Fe-Ti oxides, plagioclase, alkali feldspar and apatite although pyroxene may now be present. Texturally, acicular amphiboles of very variable size (length : breadth ratios up to 10 : 1) and corroded feldspars are set in a matrix of interlocking feldspars charged with hair-like clear apatites.

Pleochroism in the amphiboles is strong to very strong and in some xenoliths Y and Z may be almost identical, and rarely Y may be even darker than Z. The following schemes are typical:

X	Y	Z
pale yellow-brown	deep orange-brown	deep yellow-brown
pale yellow	deep orange-brown	very deep chocolate-brown
pale pink-yellow or pale pink	deep fox-red brown	deep red-brown

In several xenoliths, large phenocrysts have a core with a faint trace of green in the dominant brown colour, and the 'rim' (volumetrically greater than the core) in these cases is slightly more pink than usual. The fine-grained amphiboles may form radiating clusters, and hair-like skeletal outgrowths may develop at the terminations of larger crystals (Plate 27B), and very rarely, near vesicles, minute orientated skeletal acicular crystals may develop (Plate 27C). The larger amphiboles frequently show a single twin on (100), which may develop as a single thin twin seam. Optically the amphibole has very high birefringence (probably not less than 0.050), β = 1.701 (one measured specimen), 2V of about 80°, with negative sign and extinction of 9-16°.

Biotite flakes (X = pale yellow or colourless, Y = yellow, Z = bright pink-orange or pink-brown) occur frequently in corroded feldspars, but also in the xenoliths as a whole.

Twinned plagioclase phenocrysts (as calcic as An_{49}) are almost invariably resorbed, with the central parts becoming very 'spongy' and containing untwinned alkali feldspar, which is zoned progressively towards the centre of the patch. The rim of these plagioclases is of alkali feldspar, but corrosion of the crystal edges is absent or minimal. Sodic plagioclases may be uncorroded and inclusion-free. Zoning although usually normal, may be faintly oscillatory. Alkali feldspar phenocrysts with 2V from approximately 50° to below 20° (rarely with cross-hatch twinning), may also be corroded.

The Fe-Ti oxides occur as sub-skeletal phenocrysts (i.e. square in shape, with "arrowhead" growth on two or four corners), or as fine equant granules sometimes included in amphibole.

The intergranular matrix for the ferromagnesian minerals and feldspar phenocrysts consists of zoned feldspar, alkali and plagioclase, with undulose extinction. Clear apatites, often of hair-like dimensions, occur within this matrix or in the amphibole microphenocrysts. Larger apatites display a 'core' either of colourless fluid or dusty inclusions.

Close to the xenolith the host rock develops a coarser-grained texture and is impoverished in ferromagnesian and opaque minerals. Similarly, near vesicles, the texture of the xenolith feldspar matrix becomes coarser and a decrease in the amount of amphibole may be apparent. Vesicles are frequently infilled with secondary minerals:

fibrous zeolites, chabazite, analcite, and in one case calcite. Very often the feldspars, both in the xenolith near vesicles, and in the host rock near the rim, are replaced by a very fine-grained mass of pale pink secondary mineral, possibly a zeolite. In the host rock aegirine-rich aegirine-augite may be developed near vesicles at the xenolith rim.

Cracks permeating through xenoliths are infilled with coarse-grained alkali feldspar of the host rock, and reaction of the xenolith is more advanced.

A complete sequence of reaction may be traced for the amphiboles. Initially a thin green rim is just visible on the amphibole phenocrysts, and a green colouration is added to the overall pleochroism of the fine-grained needles, the ragged ends of the crystals being particular susceptible. The extinction angle of the amphibole increases into this green rim by as much as 14°, the rim itself increasing in green colouration outwards. Within the xenolith/host boundary the amphibole may go completely green, but there is no break down to pyroxene + oxides at this stage.

As reaction proceeds microphenocrysts take on tinges of green in their pleochroism, and small crystals at the xenolith rim have very indistinct properties, with pleochroism from green to olive-green or medium-brown and extinction up to 30°. In the coarse-grained host rock rim, aegirine-augites may be rich in opaque inclusions, and within the actual boundaries of the xenolith acicular crystals of undoubted green pyroxene and green-brown pleochroic amphiboles co-exist with abundant tiny opaque granules not necessarily related to pyroxenes. Green colouration of larger amphiboles is patchily developed.

At a more advanced stage, the amphibole may remain distinctly brown, but small stumpy prisms of green pyroxene with opaque granules co-exist with it. The amphibole phenocrysts develop initially a very thin, darker brown rim, and then become very pale. Green pyroxene is developed adjacent to, and in crystallographic continuity with, the pale zone, at which junction opaques first appear. At the xenolith boundary only large phenocrysts of amphibole exist, all of the finer-grained crystals having been replaced. The pyroxenes may themselves be zoned outwards to paler-coloured more aegirine-rich varieties (extinction changing from 42-28°), especially near vesicles.

In the extreme cases of reactions only the phenocrysts retain relic amphibole, the smaller grains consisting of pyroxene pseudomorphs, often very rich in included opaque grains (Plate 28A). The large amphiboles may break down directly to orientated pyroxenes with minor opaques, or may produce the more characteristic granular variety, with opaque grains more abundant than pyroxene granules. Single phenocrysts may show both types of reaction at opposite ends. Optically the amphibole/pyroxene boundary may be transitional or very sharp, neither being diagnostic of a particular type of breakdown. Although the pyroxene after amphibole is optically similar to the host rock pyroxene, it forms prisms (± ragged, weakly pleochroic in shades of green, extinction = 40°), whereas the host rock pyroxene is poikilitic (pleochroic green-yellow) enclosing small nephelines.

A single xenolith from the arcuate sheet of Great Stone Tops (Plate 28B) has a coarser-grained feldspar matrix (oligoclase-andesine and alkali feldspars with 2V less than 20° to about 50°), with pale green aegirine-augite prisms (extinction = 42°), rich in minute opaques, amphiboles (X = pale yellow, Y = medium green-brown, Z = dark green-brown)

PLATE 28:

Plane polarized light.

A: Advanced stage in breakdown of amphibole in xenolith (729). Only cores of amphibole remain in larger crystals; smaller acicular crystals (bottom centre) and phenocryst rims altered to oriented pyroxene ± Fe-Ti oxides. Some larger primary titanomagnetites also visible. Field: 1.7 x 2.6mm; magnification x50.

B: Xenolith of Great Stone Tops intrusive sheet (832). 'Primary' assemblage of feldspars + titanomagnetite + amphibole (now breaking down to pyroxene +oxides). Discrete pyroxenes charged with tiny opaque granules are especially abundant close to host rim. Field: 2.6 x 3.75mm; magnification x28.

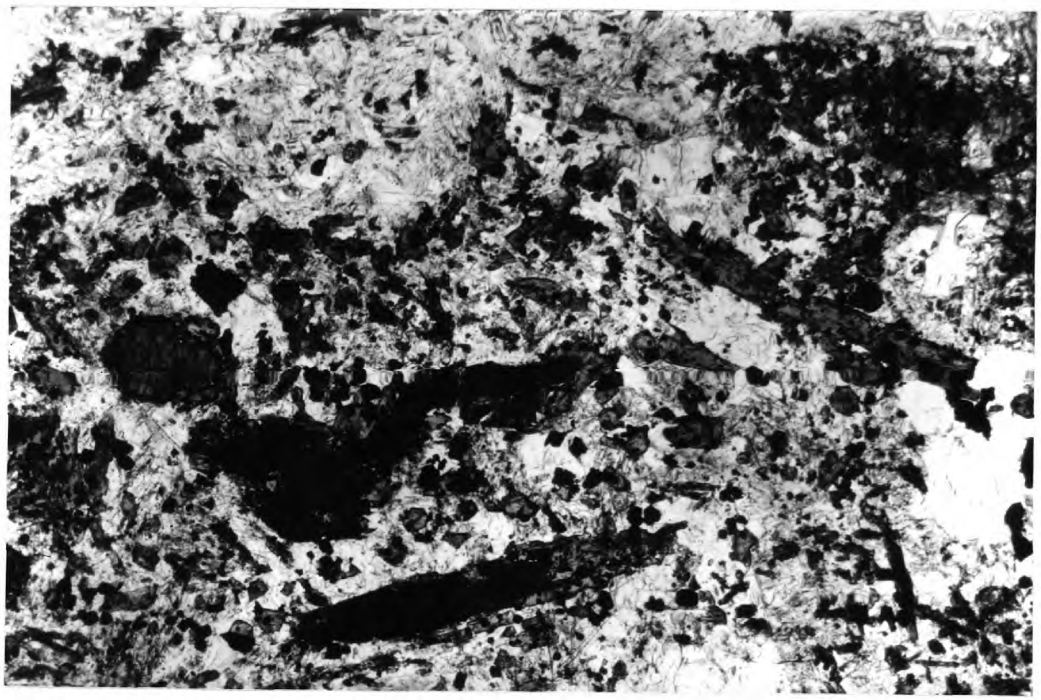

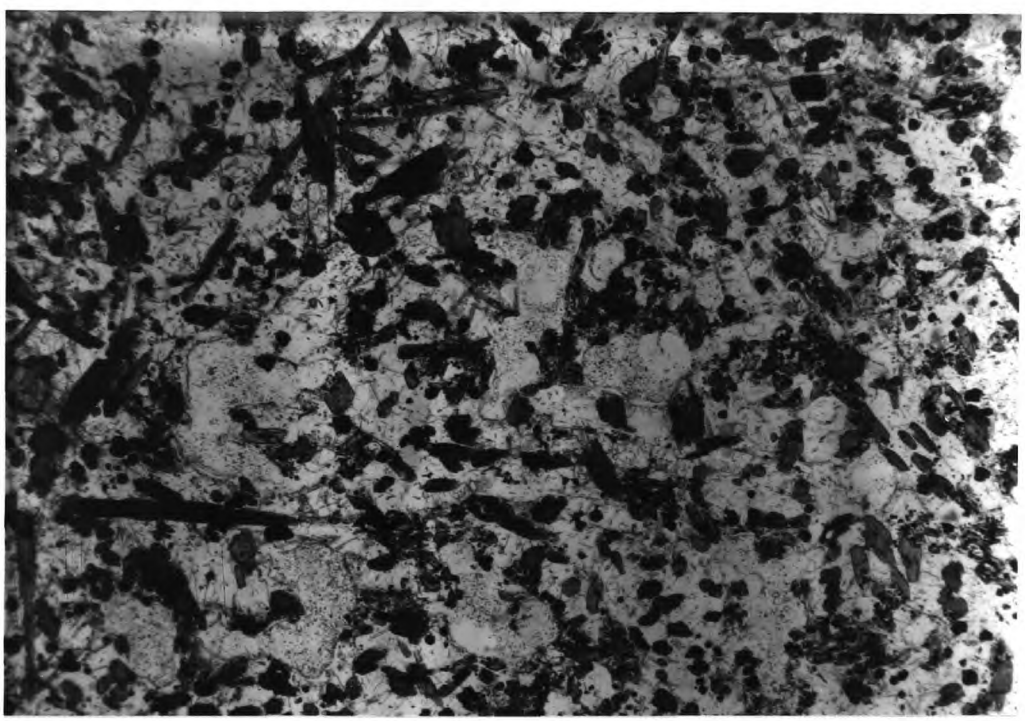

and abundant titanomagnetite coarser than those in the pyroxenes. The amphibole breaks down directly to pyroxene and oxides, the pseudomorph retaining the crystallographic orientation. No biotite was seen, but apatite is present as stout prisms or hair-like crystals in feldspar.

The 'pink' colouration of these amphiboles and the equivalent Y and Z absorptions suggest that they may be closer to a true kaersutite. In reflected light however, the only Fe-Ti oxide phase is discrete titanomagnetite (no ilmenite) suggesting lower TiO_2 than would be expected with normal kaersutite.

SECTION VII

GEOCHEMISTRY

1. Introduction.

Major and minor element contents of seventy two rocks from St. Helena have been determined by the writer. Methods of major oxide analysis were based on those of Shapiro and Brannock (1962); silica was determined by the combined gravimetric-colourimetric method of Jeffrey and Wilson (1960). Water above 110°C was determined by heating the sample to 1000-1200°C and correcting for ferrous-ferric conversion. The quoted H_2O value is therefore a "total volatiles" determination ($CaCO_3$ is present in a few specimens but only in tract amounts; nepheline is the only feldspathoid optically visible). Whole rock repeat analyses were carried out on about 25% of the samples with good correlation in all oxides.*

The elements Rb, Sr, Y, Zr and Nb were determined using an A.R.L. X-ray quantometer (2gm samples, compressed with cellulose, scanned at 40kV and 30mA, W radiation) with a precision of ± 20%. A large number of other trace elements were looked for using a Hilger large quartz spectrograph with palladium as an internal standard. Working curves were

---

* During the course of a K/Ar age dating program potassium was determined on ten analyzed rocks by J. Simons of the Department of Geology and Mineralogy, Oxford, using flame photometry with buffered solutions. The values determined here agreed with the Oxford determinations with an average deviation of ± 2.8%.

constructed by R. Berlin using G.1, W.1, S.1 and synthetic standards of varying concentrations of the metals in a synthetic phonolite base. The elements Ba, Cr, Ni, Pb, and Cu were read, others were below the detection limit of the instrument. Molybdenum and ytterbium were present in all rocks, at very low concentrations. Owing to contamination by vanadium in certain of the carbon electrodes the element was not read on any of the plates.*

The analyses of major oxides and trace elements are given in Tables 6-12. The sample localities and stratigraphic relations of the analyzed rocks are listed in numerical order (of specimen number) in Appendix I.

2. Oxidation state of iron.

The importance of the oxidation state of iron in the computation of the CIPW norm has been noted by Yoder and Tilley (p375, 1962). Alkali basalts with high Fe_2O_3 : FeO can give norms with q, hy, and hm; reduction of this ratio removes q and hm, increases the Fe : Mg ratio of normative ferromagnesian minerals, decreases the value of mt, increases ol and may reduce hy to zero and introduce ne. In a purely geochemical sense the analysis of highly oxidized rocks is to be avoided, but on St. Helena a picture of geochemical variation with time necessitated the analysis of a number of highly oxidized rocks. Frequently trachybasalts and trachyandesites were badly oxidized but it was thought better to

---

* (Arcing conditions: anode, 2.4 x 5 x 3.1mm (Ringsdorff RWIV graphite); cathode, morgenite carbon (Link SG-305-H); arc gap, 5mm; slit width, 10μ; amperage, 8A; plates, Ilford N50. Measurements: line intensity measured on A.R.L. microphotometer; relative intensities determined using self-calibration method (Ahrens and Taylor, 1961)).

analyze these intermediates than ignore them because of their oxidation state.

Watkins and Haggerty (1967) have demonstrated marked variations in ferric : ferrous ratios through single lavas which can be correlated with the 'oxidation index' of the primary Fe-Ti oxides in the rock. These variations are deuteric effects, the primary oxides being discrete titanomagnetite and ilmenite. In calculating the norms for the St. Helena rocks the Fe_2O_3 and FeO values have been recalculated for rocks which optically are shown to be highly oxidized. The Fe_2O_3 value has been lowered to the approximate value of ferric iron in similar rock types which in reflected light have an oxidation index of I (Watkins and Haggerty, p258, 1967), i.e. homogeneous titanomagnetite. It should be noted that this will not affect the Fe^{+3} content of silicates since reduction to a Fe_2O_3 : FeO ratio of a mineralogically and chemically comparable rock type automatically ensures that only the Fe_2O_3 : FeO ratio of the Fe-Ti oxides is effectively modified. This value will not be the absolute value of the primary Fe_2O_3 content on extrusion, but it will be of the right order, and will render the norm not only more useful, but more nearly correct. In some rocks, even with recalculated Fe_2O_3 and FeO values normative hypersthene and very rarely quartz is retained; this is believed to reflect some other process of alteration resulting in an abnormally high SiO_2 value. These rocks (723, 37, 705, 218, 599, 828, 269, 121) in thin section display groundmass alteration, and some contain secondary minerals, otherwise they are identical to comparable rock types giving typical 'alkaline' analyses.

A check that this method of recalculating is valid is to compare the Fe : Mg ratio of the normative

ferromagnesians with that of the modal minerals. Obviously all is not right with rocks containing modal olivine Fa_{50} or greater showing normative olivine Fa_{5-10}.

The analyzed and recalculated Fe_2O_3 and FeO values, and both norms based on these are given in Tables 6-12; the differentiation indices used in all diagrams are those from norms recalculated from the modified Fe_2O_3 : Fe ratios.

3. Oxide and element variations.

Variations in major oxides and trace elements of the seventy two analyzed rocks are shown in Figs. 30-42. Weight per cent oxides and concentrations of trace elements in parts per million are plotted against the differentiation index (D.I. = normative q+or+ab+ne+leu+kal) of Thornton and Tuttle (1960). According to these authors the percentage of the normative salic constituents of the rock should be determined from a norm recalculated to 100% free of water, ns, and minor constituents. The D.I. of the St. Helena rocks have been calculated from the normative constituents in Tables 6-12 without recalculation, a practice in common usage (see for example, Tilley and Muir, 1964; Baker, et al, 1964). Normative sodium metasilicate of 0.20 in 403 (Table 12) will not effectively influence the D.I., but the appearance of normative acmite in a number of the phonolites is responsible for the slight lowering of their differentiation indices.

The alkaline nature of the St. Helena rocks is shown in Fig. 30 which is a total alkalis/silica plot. The included lines are from Saggerson and Williams, 1964 (separating mildly alkaline, from strongly alkaline, nepheline-bearing, rocks of Tanganyika), and Macdonald and Katsura,

TABLES 6-12

Chemical analyses (major oxides and trace elements) and CIPW norms of the rocks analyzed by the writer from St. Helena. The following abbreviations are used in the norms:

q = quartz; or = orthoclase; ab = albite; an = anorthite; ne = nepheline; di = diopside; he = hedenbergite; en = enstatite; fs = ferrosilite; fo = forsterite; fa = fayalite; il = ilmenite; mt = magnetite; ap = apatite; ac = acmite; ns = sodium metasilicate; co = corundum; hem = hematite; wo = wollastonite.

- = not detected; * = trace

6: Ankaramites and porphyritic basalts.
7: Alkali olivine basalts.
8: Trachybasalts.
9: Trachyandesites.
10: Early trachytes and flank flow domes.
11: Late, highly alkaline intrusions.
12: Late, highly alkaline dykes.

Analyses and norms with double columns are for oxidized rocks: left hand figures are based on actual analyses, right hand figures are based on recalculated ferrous-ferric values.

Specimen no:	804	785	179	844	679
SiO_2	44.06	43.98	45.55	44.97	43.93
Al_2O_3	11.66	12.17	11.97	14.74	14.67
TiO_2	2.09	2.37	2.33	2.85	3.20
Fe_2O_3	1.66	3.62	2.58	2.53	4.06
FeO	8.97	7.49	9.49	9.34	8.98
MnO	0.20	0.20	0.18	0.21	0.22
MgO	15.43	14.54	12.80	8.78	7.94
CaO	12.39	10.92	11.17	10.41	9.22
Na_2O	1.58	1.90	2.13	3.06	3.32
K_2O	0.52	0.66	0.73	1.04	1.32
P_2O_5	0.32	0.24	0.29	0.43	0.51
H_2O^+	0.93	1.77	1.04	2.00	1.84
H_2O^-	0.19	0.16	0.22	0.12	0.54
TOTAL	100.00	100.02	100.48	100.48	99.75

Nb	40	-	*	40	50
Zr	65	105	110	180	190
Cr	720	635	530	280	250
Y	*	-	*	30	-
Ni	360	395	490	170	140
Co	86	90	76	58	56
Sr	230	310	330	425	455
Cu	88	77	72	62	40
Pb	-	-	-	-	*
Ba	105	90	245	270	335
Rb	-	-	-	-	30
$\frac{FeO+Fe_2O_3}{FeO+Fe_2O_3+MgO}$	0.408	0.433	0.483	0.576	0.622
or	3.07	3.90	4.31	6.15	7.80
ab	6.61	12.64	14.85	16.84	18.79
an	23.19	22.73	20.95	23.41	21.23
ne	3.66	1.86	1.72	4.90	5.04
di	22.75	20.19	19.79	14.40	12.51
he	6.21	3.51	6.38	6.17	4.56
fo	19.54	18.81	15.91	10.64	9.79
fa	6.73	4.14	6.48	5.76	4.51
il	3.97	4.50	4.43	5.41	6.08
mt	2.41	5.25	3.74	3.67	5.89
ap	0.76	0.57	0.69	1.02	1.21
H_2O	1.12	1.93	1.26	2.12	2.38
TOTAL	100.02	100.03	100.51	100.49	99.77
D.I.	13.3	18.4	20.9	27.9	31.6

TABLE 6 Ankaramites and porphyritic basalts.

TABLE 7

Alkali olivine basalts

Specimen no.	737	226	387	706	803
SiO_2	45.18	45.22	45.62	44.97	45.50
Al_2O_3	13.69	14.86	16.75	15.86	15.71
TiO_2	3.25	3.79	3.30	3.62	3.44
Fe_2O_3	4.96	6.36	2.18	4.79	3.61
FeO	7.72	7.56	9.26	8.48	8.64
MnO	0.21	0.21	0.13	0.22	0.22
MgO	8.27	5.59	5.84	4.92	5.37
CaO	10.17	10.21	9.86	9.73	9.43
Na_2O	3.32	3.14	3.31	3.59	3.47
K_2O	1.08	1.03	1.15	1.45	1.38
P_2O_5	0.50	0.39	0.48	0.55	0.60
H_2O^+	1.32	1.32	1.92	1.30	2.49
H_2O^-	0.52	0.42	0.01	0.37	0.29
TOTAL	100.29	100.10	99.81	99.85	100.15

TABLE 7

Nb	50	*	-	*	*
Zr	215	175	150	215	195
Cr	290	35	15	*	36
Y	-	-	-	*	*
Ni	330	65	50	47	*
Co	54	58	50	49	*
Sr	420	330	500	485	510
Cu	82	82	66	66	60
Pb	*	*	*	220	-
Ba	250	235	450	370	290
Rb	-	-	30	50	-
$\frac{FeO+Fe_2O_3}{FeO+Fe_2O_3+MgO}$	0.605	0.709	0.663	0.731	0.695
or	6.38	6.09	6.80	8.57	8.16
ab	21.64 18.68	26.57 22.49	22.64	22.85 20.39	24.79
an	19.26	23.41	27.45	22.86	23.22
ne	3.50 5.10	2.21	2.91	4.08 5.41	2.48
di	18.29 15.43	16.70 11.83	9.37	12.34 10.08	10.67
he	3.95 7.22	2.89 8.47	5.61	5.31 7.99	5.30
en		0.31 -			
fs		0.06 -			
fo	8.49 9.42	4.11 5.91	7.15	4.58 5.31	5.90
fa	2.32 5.57	0.90 5.35	5.41	2.49 5.26	3.70
il	6.17	7.20	6.27	6.88	6.53
mt	7.19 3.71	9.22 4.15	3.16	6.95 4.04	5.23
ap	1.18	0.92	1.14	1.30	1.42
H_2O	1.84	1.74	1.93	1.67	2.78
TOTAL	100.21 99.96	100.12 99.77	99.84	99.90 99.69	100.18
D.I.	30.16	30.79	32.35	34.37	35.43

TABLE 7

Alkali olivine basalts

Specimen no.	794	786	809		830		716	834
SiO_2	46.17	45.03	45.89		46.49		44.52	46.56
Al_2O_3	15.99	14.60	16.00		16.19		15.78	17.09
TiO_2	3.34	3.36	3.65		3.05		3.40	3.44
Fe_2O_3	4.34	2.53	4.99	2.59	5.02	2.52	3.33	1.67
FeO	8.03	10.50	7.18	9.34	7.77	10.02	8.54	10.05
MnO	0.23	0.25	0.22		0.20		0.27	0.28
MgO	5.58	6.93	4.84		5.58		5.19	4.74
CaO	9.34	8.82	9.25		8.69		8.57	8.14
Na_2O	3.68	4.15	3.81		3.70		3.75	3.95
K_2O	1.17	1.60	1.34		1.45		1.69	1.50
P_2O_5	0.50	0.67	0.66		0.58		0.58	0.60
H_2O^+	1.34	1.63	1.73		1.14		3.96	1.23
H_2O^-	0.18	0.10	0.48		0.44		0.46	0.73
TOTAL	99.89	100.17	100.04		100.30		100.04	99.98

Nb	*		*		65		*		-		40	
Zr	140		235		205		220		210		635	
Cr	58		130		13		58		41		-	
Y	*		45		*		-		*		55	
Ni	62		115		31		43		32		*	
Co	43		35		38		40		35		35	
Sr	425		670		565		600		500		520	
Cu	86		58		54		52		60		49	
Pb	420		*		-		-		-		-	
Ba	325		405		360		330		450		420	
Rb	-		30		-		-		-		-	
$\frac{FeO+Fe_2O_3}{FeO+Fe_2O_3+MgO}$	0.690		0.652		0.708		0.696		0.696		0.710	
or	6.91		9.46		7.92		8.57		9.99		8.86	
ab	27.29		18.33	28.53		25.57	28.61		25.53	22.46		27.19
an	23.66		16.49		22.60			23.29		21.24		24.47
ne	2.08		9.09	2.01		3.61	1.46		3.13	5.02		3.38
di	11.34		11.62	12.13		9.27	9.61		7.62	9.32		5.28
he	4.32		7.11	3.02		6.30	3.29		5.57	4.92		4.65
en												
fs												
fo	6.05		8.32	4.50		5.43	6.62		7.26	6.03		6.56
fa	2.92		6.43	1.42		4.67	2.86		6.71	4.02		7.29
il	6.34		6.38		6.93			5.79		6.46		6.53
mt	6.29		3.67	7.24		3.76	7.28		3.65	4.83		2.42
ap	1.18		1.59		1.56			1.37		1.37		1.42
H_2O	1.52		1.73		2.21			1.58		4.42		1.96
TOTAL	99.90		100.22	100.07		99.83	100.33		100.07	100.08		100.01
D.I.	36.28		36.88		37.10			37.23		37.47		39.43

TABLE 8. Trachybasalts.

Specimen no.	499	792	747	201	782	723	277	521
SiO_2	47.03	46.64	45.35	47.20	48.04	48.36	47.67	47.46
Al_2O_3	15.56	16.33	16.78	16.59	17.66	16.71	18.01	16.25
TiO_2	3.59	3.27	3.44	2.83	2.70	2.42	2.92	2.79
Fe_2O_3	3.24	6.00 2.50	4.83	2.64	1.17	5.31 2.31	2.07	4.01
FeO	9.12	6.49 9.64	8.85	8.81	9.36	6.48 9.18	8.13	8.05
MnO	0.37	0.22	0.26	0.25	0.21	0.25	0.18	0.27
MgO	4.49	4.76	4.57	4.28	4.42	3.04	4.24	4.38
CaO	8.34	8.13	7.22	7.88	7.14	6.66	7.68	7.34
Na_2O	4.05	4.43	4.84	4.51	4.39	3.95	4.83	4.67
K_2O	1.40	1.57	1.81	1.70	2.02	2.05	1.71	1.92
P_2O_5	0.67	0.63	0.86	1.30	0.72	1.01	0.72	0.89
H_2O^+	1.45	1.31	1.06	1.62	1.67	2.48	1.56	1.68
H_2O^-	0.58	0.20	0.22	0.38	0.26	1.14	0.39	0.30
TOTAL	99.89	99.98	100.09	99.99	99.76	99.86	100.11	100.01

Nb	70	55	100	75	50	50	*	-
Zr	235	190	315	210	340	340	250	290
Cr	-	28	-	-	25	-	23	-
Y	50	30	-	40	*	*	100	*
Ni	*	*	*	*	36	30	*	*
Co	42	37	40	25	34	21	29	27
Sr	525	475	635	700	570	575	505	540
Cu	38	50	43	310	35	31	220	30
Pb	-	-	-	720	*	-	1300	-
Ba	380	400	585	620	525	820	620	500
Rb	-	50	30	-	-	-	-	30
$\frac{FeO+Fe_2O_3}{FeO+Fe_2O_3+MgO}$	0.733	0.725	0.746	0.729	0.704	0.798	0.708	0.733
q						0.77 -		
or	8.27	9.28	10.70	10.05	11.94	12.11	10.11	11.35
ab	31.20	30.87 26.56	26.66	31.54	29.13	33.42	29.18	31.18
an	20.14	20.04	18.72	20.00	22.52	21.81	22.41	17.71
ne	1.66	3.58 5.92	7.74	3.59	4.35		6.33	4.51
di	8.19	11.18 7.48	6.07	4.86	3.47	2.57 1.68	5.25	6.63
he	5.64	1.62 5.86	3.29	3.89	3.34	1.18 2.21	3.78	3.90
en						6.38 2.72		
fs						3.35 4.11		
fo	5.17	4.67 5.88	6.00	5.89	6.59	- 2.85	5.69	5.49
fa	4.50	0.86 5.82	4.11	5.96	8.01	- 4.74	5.19	4.08
il	6.82	6.21	6.53	5.37	5.13	4.60	5.55	5.30
mt	4.70	8.70 3.62	7.00	3.83	1.70	7.70 3.35	3.00	5.81
ap	1.59	1.49	2.04	3.08	1.71	2.39	1.71	2.11
H_2O	2.03	1.51	1.28	2.00	1.93	3.62	1.95	1.98
TOTAL	99.91	100.01 99.67	100.14	100.06	99.82	99.90 99.61	100.15	100.05
D.I.	41.13	41.76	45.10	45.18	45.42	45.53	45.62	47.04

TABLE 8. Trachybasalts

Specimen no.	744	742	438	37	780	705	85
SiO_2	48.16	49.76	49.91	50.00	50.09	50.61	51.04
Al_2O_3	16.29	16.88	15.96	16.43	16.09	16.63	16.71
TiO_2	2.72	2.13	2.07	1.93	2.34	1.75	1.77
Fe_2O_3	2.48	8.35 2.35	6.66 3.16	5.65 2.65	4.55	9.06 3.06	6.78 3.28
FeO	9.14	3.59 8.99	5.67 8.82	6.78 9.48	7.33	2.74 8.14	4.95 8.10
MnO	0.26	0.22	0.42	0.20	0.25	0.25	0.24
MgO	3.65	2.72	2.79	2.51	3.23	2.24	2.02
CaO	7.81	6.75	7.00	5.41	6.80	5.35	6.24
Na_2O	4.84	4.60	4.60	4.60	5.42	4.78	5.18
K_2O	1.93	2.08	2.09	2.11	1.82	2.31	2.33
P_2O_5	0.79	0.87	1.04	0.99	0.87	0.76	1.01
H_2O^+	1.67	1.60	1.31	2.57	0.98	2.44	1.12
H_2O^-	0.31	0.78	0.34	0.78	0.21	0.93	0.76
TOTAL	100.05	100.33	99.86	99.96	99.98	99.85	100.15

Nb	65	45	110	40	65	75	85
Zr	305	285	335	315	290	365	375
Cr	-	-	-	*	-	-	-
Y	*	50	40	65	55	45	30
Ni	-	-	*	*	*	-	*
Co	*	-	37	10	23	-	12
Sr	505	580	570	670	540	730	615
Cu	24	*	35	84	22	*	26
Pb	-	-	-	*	-	*	*
Ba	560	550	550	545	500	625	650
Rb	-	30	80	30	-	60	60
$\frac{FeO+Fe_2O_3}{FeO+Fe_2O_3+MgO}$	0.762	0.746	0.815	0.833	0.786	0.841	0.854
q		0.82 -	0.31 -	0.89 -		0.27 -	
or	11.41	12.29	12.35	12.47	10.71	13.65	13.77
ab	29.47	38.92 37.43	38.92 38.32	38.92	39.61	40.45	43.33 40.94
an	17.03	19.27	16.72	17.95	14.20	17.13	15.46
ne	6.22	0.81	0.33		3.39		1.56
di	6.79	6.64 2.90	6.98 3.97	1.17 0.75	6.75	3.46 1.45	6.01 2.78
he	6.99	4.28	1.99 5.45	0.81 1.30	4.61	2.31	1.05 4.75
en		3.69 -	3.71 -	5.71 2.57		3.97 1.59	2.01 -
fs			1.21 -	4.54 5.11		2.90	0.40 -
fo	4.16	3.80	3.58	2.33	3.44	2.32	0.17 2.62
fa	5.41	7.09	6.22	5.10	2.97	4.67	0.04 5.67
il	5.17	4.05	3.93	3.67	4.44	3.32	3.36
mt	3.60	6.11 3.41	9.66 4.58	8.19 3.84	6.60	4.57 4.44	9.83 4.76
hem		4.13 -				5.90 -	
ap	1.87	2.06	2.46	2.34	2.06	1.80	2.39
H_2O	1.98	2.38	1.65	3.35	1.19	3.37	1.88
TOTAL	100.10	100.36 99.77	99.89 99.56	100.01 99.70	99.97	99.89 99.40	100.20 99.94
D.I.	47.10	50.53	51.00	51.39	53.71	54.10	56.27

TABLE 9. Trachyandesites.

Specimen no.	218	845	599	161	828	613	486
SiO_2	53.29	53.96	55.03	52.96	53.74	54.09	55.15
Al_2O_3	17.64	16.88	17.10	18.28	18.74	17.38	17.49
TiO_2	1.37	1.01	0.76	1.41	1.10	0.80	0.67
Fe_2O_3	8.20 3.20	3.70	6.88 2.88	4.01	10.53 2.53	2.77	2.54
FeO	2.07 6.57	6.53	3.05 6.65	3.39	- 7.20	6.58	6.47
MnO	0.18	0.26	0.28	0.17	0.22	0.30	0.28
MgO	0.96	1.62	1.01	2.41	0.30	1.66	1.05
CaO	3.49	4.49	4.12	5.36	3.16	4.20	4.24
Na_2O	5.33	5.56	5.44	6.53	5.81	5.99	5.94
K_2O	2.59	2.64	2.93	2.62	2.77	2.90	3.23
P_2O_5	0.56	0.49	0.33	0.25	0.80	0.43	0.36
H_2O^+	3.17	2.47	2.46	1.92	1.95	2.44	2.24
H_2O^-	0.99	0.59	0.57	0.56	0.85	0.43	0.17
TOTAL	99.84	100.20	99.96	99.87	99.97	99.97	99.83

Nb	60	65	110	125	80	*	75	
Zr	435	390	550	580	525	545	655	
Cr	8	-	-	-	-	-	-	-
Y	65	*	45	-	*	*	-	
Ni	17	-	*	*	*	*	*	
Co	-	-	*	28	-	*	-	
Sr	675	735	610	935	670	645	575	
Cu	130	*	12	32	30	13	*	
Pb	750	-	-	*	-	-	-	
Ba	1500	640	850	800	780	790	880	
Rb	40	70	50	90	50	50	70	
$\frac{FeO+Fe_2O_3}{FeO+Fe_2O_3+MgO}$	0.915	0.865	0.908	0.754	0.836	0.849	0.896	
q	5.04	1.63	3.78	-	4.38	-		
or	15.31	15.60	17.32	15.48	16.37	17.14	19.09	
ab	45.10	47.05	46.03	41.02	49.16	45.71	46.03	
an	13.66	13.31	13.59	12.83	10.45	11.97	11.52	
ne				7.71		2.69	2.29	
di		1.85	3.65	0.97	8.47		1.77	1.52
he		3.02		3.07	1.11		3.37	4.65
en	2.39	1.23	0.82	1.74		0.75	0.73	
fs	7.49	2.31		6.30		9.53		
fo		1.43		0.15	1.45	0.01	2.33	1.34
fa		2.96		0.90	0.24	0.15	5.57	5.19
il	2.60	1.92	1.44		2.68	0.47	2.09	1.52	1.27
mt	3.29	4.64	5.36	8.54	4.18	5.81	3.67	4.02	3.68
hem	5.93	-		0.99	-		10.53	-		
ap	1.33	1.16	0.78	0.59	1.89	1.02	0.85
H_2O	4.16	3.06	3.03	2.48	2.80	2.87	2.41
co	1.06				2.35		
rutile					0.85	-		
TOTAL	99.87	99.37	100.26	99.97	99.50	99.87	100.00	99.20	99.98	99.84
D.I.		62.04	62.65		63.35	64.21		65.53	65.54	67.41

TABLE 9. Trachyandesites.

Specimen no.	269	822	671	323	704	664
SiO_2	56.75	54.88	57.96	56.72	56.01	57.58
Al_2O_3	17.72	17.41	16.97	17.55	17.53	17.60
TiO_2	0.92	1.11	0.46	0.59	0.55	0.49
Fe_2O_3	4.55	2.55	2.44	4.00 2.20	5.52 2.82	3.10	3.29
FeO	3.34	5.14	6.79	4.39 6.01	2.54 4.80	5.35	4.42
MnO	0.20	0.23	0.27	0.24	0.30	0.20
MgO	1.02	1.88	1.10	1.06	0.91	1.02
CaO	3.81	3.48	2.75	3.18	3.56	2.82
Na_2O	5.98	6.04	5.97	6.37	6.74	6.70
K_2O	2.96	2.89	3.53	3.33	3.66	3.23
P_2O_5	0.33	0.77	0.13	0.18	0.19	0.13
H_2O^+	1.78	1.53	1.85	2.20	1.90	1.96
H_2O^-	0.54	0.41	0.58	0.55	0.35	0.36
TOTAL	99.90	99.86	99.96	100.03	100.15	99.80

Nb	85		115		115		120		85		105	
Zr	505		490		620		530		600		625	
Cr	-		-		-		-		-		69	
Y	60		35		45		40		45		45	
Ni	*		*		*		*		-		*	
Co	*		*		-		-		-		-	
Sr	550		545		410		475		530		395	
Cu	9		18		5		55		-		285	
Pb	-		-		*		240		-		375	
Ba	1000		790		1180		1080		975		1100	
Rb	65		50		70		80		60		95	
$\frac{FeO+Fe_2O_3}{FeO+Fe_2O_3+MgO}$	0.885		0.831		0.884		0.884		0.902		0.885	
q	2.18	-			1.31	-	0.14	-				
or	17.49		17.08		20.86		19.68		21.63		19.09	
ab	50.60		51.07		50.52		53.90	51.77	45.02		54.92	
an	12.77		11.86		9.08		9.46		6.77		8.41	
ne			0.02					1.15	6.51		0.96	
di	2.26	1.09	0.12		1.28	0.83	4.00	1.47	2.26		1.48	
he	0.95	2.30	0.20		1.84	2.36		2.90	6.01		2.52	
en	1.49	1.95			2.14	1.66	0.78	-				
fs	0.72	4.74			3.52	5.44						
fo		0.06	3.24		-	0.48		1.37	0.85		1.30	
fa		0.17	6.91		-	1.75		3.41	2.87		2.80	
il	1.75		2.11		0.87		1.12	1.12	1.04		0.93	
mt	6.60	3.70	3.54		5.80	3.19	7.26	4.09	4.49		4.77	
hem							0.51	-				
ap	0.78		1.82		0.31		0.43		0.45		0.31	
H_2O	2.32		1.94		2.43		2.75		2.25		2.32	
TOTAL	99.91	99.72	99.91		99.96	99.78	100.03	99.60	100.15		99.81	
D.I.	68.09		68.17		71.38		72.60		73.16		74.97	

TABLE 10. Early trachytic rocks and flank flow domes.

Specimen no.	745a	763	824	108	109	831	111
SiO_2	59.43	59.64	57.58	57.39	56.77	56.54	56.51
Al_2O_3	17.65	17.67	18.36	19.42	18.36	18.61	19.66
TiO_2	0.36	0.42	0.18	0.26	0.22	0.26	0.17
Fe_2O_3	5.97 2.27	2.59	3.24	4.08 2.58	4.25 2.75	3.41	2.79
FeO	0.90 4.23	3.92	4.40	1.82 3.17	2.75 4.10	3.72	2.70
MnO	0.21	0.22	0.30	0.37	0.33	0.32	0.22
MgO	0.77	0.50	0.25	0.61	0.62	0.42	0.31
CaO	1.49	2.09	2.53	2.03	2.41	2.35	2.45
Na_2O	6.90	7.62	8.08	7.26	7.46	7.74	8.01
K_2O	3.86	4.02	3.63	3.67	3.73	3.80	3.57
P_2O_5	0.03	0.08	0.13	0.09	0.08	0.12	0.14
H_2O^+	1.49	1.04	0.92	2.34	2.82	2.09	3.01
H_2O^-	0.97	0.29	0.31	0.49	0.26	0.43	0.35
TOTAL	100.03	100.10	99.91	99.83	100.06	99.81	99.89

Nb	120	90	95	110	120	120	105
Zr	680	645	670	795	725	720	690
Cr	-	-	-	-	-	-	-
Y	15	*	20	70	50	35	40
Ni	*	-	*	*	*	-	*
Co	-	-	-	-	-	-	-
Sr	280	280	425	510	615	425	535
Cu	*	-	*	17	8	*	6
Pb	-	-	-	-	*	-	*
Ba	1130	1100	900	960	1000	810	1000
Rb	70	90	140	135	150	105	150
$\frac{FeO+Fe_2O_3}{FeO+Fe_2O_3+MgO}$	0.900	0.929	0.968	0.906	0.918	0.945	0.946
q	0.57 -						
or	22.81	23.76	21.45	21.69	22.04	22.46	21.10
ab	58.39 57.72	53.68	48.92	53.82 51.97	49.86 48.02	47.31	48.09
an	5.79	2.14	3.11	9.48	5.60	4.82	7.15
ne	0.36	5.85	10.54	4.13 5.13	7.18 8.19	9.85	10.67
co				0.03			
di	1.10 0.34	1.53	0.84		2.41 1.22	1.17	0.85
he	0.87	5.12	6.70		2.44 3.80	4.07	2.67
en	1.41 -						
fs							
fo	1.23	0.38	0.16	0.18 1.06	0.30 0.68	0.35	0.26
fa	4.04	1.58	1.62	1.06 3.05	0.38 2.69	1.56	1.05
wo							
il	0.68	0.80	0.34	0.49	0.42	0.49	0.32
mt	2.54 3.29	3.76	4.70	5.92 3.74	6.16 3.99	4.94	4.05
hem	4.22 -						
ap	0.07	0.19	0.31	0.21	0.19	0.28	0.33
H_2O	2.46	1.31	1.23	2.83	3.08	2.52	3.36
TOTAL	100.04 99.66	100.10	99.92	99.84 99.68	100.06 99.92	99.82	99.90
D.I.	80.89	83.29	80.91	78.79	78.25	79.62	79.86

TABLE 11. Late highly alkaline intrusions.

Specimen no.	87	259	468	662	846	232
SiO_2	56.66	57.47	57.64	60.29	60.05	59.43
Al_2O_3	17.79	17.23	17.94	18.57	17.86	17.41
TiO_2	0.45	0.49	0.37	0.23	0.16	0.30
Fe_2O_3	4.62	2.62	3.76	2.56	5.00	2.50	1.11	2.08	2.94
FeO	3.72	5.52	4.01	5.09	2.39	4.64	3.81	3.63	3.22
MnO	0.33	0.33	0.30	0.25	0.25	0.27
MgO	0.75	0.49	0.48	0.32	0.29	0.17
CaO	2.97	3.20	2.85	2.43	2.23	1.94
Na_2O	6.88	6.80	7.03	7.03	7.44	7.25
K_2O	3.44	3.71	3.79	4.38	4.26	4.58
P_2O_5	0.14	0.29	0.10	0.08	0.02	0.10
H_2O^+	1.97	1.83	1.53	1.34	1.59	1.95
H_2O^-	0.15	0.78	0.49	0.17	0.19	0.51
TOTAL	99.87	100.39	99.91	100.01	100.05	100.07

Nb	90		140		90		165		140		190	
Zr	545		515		735		820		800		840	
Cr	-		-		-		-		-		-	
Y	50		45		35		30		35		55	
Ni	*		*		*		*		*		*	
Co	-		-		-		-		-		-	
Sr	515		670		465		140		240		140	
Cu	14		6		*		*		*		*	
Pb	-		-		-		*		-		-	
Ba	1000		1230		1280		1600		1375		1700	
Rb	120		70		100		95		105		95	
Index of agpaicity	0.85		0.88		0.87		0.88		0.94		0.97	
$\frac{FeO+Fe_2O_3}{FeO+Fe_2O_3+MgO}$	0.917		0.940		0.938		0.940		0.953		0.973	
q												
or	20.33		21.93		22.40		25.88		25.18		27.07	
ab	51.61	49.14	51.65	50.17	53.33	49.42	52.04		52.57		52.06	
an	7.50		5.54		6.20		6.18		2.76		1.44	
ne	3.58	4.91	3.19	3.99	3.33	5.45	4.03		5.63		5.03	
co												
di	2.26	1.17	1.86	1.22	2.58	1.12	0.61		0.99		0.81	
he	3.04	4.29	5.40	6.13	0.39	5.22	4.08		6.16		5.80	
en												
fs												
fo	0.57	0.93	0.25	0.46	-	0.47	0.36		0.18		0.03	
fa	0.98	4.29	0.92	2.92	-	2.80	3.09		1.45		0.32	
wo												
il	0.85		0.93		0.70		0.44		0.30		0.57	
mt	6.70	3.80	5.45	3.71	7.25	3.62	1.61		3.02		4.26	
hem												
ap	0.33		0.69		0.24		0.19		0.05		0.24	
H_2O	2.12		2.61		2.02		1.51		1.78		2.46	
TOTAL	99.87	99.66	100.42	100.30	99.92	99.66	100.01		100.07		100.09	
D.I.	74.38		76.09		77.27		81.95		83.38		84.16	

TABLE 11. Late highly alkaline intrusions.

Specimen no.	121		421	415	452	682	167
SiO_2	62.37		59.79	60.97	61.18	60.00	62.09
Al_2O_3	18.21		17.24	17.54	18.60	19.42	18.52
TiO_2	0.18		0.34	0.16	0.07	0.09	0.14
Fe_2O_3	3.70	2.00	3.49	2.72	2.31	2.21	1.86
FeO	0.80	2.33	3.47	2.99	1.55	1.10	1.76
MnO	0.19		0.25	0.23	0.15	0.18	0.16
MgO	0.04		0.25	0.11	0.24	0.13	0.07
CaO	0.85		1.97	1.81	1.23	0.79	1.26
Na_2O	6.65		6.79	7.04	7.64	7.41	7.25
K_2O	5.07		4.26	4.71	4.96	4.81	5.04
P_2O_5	-		0.11	0.03	0.04	0.02	0.06
H_2O+	1.67		1.52	1.24	1.77	3.05	1.32
H_2O^-	0.53		0.33	0.28	0.27	0.76	0.37
TOTAL	100.26		99.81	99.83	100.01	99.97	99.89

Nb	200		115	160	200	190	145
Zr	1335		930	985	1200	1300	1120
Cr	-		-	-	-	-	-
Y	75		70	70	35	40	115
Ni	38		*	*	*	*	*
Co	-		-	-	-	-	-
Sr	80		240	155	50	-	85
Cu	-		*	*	-	-	-
Pb	-		-	-	-	165	-
Ba	930		1340	1400	680	360	1350
Rb	165		125	125	135	150	160
Index of agpaicity	0.90		0.92	0.95	0.97	0.90	0.94
$\frac{FeO+Fe_2O_3}{FeO+Fe_2O_3+MgO}$	0.991		0.966	0.981	0.942	0.962	0.981
q	2.40	1.18					
or	29.96		25.18	27.84	29.31	28.43	29.79
ab	56.27		56.73	55.28	54.27	54.43	56.86
an	4.22		3.98	2.35	1.81	3.79	3.11
ne			0.39	2.32	5.62	3.94	2.43
co	0.24					0.70	
di			0.77	0.48	1.29		0.25
he			3.64	5.19	2.07		2.17
en	0.10	0.10					
fs	-	2.68					
fo			0.19	0.04		0.23	0.04
fa			1.12	0.50		0.29	0.47
wo					0.02		
il	0.34		0.65	0.30	0.13	0.17	0.27
mt	2.68	2.90	5.06	3.94	3.35	3.20	2.70
hem	1.85	-					
ap	-	-	0.26	0.07	0.09	0.05	0.14
H_2O	2.20		1.85	1.52	2.04	3.81	1.69
TOTAL	100.26	100.09	99.82	99.83	100.00	100.04	99.92
D.I.		87.41	82.30	85.44	89.20	87.80	89.08

TABLE 12. Alkaline dykes

Specimen no.	751	403	379	628	395	281	290	11	319
SiO_2	58.94	60.64	60.16	61.80	61.29	59.34	59.71	59.92	60.16
Al_2O_3	18.11	18.29	18.73	18.05	18.24	19.78	19.82	19.86	19.82
TiO_2	0.44	0.04	0.06	0.13	*	0.06	0.08	0.06	0.03
Fe_2O_3	2.87	2.75	3.57	3.29	1.82	2.22	1.94	1.69	1.76
FeO	4.08	1.18	1.34	0.82	2.61	1.24	1.27	1.70	1.35
MnO	0.25	0.23	0.17	0.15	0.23	0.20	0.15	0.18	0.21
MgO	0.59	0.09	0.06	0.08	0.12	0.18	0.19	0.05	0.13
CaO	2.66	0.83	0.97	1.10	1.15	0.85	0.97	1.07	0.93
Na_2O	6.36	8.93	8.91	8.22	7.29	9.02	8.37	8.94	8.63
K_2O	3.72	5.10	4.86	5.51	5.14	5.15	5.12	4.93	4.98
P_2O_5	0.08	-	0.04	-	0.04	0.01	0.02	0.07	0.03
H_2O^+	1.83	1.79	1.08	1.04	1.57	1.48	2.00	1.29	1.92
H_2O^-	0.26	0.19	0.21	0.17	0.31	0.24	0.36	0.17	0.15
TOTAL	100.19	100.06	100.16	100.36	99.81	99.77	100.00	99.93	100.10
index of agpaicity	0.80	1.11	1.07	1.08	0.97	1.03	0.97	1.01	0.99
$\frac{FeO+Fe_2O_3}{FeO+Fe_2O_3+MgO}$	0.922	0.978	0.988	0.981	0.974	0.951	0.945	0.986	0.966

Nb	125	140	125	185	185	140	145	125	105
Zr	760	1315	1150	1200	1230	1450	1080	1085	1385
Cr	-	-	-	-	-	-	-	-	-
Y	45	80	35	55	75	20	30	30	30
Ni	*	*	*	*	*	*	*	*	*
Co	-	-	-	-	-	-	-	-	-
Sr	300	-	50	?50	85	-	100	85	50
Cu	*	-	3	*	-	*	*	*	*
Pb	-	-	*	-	-	-	*	*	*
Ba	1100	300	545	870	610	150	740	1100	225
Rb	70	190	180	130	110	210	200	220	220
or	21.98	30.14	28.72	32.56	30.38	30.44	30.26	29.14	29.43
ab	53.82	43.33	46.34	46.83	53.64	42.69	47.77	46.68	49.01
an	9.88				1.87		1.39		0.64
ne		12.11	12.43	8.31	4.36	16.46	12.49	15.18	13.01
ac		7.96	5.38	6.51		2.86		0.83	
ns		0.20							
di	0.62	0.33	0.32	1.34	0.27	0.90	1.02	0.26	0.70
he	1.78	3.29	2.38	0.43	2.88	2.68	1.65	4.03	2.55
en	0.94								
fs	3.11								
fo	0.17	0.05			0.12	0.02			
fa	0.62	0.60			1.69	0.09		0.03	
wo			0.61	1.42			0.06		0.01
il	0.84	0.08	0.11	0.25	-	0.11	0.15	0.11	0.06
mt	4.16		2.48	1.51	2.64	1.78	2.81	2.04	2.55
ap	0.19	-	0.09	-	0.09	0.02	0.05	0.17	0.07
H_2O	2.09	1.98	1.29	1.21	1.88	1.72	2.36	1.46	2.07
TOTAL	100.20	100.07	100.15	100.37	99.82	99.77	100.01	99.93	100.10
D.I.	75.80	85.58	87.49	87.70	88.38	89.59	90.52	91.00	91.45

FIGURES 30-42

Major oxide and element variations.

30: Total alkalis : Silica
Dashed line Macdonald and Katsura (1964).
Solid line Saggerson and Williams (1964).

31: Na_2O - K_2O - CaO

32: FeO - MgO - total alkalis. Total iron recalculated as FeO.

33-42 (except 38,41) all plotted against differentiation index of Thornton and Tuttle (1960).

33: SiO_2 and Al_2O_3

34: MgO and Fe^o (as Fe_2O_3).

35: Cr, Ni, Co, Cu, Pb.

36: CaO and Sr.

37: Na_2O and K_2O.

38: Na_2O : K_2O. Crosses are for late dykes only analyzed for alkalis.

39: Ba and Rb.

40: Zr, TiO_2 and Nb.

41: Fe^o (as Fe_2O_3) : TiO_2.

42: P_2O_5 and MnO.

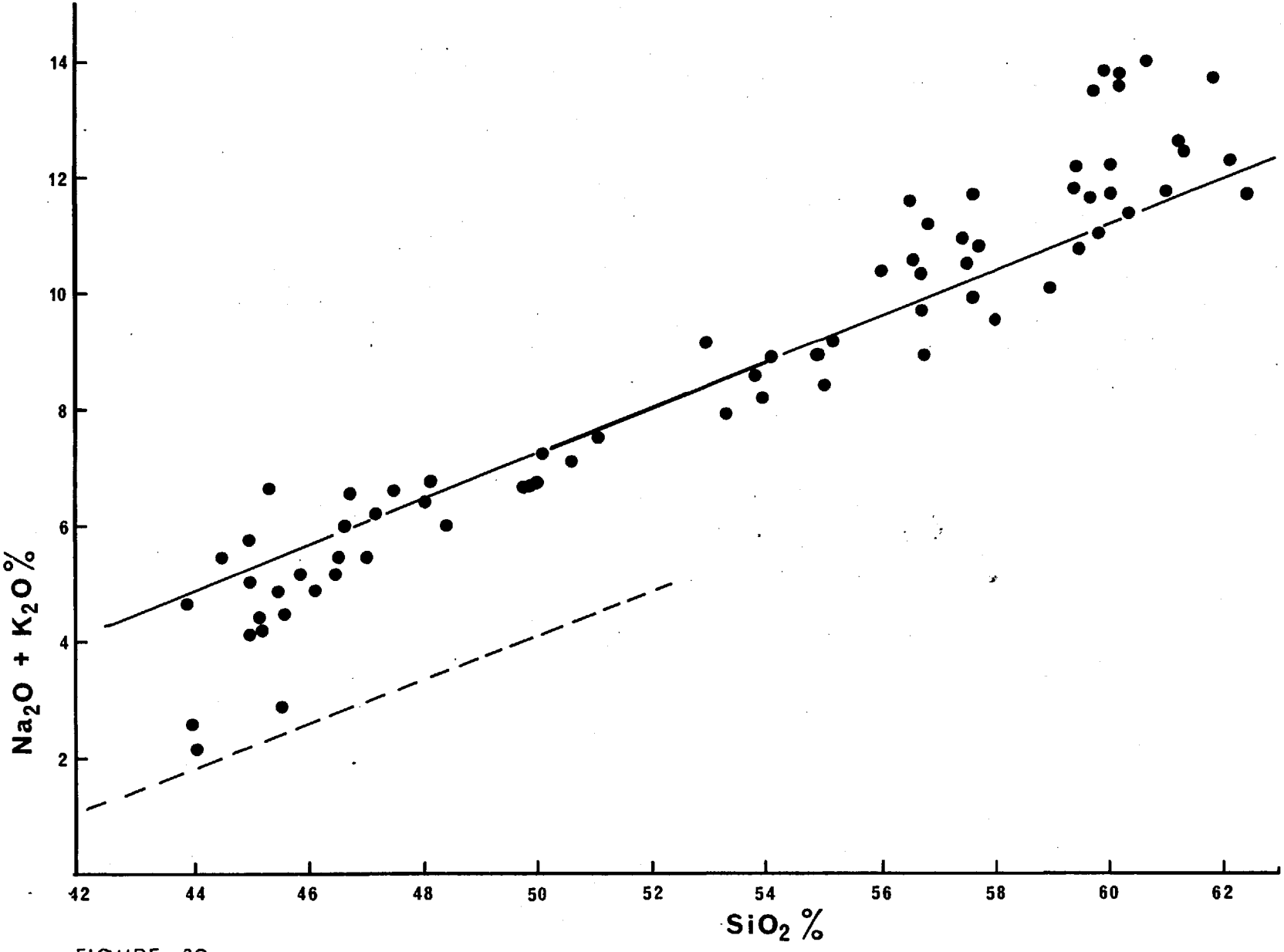

FIGURE 30

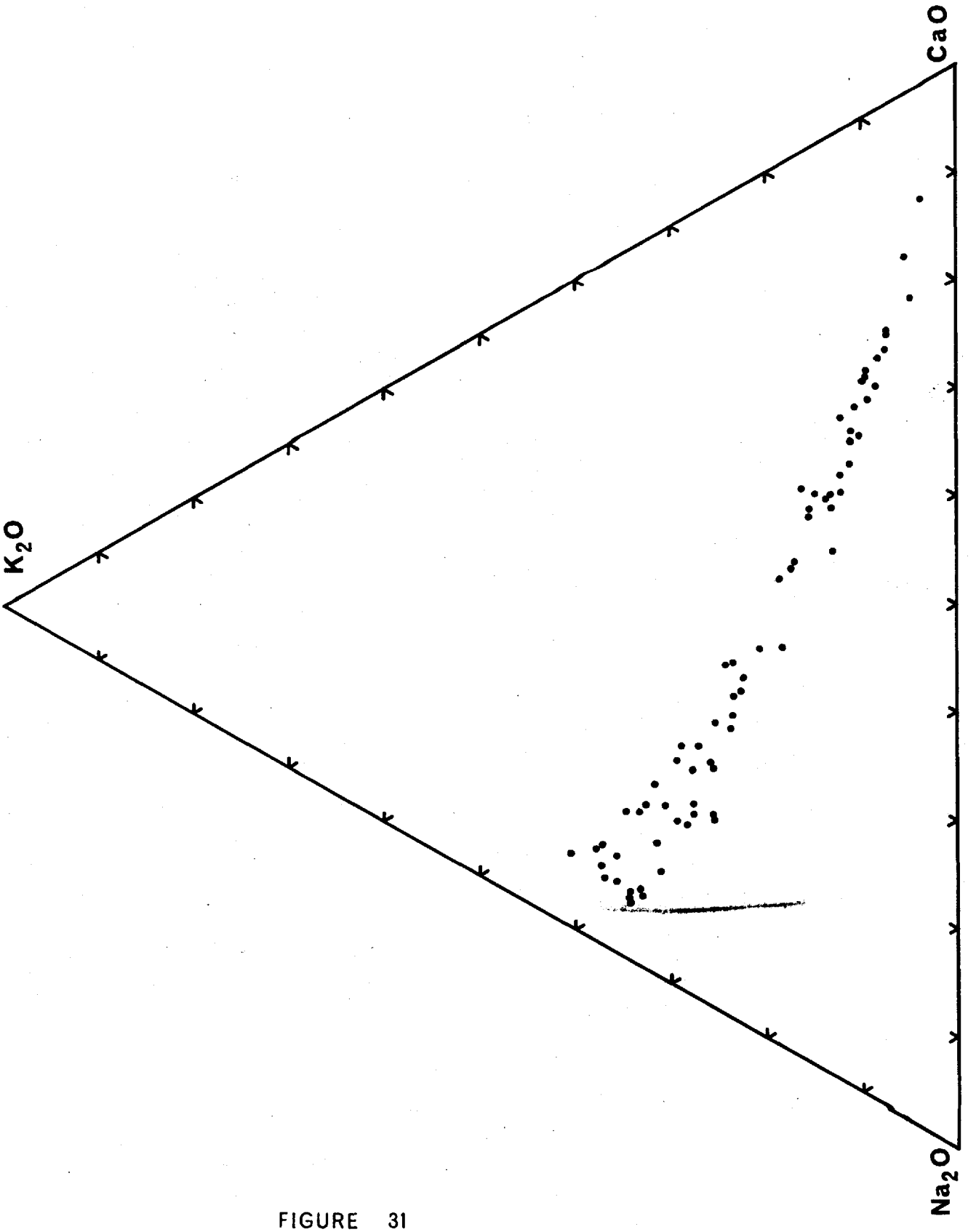

FIGURE 31

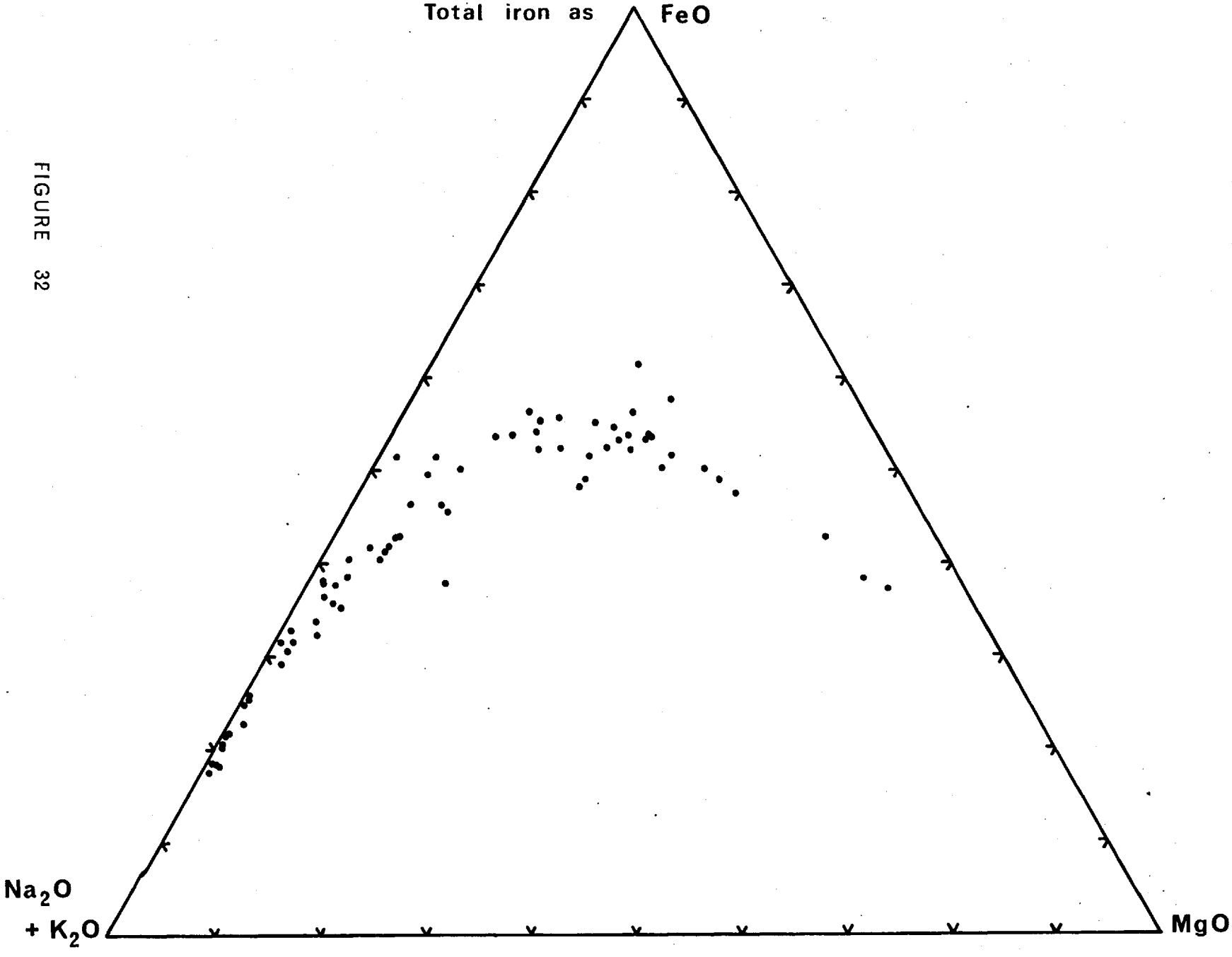

FIGURE 32

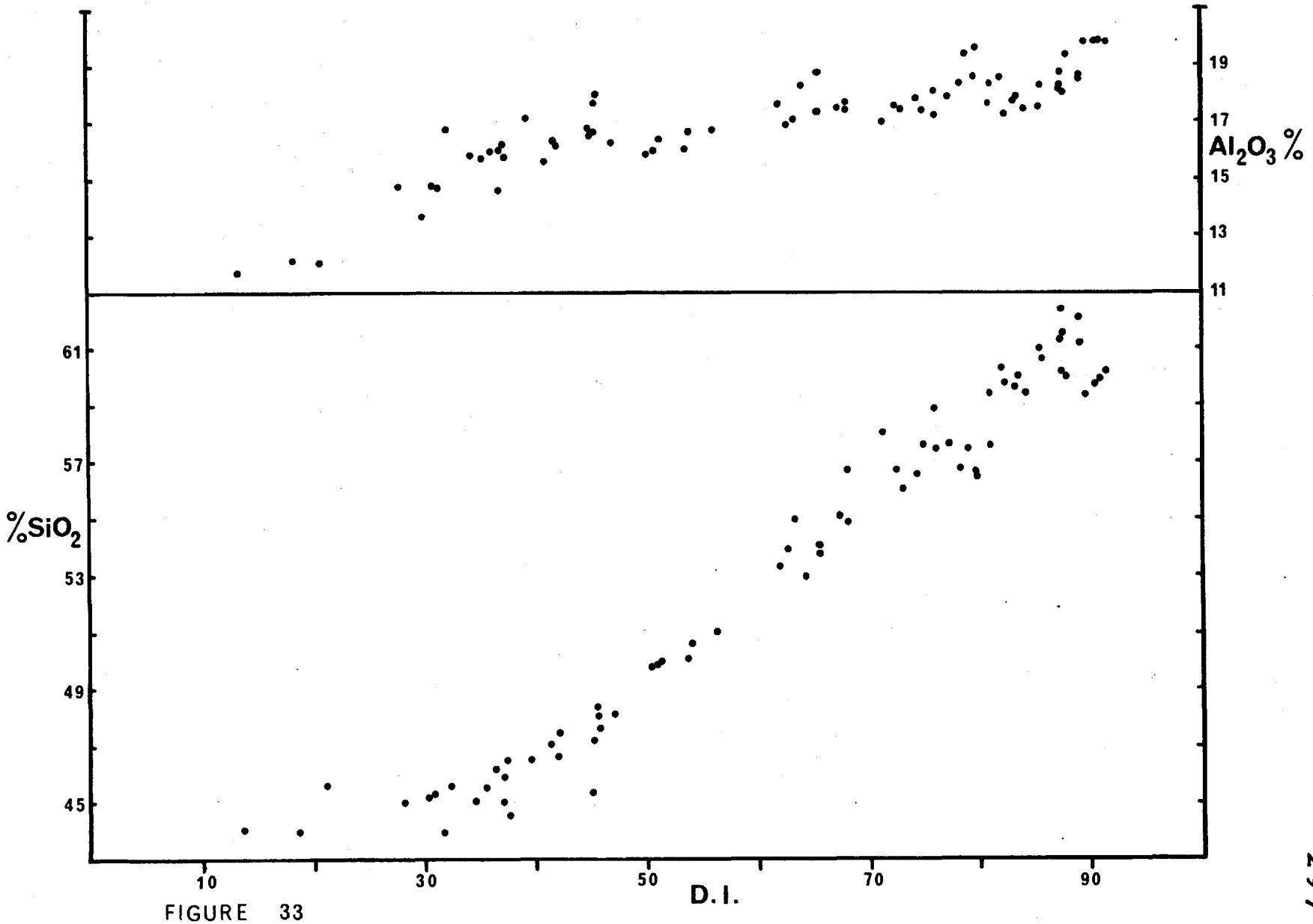

FIGURE 33

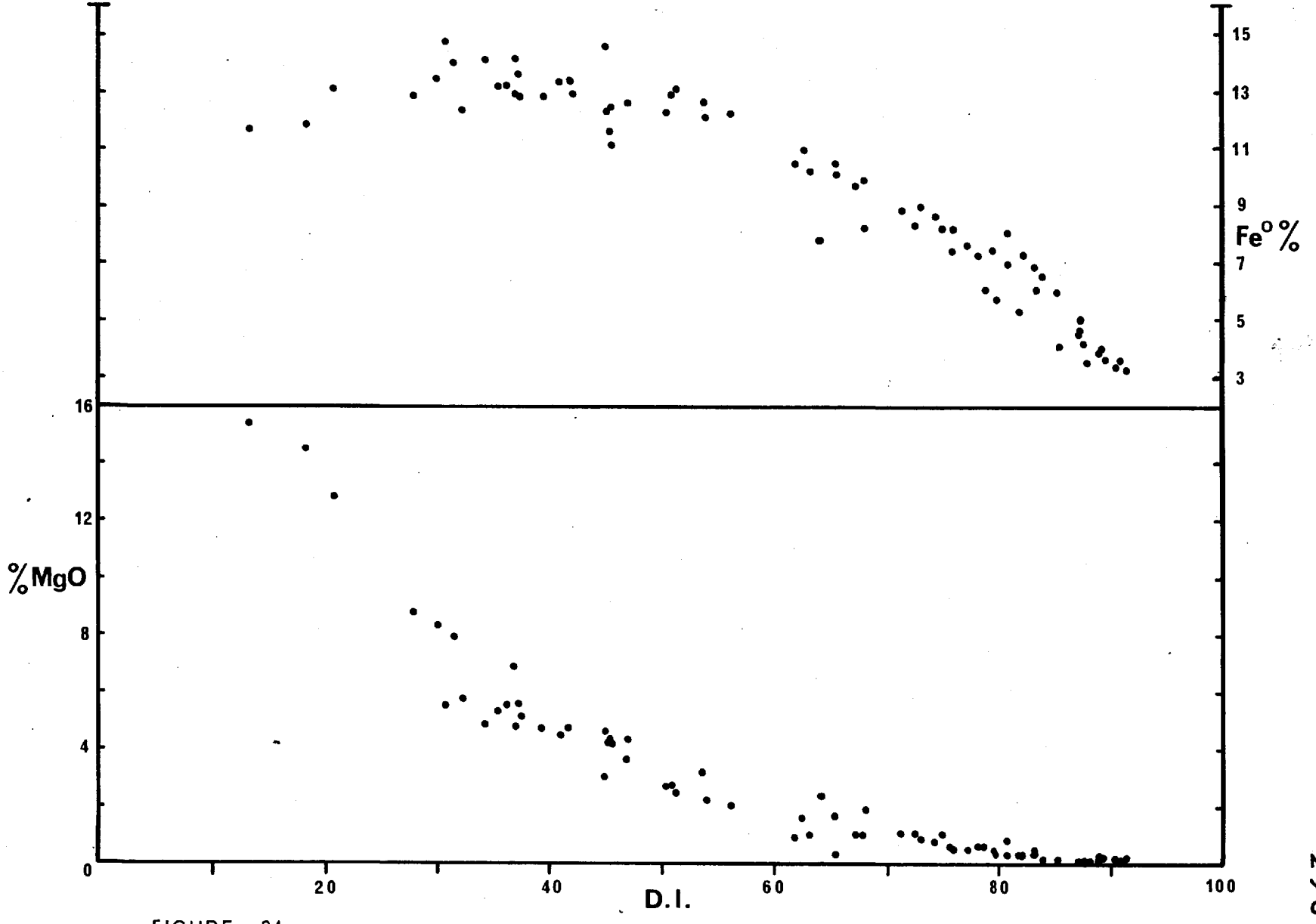

FIGURE 34

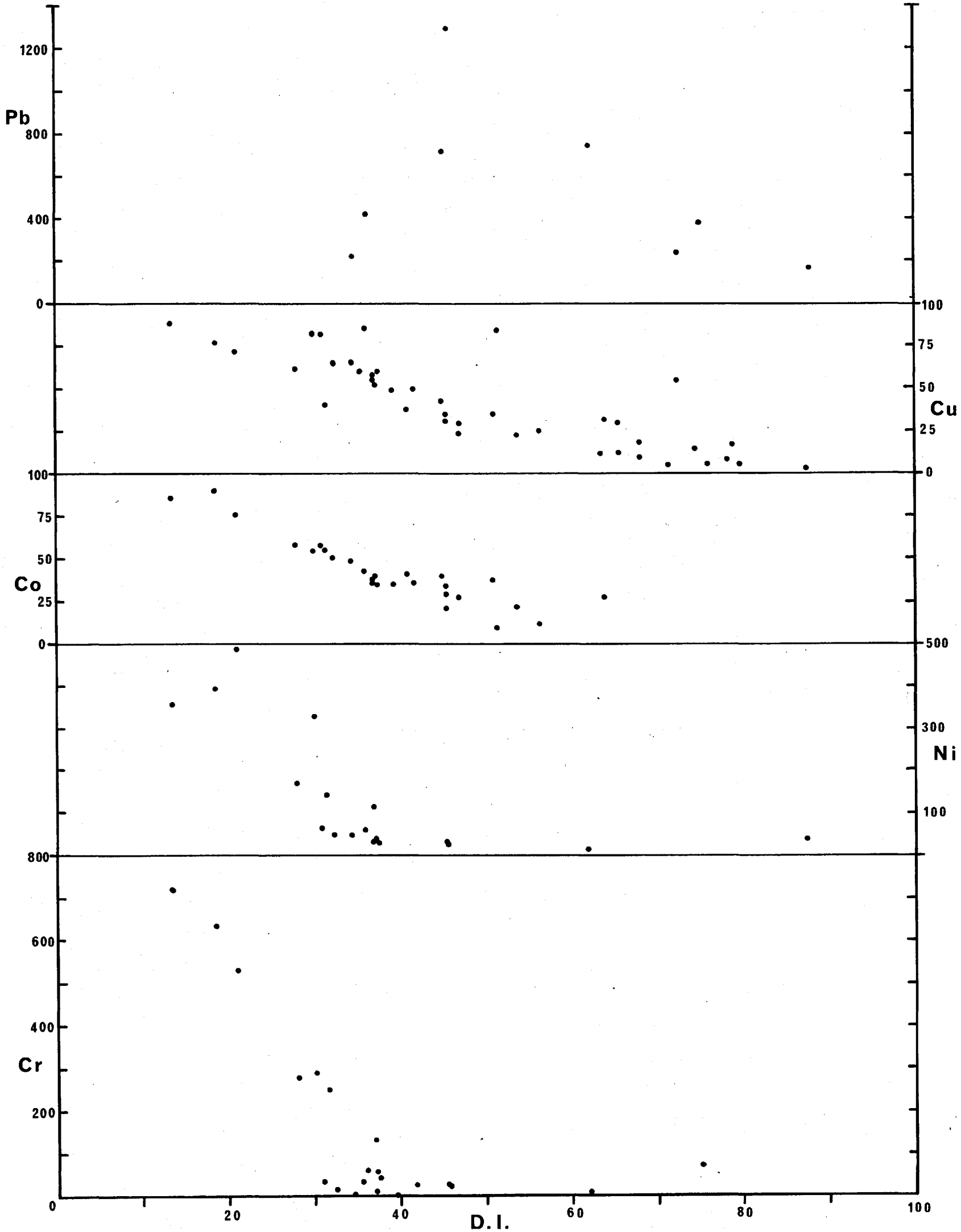

All elements in ppm

FIG : 35

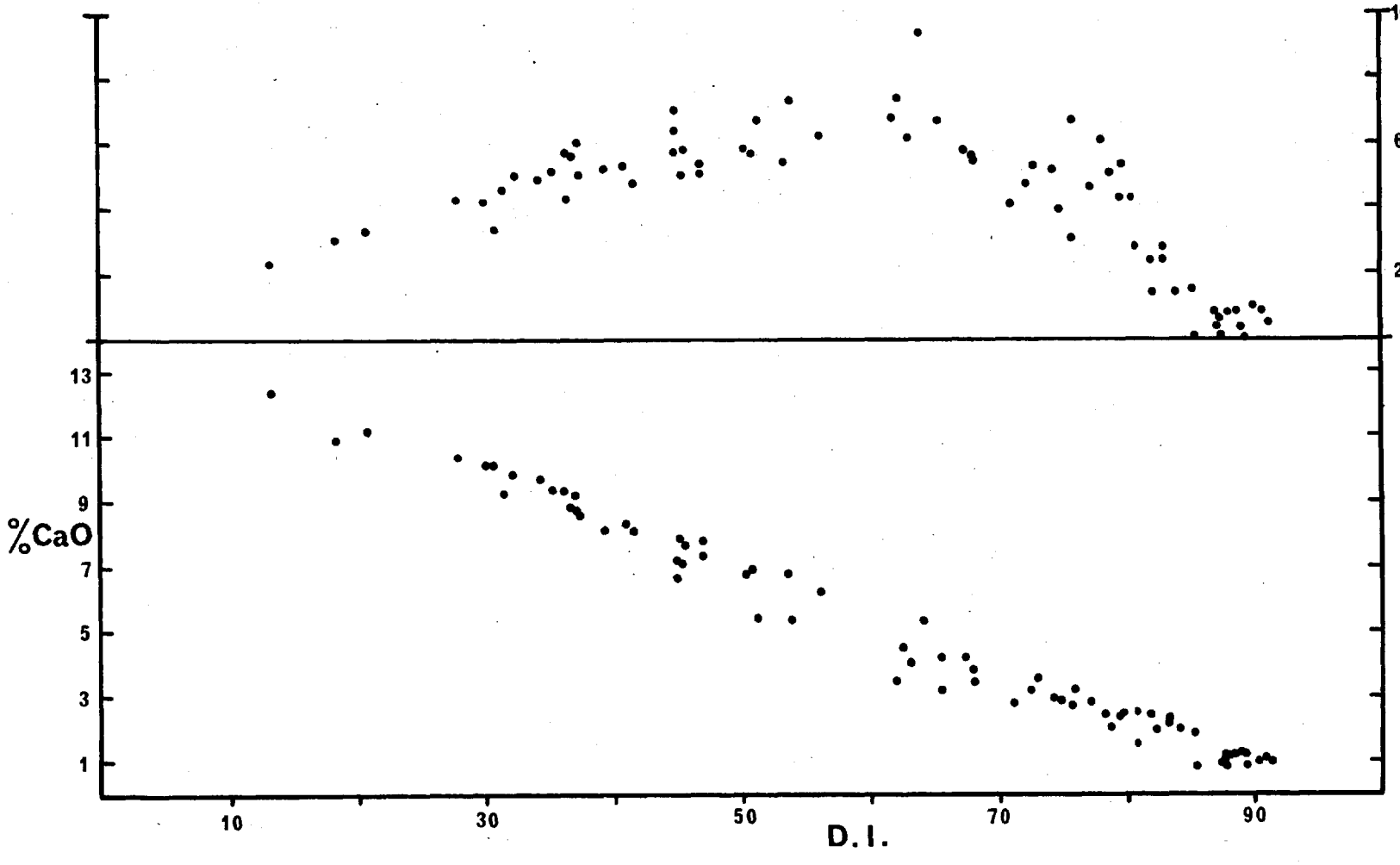

FIGURE 36

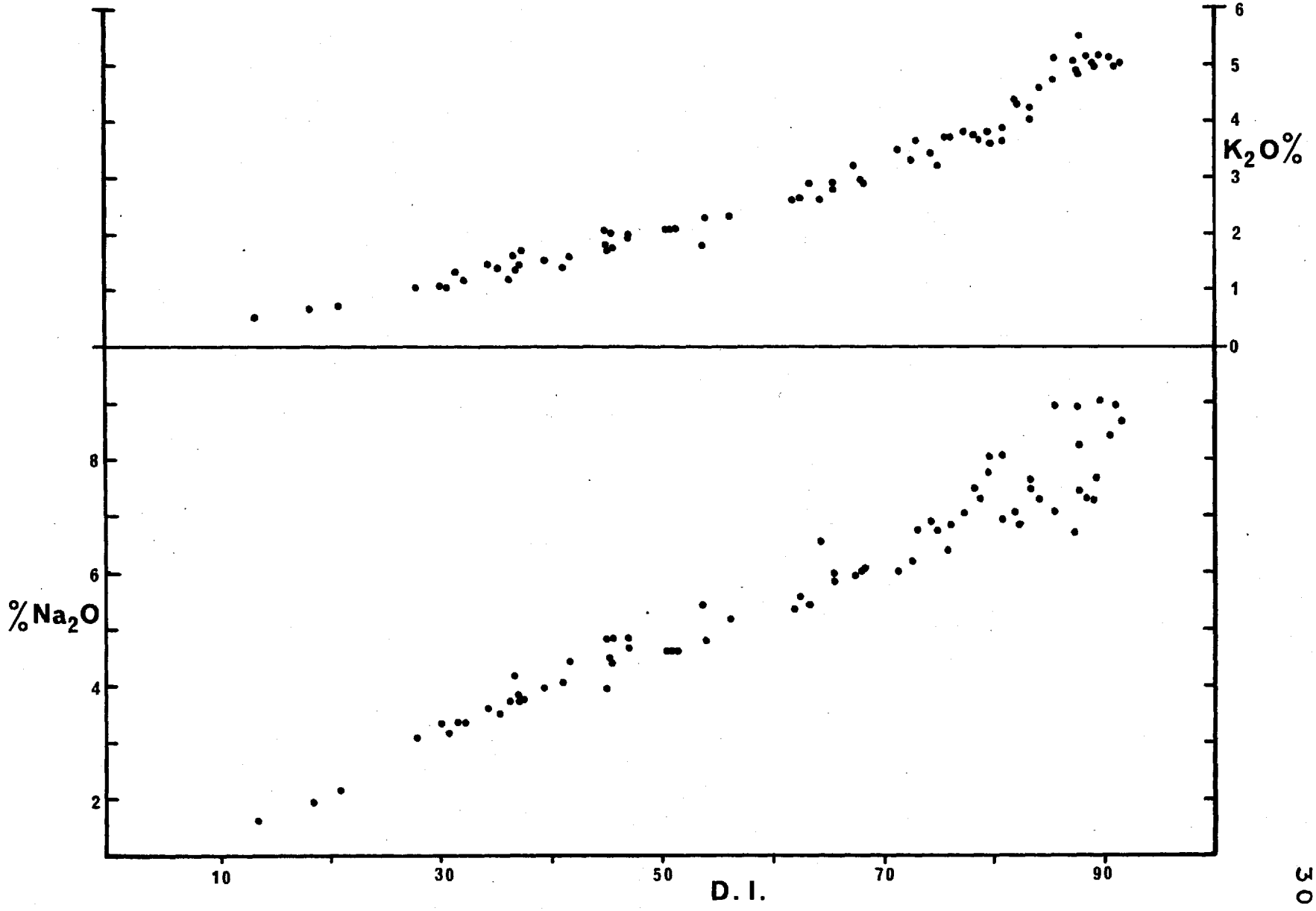

FIGURE 37

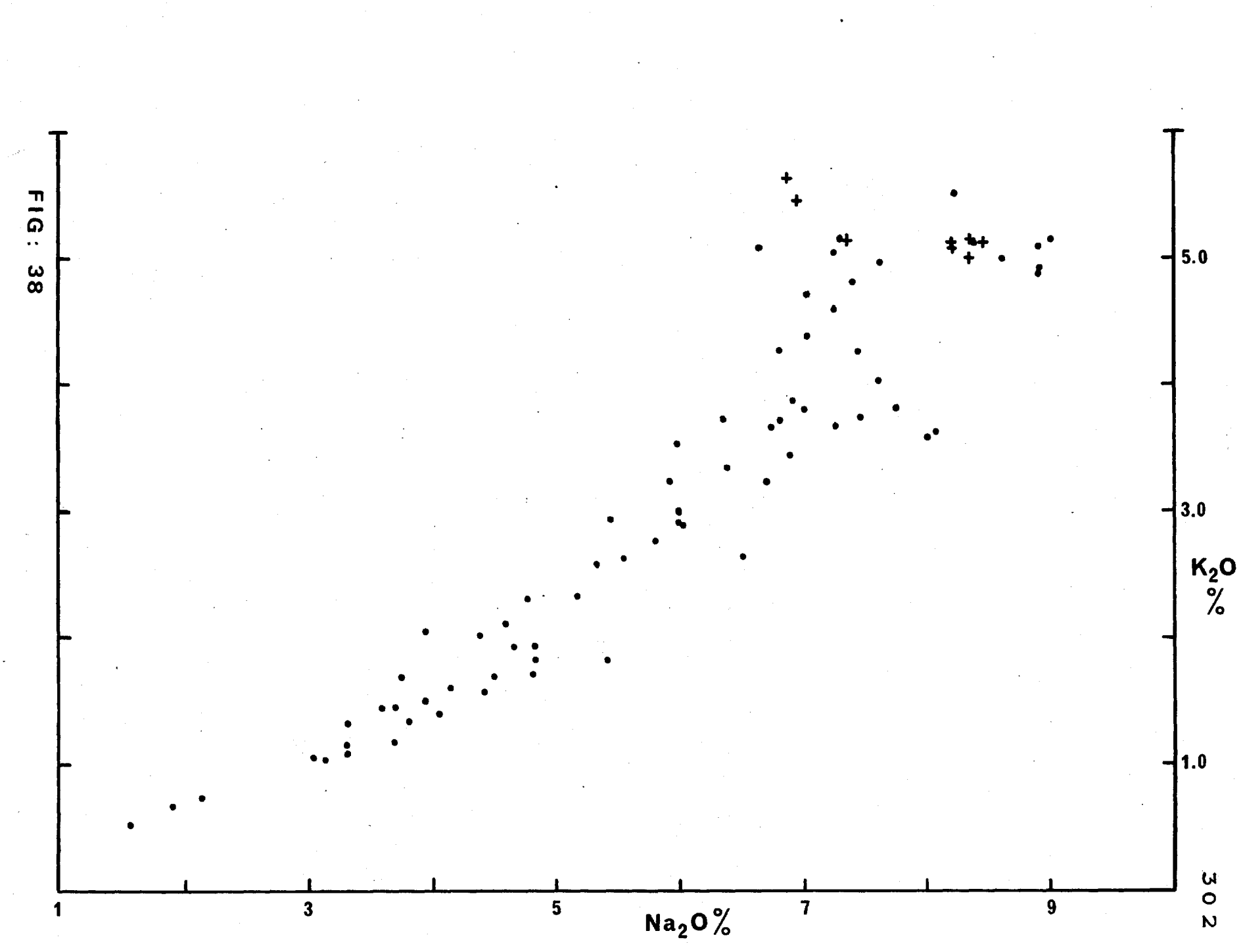
FIG: 38
5.0
3.0
1.0
K_2O %
1
3
5
7
9
Na_2O%
302

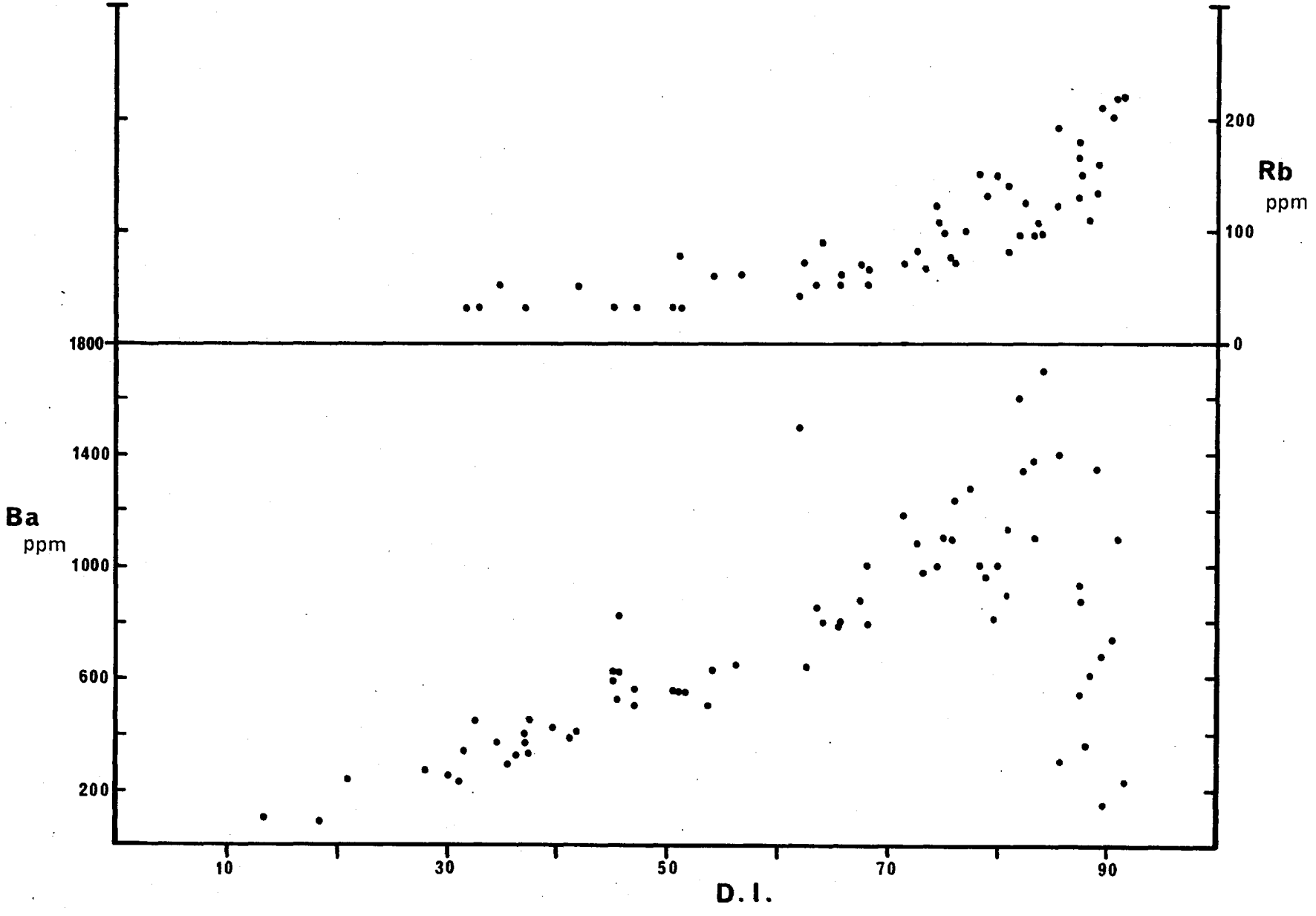

FIGURE 39

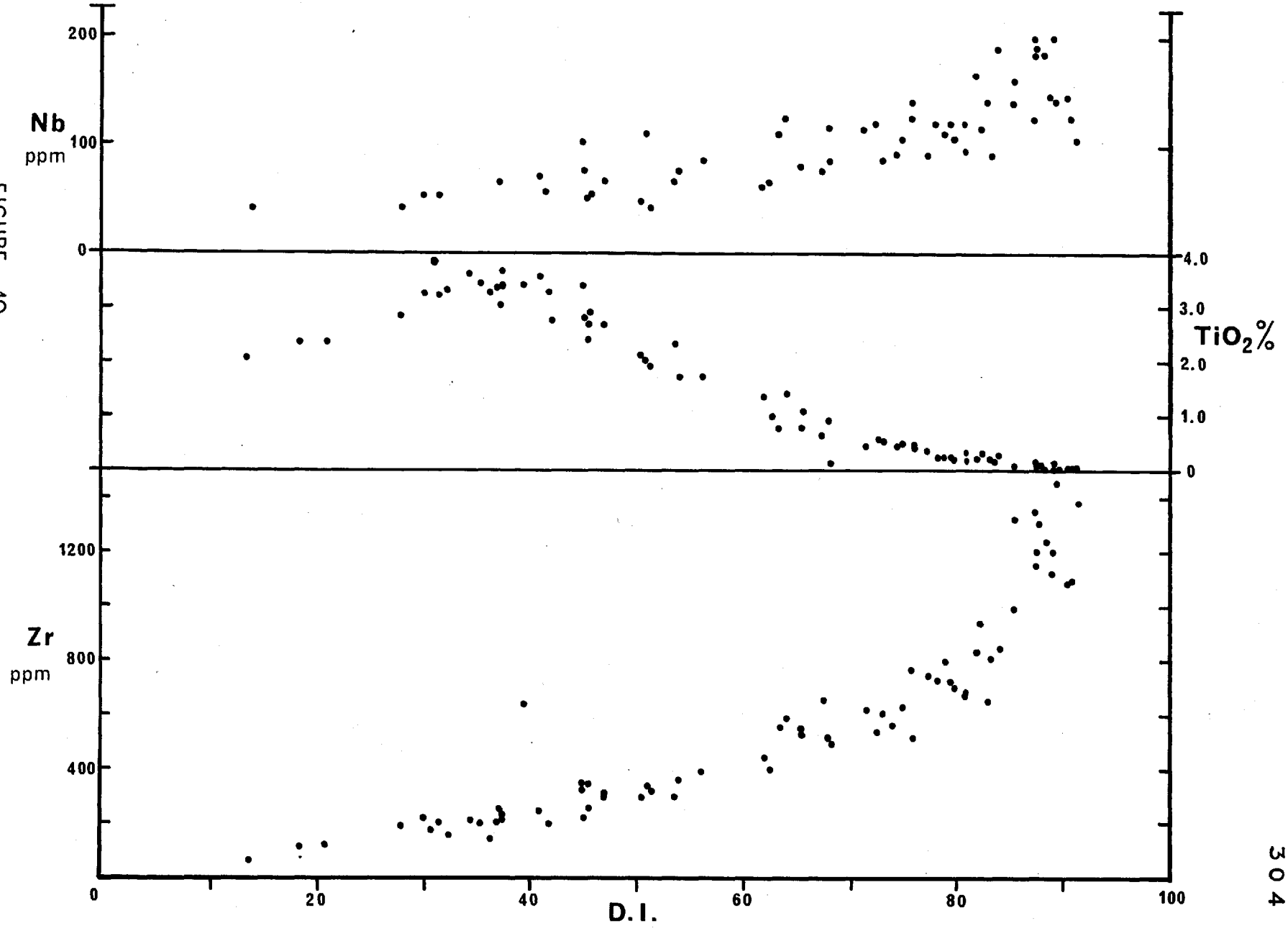
Nb
ppm
200
100
0
TiO_2%
4.0
3.0
2.0
1.0
0
Zr
ppm
1200
800
400
0
20
40
60
80
100
D.I.

FIGURE 40

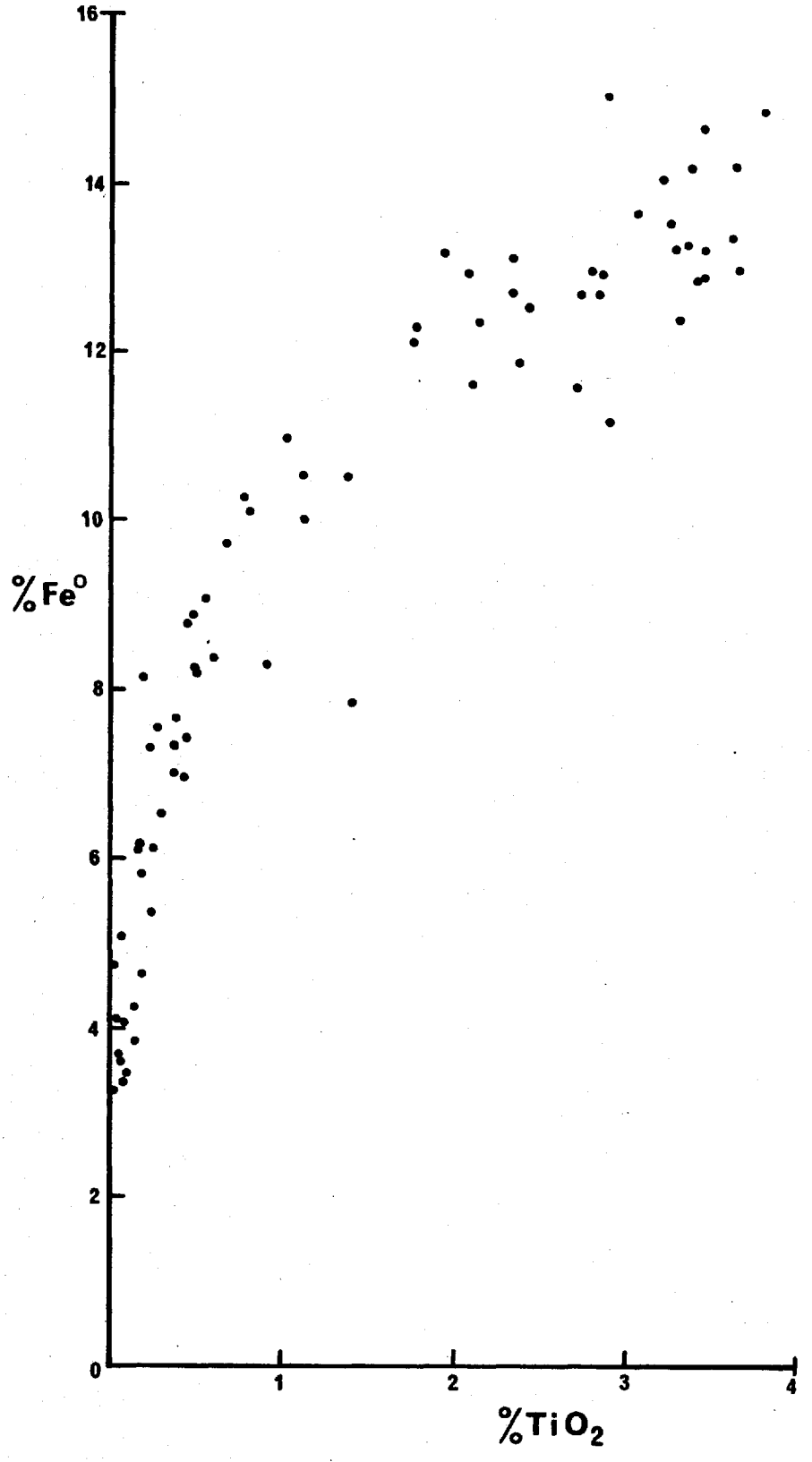

FIGURE 41

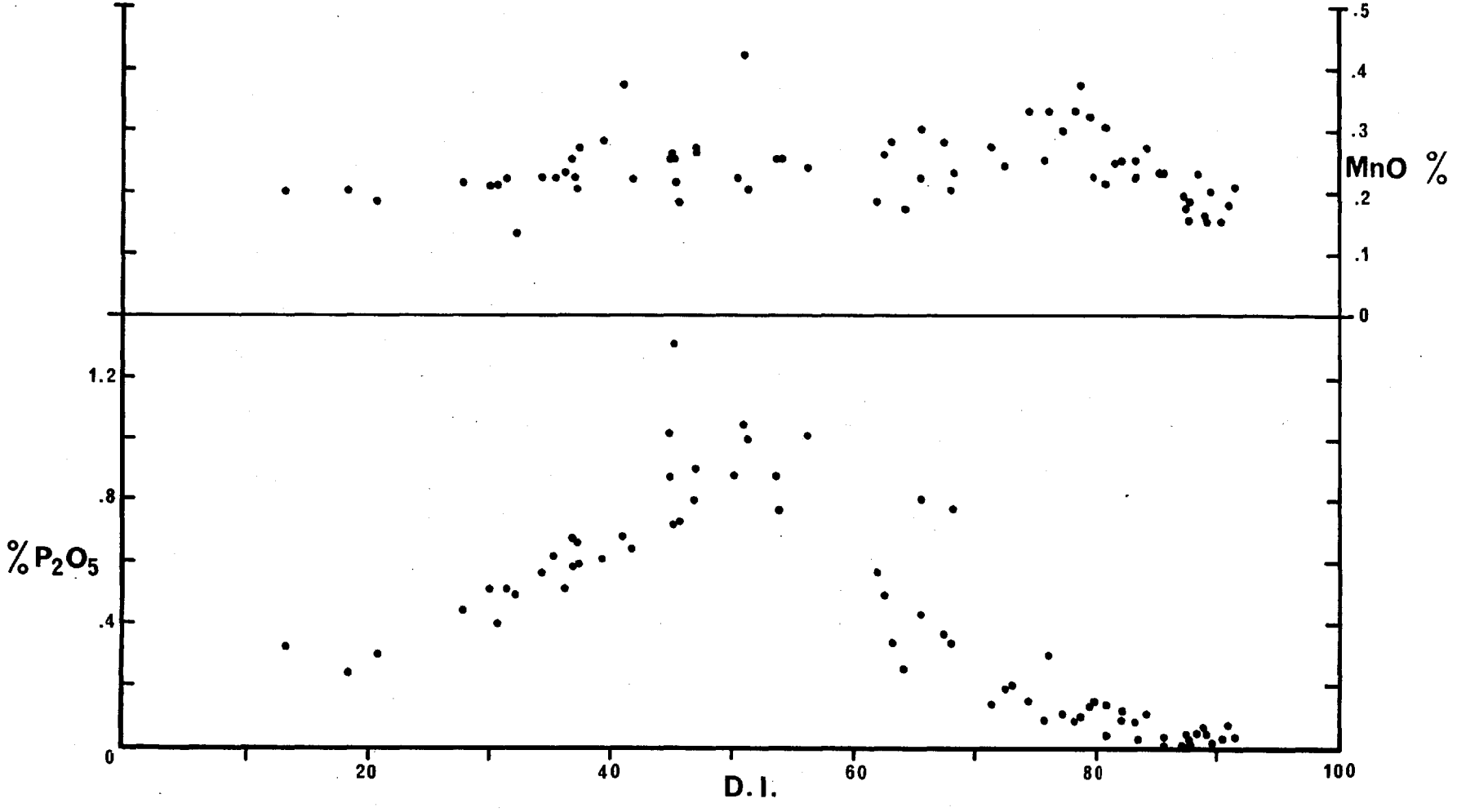

FIGURE 42

1964 (separating Hawaiian alkalic and tholeiitic fields). The proximity of the three ankaramites to this latter line merely reflects their accumulative nature. Modal nepheline first appears in rocks with D.I. > 75, but a number of intermediate and basaltic rocks plot above Saggerson and Williams' line. The more highly alkaline rocks usually plot above this line, more basic rocks below, suggesting increasing undersaturation in the late intrusives. The proximity of all points to the line demonstrates the moderate degree of undersaturation of the St. Helena rocks.

During discussions of the element variations, comparisons are made with rocks of the Tristan da Cunha group (Baker, et al, 1964), Gough Island (LeMaitre, 1962), the Polynesian and Scottish Tertiary rocks in Nockolds and Allen (1954), and the Hawaiian alkalic rocks in Nockolds and Allen (1954) and Macdonald and Katsura (1964). Other works are referenced individually.

Triangular variation diagrams are given in Figs. 31 and 32. In the FMA diagram (Fig. 32) the trend is a gentle curve towards alkali enrichment and is closely comparable to curves for other oceanic alkali volcanic series. The curve is similar to that of the Hawaiian alkalic rocks and rises closer to the FeO apex than those of Gough and Tristan reflecting higher iron values in the St. Helena intermediate rocks. The distribution in the CaO-K_2O-Na_2O diagram (Fig. 32) is only slightly curved (with slight increase in potash at the felsic end). The curve lies closer to the Na_2O apex than comparable curves for Tristan and Gough with their more potassic lavas, but compares very closely with the distribution shown by the Hawaiian alkalic rocks.

Silica (Fig. 33) shows a progressive and virtually linear increase through the series, with moderate scatter at

high values of the D.I. Alumina (Fig. 33) is very low in the accumulative rocks but increases slowly and somewhat irregularly from less porphyritic basalts to the phonolitic rocks. In the phonolites and phonolitic-trachytes the Al_2O_3 values are higher than in some other oceanic phonolites. Consequently only a few rocks have agpaicity indices (molecular Na_2O+K_2O/Al_2O_3) greater than 1.0, although the value for most of the late intrusives is 0.9 or greater.

MgO (Fig. 34) decreases continuously throughout the series, very high values coinciding with high modal olivine and diopsidic augite in the ankaramites. In the highly alkaline intrusives (D.I. = 76 and higher) MgO drops from about 0.5% to 0.2% or lower and overall is less abundant than in comparable rocks from Gough Island and the Tristan group. The low MgO accounts for the FMA curve (Fig. 31) lying closer to the FeO-alkaline sideline than the Hawaiian alkalic, Gough and Tristan curves. Total iron (Fig. 34) increases slightly from the ankaramites to a maximum at about D.I. = 30-35, after which it drops regularly to very low values in the phonolitic rocks (FeO = 3.2-4.0%).

Chromium, nickel and cobalt (Fig. 35) all decrease from high values in the ankaramites. Chromium drops very quickly to below 100 ppm in basalts, with D.I. ≈ 32, and is only detected in two rocks with D.I. > 50. High chromium values in the ankaramites and some basalts reflect the occurrence in these rocks of discrete Cr, Al, Fe spinel grains - few basalts with D.I. > 32 contain these spinels, and Cr may largely occur in early titanomagnetites. Nickel is detected in all rocks, but below about 20 ppm, in the trachyandesites, was not determined. Cobalt decreases regularly to about 25 ppm in the trachybasalts, was detected in five trachyandesites, but not in any rocks with D.I. > 70. The behaviour of these elements compares closely with that of

other volcanic areas; all three are more abundant than in the Tristan rocks, and compare more closely with the Gough, Hawaiian and Polynesian values..

Copper (Fig. 35) was detected in all rocks types including phonolites, and decreases from 90 ppm to 3 ppm. Two trachybasalts contained 310 and 220 ppm, and two trachyandesites 130 and 285 ppm - the rocks also have high Pb values (Fig. 35). Chalcopyrite has been observed in a number of basic rocks in reflected light and occurs in the same fashion as pyrite. The high Cu values for the St. Helenan rocks are therefore believed to reflect initial high copper concentration in the magma. All of the rocks containing lead (Fig. 35) are late in relation to the volcanic structure; 277, an early basalt fragment, occurs in an explosion breccia adjacent to a late phonolite dyke. The diagram has been plotted to show that Pb is not associated with late salic rocks and its unusual occurrence and high concentrations perhaps reflect hydrothermal processes.

Calcium (Fig. 36) decreases linearly from the ankaramites to the phonolitic rocks, and compares very closely with other alkali series. Strontium, (Fig. 36) increases steadily from the ankaramites to a low maximum at D.I. = 55-65, whence it decreases rapidly through the trachytes to 100 ppm in the phonolites. The enrichment in Sr in the intermediate rocks is less pronounced than in the Polynesian and Hawaiian rocks, and is similar to that of Tristan and Gough. Since Sr is likely to enter potassium-bearing minerals, and the rocks contain interstitial alklai-feldspar, then Sr is unlikely to show marked enrichment in derivatives. The sudden decrease in Sr content in the trachyandesites corresponds to the appearance of increasingly dominant alkali feldspar phenocrysts. The Sr values are lower than for Tristan and Gough in the Atlantic and the Hawaiian and

Polynesian alkali series and agree more closely with values from the Scottish Tertiary province.

Soda and potash (Fig. 37) increase steadily through the series, potassium at a slightly greater rate (Fig. 38). There is quite considerable scatter in the Na_2O figures and Na_2O : K_2O ratio at the phonolitic end of the series but there is no regular separation into rock types as in the Gough Island trachytes.

Rubidium (Fig. 39) is below the limits of detection in many of the basalts, but overall shows an increase through the series. Rb is highest in the rocks with greatest nepheline content, which although high in K_2O are not the rocks richest in potash. Barium gradually increases into the trachytes and phonolitic-trachytes (D.I. - 80-85), and suddenly decreases to very low values in certain phonolites. This type of distribution seems typical of other alkali volcanics (except the Polynesian alkali basalt - phonolite series). Barium, with its large ionic radius, will substitute for K in the alkali feldspar and consequently will show a gradual increase until the alkali feldspar is sufficiently dominant to remove most of it, leaving the final liquids greatly impoverished in Ba.

Titania (Fig. 40) is overall similar in its behaviour to iron (Fig. 41), increasing from the ankaramites and porphyritic basalts to a maximum at D.I. = 35-40. From here TiO_2 decreases linearly to D.I. = 65 and then levels off with very low concentrations in the phonolitic rocks. Titania is lower in the St. Helenan felsic rocks than in comparable rocks from other Atlantic islands.

The increase in TiO_2 and FeO in the highly porphyritic basalts reflects their probable accumulative origin, and does not reflect early enrichment. Early crystallizing

Mg-rich olivines and pyroxenes prevent the percentage of iron reaching an equivalent value to that in the fine-grained basalts (cf. the FMA diagram, Fig. 31). Similarly Ti does not appear to be taken into the early pyroxenes to any appreciable degree - it appears in the late titanaugite rim to the phenocrysts, having crystallized directly from the liquid.

Zirconium (Fig. 40) shows a gradual increase through the series with very marked enrichment in late rocks with D.I. = >85. The final Zr concentrations are higher than for other rock series quoted in Nockolds and Allen (1954), and for Gough and Tristan.

Manganese (Fig. 42) shows little positive variation, but at the felsic end (D.I. = 75-80) MnO is slightly higher, and in extreme rocks (D.I. >85) slightly lower than for other rocks in the series. (Hydrothermal manganese deposits in the east of the island are associated with flows with D.I. = 65-73.)

Phosphorous (Fig. 42) shows a more or less regular increase from ankaramites to a maximum at D.I. = 45-55, and then a progressive decrease to trace amounts in the phonolitic rocks. Trachybasalts and trachyandesites carry more modal apatite than the other rock types. High phosphorous in trachybasalts is also seen in rocks from Tristan, and to a lesser extent Gough Island (LeMaitre, Table 10, 1962; Baker, et al, Table 6, 1964). High P_2O_5 in Etnaean lavas is restricted to olivine trachyandesites (Klerkx, 1966) from a major parasitic centre; on St. Helena the high P_2O_5 is not directly related to parasitic activity.

Niobium (Fig. 40) has a distribution curve and concentration similar to those of the Tristan rocks. The rise in Nb content from below the limit of detection in many

basalts to a value of 200 ppm in some phonolitic trachytes is gradual, and the scatter probably reflects defects in the X-ray sensitivity (especially with Zr interference in intermediate and felsic rocks).

The distribution of yttrium is variable; there is an increase in abundance in the felsic rocks, but scatter is very large. Values at the felsic end appear to be overall higher than for comparable rocks from Gough and Tristan.

4. Compositional variation of volcanic products with time.

In the older north-eastern volcano virtually all of the rocks are basaltic or trachybasaltic. Only one trachyandesite dyke and one trachytic fragment (in a mixed breccia) were seen; the almost complete absence of these rock types is believed to be real. Only five analyses of rocks from the north-eastern volcano were made and only general observations can be made. Although ankaramitic dykes are not uncommon, their equivalent flows are rare; specimen 804 is from a small intrusion. Porphyritic pyroxene-olivine basalts are abundant, and feldsparphyric porphyritic flows are restricted to this volcano. In the upper 300m of the succession there is a gradual decrease in the amount of phenocrystal pyroxene and olivine, and in the top 75-100m fine-grained trachybasaltic flows are common (D.I. approx. = 50). The later intrusions on Bunker's Hill are both trachybasaltic. Overall a progressive increase in total alkalis of the lavas is more pronounced in the north-eastern volcano than in the south-west.

The differentiation indices of rocks of known stratigraphic position in the south-western volcano have been plotted in Fig. 43. There is considerable variation with time, and field relationships show that the variation

FIGURE 43:

Stratigraphic plot of volcanic products against differentiation index, for the south-western volcano.

ta: Thick trachyandesite flows of Gill Point and inland (?) equivalent. The thick trachyandesite of Headowain would be of comparable age (certainly before 737).

Lb: Lower basalts of the Upper Shield.

Ta: Upper trachyandesites.

Specimen 706 is probably a young flow as it is in the only basaltic flow of its age in Rupert's Valley.

EF: East flank products.

ST: Stone Tops trachytes

Basaltic group (east of Bencoolen) would plot between 613 and ST.

LI: Late highly alkaline intrusive rocks.

664: White Hill trachyandesite flow.

323: Tripe Bay intrusive trachyandesite.

438: High Knoll trachybasalt.

In the Main Shield, specimen 161 may be of local origin, and its exact relationship to 226 is uncertain.

Basalts are common in the younger parts of the Lower shield and the plotted data should not be taken to suggest a transitional increase in differentiation index.

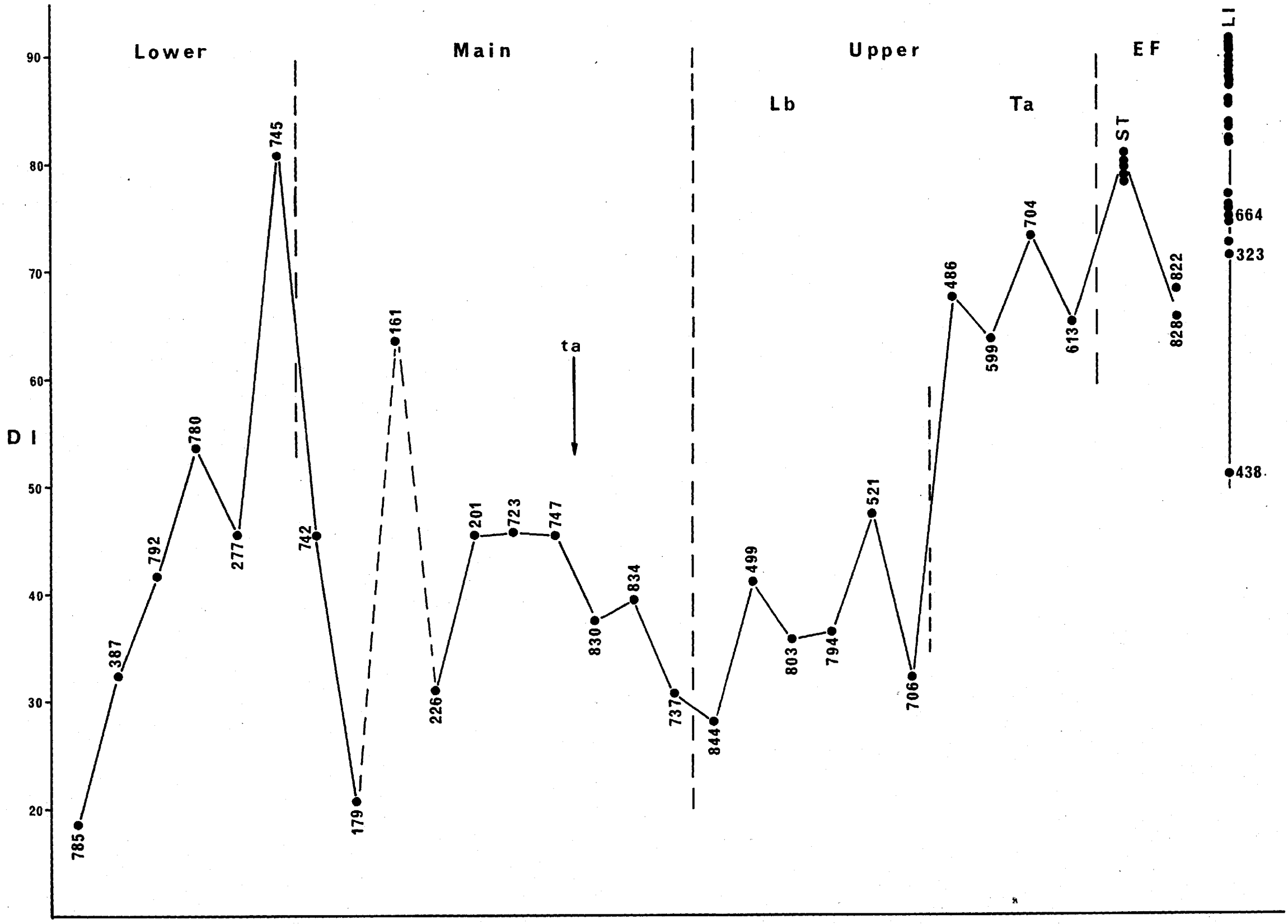
Lower
Main
Upper
EF
Lb
Ta
ST
LI
ta
DI
90
80
70
60
50
40
30
20
785
387
792
780
277
745
742
179
161
226
201
723
747
830
834
737
844
499
803
794
521
706
486
599
704
613
822
828
664
323
438

FIGURE 43

is even greater (for example, none of the main shield series trachyandesites have been analyzed). Individual groups of flows in the lower shield, and to a lesser extent in the main shield, show an upward decrease in percentage of phenocrystal pyroxenes and olivine - definite cycles with ankaramites or porphyritic basalts as early units certainly occur. In the lower and main shields there is no overall progressive variation towards increasing alkalinity. In the upper shield there is a very marked division between the lower basalts and late trachyandesites (Fig. 43). The highly alkaline condition of the lavas is broken by one group of basalts (i.e. older than the eastern flank trachytes and trachyandesites) but the bulk of the extrusives of this late age have differentiation indices greater than 65.

Extrusives forming the two shields show little or no increase in degree of undersaturation with time - basalts of any age contain comparable precentages of normative nepheline. Certain rocks of the late intrusive group however, display a marked increase in their degree of undersaturation. The significance of these variations in degree of undersaturation will be discussed in Section VIII.

5. Compositional variation of the minor intrusions.

The highly alkaline dykes and parasitic intrusions of the central and flank regions of the south-western volcano post-date all major extrusive activity (Fig. 14). Compositionally these rocks exhibit a progressive variation outwards from a central area (around and north-east of Man o' War Roost). In the central areas the intrusives are phonolites and outwards become decreasingly alkaline passing through phonolitic-trachytes and trachytes. Trachyandesitic and trachybasaltic intrusions (± associated flows) on the flanks may be related to this intrusive episode (Section III,

6). The outward progressive variation in major oxide chemistry, especially total alkalis (Fig. 44), and mineralogy has been discussed (Baker, in press). Study of trace elements in these intrusions (Table 13) confirms this progressive outward variation in degree of differentiation. Zirconium and rubidium show high values in the central area with a progressive outward decrease. Strontium is undetected in the very centre (281, 403), increase slowly to the 12% total alkalis line and then decreases rapidly through the trachytes (250-600 ppm). Barium is also low in the centre and passes outwards through a maximum, decreasing in the trachytes. With trace elements the variations are more irregular because of the lower degree of precision in their determinations.

Of particular relevance to this overall chemical variation is the variation shown by specimens from the large Riding Stones Hill intrusion. Analyses 421 (base of roof cavity), 452 (top of roof cavity) and 415 ("ring dyke" of Chapel Rock, see Fig. 44) display considerable variations in both major oxides and trace elements (Table 11). The compositional values of the dyke are intermediate to the values of the base and top of the cavity, and more closely in keeping with the element variation of the intrusive rocks as a whole than are the values for 452 and 421.

An origin for these compositional variations is proposed in Section VIII.

6. Volume considerations and the intermediate rocks.

A great deal of controversy has followed the statement by Chayes (1963a) that in oceanic environments intermediate lavas are less abundant than end members of the series (ie. basalt and trachytes, rhyolites or phonolites). In his concluding remarks he suggested that a problem as

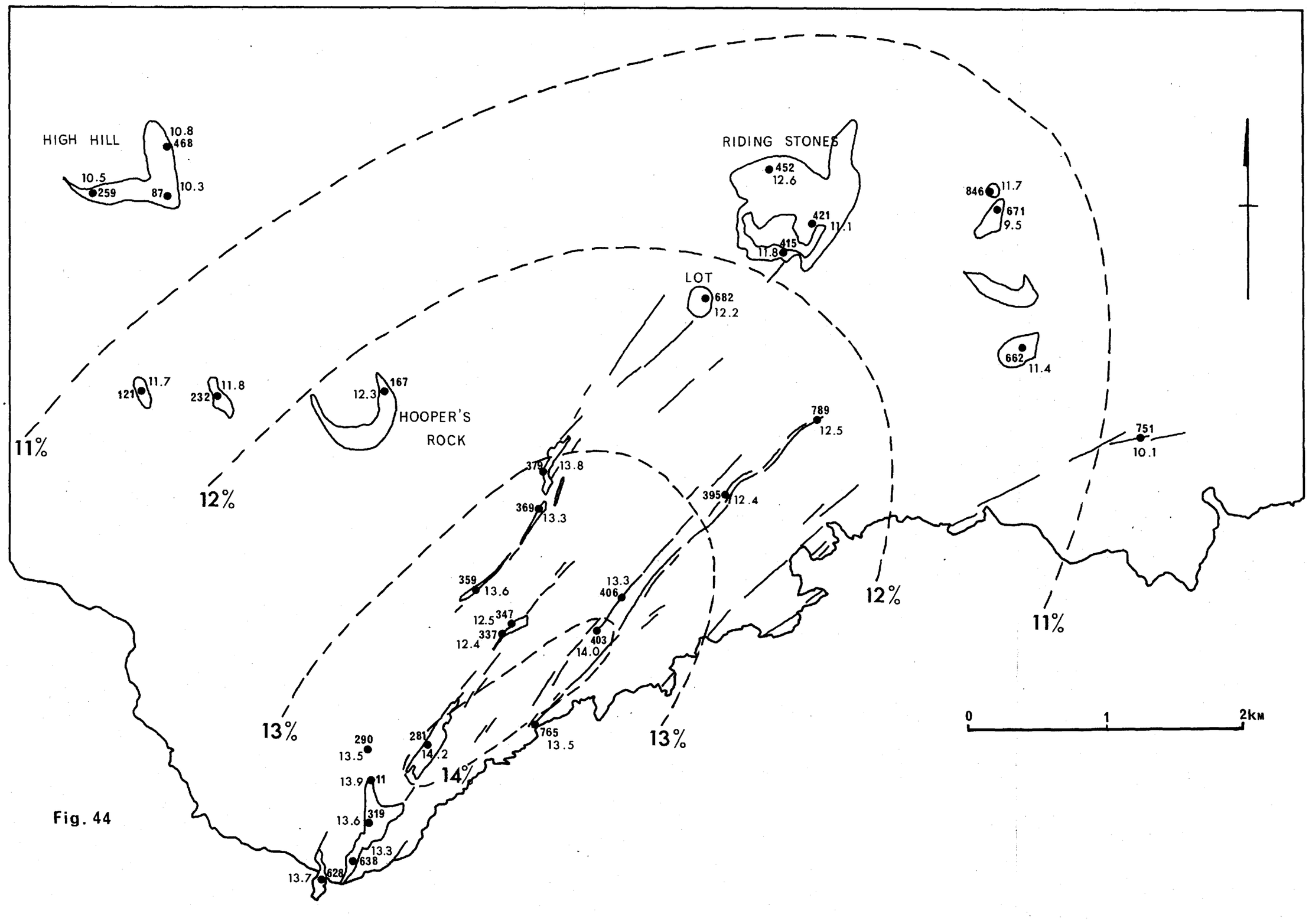
HIGH HILL
10.8
468
10.5
259
87
10.3
RIDING STONES
452
12.6
421
11.1
415
11.8
846
11.7
671
9.5
LOT
682
12.2
662
11.4
121
11.7
232
11.8
12.3
167
HOOPER'S
ROCK
789
12.5
751
10.1
379
13.8
395
12.4
369
13.3
359
13.6
13.3
406
12.5
347
337
12.4
403
14.0
11%
12%
13%
14%
290
13.5
281
14.2
765
13.5
13.9
11
13.6
319
13.3
638
13.7
628
0
1
2KM

Fig. 44

Specimen number	D.I.	Normative ne	Total alkalis	Zr	Rb	Sr	Ba
281	89.6	16.5	14.2	1450	210	-	150
403	85.6	12.1	14.0	1315	190	-	300
319	91.5	13.0	13.6	1385	220	50	225
11	91.0	15.2	13.9	1085	220	85	1100
628	87.7	8.3	13.7	1200	130	50	870
379	87.5	12.4	13.8	1150	180	50	545
167	89.1	2.4	12.3	1120	160	85	1120
682	87.8	3.9	12.2	1300	150	-	360
395	88.4	4.4	12.4	1230	110	85	610
121	87.4	-	11.7	1335	165	80	930
232	84.1	5.0	11.8	840	95	140	1700
415	85.4	2.3	11.8	985	125	155	1400
421	82.3	0.4	11.1	930	125	240	1340
452	89.2	5.6	12.6	1200	135	50	680
846	83.4	5.6	11.7	800	105	240	1375
671	71.4	-	9.5	620	70	410	1180
662	82.0	4.0	11.4	820	95	140	1600
259	76.1	4.0	10.5	515	70	670	1230
87	74.4	4.9	10.3	545	120	515	1000
468	77.3	5.5	10.8	735	100	465	1280
751	75.8	-	10.1	760	70	300	1100
323	72.6	1.2	9.7	530	80	475	1080
438	51.0	0.3	6.7	335	80	570	550
85	56.3	1.6	7.5	375	60	615	650

TABLE 13

important as this should warrant programmes of more careful sampling (op. cit. p1532). In reply to Chayes, Macdonald (1963) summarized volume relations of the rocks forming the alkali caps (constituting about 1% of the volcano volume) in the Hawaiian volcanoes. These volumes were: alkali basalt + ankaramite = 41% + 1.7%; hawaiite + mugearite = 56.5%; trachyte + rhyodacite = 1.1%. Hawaiites and mugearites approaching basalts were far more abundant than those approaching trachyte. Harris (1963), discussing relationships of the rock types from the Tristan group, stressed the possibility of collecting and analytical biases and demonstrated that this would at least modify peak heights, and could turn a minor abnormality into a major (apparent) abnormality. He also showed that the degree of erosion of the volcano can influence the proportions of exposed rocks (op. cit. p5104-5), especially in terms of minor parasitic intrusions; i.e. the volume of intrusive trachytes could exceed that of trachyandesites and basalts in similar modes of occurrence, and the volume of trachytic intrusives may increase in deeply eroded central parts of the volcano. Harris concludes: "Only if an island has been subjected to a thorough field study and detailed mapping is the ratio of trachyandesite to trachyte in the specimens collected there likely to represent their relative areal abundance." (p5106, 1963).

Chayes' (1963b) objection to these data is that in Hawaii they are from an island group extraordinarily poor in trachytes, and in the case of Tristan they are from islands "in which trachyandesite is apparently unusually abundant" i.e. in carefully sampled islands the distributions disagree with his hypothesis and are therefore anomalous. He adds (op. cit. p5109): "It is now clear beyond cavil that the published analyses of salic oceanic lavas are far more

numerous than published analyses of oceanic lavas of trachy-andesitic composition. The obvious interpretation is that on the oceanic islands lavas of the first type are far more abundant than those of the second."

In his conclusions above, Harris mentioned "areal abundance", and in the compilation of the Tristan rock type relations (Baker, et al, p493, 1964) the authors suggest that caution should be exercised in study of the histogram because of this non-volumetric bias. In the light of the above discussion it is appropriate to study the abundances of the rock groups on St. Helena. The island has been mapped in detail, and because of the deep erosion virtually all of its subaerial products are exposed. However, the study of volume relations may be further complicated because of the erosional state of the island, and the degree of erosion at the varying stages of its growth. Early material may be eroded or may be protected from erosion by a cover of later rocks, potentially of different composition - attempts to overcome these factors are made.

Intermediate rock types occur on St. Helena, and are quite common in spite of Daly's statement: "Not far from ninety-nine per cent of the volume of visible Saint Helena is of femic, basaltic nature. The remainder is almost entirely salic, phonolitic.....lavas intermediate in composition between basaltic and highly salic types are exceedingly rare, if not quite absent" (p62, 1927). The trachyandesites (within the tight limits of Chayes' 'Daly gap') are recognizable in the field, and may be mapped as such, in only rare cases do they resemble certain trachytes (Section V). Trachybasalts may be readily discernible, never resemble trachyandesites, but frequently are indistinguishable from basalts. Classification of rock types is given in Section V , and both field and chemical data have been used

to compile the various percentages presented in Table 14. The various methods of compilation have been selected because they may be or have been used in a 'systematic' study of a volcanic region.

i. Grid system.

Using grids of 1000 and 500 yards (War Office map is subdivided at 1000 yard intervals) the rock type at each intersection was recorded. The trachybasaltic figures are certainly too low because of the uncertainty of distinguishing them from basalts in the field.

ii. Areal distribution.

Areas of rock types exposed are listed; again trachybasalts are under-counted.

In methods i and ii the percentages are modified by the occurrence of the late trachyandesite flows which cover an area of about 16km^2 (island approx. 120km^2).

iii. Volume analysis.

The sub-aerial volume has been estimated at approximately 60km^3 and existing distribution of rock types are estimated in Table 14 (3a). A figure of 80km^3 was used for the estimated original volume of the sub-aerially extruded material; this is almost certainly low (perhaps by as much as 30%) but an error of this nature will not modify Table 14 line 3b, except to reduce trachyandesites and phonolites by about $\frac{1}{5}$ (line 3c).

Trachybasalts occur as several small intrusions, one major group of flows (Old Joan centre) and numerous flows in the 'basaltic' groups in the upper levels of the main shield series and the north-eastern volcano. Some flows are recognizable in the field (by their purple sheen) and the proportion of these and the distribution throughout the pile

	Basalt	Trachybasalt	Trachyandesite	Trachyte + phonolite
1a	115 77.7%	7 4.7%	22 14.9%	4 2.7%
1b	441 75.4%	36 6.2%	96 16.4%	12 2.0%
2	11921 83.0%	332 2.3%	1906 13.3%	198 1.4%
3a	58.2 96.9%[2]		1.41 2.3%	0.5 0.8%
3b	~76 ~95%[3]		~3.2 ~4%	~0.75 ~1%
3c	~96.3%		~3%	~0.7%
4	216 28.7%	104 13.8%	134 17.7%	303 39.8%
5	16 22.2%	15 20.8%	13 18.1%	28 38.9%

Footnotes 1-3 explained in text.

KEY:

1a: Grid count. Rock types occurring at intersections of square grid at 1000 yard intervals.

1b: Ditto at 500 yard intervals.

2: Areal distribution of rock types in units $x10^4$ yds^2.

3a: Volume relationships assuming $60km^3$ volume of existing sub-aerial island.

3b: Ditto assuming $80km^3$ volume of island without erosion.

3c: Ditto assuming $100km^3$ volume without erosion.

4: Rock types in field collection.

5: Rock types analyzed chemically.

TABLE 14

of the analyzed types suggests that a volume of not less than $8km^3$ (i.e. greater than 10% of the total extruded products) is made up of trachybasaltic rocks. However, a value of more than 25% of the total volume would certainly be too high.

Explanation of footnotes in Table 14.

1. The Gill point trachyandesite flow, if continuous to Rock Rose (Section III, 3a) has a volume of approximately $0.7km^3$ (1.2% total volume of the island) or $0.8-0.9km^3$ allowing for marine erosion.

2. The trachybasalts from the Old Joan Hill centre have a volume of approximately $0.8km^3$ (1.3% total) or allowing for erosion approximately $1.0km^3$.

3. The Man o' War ankaramites (Section III,2c) had an estimated volume of approximately $3.5km^3$ (4.3% of the total estimated sub-aerial products).

In volume considerations then, figures of: basalts = 75-85%; trachybasalts = 20-10%; trachyandesites = 4%; and trachytes + phonolites = 1%, are believed to be close approximations for the total sub-aerial volcanic products.

Within the central 'feeder' area of the south-western volcano (Sandy Bay), dyke counts based on thicknesses and not volumes gave:

basalts + trachybasalts	= 91%
trachyandesites	= 6%
phonolites + trachytes	= 3%

Again the descending order is obvious with basaltic rocks greatly predominant and trachyandesites more abundant than the salic rocks. These late salic dykes are only developed

in the Sandy Bay area and 3% is in fact anomalously high. If figures for rock types collected and rock types analyzed are considered the percentages are greatly modified (Table 14, lines 4 and 5). The salic rocks were highly overcollected because of the interest in these late products.

A final bias to collecting and analysis is concerned with the occurrence of parasitic intrusions. Intrusions tend to be less prone to erosion than the surrounding rocks; trachytes and phonolites on many islands occur largely as minor intrusions, and small intrusions are always of great interest to a field geologist - a break from the regularity of the monotonously dipping flank lavas. The intrusions on St. Helena, none of which was coarser-grained than the equivalent extrusives, break down as follows:

	Parasitic	Minor (irregular)	Total	%
Basalt	-	3	3	9
Trachybasalt	3	2	5	16
Trachyandesite	4	3	7	22
Trachyte + Phonolite	14	3	17	53

The order is completely reversed, and should also be compared with the dyke percentages given above.

Plotting histograms of the major oxides, differentiation index, or any other parameter of the analyses of the St. Helena rocks will give an apparent bimodal distribution. A study of the chemistry, petrography and volume relations of the rock types shows a gradation from ankaramites to phonolites. Similarly LeMaitre (1962) and Baker, et al (1964) writing on Gough and Tristan stress the gradational and continuous variation from basaltic to salic

ends of their series. Chayes (1963b) requires that petrologists accept his "bimodal distribution" of oceanic rock types and start to rethink their hypotheses of petrogenesis. Where petrologists, and much more significantly, petrologists who are field geologists, who have collected their rocks and know the occurrence of the rock types, in careful study of volcanic islands find no central minimum in distribution, then it is Chayes who must reconsider his theories.

Analyses from a number of oceanic alkali rock series do show minor 'gaps' in intermediate positions (see Figs. 33-42, D.I. = 56-62). The significance of these may become apparent as (even a few) more islands are studied in detail. Until more definite relationships between these types and their associates are established by field and laboratory studies, there appears no reason to abolish theories of crystal fractionation as Chayes (1963a and b) has proposed; even on existing data there is reason to treat the 'Daly gap' with less awe than Chayes woud have us do.

SECTION VIII

PETROGENESIS

1. Introduction.

In this section various aspects of the petrology of St. Helena volcanic rocks are considered. Initially the origin of petrological variations of the exposed rocks is considered, and particular attention is focussed on the late highly alkaline intrusives. Secondly, some views on the origin of the xenoliths are put forward. Finally, the origin of the St. Helena parental magma is considered, and the petrochemical features of the island are compared with those of other islands in the South Atlantic, and a mechanism which could produce the observed variations between them is suggested.

2. Differentiation.

There is no evidence to suggest that St. Helena is anything but truly oceanic in its structure and origin, and the genesis of its rocks can be considered as unaffected by any process of sialic contamination. Several lines of evidence strongly support the view that rocks exposed on St. Helena were derived from an alkali olivine basalt parent magma by a process of crystal differentiation.

a. Mineralogical and chemical evidence.

In thin section even the most basic rocks contain alkali feldspar, occurring either interstitially or as late crystallizing patches petrographically approaching trachyte. Wilkinson (1966) showed that the interstitial glass of an alkali olivine basalt was comparable to a trachyte

in composition. He remarked on the contrasting chemistries of the host rock and its interstitial glass, but pointed out that rocks of intermediate composition were also known as differentiates in mildly alkaline intrusions (op. cit. p858). The apparently continuous zoning in the constituent minerals of the St. Helena basalts and trachybasalts, suggests that successive liquids remaining in a crystallizing flow unit may in fact pass through compositions equivalent to that of intermediate rocks.

There is a progressive compositional variation in constituent minerals from ankaramites to phonolites (Section VI). Progressive chemical variations of the rocks are shown in Figs. 30-42, and the variation in normative feldspar composition is shown in Fig. 45, where early crystallizing calcic plagioclase becomes increasingly sodic, with the orthoclase content increasing throughout the series.

The salic constituents of the trachytic and phonolitic rocks have been recalculated in terms of $NaAlSiO_4$, $KAlSiO_4$, SiO_2, and plotted in 'petrogeny's "residua" system' (Bowen, 1937), with data for the system (P_{H_2O} = 1000 kg/cm^2) taken from Hamilton and Mackenzie (1965) (see Fig. 46). The rocks plot as a group in the low temperature part of the system below the alkali feldspar join. The more undersaturated rocks plot closer to the phonolite minimum than do the trachytes, suggesting a derivation of the phonolitic rocks from the trachytes with their higher temperatures of crystallization. At pressures of water less than 1000 kg/cm^2 the nepheline-feldspar field boundary should move towards the feldspar join (Hamilton and Mackenzie, p228, 1965). If P_{H_2O} was less than 1000 kg/cm^2 for the St. Helena volcanic rocks, the most undersaturated rocks (281, 11, 319) would fall even closer to the phonolite minimum than shown in Fig. 46.

FIGURE 45:

Plot of normative feldspars of the analyzed St. Helenan rocks (S-S).

The trend is closely comparable with those of the Hawaiian alkali rocks, ha-ha (Macdonald and Katsura, 1964), and the Hebridean alkali rocks, he-he, taken from Tilley and Muir (1964). The Gough Island trend, G-G (LeMaitre, 1962), although 'parallel', reflects the potassic nature of rocks from this island.

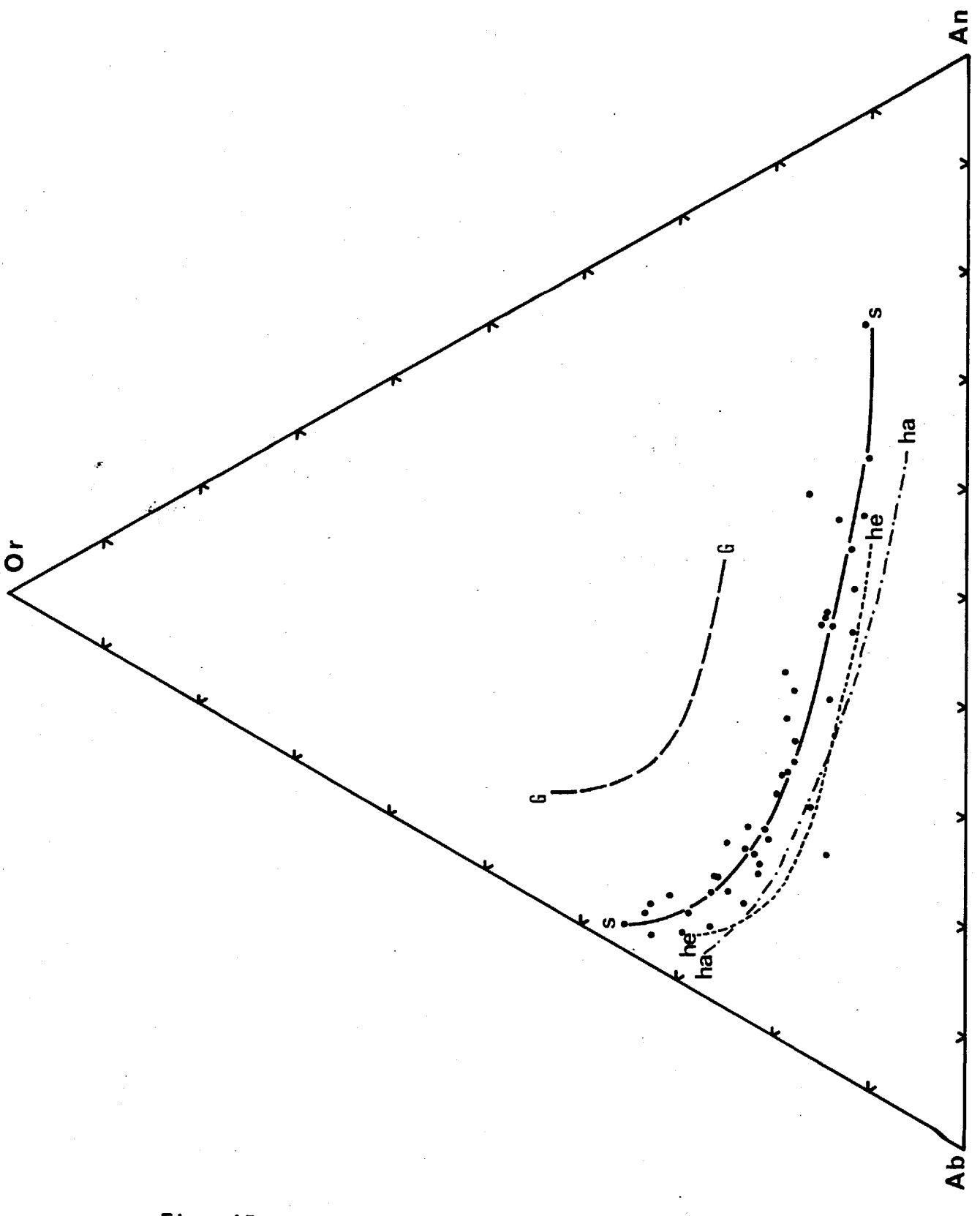

Fig. 45

FIGURE 46:

The St. Helena salic rocks (normative ne + or + ab $>$ 80%; except 87, 259, 468, 108, 109, 111, 831, 751 with D.I. = 74-80) plotted in the system SiO_2 - $NaAlSiO_4$ - $KAlSiO_4$, with data at P_{H_2O} = 1000 kg/cm^2 taken from Hamilton and MacKenzie (1965). Inset is a larger scale (x2) plot showing the specimen numbers.

m = alkali feldspar minimum.

M = $NaAlSi_3O_8$ - $KAlSi_3O_8$ - $NaAlSiO_4$ - $KAlSiO_4$ temperature minimum.

Note grouping of Stone Tops trachytes (108, 109, 111, 824, 831), early trachytes (745, 763), and the High Hill trachyte (87, 259, 468) and one dyke (751) of the late intrusive phase on the sodic side of the thermal valley.

The phonolitic-trachytes and phonolites of the late intrusives plot in, or just on the potassic side of the thermal valley. Note that of the Riding Stones specimens, 452 (top of cavity infilling) plots at lower temperature than the others (415, 421).

Specimen 121 is altered, its position largely reflecting its high silica value.

P_{H_2O} = 1000 kg/cm^3

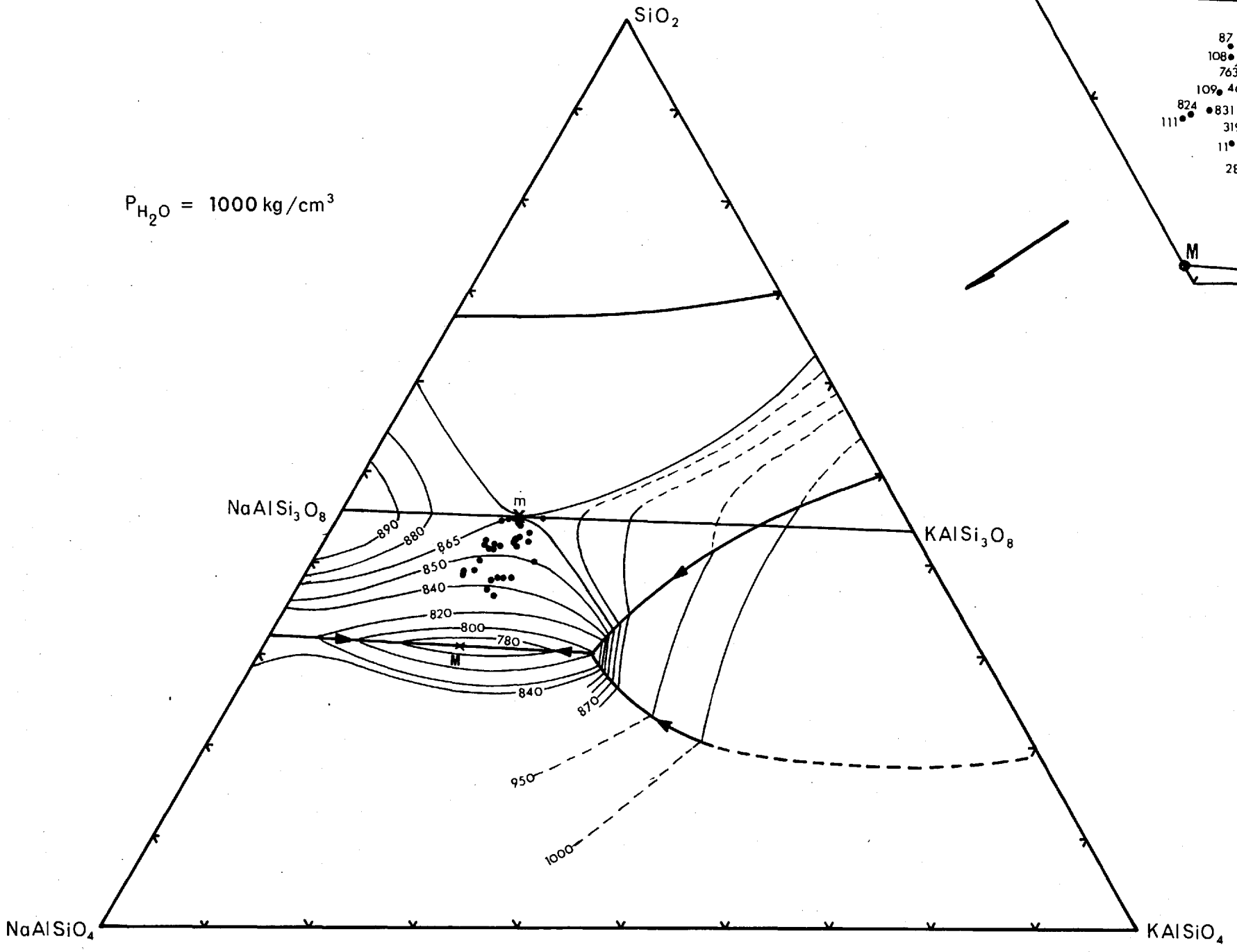

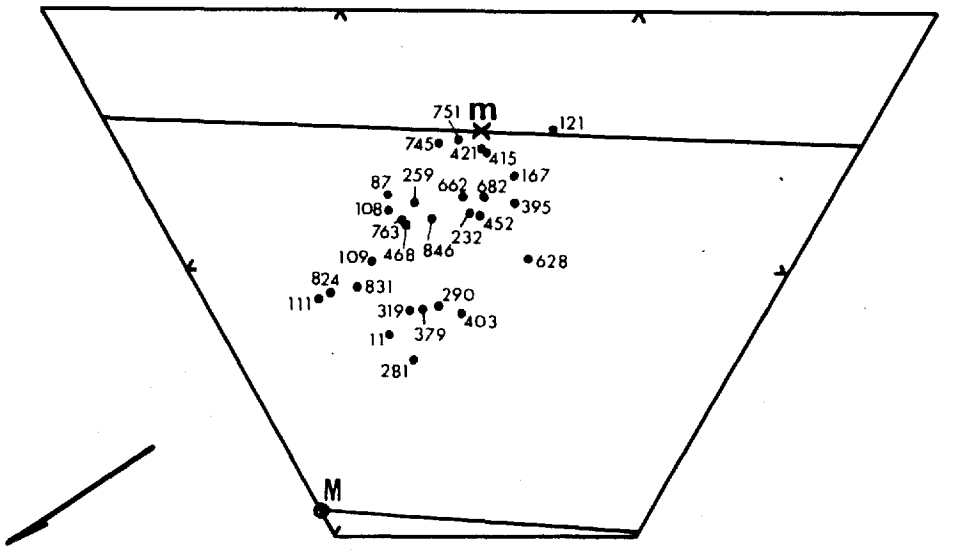

WEIGHT %

FIG. 46

The most undersaturated rocks, although not themselves potassic, fall in, or just on the potassic side of, the low temperature trough. These rocks contain normative acmite (with a trace of ns in 403) and the removal of soda from the system for inclusion into the pyroxene could probably explain this apparently slightly anomalous distribution. The rocks which plot on the sodic side of the thermal valley are the Stones Tops trachytes (108, 109, 111, 824, 831), two early trachytes (745, 763), the High Hill intrusion on (87, 259, 468) and one dyke (751). The High Hill trachytes, 745 and 751 have normative salic constituents $< 80\%$, and those of the Stone Tops lie between 78-80%; inclusion of these within the system is not strictly valid and is likely to lead to some distortion. Rocks of High Hill and Stone Tops contain analcite and zeolites producing the high Na_2O : K_2O ratios which may account for their distortion on the sodic side. The distribution of these trachytes and the late phonolites can therefore be explained by the above points, and does not require the late differentiates to cross the thermal valley.

Variations shown by the rocks of the Riding Stones Hill intrusion offer further evidence for differentiation of the late phonolitic-trachytes. The analyses (Table 11) of 452 from the top of the roof-infilling and 421 from the bottom are believed to reflect minor in-situ differentiation of the originally intruded magma, the composition of which is given by analysis 421 (from the feeder 'ring' dyke). A process allowing slight settling of more basic constituents and rise of alkali constituents (possibly aided in this intrusion by volatile transfer - see Section IV) could produce the contrasting chemistries (compare also Figs. 46 and 48).

A final point in favour of derivation of the late highly alkaline rocks by a process of crystal differentiation is found in the volume considerations of the different rock

types. This problem was discussed in Section VII where the volumes of the different rock types exposed above sea level were estimated at: basalts = 75%-85%; trachybasalts = 10%-20%; trachyandesites = 4%; and trachytes and phonolites = 1%.

These figures are fully in keeping with a theory of derivation of successively smaller volumes of increasingly differentiated rocks from more basic 'parents'.

b. Role of oxygen pressure.

The path followed by a liquid crystallizing within the system MgO - FeO - Fe_2O_3 - SiO_2, depends upon whether the conditions are of constant total composition or of constant partial pressure of oxygen (Osborn, 1959). The paths are shown in Fig. 47b and compared with those of Skaergaard, the Cascades, and the Thingmuli tholeiitic trend (from Carmichael, 1964). The trend for the St. Helena rocks (Fig. 47a) is approximately linear, although the scatter is quite high. The rocks with total iron : total iron + magnesia less than 0.65 are accumulative and their low ratio reflects the influence of Mg-rich pyroxenes and olivines; these points were not included when fitting the trend line. The trend approximates to a curve of fractional crystallization under conditions of nearly constant Po_2. The position and slope of the curve compared to the curves for the synthetic system are in keeping with conditions of low Po_2 (Osborn, 1959) possibly increasing slightly at the salic end. This overall slight increase may be confirmed by comparing the Fe_2O_3 : FeO ratios of the various rock types from St. Helena (Fe_2O_3/FeO : basalts approx. 0.2, trachytes 0.8-1.0, and phonolites 1.2-2.0).

The occurrence in the St. Helena rocks of titanomagnetite with only very rare ilmenite is in keeping with low

FIGURE 47:

a: Ratio $FeO + Fe_2O_3/FeO + Fe_2O_3 + MgO$ against silica for the St. Helena rocks. Specimens 679, 737, 844, 179, 785, 804 are ankaramites and porphyritic pyroxene-olivine basalts of accumulative origin.

b: Similarly plotted for comparison: a, b, c: synthetic liquids from the system $MgO - FeO - Fe_2O_3 - SiO_2$ (Osborn, 1959), c = constant total composition, b = constant partial pressure of oxygen, a = higher constant partial pressure of oxygen.

Sk-Sk = Skaergaard trend.
T-T = Thingmuli trend
C-C = Cascade trend

All data taken from Carmichael (1964).

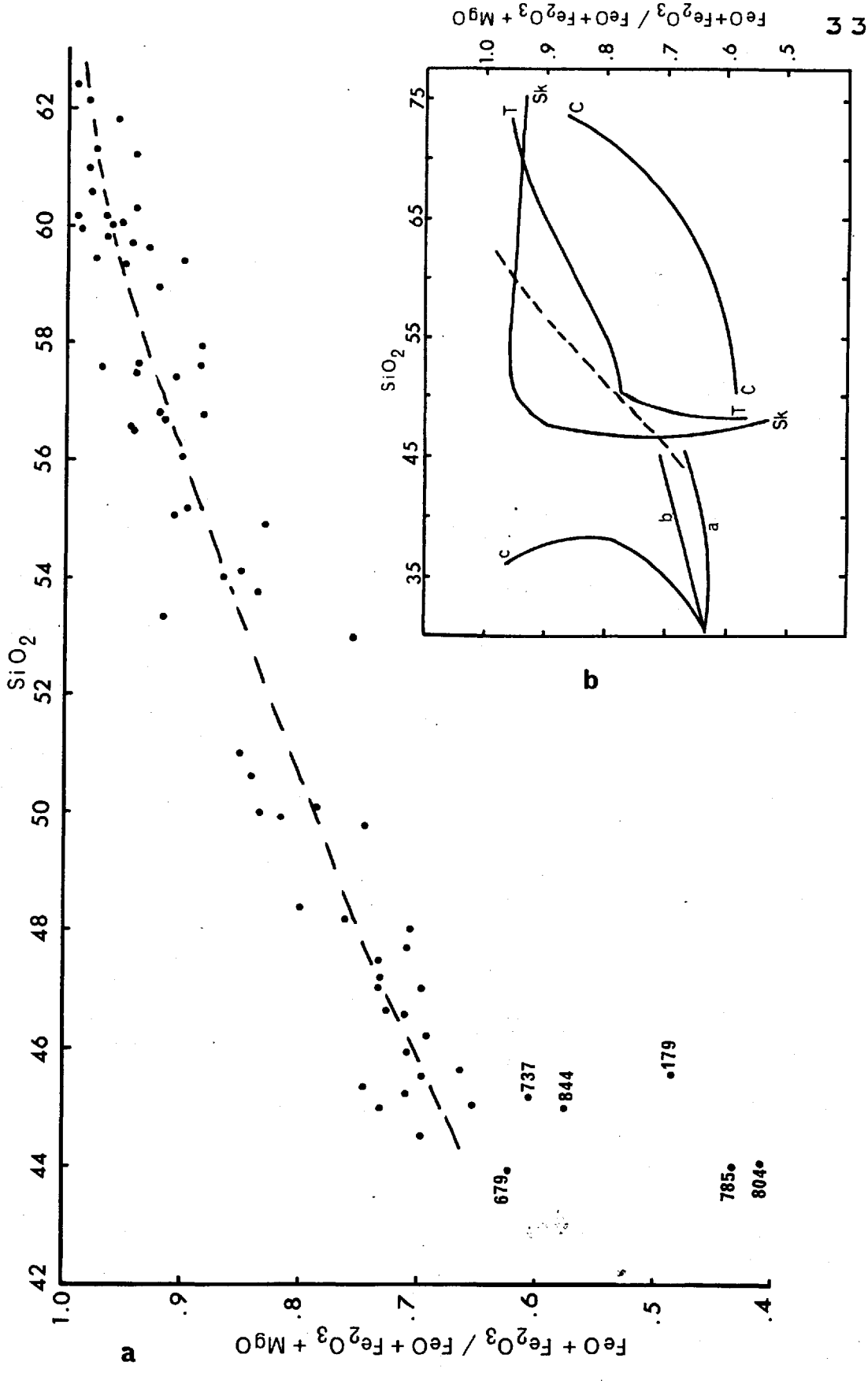
SiO2
42
44
46
48
50
52
54
56
58
60
62
1.0
.9
.8
.7
.6
.5
.4
FeO + Fe2O3 / FeO + Fe2O3 + MgO
a
679
737
844
179
785
804
SiO2
35
45
55
65
75
1.0
.9
.8
.7
.6
.5
FeO+Fe2O3 / FeO+Fe2O3 + MgO
T
Sk
C
T
C
Sk
c
b
a
b

Fig. 47

partial pressures of oxygen (Lindsley, 1963).

c. Composition of the parental basalt.

Study of Figs. 30-42 shows that the variations of all major and a number of minor elements are regular from a point with D.I. approximately equal to 30. Fine-grained basalts with this differentiation index are believed to be parental to the St. Helena alkali rocks. Rocks with differentiation indices less than 30 are believed to be accumulative and show correspondingly high values of MgO, CaO, Ni, Cr, Cu, Co, relatively low FeO and TiO_2, and low K_2O and Al_2O_3. Petrographically they are characterized by high contents of phenocrystal pyroxene and olivine, and their origins may be compared with, for example, the picritic rocks of Kilauea (Murata and Richter, 1966). These authors interpret the chemical variations of the 1959 basalts as dominantly dependent on settling of olivine through the magma. Groups of flows in the south-western volcano of St. Helena were described (Section VII, 4) in which the lowest flows contained a high percentage of modal pyroxene + olivine and later members were fine-grained, lacked phenocrysts and chemically had higher differention indices.

Fine-grained basalts with D.I. = 30-40 are very abundant on St. Helena. Rocks of this type have been averaged in groups (D.I. = 30-35, D.I. = 35-40, and D.I. = 30-40) and are presented, with their norms in Table 15. The average may be compared with individual analyses (Table 7) of known stratigraphic position (Fig. 43), and it is obvious that basalts comparable to the average nepheline normative (approx. 4%) basalt have been produced by both volcanoes at varying intervals throughout large parts of their histories. Intermediate rocks also occur at a number of levels in the south-western volcano, and these too, have comparable

	I		II		III	
SiO_2	45.33		45.78		45.60	
Al_2O_3	15.79		15.94		15.88	
TiO_2	3.54		3.37		3.44	
Fe_2O_3	4.24	2.86	3.65	2.83	3.88	2.84
FeO	8.49	9.72	8.68	9.41	8.60	9.54
MnO	0.20		0.24		0.22	
MgO	5,43		5,48		5.46	
CaO	9.81		8.80		9.20	
Na_2O	3.38		3.84		3.66	
K_2O	1.25		1.46		1.38	
P_2O_5	0.51		0.60		0.56	
H_2O ±	2.03		2.24		2.15	
	100.00	99.85	100.08	99.99	100.03	99.93
or	6.90		8.62		8.13	
ab	24.20	22.57	25.40	24.40	24.92	23.66
an	24.24		21.96		22.87	
ne	2.37	3.25	3.51	4.38	3.25	3.93
di	12.27	10.49	9.90	9.08	10.84	9.64
he	4.78	7.82	4.55	5.48	4.64	6.02
fo	5.44	6.07	6.33	6.61	5.98	6.39
fa	3.12	4.93	4.16	5.34	3.74	5.18
il	6.72		6.41		6.53	
mt	6.14	4.15	5.29	4.10	5.63	4.12
ap	1.19		1.42		1.33	

I Average of four basalts D.I. 30-35 (Table 7, 226, 387, 706, 803).

II Average of six basalts D.I. 35-40 (Table 7, 794, 786, 809, 830, 716, 834).

III Average of ten basalts D.I. 30-40 above.

TABLE 15

compositions irrespective of their stratigraphic position.

It is reasonable therefore, to consider that variations in derived rock types result from processes at high levels on a parental basalt of nearly constant composition produced periodically throughout the sub-aerial development of the island (i.e. some 7 m.y.). This recurrence of chemically comparable rock types was noted in the Tristan Volcanological Report (op. cit.), although the rocks forming the exposed parts of Tristan da Cunha represent a much shorter time span than they do on St. Helena (approx. 1 m.y. - Gass, 1967).

3. Late intrusive rocks.

Compositional variations within the late highly alkaline intrusive rocks have been described above (Section VII, 5), and a possibly close relationship between these rocks and the compositionally intermediate flank intrusions has been suggested. These variations are believed to reflect the tapping at varying levels of a differentiated magma chamber at a high level in the volcanic structure. If the chamber is progressively zoned downwards from the most alkaline rocks at the top, then intrusions further down the flanks will tap successively lower (more basic) levels. The compositional variations of these rocks are plotted in an FMA diagram (Fig. 48) - their strikingly close proximity to a single 'trend line' should be compared with the salic rocks alone plotted in Fig. 46.

Systematic changes in the chemistry of extrusives away from a volcanic centre (± with time) have been described by Thorarinsson (1950), Vlodavetz (1959), and Richter et al (1964), and processes of crystal settling to account for variations in extrusives in Hawaii have been proposed by

FIGURE 48:

Analyses of rocks of the late intrusive phase plotted in an FMA diagram. Line is overall trend for St. Helenan analyses taken from Fig. 32. Percentage figures are for total alkalis.

664 = White Hill trachyandesite flow believed to be extrusive equivalent.

438 = High Knoll trachybasalt.

Note spread of analyses of Riding Stones intrusion: 421, 415, 452.

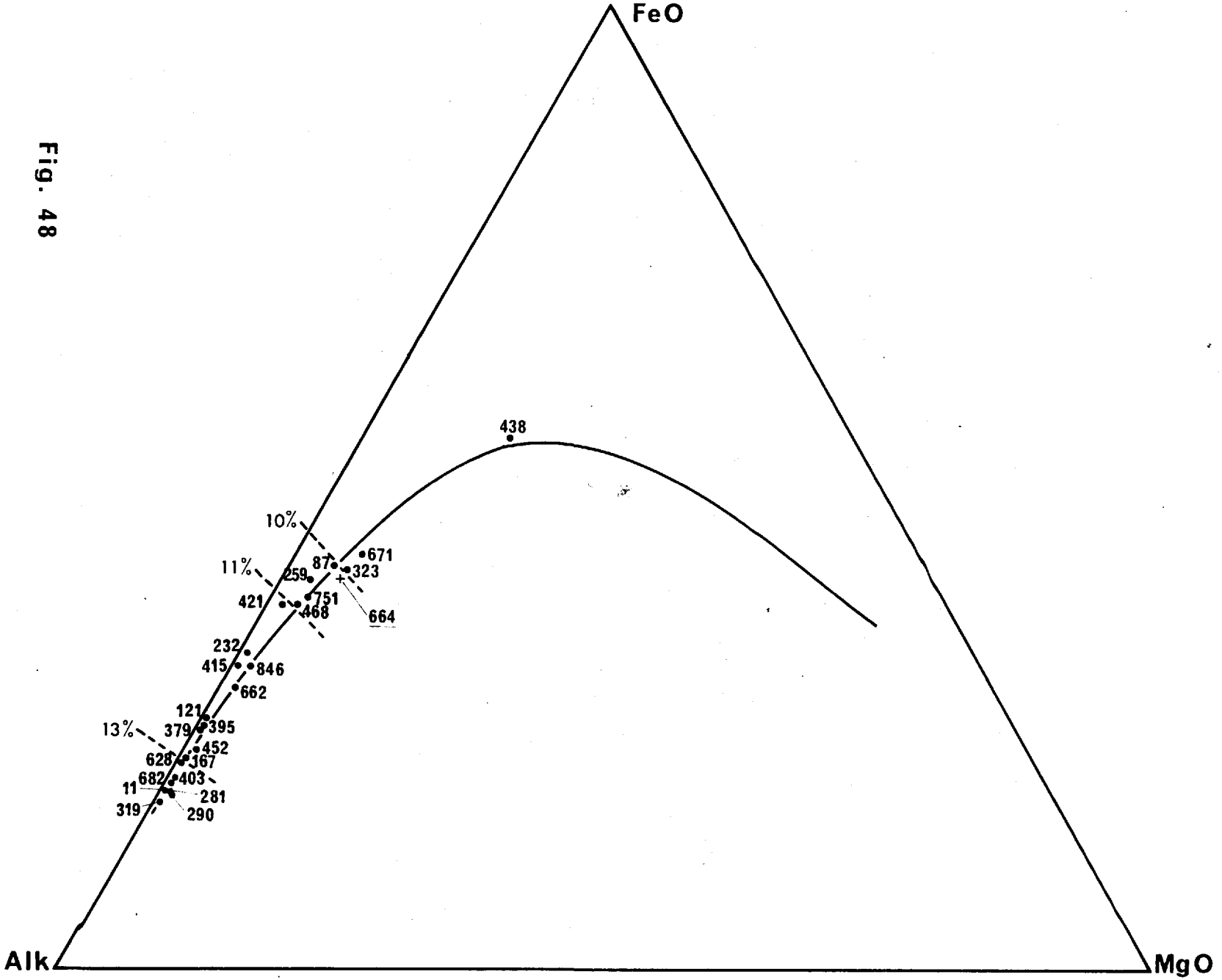
FeO
Alk
MgO
438
10%
11%
13%
671
87
323
259
421
751
468
664
232
415
846
662
121
379
395
452
628
367
682
403
11
281
319
290

Fig. 48

Macdonald (1944) and Moore (1965). Smith and Bailey (1966) have postulated that compositional variations in the Bandelier tuff (rhyolitic ash-flow) reflect tapping of a differentiated chamber which became increasingly basic with depth. The concept of an in situ differentiated magma chamber is not new, and much data demonstrate that it is a fundamental geological process. The chemical variations described by the above authors have usually been slight (approx. 5% SiO_2, 1-2% total alkalis) but in accumulative rocks (picrites) variations are very large (e.g. Murata and Richter, 1966). The variations displayed by intrusive rocks on St. Helena require a compositional variation from basalt to phonolite in a chamber as little as 2km below the volcano surface (Section IV).

Separation of large quantities of olivine, pyroxene and minor plagioclase from the initially introduced liquid basalt can occur within a period of several months, the crystal-impoverished part of the chamber becoming cooler (Richter et al, 1964) but remaining nearly 100% liquid (Murata and Richter, p198, 1966). It is perfectly reasonable to suppose that if the body of magma cools only slowly, in situ crystal differentiation can progressively enrich a decreasing volume in the upper layers of the chamber in low melting point constituents - i.e. trachytic compositions. Baker et al (p1455-56, 1967) have shown that the period of time covering the cessation of upper shield activity to emplacement of the highly alkaline intrusives could have been in the order of a million years.

A body of magma at such high level in the volcano structure, maintained at a high temperature for a considerable period of time should have affected the overlying pile to some extent. It is of some significance, then, that the secondary zeolite and carbonate mineralization of the

south-western volcano attains a maximum almost completely coincident with the total alkalis maximum of Fig. 44 (Encl. 6). That this mineralization may be contemporaneous with the cooling of the magma body is further supported by the incidence of local areas of intense zeolitization adjacent to individual late intrusions (e.g. Hooper's Rock, Riding Stones Hill, Encl. 6).

That the factors controlling the differentiation of trachytes (either towards the phonolitic or granitic minimum) are critical has been noted by LeMaitre (pp1334-5, 1962) and Nolan (1966). The trachytes within the late magma chamber on St. Helena moved towards the phonolitic minimum (Fig. 46), the gradational nature of the process being reflected in both chemistry and mineralogy.

Nolan (op. cit. p151) says: "It seems likely that the variation in the nature of the final liquid residuum depends mainly on slight original variations in the parent basaltic magma. Notable departure in either direction from the saturated condition of the parent magma will normally persist in the end differentiates". This appears to have been the case in the rocks of Gough Island (LeMaitre, 1962), which are very weakly nepheline normative - early trachytes plot on or just below the Ab-Or join, and later aegirine-augite trachytes follow the slope down towards the phonolite minimum (op. cit. p1334). Similarly, the slightly more strongly nepheline-normative parental basalts of St. Helena have given rise to end-differentiates which plot closer and closer to the phonolite minimum.

In Section III, 6e, a number of intermediate dykes and flows in the White Hill area, contemporaneous with, or later than, this intrusive phase were described. The trachy-andesitic flows (664, Table 9) are considerably more alkaline

(D.I. = 75) than the earlier upper shield flows, and petrographically are close to the 'basic' trachytes such as 751. Sheep Knoll, (671, Table 9) which is associated with the late intrusives is less alkaline than would be expected (cf. 846, 662, Fig. 44), and chemically is comparable to 664.

It is suggested that these local extrusives represent material extruded from the differentiated chamber at a time comparable to that of the major intrusive phase. They are less alkaline (total alkalis = 9.9% in the 11-12% total alkali zone) than similarly situated intrusions, because they have locally drained the chamber to a greater depth, and/or because the slightly earlier intrusions have depleted the chamber locally in magma with total alkali composition equivalent to 11-12%. The trachyandesitic composition of Sheep Knoll (total alkalis = 9.5%) may result from a similar process. This intrusion is, however, later than the Powell's Valley Hill trachyte (Section IV) and its more basic composition may result from emplacement after extrusion of the White Hill trachyandesite from a chamber depleted in more alkaline magma.

The Sandy Bay Barn trachybasalts are probably later than the trachyandesites, and are certainly later than the trachytic dyke 751 (Section III, 6e). The composition of the flows may reflect a continuation of the above process of local draining of the chamber to more basic levels (cf. compositional variation in the High Knoll parasitic mass, Section III, 6d).

4. Origin of the Bencoolen trachyandesites.

The parasitic Bencoolen flows are petrographically unique on St. Helena. The flow group is developed in (fed from) an area in which local pockets of magma of varying

composition, have been developed on several occasions (see Section III, 5). The phenocrysts of the flow group are of alkali feldspar and slightly zoned plagioclase (cores as calcic as An_{54}). Both types were intensely corroded before crystallization of thick rims of zoned plagioclase (± reverse → normal → ± alkali feldspar, see Section VI). Groundmass feldspars are normally zoned plagioclases with alkali feldspar occurring as rims and interstitially. Ferromagnesian minerals and Fe-Ti oxides appear comparable to those found in normal trachyandesites although the olivine (Fa_{41}) is more forsteritic than in chemically comparable rocks. A possible origin for this rock type is proposed below.

A pocket of crystallizing magma (plotting in the two feldspar field of the system An-Ab-Or) was producing normally zoned plagioclases and potash-feldspars. A more basic liquid (?trachybasaltic) forced into the magma body caused intense corrosion of the feldspar phenocrysts, probably resorbing completely finer-grained crystalline material. The basic liquid was mixed thoroughly producing a virtually homogeneous liquid of trachyandesitic bulk composition, precipitating basic andesine zoned out to alkali feldspar onto the eroded 'trachytic' phenocrysts.

5. Origin of the xenoliths.

The three kinds of xenoliths described in Section VI (feldspathic clots, gabbroic, amphibole-bearing) are believed to have originated by three different processes.

a. Feldspar clots.

The small plagioclase clots have a corroded zone outside which the feldspar is normally zoned in comparable fashion to the host rock feldspars, they almost invariably contain abundant euhedral apatites, are more calcic than

their host, and may consist only of one 'xenocryst'. The composition, and the degree of corrosion by the host rock, of the plagioclase crystals show that they, and their included apatites, were derived from a more basic magma.

It is suggested that the multiple or individual xenocrysts containing apatites have been 'picked up' by the erupting magma from the lower levels in a magma chamber and brought into a less basic environment resulting in marked corrosion. Two of the clots are associated with small intrusions related to high level pockets of magma, and the extent of the flows containing the other two is uncertain.

The alkali feldspar-rich xenolith of the Bencoolen flow (Section VI, 2b) contains primary amphibole. Its position in the very base of the flow group and its sodic mineralogy suggest that it is a fragment of a roof accumulation within the originally trachytic magma body that is postulated above as the source material for the flows.

b. The gabbroic xenoliths.

The gabbroic xenoliths are compositionally and mineralogically slightly more basic, coarse-grained, varieties of the basaltic flow and dykes which include them. The xenoliths are petrographically true orthocumulates (Wager et al, 1960), the zoned rims to the plagioclase and pyroxene having crystallized from intercumulus liquid. These xenoliths, therefore, are probably coarse-grained cumulate material from low levels in a magma chamber included in material extruded from the upper parts of the chamber. The accumulative origin of 'plutonic' xenoliths of similar petrography is widely accepted (see for example White, 1966).

c. Amphibole-bearing xenoliths.

The following features concerning the amphibole-bearing xenoliths must be taken into consideration when proposing their origins*.

i. Their occurrence is restricted to highly alkaline rocks of the late intrusive phase.

ii. Their distribution is localized in an area approximately 5km in diameter, coincident with the central regions of the early basaltic dyke swarms and the proposed late magma chamber (Fig. 49).

iii. The xenoliths containing acicular amphiboles occur in a well-defined narrow central zone approximately 2 x 1km (Fig. 49).

iv. Coarse-grained varieties are very rare and very small; the xenoliths with acicular amphiboles are larger, and abundant within their limited zone of occurrence.

v. Varieties with acicular amphiboles are highly vesicular and contain abundant late apatite, suggesting a high concentration of volatiles. Their shape and orientation suggests that they were plastic at the time of their incorporation in the host dykes.

vi. The original assemblage of pyroxene + feldspar ± olivine + Fe-Ti oxides + apatite was breaking down to a hydrous assemblage (amphibole ± biotite) before incorporation in their host rocks. Reaction within their host rocks resulted in breakdwon of amphibole to pyroxene + Fe-Ti oxides.

---

* With the exception of one xenolith from an arcuate sheet at Great Stone Top (see below).

FIGURE 49:

Distribution of the amphibole-bearing xenoliths; all are associated with the late intrusive phase, phonolites and phonolitic-trachytes.

a = coarse-grained
f = coarse-grained, feldspar-rich.
v = finer-grained vesicular varieties with acicular amphiboles.

Only highly alkaline intrusives are shown; dashed lines are total alkalis contours taken from Fig. 44.

Areas without xenoliths were extensively searched for them.

Pyroxene-oxide pseudomorphs after amphibole occur in the arcuate Hooper's Rock intrusion. Corroded feldspar 'xenocrysts' in Rush Knoll (236, a) are identical to xenolithic feldspars.

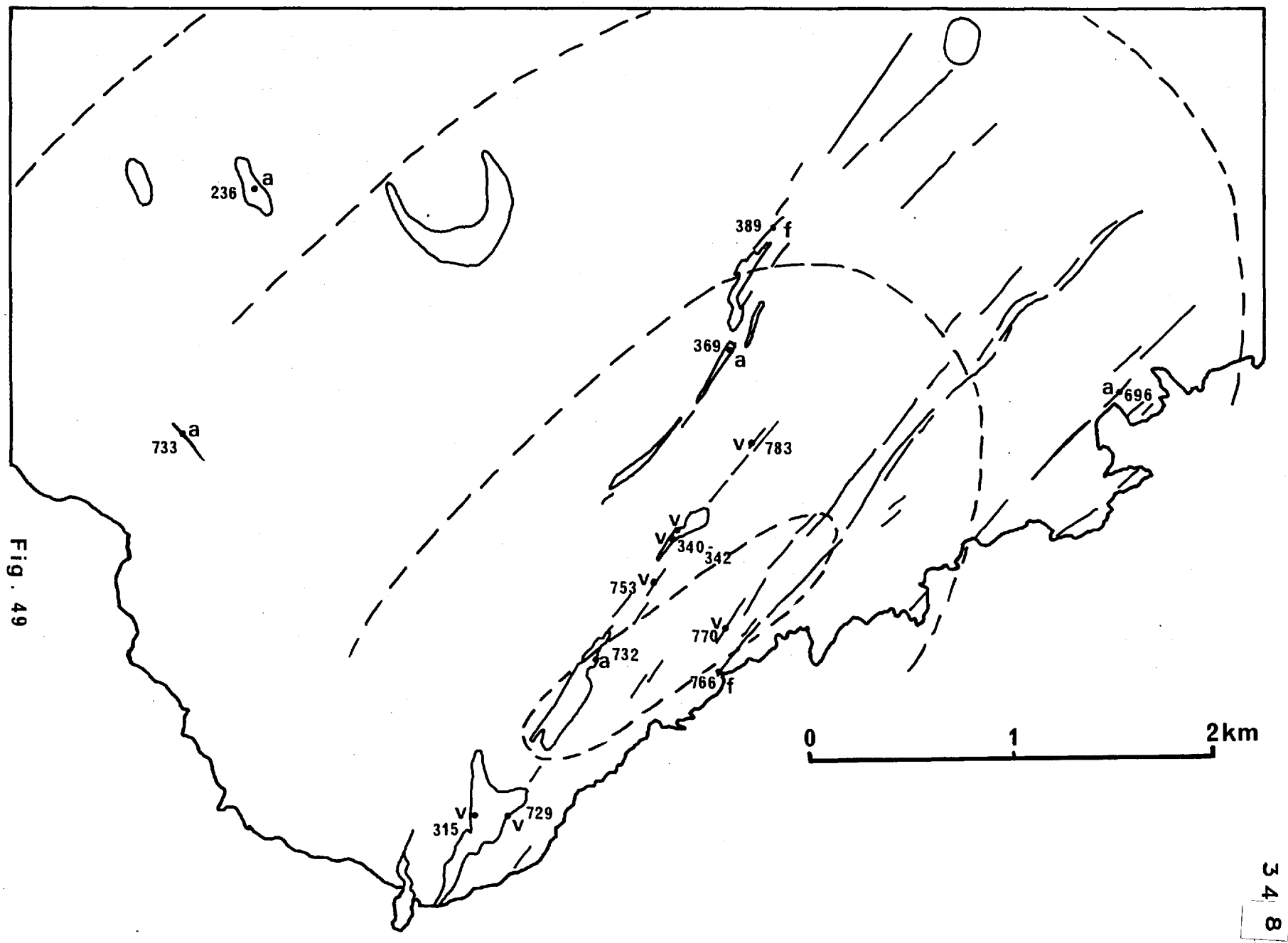
236 a
389 f
369 a
733 a
783 v
696 a
340
342
753 v
770 v
732 a
766 f
315 v
729 v
0
1
2km

Fig. 49

vii. Mineralogically the compositions of all the xenoliths appear closely comparable (?more alkaline for vesicular, fluid varieties) and are monzonitic or syenogabbroic.

viii. Discrete 'xenocrysts' with rims of pyroxene and Fe-Ti oxides also occur in these highly alkaline intrusives.

Several points suggest that the incorporation of xenoliths into the late, highly alkaline intrusive rocks is coincidental:

i. The xenoliths were either crystalline or plastic at the time of incorporation in a magma containing appreciable liquid.

ii. The xenoliths are more basic than the rocks which enclose them.

iii. The alkaline intrusives exhibit a progressive chemical, mineralogical and petrographical variation outwards from a central area. The extremely undersaturated nature of the Man o' War Roost phonolite (281) and comparable rounded inclusions in an adjacent dyke (403) suggest that this nepheline-rich phase is representative of the uppermost part of the magma chamber.

iv. The alkaline intrusives contain no apatite; the xenoliths are exceedingly rich in it.

v. The vesicular xenoliths with acicular amphiboles reflect high volatile content - the alkaline intrusives show no evidence for comparable high volatile content.

vi. Amphiboles are unstable in all rock of the intrusive phase.

The possibility that the xenoliths represent a 'roof facies' of the magma chamber would appear untenable in terms of the above points.

The possibility that the more basic xenoliths are cumulates from deeper levels in the chamber is discredited by the fact that incorporation of crystalline material from depths in the chamber would require strong magma currents and high rates of extrusion (see for example (Murata and Richter, 1966), causing widespread stirring of the magma. The gradational outward variation in petrology of the alkaline rocks shows no evidence for anything but undisturbed tapping of a magma body with regularly variable composition. The existence of crystalline material with compositionally comparable material which was plastic at the time of incorporation rules out the origin of the xenoliths from accummulative lower levels.

The only alternative is to accept that the xenoliths are derived from outside and above the late high level magma chamber

The mechanism proposed here for the origin of the amphibole-bearing xenoliths on St. Helena assumes the intrusion of a flat laccolithic basaltic mass into the southwestern shield at a higher level than the top of the late magma chamber. If this upper sheet cooled symmetrically inwards from top and bottom, the central parts could crystallize as coarse-grained intermediate rocks (monzonites). Volatiles would migrate into, and be concentrated in, the central parts causing pyroxene to break down to amphibole and the crystallization of abundant apatite. The last crystallizing fraction of the sheet would be very volatile-rich, conceivably taking a considerable length of time to crystallize. Fissuring preceding the intrusion of the highly

alkaline rocks from the magma chamber below would cut the essentially consolidated sheet, the basaltic rocks would fracture cleanly, the coarser-grained central rocks, could be expected to fracture less cleanly, with fragments and discrete crystals falling into the fracture to be caught up in the dykes. The very central portion of volatile-enriched final differentiate could be incorporated in the phonolitic mass as relatively immiscible, plastic fragments, which distorted during flow. Consequently coarse-grained xenoliths could occur anywhere within the limit of coarse-grained rocks in the sheet, whereas xenoliths representing the final (still plastic) fraction could only occur above the area of latest crystallization.

Yagi (1953) has described alkali doleritic intrusive rocks (chemically comparable to St. Helena varieties) from the Morotu district, Sakhalin, in which in situ differentiation has produced small quantities of late monzonites and syenites. The intrusions, in the form of sheets, laccoliths and dykes, may be up to three kilometres in maximum dimension. In general the marginal parts are of dolerite, and the inner parts of coarser-grained leucocratic monzonite or syenite (p772); locally residual volatile-rich monzonitic or syenitic liquids have migrated into fissures in the crystalline doloritic parts (op. cit. p806). The intrusions have cooled from the margins, becoming progressively more alkaline (and volatile-rich) towards the central regions, which have remained highly fluid after crystallization of the main mass of the intrusions. The textures shown by xenoliths containing acicular amphiboles (Section VI, 2) should be compared with late syenites figured by Yagi (Plate 4, Fig. 2).

Why the processes of differentiation in magma bodies on St. Helena should simultaneously given rise to such

different mineralogical assemblages is uncertain. However, the theory that "the continuing concentration of volatiles in the residue as crystallization proceeded was no doubt a major factor" (Yagi, p806, 1953) may hold the key to this problem.

The occurrence of a vesicular xenolith comparable to those with acicular amphiboles, in a sheet related to Great Stone Top, presents another problem. It has been suggested above that the Stone Top trachytes are unrelated to the late intrusives of the south-western volcano. The existence of a comparable sheet overlying the high level magma body responsible for the Stone Tops flow domes is highly unlikely. The origin of this single (observed) xenolith is almost certainly dependent upon the interpretation of the origin of the pyroxene-oxide pseudomorphs after amphibole, so common in the Stone Tops flows, and in intermediate flows of parasitic origin elsewhere.

High pressures of volatiles are considered to have been characteristic of small bodies of magma within the volcano. Under these conditions it is probable that the stable ferromagnesian silicates would have been amphibole. Release of pressure in the magma by fracture of overlying rocks, and rapid escape of volatiles could move the ferromagnesian assemblage into a stable pyroxene field, resulting in the breakdown of amphibole to Fe-Ti oxides and a pyroxene during rise to the surface.

The occurrence of pyroxene-oxide pseudomorphs after amphibole appears to be restricted on St. Helena to trachyandesitic and trachytic lavas almost certainly only of parasitic origin. Pseudomorphs of this type may contain no amphibole, may eventually disintegrate to such an extent that the former presence of the hydrous phase is almost destroyed

- identification of clusters of granular Fe-Ti oxides ± pyroxene in rocks of this type may be a method of establishing pre-eruption conditions in the magma.

The more alkaline Stone Tops xenolith, although superficially similar to those included in the late intrusive rocks, may therefore represent a (?roof) facies of the Stone Tops trachytic magma body.

6. Origin of the St. Helena parental magma.

The composition of the basalt believed to be parental to the rocks exposed on St. Helena was given in Table 15. The basalt is nepheline normative (4%) and exhibits little compositional variation throughout the subaerial activity of the volcanoes.

The mantle at depths of magma genesis is believed to consist of peridotite, although the exact constitution varies from author to author: Yoder and Tilley (1962), O'Hara (1965), O'Hara and Yoder (1967) and Green and Ringwood (1967). It is also generally held that basalt types are the products of variable degrees of partial melting of this peridotite, (Reay and Harris, 1964; Green and Ringwood, 1967). Green and Ringwood (op. cit. pp159-167) showed that at pressures equivalent to depths of 35-70km, lower degrees of partial melting produced more alkalic basaltic types. The composition of the basalt at the surface is therefore dependent upon the depth of partial fusion (depth of magma segregation - Green and Ringwood, 1967), the amount of fusion, and the ensuing modifications brought about during rise of the magma to the surface - O'Hara (1965), O'Hara and Yoder (1967), Green and Ringwood (op. cit.). It seems reasonable to accept that all of these processes are important, although to distinguish between the weights placed on particular mechanisms

by particular authors is impossible in this study. Seismic activity at depths of 50-60km below the tholeiitic shield of Kilauea preceding an eruption has been interpreted by Eaton and Murata (1960) as indicative of the depth of magma genesis.

On the basis of seismic, experimental and theoretical evidence therefore, it is suggested that the 'parental' basalt of St. Helena originated by partial melting of a peridotite mantle at depths in the order of 60-70km.

7. Petrochemical variations of Atlantic islands.

In 1961 Almeida, from a comparative study of 11 Atlantic volcanic series, suggested the existence of two petrochemical groups. The hyperalkaline, highly undersaturated group, comprising Trindade, Fernando de Noronha, Cape Verde Islands, Sao Tome, Principe, and the Canaries, was contrasted with the mioalkaline, weakly undersaturated or saturated group of Madeira, Tristan, Gough, St. Helena, Ascension and the Azores. Baker et al recognised a variation in petrochemistry outwards from the mid-Atlantic ridge, and concluded their comparative studies of South Atlantic islands: "The trend, therefore, would appear to be one of increased silica undersaturation, with increase in distance from the centre of the ridge" (1964, p539). More recently, in a comprehensive study of the volcanic islands in the Atlantic and east Pacific, McBirney and Gass (1967) have demonstrated a progressive outward decrease in the Niggli q value of late differentiates from oceanic ridges towards the margins of the ocean basins. The basic ("primitive") rocks show a comparable but slight outward variation.

A comparative study has been made here of the chemical variations of volcanic series from Atlantic islands in an attempt to demonstrate quantitatively their relationship

to distance from the mid-Atlantic ridge. Because of irregularities in the shape of the South Atlantic resulting in increased distance of coastlines from the ridge southwards, the ratio: distance of island to ridge/distance of mainland to ridge has been considered. This ratio allows for any relationship existing between the mid-oceanic ridge and the ocean basin rims. The islands and their geographical relationship to the mid-Atlantic ridge and the coastline are shown in Fig. 50.

While the choice of Niggli q value by McBirney and Gass (op. cit.) has shown very strikingly an outward variation for the late derivatives, the use of analyses of all rock types will give a more representative, though somewhat more confused picture. All published analyses for islands and island groups are presented graphically in terms of plots of total alkalis against silica (Figs. 51-57). This method of presentation reflects the undersaturation of the rocks accurately and simply. Analyses of rocks from the Tristan group, Gough and St. Helena are given in Fig. 51; these rocks are all slightly or moderately nepheline normative and the islands are at comparable distances from the ridge crest. In Fig. 52 the rocks of the Tristan group alone are plotted, their slightly more undersaturated nature is obvious and the rocks of Inaccessible and Nightingale are in general less undersaturated than those of Tristan itself.

Figs. 53 and 54 contrast the degree of undersaturation of Ascension and Bouvet (virtually on the ridge crest) with the extremely undersaturated rocks of Trindade, Fernando de Noronha and Principe (at considerable distances from the crest). In Figs. 55-57 analyses of rocks from Madeira, the Azores, the Canary Islands and the Cape Verde Islands are shown. Rocks of the Cape Verdes display

FIGURES 50-57:

Comparative study of the Atlantic Islands.

FIG. 50: Geography of the Atlantic showing the crest of the Mid-Atlantic Ridge (and cross faults) taken from Menard (1965).

FIGS. 51-57

Total alkalis plotted against silica.

FIG. 51: Gough Island (LeMaitre, 1962), St. Helena, Tristan da Cunha group (Baker et al, 1964); the dashed lines are used in Figs. 52-57 merely as reference lines. Gough analyses plot overall lower than others.

FIG. 52: Tristan da Cunha, Inaccessible and Nightingale (op. cit.).

FIG. 53: Ascension Island (Daly, 1925), Bouvet (Broch, 1946), and basalts dredged from the northern part of the Mid-Atlantic Ridge (Muir and Tilley, 1964).

FIG. 54: Bermuda (Pirsson, 1914), Fernando de Noronha (Almeida, 1955), Principe (Neiva, 1954), Trindade (Almeida, 1961).

FIG. 55: Cape Verde Islands (Neiva, 1940): solid circles = S. Antao; open circles = S. Vincente; crosses = Sal, Maio, S. Tiago, Fogo; B = Boa Vista.

FIG. 56: The Canary Islands: small circles = La Palma, H = Hierro; crosses = Tenerife, Gran Canaria, Gomera; open large circles = Fuertaventura; filled large circles = Lanzarote. Data from Hausen (1956, 1958, 1959, 1961) Bravo (1964), and additional unpublished analyses from Tenerife, W.I. Ridley.

FIG. 57: Azores (Hadwen and Walker, in press), Madeira (Gagel, 1912; Finckh, 1914).

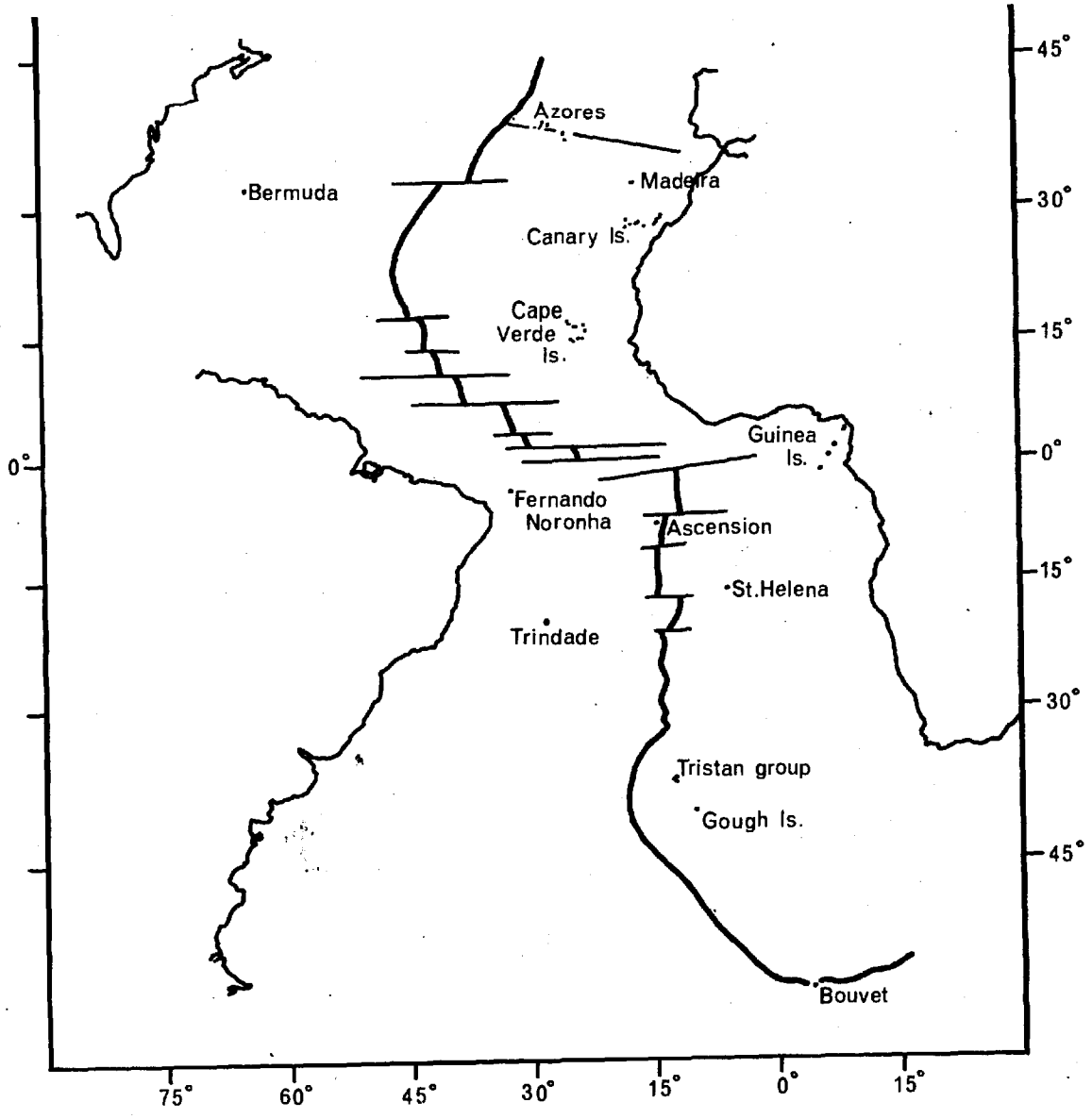
Azores
Bermuda
Madeira
Canary Is.
Cape Verde Is.
Guinea Is.
Fernando Noronha
Ascension
St.Helena
Trindade
Tristan group
Gough Is.
Bouvet
45°
30°
15°
0°
15°
30°
45°
75°
60°
45°
30°
15°
0°
15°

Figure 50

FIG. 51

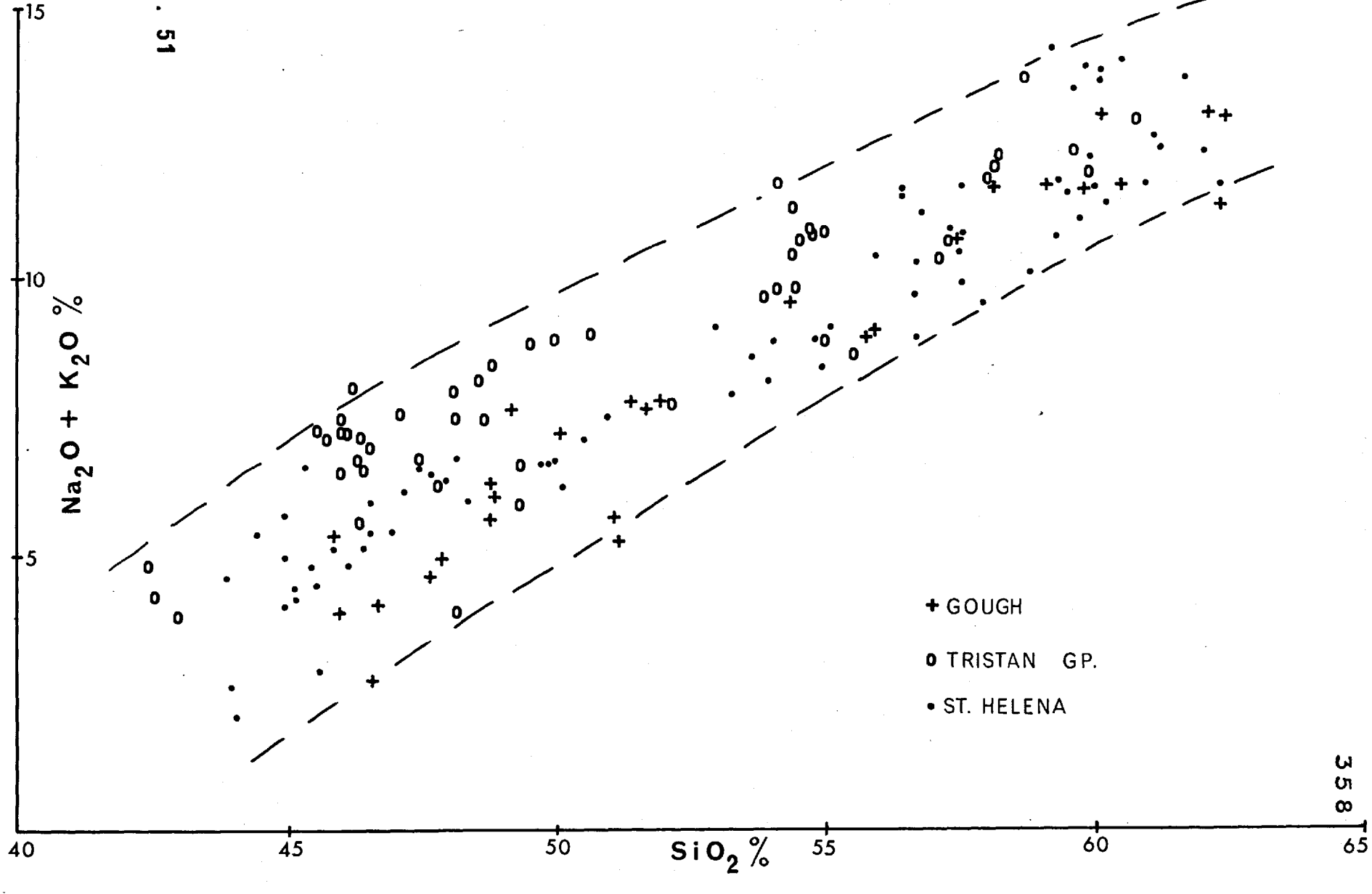
15
10
5
$Na_2O + K_2O$ %
40
45
50
55
60
65
SiO_2 %
+ GOUGH
o TRISTAN GP.
• ST. HELENA

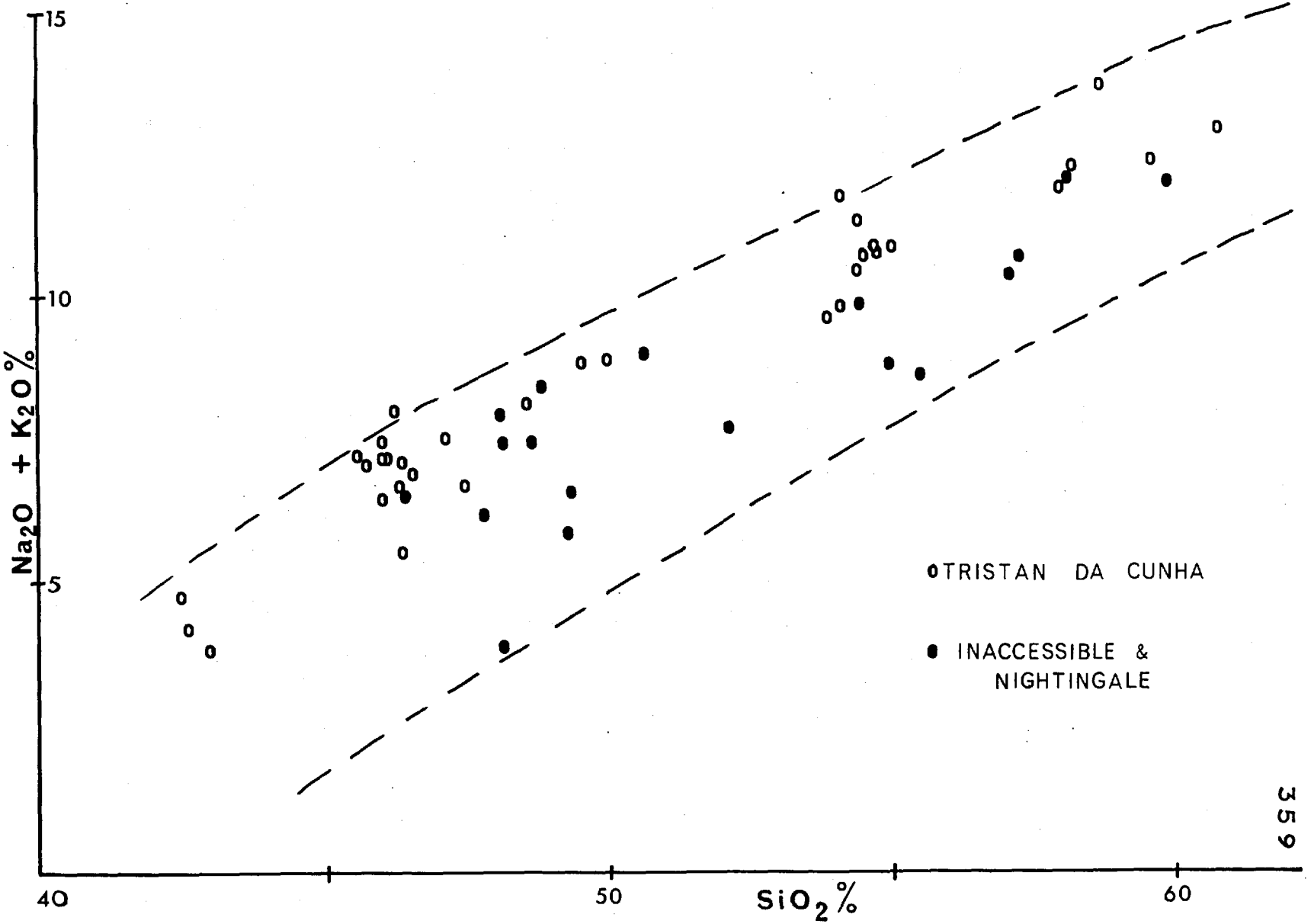
15
10
5
$Na_2O + K_2O\%$
40
50
60
$SiO_2\%$
TRISTAN DA CUNHA
INACCESSIBLE & NIGHTINGALE

Fig. 52

Figure 53

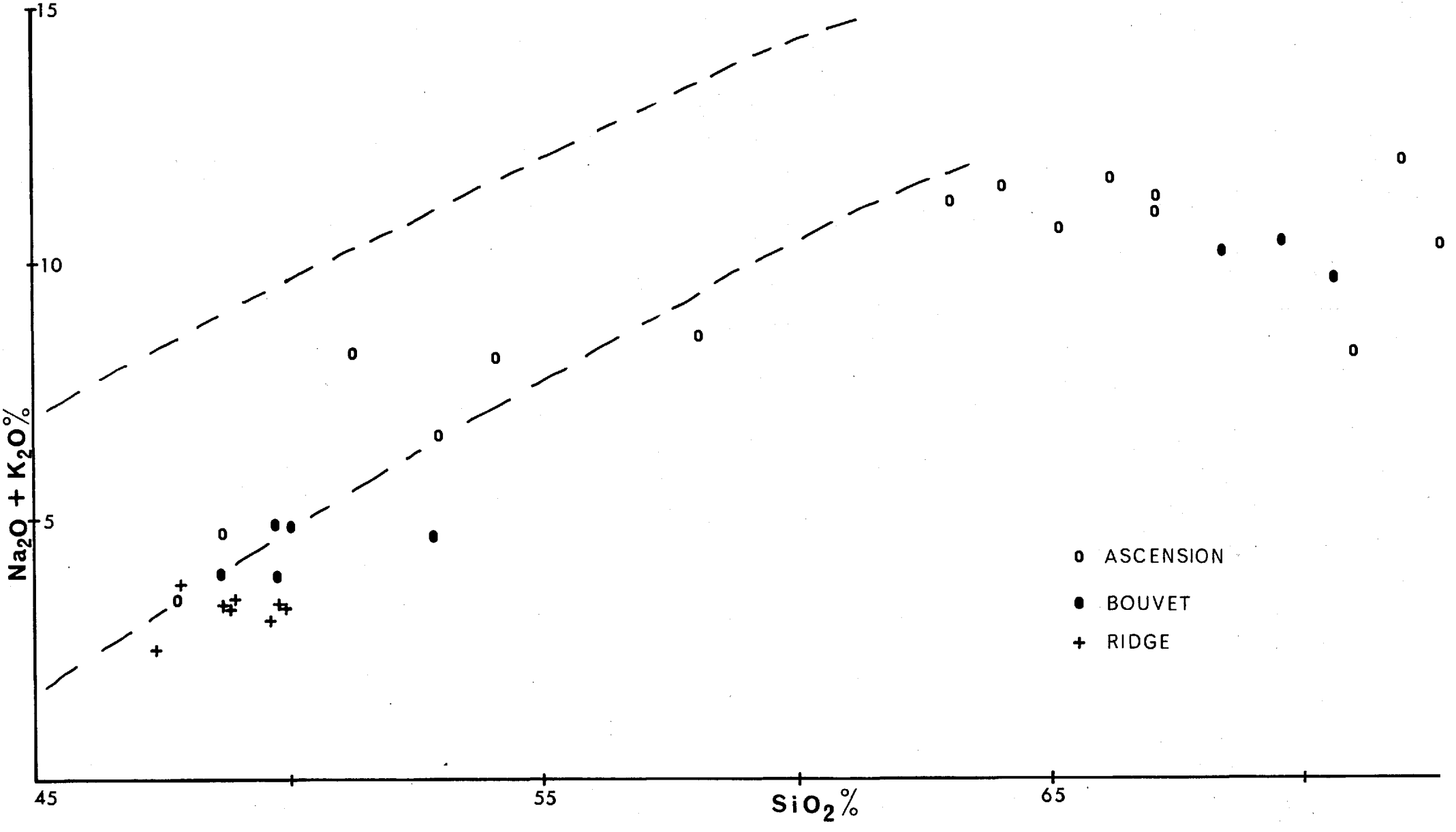

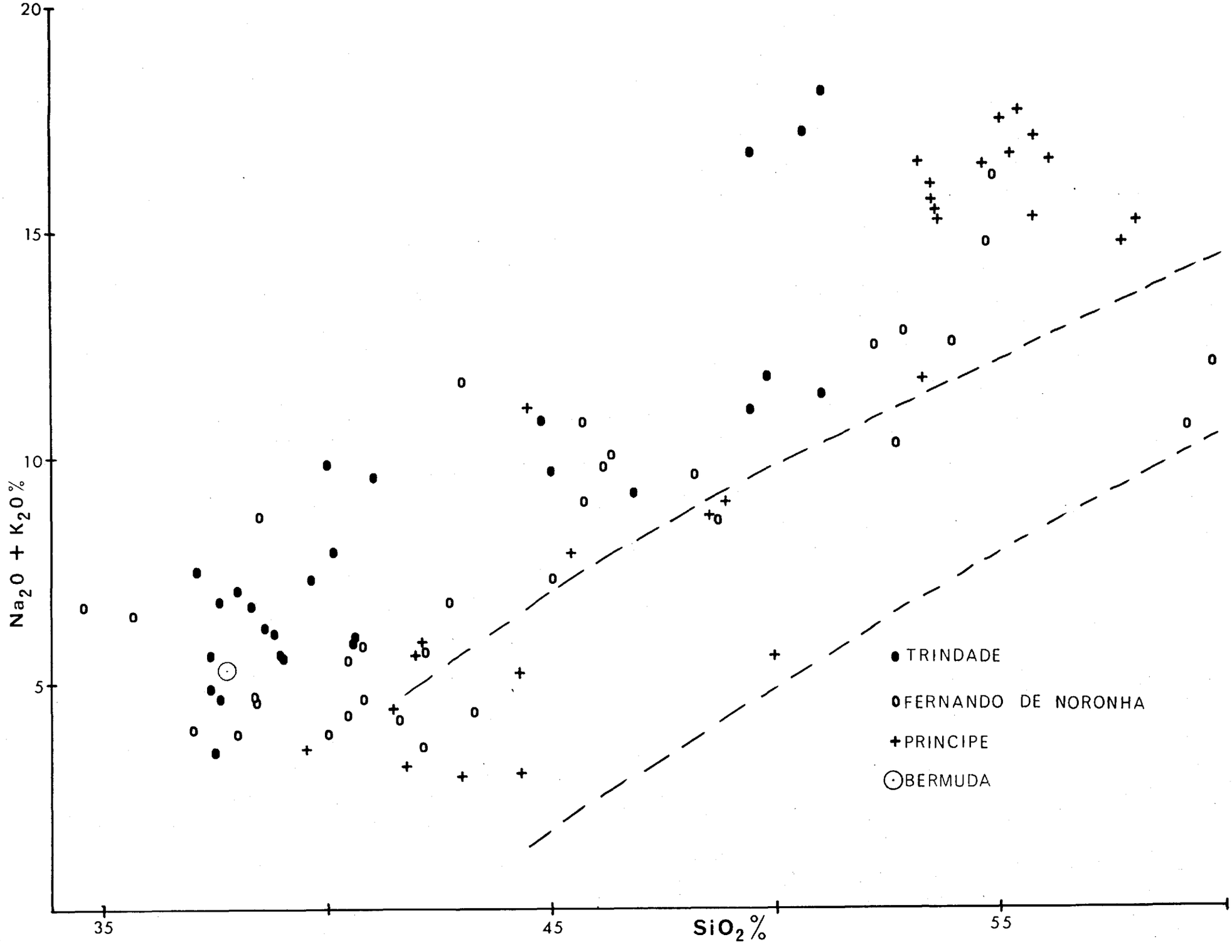
20
15
10
5
$Na_2O + K_2O\%$
35
45
55
$SiO_2\%$
TRINDADE
FERNANDO DE NORONHA
PRINCIPE
BERMUDA

Fig. 54

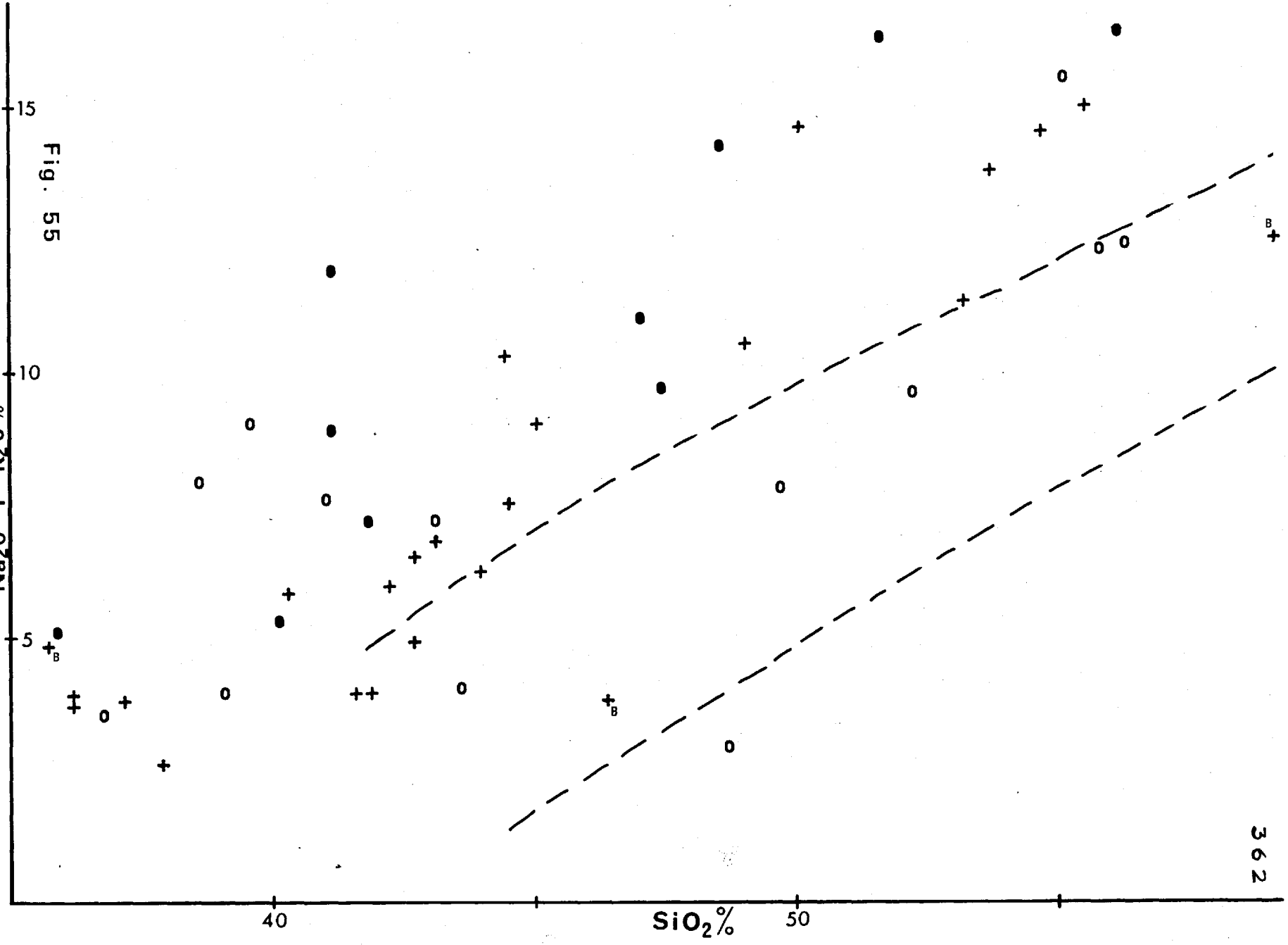

Fig. 55

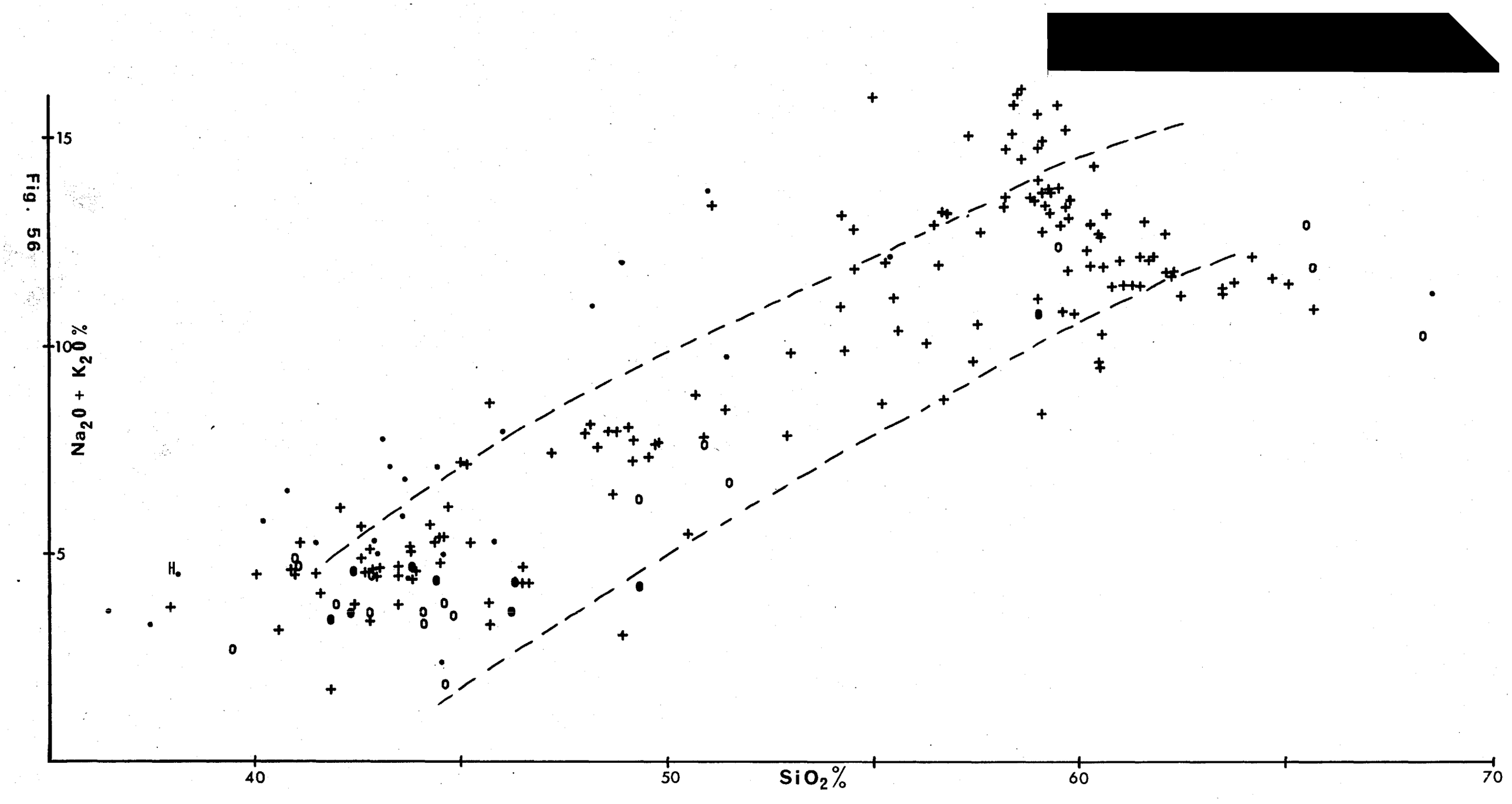
Fig. 56
15
10
5
$Na_2O + K_2O$ %
40
50
60
70
SiO_2 %

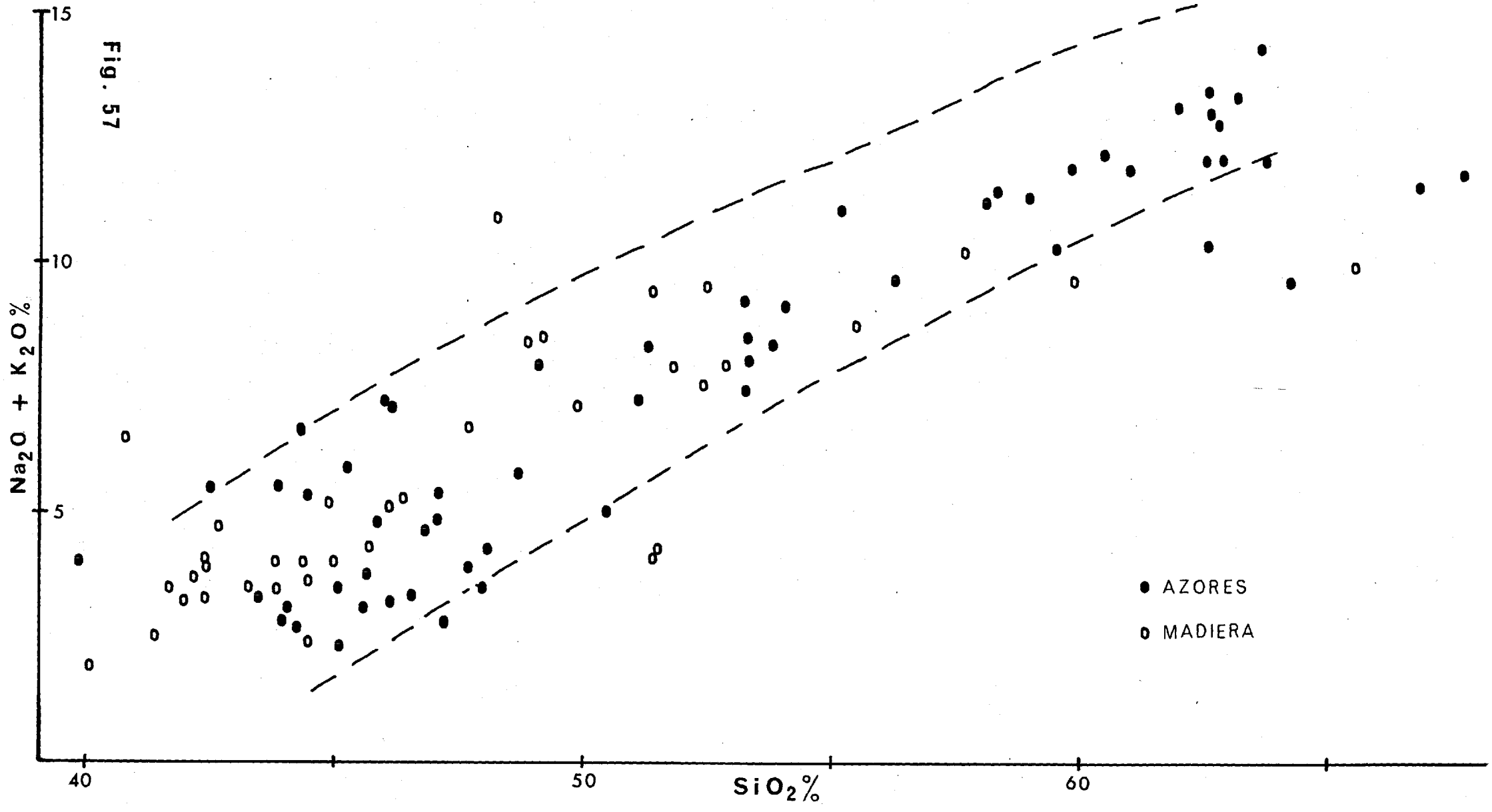

Fig. 57

considerable scatter but are largely very undersaturated and comparable to Trindade types. Analyses from the Canaries, Madeira and the Azores are collected from numerous sources, many of which are very old, and in these cases it is difficult to separate real and apparent scatter. In the main the Canary Island rocks are comparable to, or slightly more undersaturated than, the Tristan rocks, especially at the basic end (Fig. 56). Analyses from Madeira and the Azores are closely comparable and differ only slightly from the Gough-Tristan-St. Helena group (Fig. 57); affinities towards both rhyolitic and phonolitic derivatives are however, encountered in the Azores. The highly undersaturated melilite -nepheline basalt from Bermuda (nearly 2000km west of the ridge crest), is comparable to Trindade specimens (Fig. 54).

From these figures it is obvious that exposed rock types on islands in the South Atlantic display a variation in degree of undersaturation as a function of their position relative to the mid-Atlantic ridge and the continental margins. For the other islands, Azores, Madeira and the Canaries, the pattern is not so apparent and there is considerable scatter, but in general they are in keeping with the hypothesis.

Study of Hawaiian volcanism has shown that the alkalic rocks are later than the main tholeiitic shields (Macdonald and Katsura, 1964). With increasing degree of alkalinity there is evidence of a slowing down in rates of volcanism (op. cit.). It is therefore of considerable importance to attempt to establish **within the South Atlantic** islands the control not only of geography on the chemical variations but also of time. Wilson (1963) attempted to show an increase in the age of islands away from the mid-Atlantic ridge. Recent work, however, while agreeing that in general volcanism <u>on</u> the ridge is young, does not support any overall

regular pattern. Dates from Trindade and Fernando de Noronha are Pliocene to Recent (Prof. F.F.M. de Almeida, personal communication); St. Helena ranges from 14.6-6.8 m.y. in age (Baker et al, 1967); a phonolite plug from the Vema seamount gave an age of 11 m.y. (Simpson and Heydorn, 1965); ages from the Canaries vary from 20 m.y. to Recent (Abdel-Monem et al, 1967); historical eruptions have occurred on Tristan, Bouvet, the Azores, the Cape Verdes, and the Canaries. Increasing undersaturation away from the ridge cannot be explained in terms of absolute time relations - i.e. the age of the subaerial volcanic products in relation to the initiation of volcanism (submarine) for a given island may be highly significant, the absolute age determined for islands relative to each other is not.

Within islands or island groups the chemical variation of the volcanic products is somewhat variable. On St. Helena the composition of the parent basalt has remained virtually constant for 7 m.y. In the Tristan group the older Inaccessible and Nightingale are less undersaturated (Fig. 52), but all retain characteristic element concentrations. On Tenerife there is the possibility of a slight increase in undersaturation with time (Ridley, 1968). (In the Hawaiian islands younger rocks of a given volcano may be considerably more undersaturated than the earlier alkali rocks.)

Geographically, islands in a given group also provide conflicting information. Inaccessible and Nightingale are closer to the ridge than Tristan and are less undersaturated. In the Canaries there is no systematic variation in undersaturation although overall Fuertaventura and Lanzarote may be the least undersaturated (Fig. 56). A similar situation (least undersaturated furthest from the ridge) is suggested by analyses from the Cape Verdes (Fig. 55). Since the exact geophysical relations of the Cape Verdes, the

Canaries, the islands of the Gulf of Guinea, and the Azores to the continental shelf and to major fault zones are uncertain, these islands must be treated with great care. Perhaps of considerable significance is the overall decrease in undersaturation within the Cape Verdes and the Canaries towards the continental margins.

Gravity and seismic anomalies for the mid-Atlantic ridge have been interpreted by Talwani et al (1965) as the result of a very flat lens, up to 3000km across, of lower density (3.15 gm/cm^3) material in the 3.40 gm/cm^3 mantle at a depth of approximately 20km below the ocean. A possible cause for this density has been suggested by Morgan (1965) who interpreted it as a zone of hotter material (300^oC hotter than the surrounding mantle below the ridge). From different lines of evidence Bott (1965) has suggested that oceanic ridges reflect a degree of partial melting in the mantle at the apex of convection currents beneath them. The magma so produced rises towards thesurface "owing to its relatively low density. It is likely to form a network of dykes and magma chambers in the layer overlying the cell" (op. cit., p843). Bott envisaged some degree of partial melting extending outwards in a zone (approx. 60km below the ocean floor) for a considerable distance away from the main partial fusion zone below the ridge (Fig. 4, p843). Mechanisms similar to those proposed by Morgan and Bott would produce a zone of higher temperature within the upper mantle extending out from the ridge for a considerable distance, and could account for the heat-flow variations in the Atlantic.

The most recent compilation of heat-flow data from the Atlantic (Von Herzen, 1967) shows local areas of high heat-flow of varying intensity along the ridge, and overall lower heat-flow on either side. Von Herzen has shown very

strikingly the relationship of temperature gradient in the mantle to surface heat-flow measurements (pp220-1), i.e. the progressive deepening of isotherms away from the ridge.

It is suggested here that the increase in undersaturation outward from the mid-Atlantic ridges is a reflection of this higher temperature zone and its associated (?potential) zone of partial fusion within the mantle decreasing away from the ridge. Outwards from the ridge the potential amount of partial melting would be progressively reduced depending upon the rate at which the temperature difference decreases. Partial melting at depths of 35-70km produces increasingly undersaturated liquids with decreasing percentage of melting or increasing pressure (i.e. depth) (Green and Ringwood, 1967). Outwards from the ridge therefore, increasingly undersaturated basalts (parental to their low pressure high level differentiates) should be erupted at the surface. At the mid-Atlantic ridge, the high degree of partial fusion, occurring at a higher level over a larger volume (Morgan, 1965; Bott, 1965) could produce tholeiitic or high-alumina basalts (Green and Ringwood, op. cit.). These would be intruded as dyke swarms giving rise to tholeiitic submarine eruptions (Engel and Engel, 1964; Muir and Tilley, 1964; see also Fig. 53 above). Similarly, individual volcanoes (i.e. Ascension and Bouvet) would be oversaturated or saturated. Individual island volcanoes could continue to act as point sources for the extrusion of magma as they already have associated zones of weakness beneath them allowing easier uprise of magma.

In many respects this hypothesis is similar to that of McBirney and Gass (1967) but disagrees with that of Aumento (1967) who would require the islands on or adjacent to the ridge to have a capping (at least) of alkali rocks.

The dredging of a nepheline normative basalt from the mid-Atlantic ridge near Saint Paul's Rocks (Melson et al, 1967b) demonstrates that highly alkali basalts can form on the ridge. The close proximity of the dredged material to the amphibole-bearing coarse-grained Saint Paul's Rocks (Melson et al, 1967a) suggests that the assemblages from this area may not necessarily be typical of the ridge as a whole. The fact that basalts dredged from the mid-Atlantic ridge show variations from truly tholeiitic to intermediate types (i.e. towards alkali varieties) may be a reflection of variations in observed heat-flow along the ridge (Von Herzen, 1967) and associated variations in depths of magma genesis.

This hypothesis does not detract from or add to the theory of a spreading ocean floor proposed by Dietz (1961). The process obtained substantial positive support from the theories of Vine and Matthews (1963) and may others (see Vine, 1966) based on the distribution of ocean ridge magnetic anomalies. Recent investigations on sediment distribution in the Atlantic by Ewing and Ewing (1967) however require a period of quiescence in ocean floor spread from before 10 m.y. B.P. for 30-40 m.y. The hypothesis postulated above, for petrochemical variations, allows for either the build up of islands more or less in situ (no spread) or continued build up during ocean floor spread. In the first case the composition of visible products will be approximately comparable to the earliest produced material of the pile. In the second case the composition of material extruded to form the pile will change progressively away from the ridge, the exposed extrusives reflecting the position attained by the island (and its accompanying partial melting zone in the mantle). Data for "the life of ocean islands" taken ffom Gass (1967) for the Tristan group seem insufficient criteria to discredit theories of outward

migration of islands from oceanic ridges (McBirney and Gass, 1967) especially when the constructive phase of subaerial volcanism alone may extend over several million years. Dredging the tops of the numerous seamounts in the Atlantic and a deep bore-hole through an oceanic island off the ridge should provide very valuable data on this problem; with its postulated high level, differentiated, magma chamber St. Helena would seem an obvious choice for siting a bore-hole.

SECTION IX

SUMMARY OF VOLCANIC HISTORY

Submarine volcanic breccias were uplifted approximately 400m before, and possibly in part during, the earliest shield-forming activity in the north-east. The oldest subaerial products were extruded about 15 million years ago onto a surface eroded into these breccias. The rocks forming the north-eastern shield were fed from countless, thin fissures, dominantly trending north-south, and preserved to-day as a striking dyke swarm centred on Knotty Ridge. Early, and often very violent, explosive activity produced widespread deposits of scoria and tuff, but later volcanism became dominantly effusive. Occasional explosive eruptions however, produced thin tuff horizons interbedded with the lavas which constitute the bulk of the shield. During the late stages of the formation of the shield the eruptive 'centre' probably moved slightly to the north. Parasitic activity, rare throughout the building of most of the shield, was not uncommon during the youngest stages.

After an interval of two or three million years, when activity had been centred in the south-west, highly vesicular lavas and agglomerates were extruded, probably from north-south fissures, onto the deeply eroded western flank of the shield.

Virtually all of the exposed rocks of the north-eastern volcano are basaltic or trachybasaltic; other types constitute less than 0.1% by volume. Towards the top of the shield there is a decrease in the number of porphyritic basalt and an increase in numbers of trachybasalts. Two late

parasitic intrusions are also trachybasaltic. Extrusives of the youngest highly scoriaceous group are now extensively altered but consisted of basalts and/or trachybasalts.

Three lines of evidence suggest a relatively abrupt shift in the centre of activity after build-up of the north-eastern shield:

i. Lack of parasitic activity in the north-east.
ii. Lack of highly differentiated rock types in the north-east.
iii. K/Ar age determination on the top of the north-eastern and the bottom of the south-western shields.

Points i and ii may suggest the lack of a major magma chamber in the late stages of shield development. Point iii in itself is not conclusive because of possible errors of $\pm$ 1.0 million years on the absolute ages.

The bulk of the extrusives (Lower and Main Shields) of the south-western volcano were fed from a NE-SW fissure system, preserved as the second striking dyke swarm in Sandy Bay. A minor NW-SE dyke concentration in Manati Bay represents the feeders for a minor part of the Main Shield extrusives. The younger flows of the Upper Shield were fed from an area north-east of the major dyke concentrations.

In the south-west activity commenced about 11.5 million years ago, and built the complex Lower Shield. Periods of relatively quiet extrusion of basaltic flows were separated by explosive episodes during which scoria cones were built up over considerable areas of the volcano. Successive flow groups flooded the irregular topography and maintained a shield-like form.

The Lower Shield attained a height of over 500m before the dominantly effusive activity of the Main Shield

commenced about 10 million years ago. Explosive activity changed transitionally but abruptly from local eruptions in the Lower Shield to activity from the volcano's centre producing widepsread tuffs. Explosive parasitic activity also continued throughout the building of the Main Shield and numerous scoria cones more than 350m high were formed. About 800m of lavas and interbedded tuffs forming the Main Shield were extruded in about a million years.

Rocks of the Lower Shield are dominantly basaltic, with ankaramites abundant at low levels; individual groups of flows may have ankaramites at the bottom, progressively less crystal-rich types upwards, and even trachybasalts at the top. Intermediate rocks are not uncommon in the higher levels of the Lower Shield, and trachytes occur in the youngest deposits.

The Main Shield is composed dominantly of basaltic and trachybasaltic rocks, and several thick voluminous trachyandesites. Ankaramites are very uncommon, although porphyritic basalts occur throughout the sequence, most commonly at lower levels.

The north-eastern and south-western volcanoes were deeply eroded before extrusion of the Upper Shield rocks began more than nine million years ago. Early basaltic flows of the Upper Shield were themselves eroded before extrusion of a group of thick trachyandesites. The youngest trachyandesite was extremely voluminous, and poured out over a surface cut deeply into the older flows. The wide lateral extent and almost perfectly horizontal tops of all flows of the Upper Shield reflect their extreme fluidity. Effusive activity building the Upper Shield was interrupted by intermittent explosive activity from the eruptive centre, but not by parasitic explosive activity.

Activity continued on the eastern flanks of the south-western volcano, where a succesion of basalts was followed by the extrusion of the thick trachytic flow domes of Stone Tops, and the younger, petrographically distinct, trachyandesites of Bencoolen and Boxwood Hill.

After cessation of major shield-forming activity, the south-western volcano was intruded, about 7.5 million years ago, by a group of compositionally variable, highly alkaline rocks. The intrusions, and flows where they locally broke the surface, were fed from a differentiated magma chamber about 2km below the volcano surface.

In the late stages of the volcanic history of St. Helena there is evidence of the activity slowing down. The north-eastern volcano was built in approximately three million years, and the Lower and Main Shields of the south-western volcano were built in approximately 2 million years. The volumetrically inferior Upper Shield, with its numerous erosion surfaces, was built in 1-2 million years, and the highly alkaline intrusions were about 1 million years later.

Activity, other than fumarolic, younger than the highly alkaline intrusive phase is not apparent. Secondary mineralization of the central areas of the volcanoes has resulted in the development of carbonate in the north-eastern shield, and zeolites and carbonates in the south-western shield. Psilomelane of hydrothermal origin is associated with late trachyandesites of the Upper Shield. Local fumarolic activity is believed to account for wide-spread alteration of all rock types to clay-rich assemblages, and local development of halloysite segregation veins. Comparable but less extreme alteration probably resulted from weathering.

APPENDIX I

LOCALITIES OF ANALYZED SPECIMENS

11 Phonolite dyke extension; northern margin, north Asses Ear

37 Trachybasaltic flow(2m); locally top flow of NE Shield, James Valley, W side on Ladder Hill road

85 Trachybasaltic flow(>5m) from High Knoll intrusion; top of Ladder Hill road

87 Trachytic roofed 'ring' intrusion; SE side High Hill elevation 635m

108 Trachyte flow 250m W of summit of Great Stone Top dome

109 Trachyte flow (? underlying 108) 2m W of above locality

111 Trachyte flow dome; summit block Little Stone Top

121 Altered (phonolitic-)trachyte; intrusion of uncertain form, north cliff top of Wild Cattle Pound

161 Trachyandesite (? local) flow, Main Shield; first bend on path to Horse Ridge from end of West Road

167 Phonolitic-trachyte roofed 'ring' intrusion; north end Hooper's Rock mass

179 Ankaramitic basalt flow (>4m), low level of Main Shield; trig. point 2269 Hooper's Ridge

201 Trachybasaltic sheet; 500m SW White Point

218 Altered trachyandesite roofed 'ring' intrusion; NW side White Point

226 Basalt flow, Main Shield; elevation 570m, Thompson's Wood, SW Toby's Ledge

232 Phonolitic-trachyte 'laccolith'; Rush Knoll

259 Trachyte; cliff top SW side High Hill intrusion

269 Trachyandesite flow from Blue Point parasitic centre; centre of ridge to Man o' War Roost elevation 545m

277 Trachybasaltic fragment in breccia adjacent to phonolite of Man o' War Roost; ridge from Blue Point

281 Phonolite dyke; Man o' War Roost, NW side

290 Phonolite boulder, breccia 100m N Asses Ears

319 Phonolite dyke extension, margin of south Asses Ear, W side

323 Trachyandesite block from arcuate sheet of Tripe Bay North

379 Phonolite dyke; 50m N of northern summit White Rocks

387 Basaltic flow; near top Man o' War flows (Lower Shield) NNE White Rocks

395 Phonolitic-trachyte dyke, centre of N dyke of major pair, Broad Gut

403 Phonolite dyke (2m), elevation 250m, 600m E Lot's Wife

415 Phonolitic-trachyte 'ring' dyke, summit Chapel Rock

421 Phonolitic-trachyte base of infilled roof cavity Riding Stones intrusion, 250m NE Chapel Rock

438 Trachybasaltic apophysis NNE end High Knoll intrusion, elevation 500m

452 Phonolitic-trachyte, upper part roof of Riding Stones Hill, SW of limit of exposure

468 Trachyte; NNE end of intrusion I of High Hill

486 Trachyandesite flow; late member Upper Shield, 450m E Bencoolen

499 Trachybasalt flow; late member Upper Shield Lower Basalts, 125m E east corner Bencoolen

521 Trachybasalt flow, top flow Upper Shield Lower Basalts, waterfall 1km WNW Gill Point

599 Trachyandesite; top flow Upper Shield, cliff top of Fisher's Valley, 1km W Prosperous Bay Signal Station

613 Trachyandesite, Upper Shield; Bradley's Ruins,Fisher's Valley

628 Phonolite dyke; centre N side Castle Rock

662 Phonolitic-trachyte 'pipe', summit White Hill East

664 Trachyandesite flow, White Hill group of flows, elevation 480m SSE White Hill

671 Trachyandesite 'pipe', Sheep Knoll, S face elevation 640m

679 Porphyritic pyroxene-olivine basalt, low level in north-eastern shield, N end Netley Gut

682 Phonolitic-trachyte pipe; summit Lot

704 Trachyandesite flow, Upper Shield; 400m N Alarm Cottage

705 Trachybasalt irregular pipe; Bunker's Hill parasitic centre, north-eastern volcano

706 Basalt flow, Upper Shield; 850m NNW Bunker's Hill

716 Basaltic irregular arcuate sheet cutting Main Shield, 300m S Hooper's Rock

723 Altered trachybasalt flow from Old Joan centre, Main Shield; 1km WNW Old Joan Hill

737 Basalt flow, Main Shield; 1km W High Peak, elevation 720m

742 Trachybasalt flow, low level Main Shield (below 179); Horse Ridge, spot height 1829

744 Trachybasalt dyke (1.5m); 700m NE Lot's Wife elevation 290m

745a Trachyte fragment in Devil's Cap pyroclastics (Lower Shield); 70m ESE Devil's Cap

747 Trachybasalt flow, Main Shield; NE side Powell's Valley, elevation 150m

751 Trachyte dyke (8m); stream bed Powell's Valley elevation 90m

763 Trachyte 'laccolith', 100m SE Devil's Cap

780 Trachybasalt, irregular arcuate intrusion forming hillock 800m E Horse's Head

782 Trachybasalt dyke; 250m NE Lot's Wife, elevation 215m

785 Ankaramite, upper levels Horses Head flows, Lower Shield; centre of promontory 500m ENE The Chimney

786 Basalt dyke (>35m); immediately east Rock Mount

792 Trachybasalt flow (Beach trachybasalts, Lower Shield); ridge 200m N Sandy Bay Beach

794 Basalt flow (>7m), Upper Shield; sharp bend in road, elevation 555m, 900m W Mount Actaeon

803 Basalt flow (>20m), Upper Shield; E side gorge, seaward end Fisher's Valley

804 Ankaramite intrusion (centre of arcuate mass) Prosperous Bay Beach

809 Basalt (? dyke) North-eastern shield; SW side The Barn, track to summit, elevation 420m

822 Trachyandesite flow (Bencoolen group); W side of spot height 1430, Boxwood Hill

824 Trachyte; lowest flow of Great Stone Top, Sharks Valley

828 Trachyandesite flow; cliffs N end Bencoolen

830 Basalt flow, Main Shield; centre Tipley's Ridge, 480m

831 Trachyte, inclined cone-like sheet feeder to Great Stone Top; E cliff face

834 Basalt flow (4m), high level Main Shield; path to Saddle 50m S of bend ESE spot height 2160, elevation 600m

844 Ankaramitic basalt (>35m), associated Upper Shield; ridge Diana's Peak to Sheep Knoll, elevation 700m

845 Trachyandesite dyke, same ridge as 844, elevation 665m

846 Phonolitic-trachyte ?pipe-like mass; 100m N Sheep Knoll summit

APPENDIX II

SECONDARY MINERALIZATION

The basal breccias of the north-eastern volcano are pervaded by calcite, occurring as veins and vesicle infillings. The carbonate has been extensively taken into solution and re-precipitated as cement for detrital deposits or as travertine in stream beds. The minerals are colourless or white, but varying amounts or iron are responsible for colour banded varieties.

Zeolites and carbonates occur abundantly in Sandy Bay up to elevations of approximately 500m (Encl. 6). The zone of alteration is dome-shaped, rising from Manati Bay in the west to a maximum (by extrapolation) east of Lot's Wife, and dropping gradually into Powell's Valley in the east. Zeolites are found outside this area and especially are associated with the country rocks around late, highly alkaline intrusions (Encl. 6). The area of weak zeolization in James Valley, increasing in intensity to Sugarloaf Hill, is unrelated to exposed intrusive activity. However, the concentration at Gill Point is related to parasitic scoria activity. The concentration of zeolites largely into the central regions of the volcano and associated with late highly alkaline intrusions may reflect their close relationships to the late high level magma chamber.

Chabazite, as "cubes", is the most abundant zeolite, and occurs as the form "phacolite" only above the Hooper's Rock phonolitic-trachyte. Fibrous zeolites (including thomsonite, scolecite and mesolite) are also common, and may occur as concentric overgrowths one on another. Phillispite

and at least one other non-fibrous zeolite were found, and at low levels in Sandy Bay analcite was identified. In Sandy Bay calcite co-exists with the zeolites as fibrous, radiating or crystalline material. Certain large vesicles have beautifully developed, concentrically banded carbonate infillings, iron-rich varieties occurring in sharp early zones. Occasionally vesicles retain hollow cores into which bladed carbonates have grown, in one case producing interfering roseate clusters. Fibrous aragonite, often pale-yellow in colour, occurs in Rupert's Valley within the zone of zeolitization.

The distribution of zeolites on St. Helena does show similarities to the zonal arrangement described by Walker (1960) from Iceland, and their detailed mineralogy could prove an interesting study.

Gypsum occurs in several localities (Encl. 6) in the east of the island and in Broad Gut (Sandy Bay). Legend has it that the cast for Napoleon's death-mask was made from gypsum collected on George Island, but this seems unlikely. In Broad Gut the the gypsum occurs as exceedingly rare, very beautiful, rosettes up to 15cm across; more usually flakes (2-5cm) are found. The mineral occurs in intensely altered areas (often of pyroclastics) with restricted drainage and subject to infrequent rainfall.

Manganese ores, probably of hydrothermal origin, occur in the east of the island (Encl. 6). Anastomosing flat-lying veins and stringer, locally totally 1m in thickness, are associated with the highly altered bases of the top three (but more usually the youngest) trachyandesites of the upper shield. This material was identified as psilomelane and analyzed by Hirst (1951), although he did not relate it to the specific group of flows. In several localities 'wad' has

been deposited in stream valleys below the outcrops.

Empty vesicles in basalts elsewhere on the island may be coated by a thin sheen of black or black-brown material believed to be manganiferous. One specimen of dendritic manganese in a vesicle with zeolites at the rim, was also found in a basaltic block.

Goethite - hematite nodules (0.5-3cm) occur on Longwood and Deadwood Plains, and sporadically elsewhere. At one locality on Longwood Plain, a crust (4-10cm) of comparable composition occurs. The material appears to be concentrated during the weathering of the late trachyandesites (it is or interest, however, that the nodules contain only traces of manganese - Dr. D.S. Cronan, personal communication).

Phosphatic deposits covering a large area of Prosperous Bay Plain, locally to depths of more than 1m (Encl. 3) were interpreted by Daly as representing an ancient bird rookery.

In areas believed to be largely hydrothermally altered, veins, and bulbous pods of halloysite occur (Encl. 6). The material varies considerably in its appearance, may be massive or finely banded with colours ranging from black to white. It is found as segregation pods, extensive cross-cutting veins, from in situ alteration of lavas, and as material occurring in the scoriaceous bases of flows. Sixteen specimens, representing a complete cross-section of the widely variable material, were identified by Dr. R.J. Davis of the Natural History Museum. Fifteen specimens were of halloysite (7Å or 10Å varieties), with traces of magnetite, hematite, or members of the plumbogummite group. One pale yellow specimen was of hisingerite. The X-ray powder films and specimens are retained at the Natural History Museum (ref. 916 F to 931 F inclusive).

Minor alteration producing halloysite occurs extensively throughout the island, but the intensely altered patches are restricted, as seen in Enclosure 6. The south-west, Longwood and Deadwood Plains, and Stone Tops Ridge are all very heavily altered. There is no apparent correlation between this type of alteration and parasitic activity. Data from wells demonstrate that alteration extends to depths in excess of 25m. Locally, at the surface, sharp divisions are developed adjacent to relatively fresh material - the halloysite is unlikely to originate wholly by weathering.

APPENDIX III

PALAEOCLIMATE

An 8m sequence of fine-grained, well-bedded detrital deposits, is overlain by the youngest trachyandesite of the Upper Shield (8.6 ± 0.4 m.y.) at the landward end of Turks Cap Ridge. The deposits contain a rich floral assemblage of some 30 species, now largely extinct on the island, which is being studied by Dr. M.J. Muir of this Department. The beds were originally deposited in a broad depression related to the drainage pattern of the south-western volcano (Main Shield stage). The carbonaceous material was therefore laid down between 8.6 and about 9.6 million years ago (i.e. Middle Pliocene). Several of the units in the sequence contain numerous in situ rootlets and carbonaceous partings up to 5mm thick. The deposits were therefore laid down in a poorly, drained, swampy area into which streams from the high ground inland brought an additional plant assemblage. The nature of the assemblage and these deposits, together with geological evidence of extensive weathering of the Upper Shield during its formation, strongly suggest wetter conditions in the Pliocene than presently found.

The distribution of pyroclastic material shows an asymmetry towards the north-west as a result of dominant south-easterly winds acting throughout the entire sub-aerial activity of the volcanoes; i.e. from Upper Miocene to Middle Pliocene.

Along the southern, and parts of the north-eastern coasts of the island, patches up to 10m thick of dune bedded, wind-blown calcareous sand occur (Fig. 58). The deposits

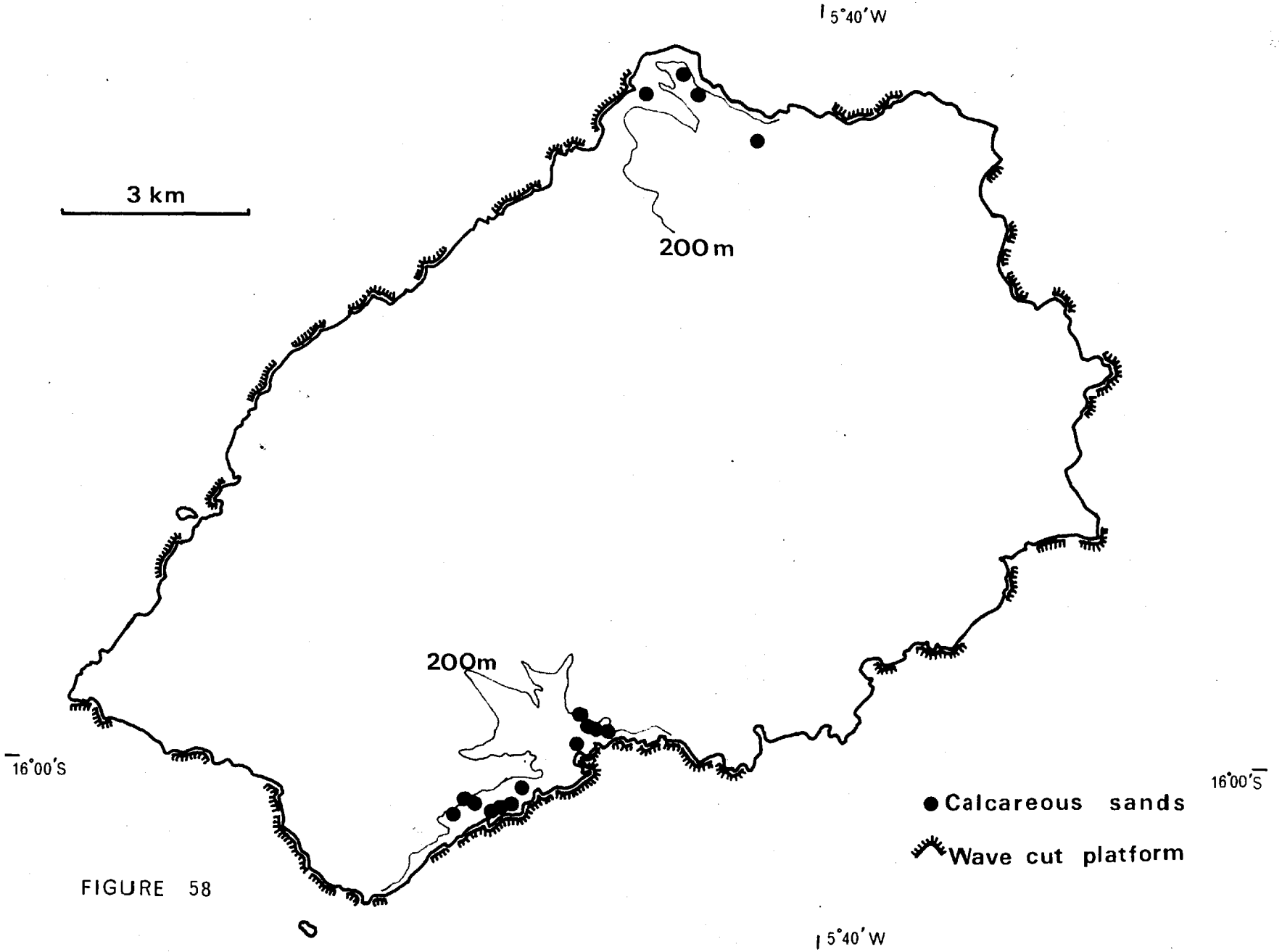
15°40'W
3 km
200m
200m
16°00'S
16°00'S
Calcareous sands
Wave cut platform
15°40'W

FIGURE 58

have been largely eroded, and consist of well sorted, coarse (1.0-1.5mm), moderately well cemented calcareous material with a small percentage of rock fragments. The sands occur up to elevations of 425m above sea level in the NE and 200m above sea level in the south. No calcareous sand beaches occur on the island at the present time. More commonly the present day beaches are of rounded boulders although a few contain small areas of coarse, black volcanic sand.

The faunal assemblage of the calcareous sand has been studied by M. Norvick and S.F. Schuyleman of Imperial College who identified the following:

Eponides	sp	
Rotalia	sp	
Asterigerina	sp	
Heterostegina	sp	
Amphistegina	sp	
Quinqueloculina	sp	
Gastropoda	10spp	
Polyzoa	5spp	
Cidaris	sp	spines (abraded)

Fragments of: lamellibranchs, schleractinian corals, and ophiuroid schlerites,

Serpulid warm tubes.

They suggested that the assemblage was of a warm shallow water fauna, probably sub-tropical or tropical. No species give a definite date, the whole assemblage could be Miocene to Recent.

The island shows certain features interpreted as results of an approximately 5m eustatic lowering of the sea level. Along the north and north west coasts a large number of 'dry' caves have their lips 2-3m above mean sea level (diurnal tidal variation on St. Helena is approximately 0.5m, although an annual variation of 1.3m is possible). The cave flows are covered by rounded basaltic boulders and are untouched by the sea except during the often intense "rollers"

of February and March when a certain amount of water may enter. Present day caves, being actively eroded, have their lips some 2m below mean sea level. Isolated patches of a raised beach deposit of rounded volcanic boulders cemented by calcareous and co-minuted volcanic material, occur all round the island (Fig. 58) from 1-3m above mean sea level. Along the southern coast the less consolidated volcanic rocks are cliffed on the landward side of the raised beach, and are being actively eroded only where the raised beach has been destroyed. One magnificent stack, The Chimney, is preserved on the raised beach in the south, standing 35m from the present shore line with its base 2m above mean sea level.

The calcareous sands must have originally formed an extensive beach along the southern coast with smaller pockets in the north-eastern bays. In all cases the attitudes of the sands demonstrate derivation from approximately south easterly directions - even in the NE the deposits are bedded in the direction of existing strong eddies. The thick north-eastern deposits rest at the top of a 200-450m cliff with a face dipping at 50-70° into the sea. The winds necessary to shift such large amounts of coarse material up to these altitudes must have been extremely powerful. Coarse material may be blown inland to-day but certainly does not form extensive, well-bedded deposits at elevations of 200m or more.

It is conceivable that during the Pleistocene, as a result of a northward shift in the limit of pack-ice, wind intensities could have been stronger. Calcareous beach sands from the cominution of a warm water fauna, of Pliocene or possibly intraglacial origin could thus have been blwon inland by strong Pleistocene winds. Subsequent marine erosion cut cliffs in the volcanic rocks with their sand capping, and built up cemented wave cut platform deposits

prior to the last eustatic drop in sea level.

The interpretation of the evidence presented above, of a warmer and wetter climate on St. Helena during the Pliocene, followed by more severe climatic conditions in the Pleistocene is in keeping with recent data on Late Tertiary palaeoclimatology (see for example, Nairn, 1961).

REFERENCES:

ABDEL-MONEM, A., WATKINS, N.D., and GAST, P.W. Volcanic history of the Canary Islands. Trans.Am.Geophys.Union 48, Abs., 226-7 (1967).

AHRENS, L.H. and TAYLOR, S.R. Spectrochemical analysis. Second edition. Pergamon, London. (1961).

ALMEIDA, F.F.M. de. Geologia e petrologia do Arquipelago de Fernando de Noronha. Min.Agr.Div.Geol.Min.Brasil Monografia XIII (1955).

--. Geologia e petrologia da ilha da Trindade. Div.Geol. Miner.Brasil Monografia XVIII (1961).

ANDERSON, E.M. The dynamics of the formation of cone-sheets, ring-dykes and cauldron subsidences. Proc.Roy.Soc. Edinburgh 56, 128-63 (1936).

AOKI, K. Petrology of the alkali rocks of the Iki Islands and Higashi-matsuura District, Japan. Sci.Rept.Tohoku Univ. 6, ser.III, 261-310 (1959).

AUMENTO, F. Magmatic evolution on the Mid-Atlantic Ridge. Earth Planet.Sci.Letters 2, 225-30 (1967).

BAKER, I. Compositioal variation of minor intrusions and the form of a volcano magma chamber. Q.J.G.S. In press.

--, GALE, N.H. and SIMONS, J. Geochronology of the Saint Helena volcanoes. Nature 215, 1451-6 (1967).

--, and HAGGERTY, S.E. The alteration of olivine in basaltic and associated lavas. Part II: Intermediate and low temperature alteration. Contr.Mineral.Petrol. 16, 258-73 (1967).

BAKER, P.E., GASS, I.G., HARRIS, P.G. and LEMAITRE, R.W. The volcanological report of the Royal Society expedition to Tristan da Cunha, 1962. Phil.Trans.Roy.Soc.London ser. A, 256, 439-578 (1964).

BHATTACHARJI, S. and SMITH, C.H. Flowage differentiation. Science 145, 150-3 (1964).

BOTT, M.H.P. Formation of oceanic ridges. Nature 207, 840-3 (1965).

BOWEN, N.L. Recent high temperature research on silicates and its significance in igneous geology. Am.J.Sci. 33, 1-21 (1937).

BRAVO, T. Estudio geologico y petrografico de la isla de la Gomera. Estudios geol. 20, n.1-2, 1-56 (1964).

BAILEY, E.B. and others. Tertiary and post-Tertiary geology of Mull, Loch Aline and Oban. Geol.Surv.Scotland Mem. (1924).

BROCH, O.A. Lavas of Bouvet Island. Norske Videnskamps Akademi Oslo 25, 3-26 (1946).

CANN, J.R. and VINE, F.J. An area on the crest of the Carlsberg Ridge: Petrology and magnetic survey. Phil.Trans. Roy.Soc.London ser.A, 259, 198-217 (1966).

CARMICHAEL, I.S.E. The petrology of Thingmuli, a Tertiary volcano in eastern Iceland. J.Petrol. 5, 435-60 (1964).

CHAYES, F. Relative abundance of intermediate members of the oceanic basalt-trachyte association. J.Geophys.Res. 68, 1519-34 (1963a).

--, Relative abundance of intermediate members of the oceanic basalt-trachyte association - reply to discussions. J.Geophys.Res. 68, 5108-9 (1963b).

CROSS, W. Lavas of Hawaii and their relations. U.S.G.S. Prof.Pap. 88 (1915).

DALY, R.A. Magmatic differentiation in Hawaii. J.Geol. 19 289-316 (1911).

--, The geology of Ascension Island. Proc.Am.Ac.Arts Sci. 60, 1-80 (1925).

--, The geology of Saint Helena Island. Proc.Am.Ac.Arts Sci. 62, n.2 (1927).

DARWIN, C. Naturalist's voyage round the world. Second edition 486-91, John Murray: London (1873).

--, Geological observations. Second edition 83-109 Smith,Elder and Co: London (1876).

DEER, W.A., HOWIE, R.A. and ZUSSMANN, J. Rock forming minerals. 5 vols. Longman's: London (1962,1963).

DIETZ, R.S. Continent and ocean basin evolution by spreading of the sea floor. Nature 190, 854-7 (1961).

EATON, J.P. and MURATA, K.J. How volcanoes grow. Science 132, 925-38 (1960).

ENGEL, A.E.J. and ENGEL, C.G. Composition of basalts from the Mid-Atlantic Ridge. Science 144, 1330-2 (1964).

EWING, J. and EWING, M. Sediment distribution on the mid-ocean ridges with respect to spreading of the sea floor. Science 156, 1590-2 (1967).

FINCKH, L. Die Gesteine der Inseln Madeira and Porto Santo. Zeit.Deutsh.Geol.Gesellsch. 65, 453-517 (1914).

GAGEL, C. Studien über den Aufbau and die Gesteine Madeiras. Zeit.Deutsch.Geol.Gesellsch. 64, 344-491 (1912).

GARSON, M.S. Stress pattern of carbonatite and alkaline dykes at Tundulu ring structure, Southern Nyasaland. Int.Geol.Cong. 20th Session: publ.Assoc.Serv.Geol.Africa 309-23 (1959).

GASS, I.G. Geochronology of the Tristan da Cunha group of islands. Geol.Mag. 104, 160-170 (1967).

GIBSON, I.L., KINSMAN, D.J.J. and WALKER, G.P.L. The geology of the Faskrudsfjordur area, Eastern Iceland. Greinar IV, 2. Visind.Islendinga. 1-52 (1966).

GREEN, D.H. and RINGWOOD, A.E. The genesis of basaltic magmas. Contr.Mineral.Petrol. 15, 103-90 (1967).

HADWEN, P. and WALKER, G.P.L. A geological review of the Azores. Proc.Geol.Assoc. In press.

HAGGERTY, S.E. and BAKER, I. The alteration of olivine in basaltic and associated lavas. Part I: High temperature alteration. Contr.Mineral.Petrol. 16, 233-57 (1967).

HAMILTON, D.L. and MACKENZIE, W.S. Phase equilibrium studies in the system $NaAlSiO_4$ (nepheline)-$KAlSiO_4$ (kalsilite)-SiO_2-H_2O. Mineral.Mag. 34, 214-31 (1965).

HARKER, A. The Tertiary igneous rocks of Skye. Geol.Surv. Scotland Mem. 256-69 (1904).

HARRIS, P.G. Relative abundance of intermediate members of the oceanic basalt-trachyte association - a discussion. J.Geophys.Res. 68, 5103-7 (1963).

HAUSEN, H. Contributions to the geology of Tenerife. Soc. Scient.Fenn.Comm.Physico-Math. 18, n.1 (1956).

--, On the geology of Fuertaventura. Soc.Scient.Fenn.Comm. Physico-math. 22, n.1 (1958).

--, On the geology of Lanzarote. Soc.Scient.Fenn.Comm. Physico-Math. 23, n.4 (1959).

--, New contributions to the geology of Grand Canary. Soc.Scient.Fenn.Comm.Physico-Math. 27, n.1 (1962).

HEEZEN, B.C. and THARP, M. Physiographic diagram of the South Atlantic Ocean. Geol.Soc.Am. (1961).

HIRST, T. Observations on the geology and mineral resources of Saint Helena. Colonial Geol.and Min.Resources 2, n.2, 116-28 (1951).

IDDINGS, J.P. Igneous rocks. Vol.2. John Wiley: New York (1913).

JACOBSON, R.R.E., MACLEOD, W.N. and BLACK, R. Ring-complexes in the younger granite province of Northern Nigeria. Geol.Soc.London Mem. 1 (1958).

JAMBOR, J.L. and SMITH, C.H. Olivine composition determination with small diameter X-ray powder cameras. Mineral. Mag. 33, 730-43 (1964).

JEFFERY, P.G. and WILSON, A.D. A combined gravimetric and photometric procedure for determineng silica in silicate rocks and minerals. Analyst London 85, 478-86 (1960).

JOHNSON, W. and MELLOR, P.B. Platicity for mechanical engineers. Van Nostrand Co.: London (1962).

KLERKX, J. La cristallisation de l'apatite dans les laves de l'Etna. Ann.Soc.Geol.Belg. 89, Bull.5-10, 449-58 (1966).

LACROIX, A. Sur quelques roches volcaniques melanocrates des Possessions francaises de l'ocean Indien et du Pacifique. Compt.Rend.Seances Acad.Sci.Paris 163, 177-83 (1916).

LEMAITRE, R.W. Petrology of the volcanic rocks, Gough Island, South Atlantic. Bull.Geol.Soc.Am. 73, 1309-40 (1962).

LINDSLEY, D.H. Fe-Ti oxides in rocks as thermometers and oxygen barometers. Carnegie Inst.Washington Ybk. 62, 60-6 (1963).

MACDONALD, G.A. The 1840 eruption and crystal differentiation in the Kilauea magma column. Am.J.Sci. 242, 177-89 (1944).

--, Hawaiian petrographic province. Bull.Geol.Soc.Am. 60, 1541-96 (1949).

--, Dissimilarity of continental and oceanic rock suites. Bull.Geol.Soc.Am. Abs. 68, 1761-2 (1957).

--, Dissimilarity of continental and oceanic rock suites. J.Petrol. 1, 172-7 (1960).

--, Relative abundance of intermediate members of the oceanic basalt-trachyte association - a discussion. J.Geophys.Res. 68, 5100-2 (1963).

--, Hawaiian calderas. Pacific Sci. 19, 320-34 (1965).

--, and KATSURA, T. Chemical composition of Hawaiian lavas. J.Petrol. 5, 82-133 (1964).

MCBIRNEY, A.R. and GASS, I.G. Relations of oceanic volcanic rocks to mid-ocean rises and heat flow. Earth Planet. Sci. Letters 2, 265-76 (1967).

MELLISS, J.C. Saint Helena: a physical, historical, and topogrophical description of the island, including its geology, fauna, flora, and meterorology. L.Reeve and Co. London (1875).

MELSON, W.G., JAROSEWICH, E., BOWEN, V.T. and THOMPSON, G. Saint Peter and Saint Paul rocks: a high temperature, mantle-derived intrusion. Science 155, 1532-5 (1967).

--, --, CIFELLI, R. and THOMPSON, G. Alkali olivine basalt dredged near Saint Paul's Rocks, Mid-Atlantic Ridge. Nature 215, 381-2 (1967).

MENARD, H.W. The world-wide oceanic rise-ridge system. In A Symposium of Continental Drift, 109-22 Royal Society, London (1965).

MOORE, J.G. Petrology of deep-sea basalt near Hawaii. Am. J.Sci. 263, 40-52 (1965).

MORGAN, J.W. Gravity anomalies and convection currents: Part 2: The Puerto Rican Trench and the Mid-Atlantic Rise. J.Geophys.Res. 70, 6189-6204 (1965).

MUIR, I.D. and TILLEY, C.E. Mugearites and their place in alkali igneous rock series. J.Geol. 69, 186-203 (1961).

--, --. Basalts from the northern part of the rift zone of the Mid-Atlantic Ridge. J.Petrol. 5, 409-34 (1964).

MURATA, K.J. and RICHTER, D.H. The settling of olivine in Kilauean magma as shown by lavas of the 1959 eruption. Am.J.Sci. 264, 194-203 (1966).

NAIRN, A.E.M. (Editor). Descriptive palaeoclimatology. Interscience Publications (1961).

NEIVA, J.M.C. Consideracoes sobre o quimismo das formacoes eruptivas do Arquipelago de Cabo Verde. Mus. e Lab. Mineral. e Geol.Fac.Cienc.do Porto 17 (1940).

--, Chimisme des roches eruptives des iles de S.Thome et Prince. Compt.Rend.du Congres d'Alger XXI (1954).

NOCKOLDS, S.R. Average composition of some igneous rocks. Bull.Geol.Soc.Am. 65, 1007-32 (1954).

--, and ALLEN, R. Geochemistry of some igneous rock series. Geochim. Cosmochim. 5, 245-85 (1956).

NOLAN, J. Melting-relations in the system $NaAlSi_3O_8$-$NaAlSiO_4$-$NaFeSi_2O_6$-$CaMgSi_2O_6$-H_2O. Q.J.G.S. 122, 119-158 (1966).

O'HARA, M.J. Primary magmas and the origin of basalts. Scott.J.Geol. 1, 19-40 (1965).

--, and YODER, H.S. Formation and fractionation of basic magmas at high pressures. Scott.J.Geol. 3, 67-117 (1967).

OLIVER, J.R. The geology of Saint Helena. Benjamin Grant: Saint Helena (1869).

OSBORN, E.F. Role of oxygen pressure in the crystallization and differentiation of basaltic magma. Am.J.Sci. 257, 609-647 (1959).

PIRSSON, L.V. Geology of Bermuda Island. Am.J.Sci. ser.4 38, 331-44 (1914).

REAY, A. and HARRIS, P.G. The partial fusion of peridotite. Bull.volc. 27, 115-27 (1964).

RICHEY, J.E. and THOMAS, H.H. The geology of Ardnamurchan, N.W.Mull and Coll. Geol.Surv. Scotland Mem. (1930).

RICHTER, D.H., AULT, W.U., EATON, J.P. and MOORE, J.G. The 1961 eruption of Kilauea Volcano, Hawaii. U.S.G.S. Prof. Pap. 474-D (1964).

RIDLEY, W.I. Geology of the Las Canadas area, Teneriffe. Unpublished Ph.D.Thesis, Univ.London (1968).

ROBSON, G.R. and BARR, K.G. The effect of stress on faulting and minor intrusions in the vicinity of a magma body. Bull.volc. 27, 315-30 (1964).

SAGGERSON, E.P. and WILLIAMS, L.A.J. Ngurumanite from Southern Kenya and its bearing on the origin of rocks in the Northern Tanganyika alkaline district. J.Petrol. 5, 40-81 (1964).

SHAPIRO, L. and BRANNOCK, W.W. Rapid analysis of silicate, carbonate and phosphate rocks. U.S.G.S.Bull. 1144A (1962).

SIMPSON, E.S.W. and HEYDORN, A.E.F. Vema seamount. Nature 207, 249-51 (1965).

SMITH, R.L. and BAILEY, R.A. The Bandelier tuff: a study of ash-flow eruption cycles from zoned magma chambers. Bull. volc. 29, 83-104 (1966).

TALWANI, M., LE PICHON, X. and EWING, M. Crustal structure of the mid-ocean ridges. 2: Computed model from gravity and seismic refraction data. J.Geophys.Res. 70, 341-52 (1965).

THORARINSSON, S. The eruption of Mount Hekla 1947-1948. Bull.volc. 10, 157-68 (1950).

THORNTON, C.P. and TUTTLE, O.F. Chemistry of igneous rocks. 1: Differentiation Index. Am.J.Sci. 258, 664-84 (1960).

TILLEY, C.E. and MUIR, I.D. Intermediate members of the oceanic basalt-trachyte association. Geol.Fören.Förhand. 85, 434-43 (1964).

TYRRELL, G.W. Petrology of Heard Island. B.A.N.Z. Antarctic Research Expedition 1929-31. Rep.Ser.A 2, Pts. 3-4 (1937).

VINE, F.J. Spreading of the ocean floor: new evidence. Science 154, 1405-15 (1966).

--, and MATTHEWS, D.H. Magnetic anomalies over ocean ridges. Nature 199, 947-9 (1963).

VLODAVETZ, V.J. On the underground structure of some volcanoes on Kamchatka. Bull.volc. 20, 113-20 (1959).

VON HERZEN, R.P. Surface heat-flow and some implications for the mantle. In: The Earth's Mantle. 197-230 Pergamon (1967).

WAGER, L.R., BROWN, G.M. and WADSWORTH, W.J. Types of igneous cumulates. J.Petrol. 1, 73-85 (1960).

WALKER, F. Mugearites and oligoclase-basalts. Geol.Mag. 89, 337-45 (1952).

WALKER, G.P.L. Zeolite zones and dike distribution in relation to the structure of the basalts of eastern Iceland. J.Geol. 68, 515-28 (1960).

WATERS, A.C. Determining direction of flow in basalts. Am. J.Sci. 258A, 350-66 (1960).

WATKINS, N.D. and HAGGERTY, S.E. Primary oxidation variation and petrogenesis in a single lava. Contr.Mineral.Petrol. 15, 251-71 (1967).

WATTS, W.W. (Chairman). Report of the Committee on British Petrographic Nomenclature. Mineral.Mag. 19, 137-47 (1921).

WELLS, A.K. Mugearites and oligoclase-basalts. Geol.Mag. 91, 14-16 (1954).

WENTWORTH, C.K. and MACDONALD, G.A. Structures and forms of basaltic rocks in Hawaii. U.S.G.S.Bull. 994 (1953).

WHITE, R.W. Ultramafic inclusions in basaltic rocks from Hawaii. Contr.Mineral.Petrol. 12, 245-314 (1966).

WILKINSON, J.F.G. Reidual glasses from some alkali basaltic lavas from New South Wales. Mineral.Mag. 35, 847-60 (1966).

WILSON, A.D. A new method for the determination of ferrous iron in rocks and minerals. Bull.Geol.Surv.Great Britain 9, 56-8 (1955).

WILSON, J.T. Evidence from islands on the spreading of ocean floors. Nature 197, 536-8 (1963).

YAGI, K. Petrochemical studies on the alkalic rocks of the Morotu District, Sakhalin. Bull.Geol.Soc.Am. 64, 769-810 (1953).

YODER, H.S. and TILLEY, C.E. Origin of basalt magmas: an experimental study of natural and synthetic rock systems. J.Petrol. 3, 343-532 (1962).

SOUTH-WESTERN VOLCANO

GEOLOGY – MAIN AND UPPER SHIELDS

5°45′ 5°40′ 15°55′ 16°00′

SOUTH-WESTERN VOLCANO
NORTH-EASTERN VOLCANO
JAMESTOWN
TURK'S CAP
HORSE POINT
HIGH KNOLL
phosphate
PROSPEROUS BAY PLAIN
THE SADDLE
MOUNT ACTAEON
GILL POINT
HEADOWAIN
HIGH PEAK
HIGH HILL
RIDING STONES
SHEEP KNOLL
POWELLS VALLEY HILL
LONG RANGE
WHITE HILL
TRIPE BAY
RUSH KNOLL
WHITE POINT
OLD JOAN HILL
HOOPER'S ROCK
LOWER SHIELD
BLUE POINT
Intermediate flows of the White Hill area (w)

LATE ALKALINE INTRUSIONS
EASTERN FLANK FLOWS
UPPER SHIELD
TRACHYANDESITES
LOWER BASALTS
MAIN SHIELD
flows
intrusives
INTERMEDIATE (PARASITIC)
PARASITIC CONES
INTERMEDIATE FLOWS
BASALTS (and TRACHYBASALTS)

0 1 2 3 Km

Enclosure: 3

IB 67

SOUTH - WESTERN VOLCANO -

GEOLOGY OF THE LOWER SHIELD

16°00'

15°45'

15°43'

16°01'

MANATI BAY

DEVIL'S HOLE

BLUE POINT

CASTLE ROCK

ASSES EARS

MAN O' WAR ROOST

FRIGHTBUS ROCK

NIGGERHEAD

LOT'S WIFE

WHITE ROCKS

THE CHIMNEY

SANDY BAY BEACH

HORSES HEAD

FAIRYLAND

LOT

RIDING STONES HILL

0 500m 1000m

MAIN SHIELD EXTRUSIVES

INTRUSIVES
- PHONOLITIC
- INTERMEDIATE
- BASALTIC

DEVIL'S CAP PYROCLASTICS

DEVIL'S HOLE BRECCIAS

WHITE ROCK SERIES
- pyroclastics: UPPER FLOWS
- flows: UPPER PYROCLASTICS
- LOWER FLOWS
- LOWER PYROCLASTICS

BEACH TRACHYBASALTS

MAN O' WAR FLOWS

SANDY BAY SERIES
- flows
- pyroclastics

HORSES HEAD FLOWS

ALLUVIUM

Enclosure : 2

IB 167

SAINT HELENA –

PARASITIC CENTRES

(except Lower Shield of SW Volcano)

5°45′ 5°40′

15°55′ 15°55′

JAMESTOWN

HIGH KNOLL

THE SADDLE

HIGH HILL

WHITE POINT

LOWER SHIELD

16°00′ 16°00′

Estimated original size of cone:

- ○ <100 m
- ⊙ 100 – 200 m
- ● >200 m

70 Estimated height of base (m) (above sea level)

N NE Volcano

0 1 km 2 3

Enclosure: 5

IB '67

SAINT HELENA — SECONDARY MINERALIZATION

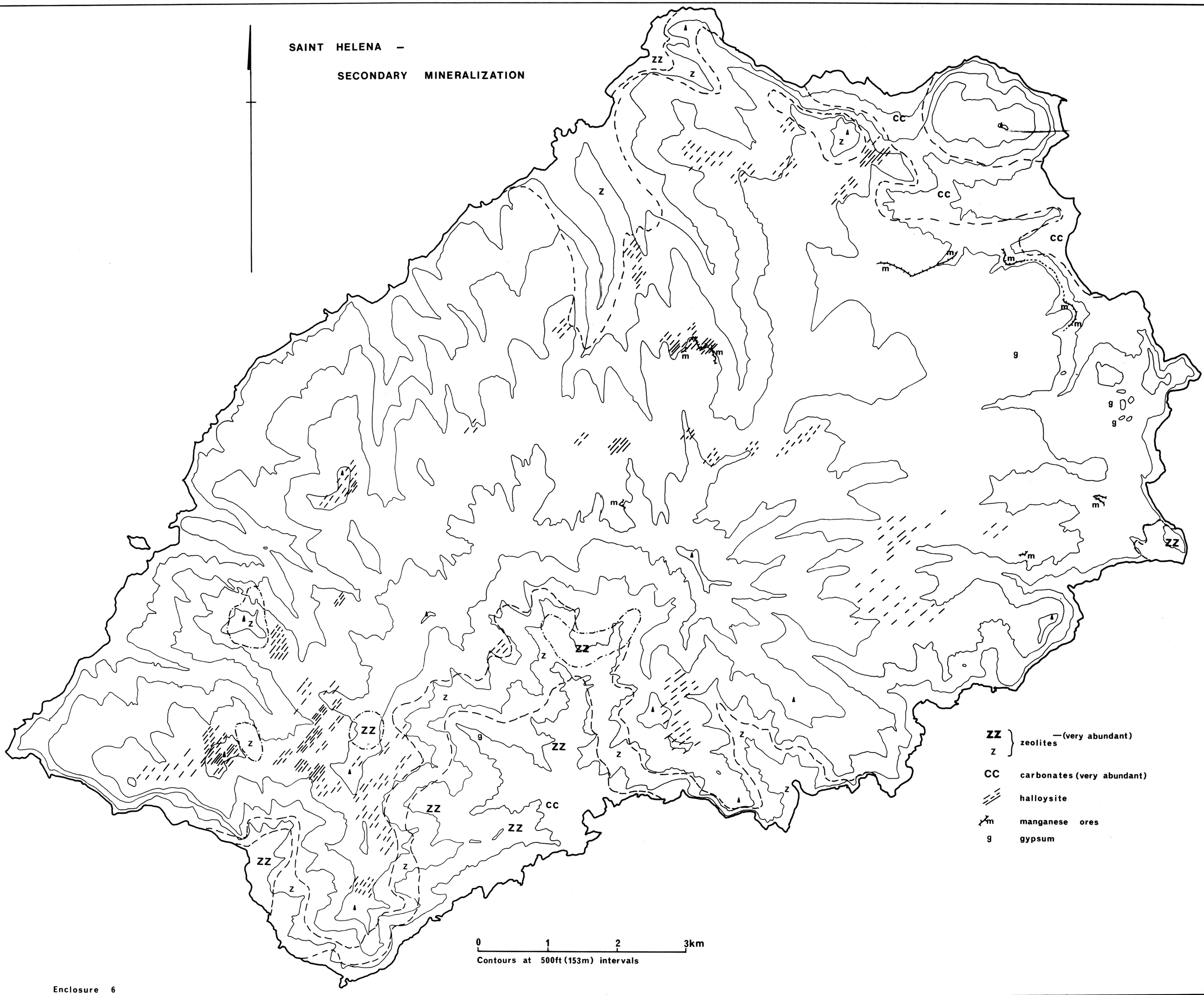

Enclosure 6

IB '67

SAINT HELENA

TOPOGRAPHY

5°46'
5°44'
5°40'
15°56'
15°58'
16°00'

Segerhoat Hill
Flagstaff Bay
Banks Valley
The Barn
Flagstaff Hill
Rupert's Hill
JAMESTOWN
Rupert's Valley
Knotty Ridge
Deadwood Plain
Turks Cap
Bryan's Rock
Horse Point
Prosperous Bay
Banker's Hill
High Knoll
Longwood Plain
King & Queen Rocks
LONGWOOD
Fisher's Valley
Horse Pasture
Prosperous Bay Plain
Woody Ridge
The Saddle
Egg Island
Swanley Valley
Old Woman's Valley
Stitch's Ridge
Benecoolen
Cason's Gate
Mount Actaeon
Gill Point
Shore Island
Headowain
Cole's Rock
Diana's Peak
Levelwood
Sharks Valley
Little Stone Top
Great Stone Top
Fairyland
High Peak
High Hill
Sheep Knoll
Boxwood Hill
George Island
Blue Hill
Rock Mount
Riding Stones Hill
Thompson's Valley
Deep Valley
Long Range
SANDY BAY
Tripe Bay
White Hill
Wild Cattle Pound
Broad Gut
Powell's Valley
Thompson's Wood
Hopper's Ridge
White Point
Horse Ridge
Man and Horse
White Rocks
Sandy Bay Barn
Old Joan Hill
Wild Ram Hill
Gates of Chaos
Sandy Bay Beach
Horse's Head
Devil's Cap
Lot's Wife
Manati Bay
The Chimney
Blue Point
Niggerhead
Devil's Hole
Man o' War Roost
Frontbus Rock
Asses Ears
Black Rocks
Castle Rock
Speery Island

Kilometers
0 1 2 3
Contours at 100m intervals

Enclosure: 1

IB '67

SOUTH-WESTERN VOLCANO – DYKE DISTRIBUTION

5°45′ 5°40′

15°55′ 15°55′

16°00′ 16°00′

NORTH-EASTERN VOLCANO

JAMESTOWN

MAIN EXPOSURE OF UPPER SHIELD SERIES

U

THE PEAKS

STONE TOPS

DEEP VALLEY

POWELL'S VALLEY

LOT

LOT'S WIFE

MANATI BAY

LIMIT OF LOWER SHIELD

<.05 .05 .06 .07 .08 .10 .11 .12 .13 .14 .15 .16 .18 .19 .20 .22 .23 .24 .26 .27 .28 .30 .32 .36 .40 .45

0 1 2 3 km

Enclosure: 4

IB '67